

**Highly Conjugated, Substituted Polyacetylenes via the Ring-Opening
Metathesis Polymerization of Monosubstituted Cyclooctatetraenes**

Thesis by
Christopher B. Gorman

In partial fulfillment of the Requirements
For the Degree of
Doctor of Philosophy

California Institute of Technology
Pasadena, California

1992

(Defended August 13, 1991)

To my family
Mom, Dad, Greg, and Anne

Acknowledgments

After making some materials, I quickly found out that a lot of the neat characterization experiments in the literature are "non-trivial." I want to thank several people for assistance and advice on interpretation. Glenn Heffner in Dale Pearson's group at UC Santa Barbara did some light scattering experiments and helped sort out the possibilities for determining size and shape information on these molecules. I thank Dr. Joseph Perry for making some initial nonlinear optical measurements and teaching me a thing or two about NLO. I also appreciate the efforts of Hyun Chae Cynn in Dr. Malcom Nicol's group at UCLA in obtaining Raman spectra. While on the subject of lasers, I should mention Bruce Tiemann. Besides being an excellent anecdotal reference (to several decimal places) on optics and methods for packing nitrogen atoms into a molecule, he synthesized several compounds for me and can really get a lot of surface area out of a piece of lithium. Also, I'd like to thank Lynda Johnson for the facile (one-pot?) synthesis and the gift of a family of robust tungsten alkylidenes. I'm sorry I didn't get to try them all.

When I started doing research here, I found myself under the auspices of a man who saw the world a bit differently than I did. Despite that, Bob Grubbs dealt with my argumentative way of reasoning things out, let me take my project in directions he hadn't planned, and was honest and exceptionally kind with me when I needed advice. I don't think I could have done the same in similar circumstances, and I thank him for always trying to intervene in a positive way. I have also had the good fortune to interact with Dennis Dougherty, who taught me a lot of important ways of thinking about chemistry, and Nate Lewis, who

was willing to grind a group meeting to a halt and explain enough about semiconductor/X junctions so I could follow. I found teachers in both of their groups and want to thank them all, especially Dave Shultz, Mike Sailor, and Tom Jozefiak for making a lot very clear in a short time.

I have had some incredibly rewarding collaborations in the lab as well, and a few important people taught me the bulk of what I know about doing chemistry. Jeff Moore continues to be an experimental powerhouse. If I could do chemistry as thoughtfully and as efficiently as he does, I'd have it made. I just hope that his wife doesn't find that pack of Camels in his desk. If possible, Eric Ginsburg and I would have done our computations on a computer with two keyboards (and fought over who could use the mouse), and I don't think I did an experiment while he was here that he didn't scrutinize. Although we were destined not to agree on anything, he forced me to look at every data point twice, and that turned out to be a good thing. An argument can be worth a thousand experiments, and I thank him for his vital role in piecing this whole thing together. Seth Marder continues to be insightful (if not profound) and a ne'er-too-oft dining partner. I thank him for his friendship and an ongoing effort to get and keep me on the right track. Nothing can summarize years of banter, but listen, learn and collaborate, and you'll be fine.

I thank Andrew Conley and Kian-Tat Lim for their friendship, and Anne for everything.

Fellowships from the NASA Jet Propulsion Laboratory and the American Chemical Society Division of Organic Chemistry (Sponsored by SmithKline & French Laboratories) are most gratefully acknowledged

Abstract

A number of monosubstituted cyclooctatetraenes were polymerized via ring-opening metathesis polymerization, producing derivatives of polyacetylene that were highly conjugated. Most of these polymers were soluble in the nascent, high-cis form, and some remained soluble upon isomerization to the trans form. The polymers had a high molecular weight (as determined by gel permeation chromatography) and were composed of polyacetylene backbones (as determined by Raman spectroscopy).

Not all of the polymers were completely soluble after isomerization to the trans form. Observations relating the steric bulk of the side group with solubility behavior indicate a tradeoff between solubility and conjugation. Structural variation permitted the synthesis of very highly conjugated, yet soluble polyacetylenes. For example, *trans*-poly-*s*-butylCOT, had a low-energy optical absorption (560 nm in tetrahydrofuran, 586 nm in CS₂) corresponding to extended conjugation. The polymer was formed as an amorphous film, yet it had a conductivity after iodine doping of 0.03 S/cm. THG measurements at 1064 nm gave $|\chi(3)| = 2 \pm 1 \times 10^{-11}$ esu for polytrimethylsilylCOT. Activation parameters for cis/trans isomerization of *trans*-poly-*s*-butylCOT in solution were obtained. NMR spectroscopy revealed that two isomers exist in the so-called "trans" form, suggesting the existence of cis/trans and trans/trans diads in the polymer. The trisubstituted olefin at which the side-group is attached can isomerize between the cis and the trans forms with a very low barrier ($\Delta G^\ddagger = 18.9 \pm 0.4$ kcal/mol was measured at 50 °C by magnetization transfer in benzene).

Both semi-empirical (AM1) and empirical (MM2) calculations on model compounds were used to provide a model relating side group sterics with twisting in the polymer main chain. Molecular dynamics was used to probe the

magnitude of motion in the polymer main chain. AM1 heat-of-formation calculations were used to explore the cis/trans preference of a trisubstituted double bond in a polyene chain.

Polyacetylenes bearing chiral side groups were synthesized and explored. Strong Cotton effects were observed for the backbone $\pi \rightarrow \pi^*$ transition. The data suggest that the side group geometrically perturbs the main chain, possibly twisting it in predominantly one screw sense.

TABLE OF CONTENTS

Abstract.....	vi
TABLE OF CONTENTS.....	viii
LIST OF TABLES	xi
LIST OF FIGURES AND SCHEMES.....	xii
CHAPTER 1: CONJUGATED POLYMERS: THE INTERPLAY BETWEEN SYNTHESIS, STRUCTURE, AND PROPERTIES	1
1. Introduction	2
2. Structural features of conjugated polymers	3
3. Polymer synthesis - Basic methods.....	5
3.1 Step-Growth Polymerization.....	7
3.2 Chain-Growth Polymerization.....	9
3.3 Ring-Opening Polymerization	12
4. Direct Synthetic Methods.....	13
4.1. Electrochemical Synthesis	13
4.2. Synthesis by Step-Growth Polymerization.....	18
4.2.1. Polyaniline (PAN)	18
4.2.2. Poly(phenylene sulfide).....	19
4.2.3. Polythiophene and its derivatives.	20
4.2.4. Other 5-membered Heterocyclic Derivatives.....	24
4.2.5. Polyparaphenylene (PPP).	27
4.2.6. Polysilanes.....	28
4.2.7. Polymers of Phthalocyanines.	30
4.2.8. Other Conjugated Metal Coordination Polymers.	31
4.2.9. Ladder Polymers.	32
4.3. The Unusual Topochemical Polymerization to form Polydiacetylenes	35
4.4. Chain-growth Polymerizations	37
4.4.1. Polyacetylene via Ziegler-Natta polymerization.....	37
4.4.2. Ring-Opening Metathesis Polymerization routes to Polyacetylenes	40
5. Polymers from precursors.....	42
5.1. Polyparaphenylene (PPP)	42
5.2. Poly(Phenylene Vinylene) (PPV) and other Vinylene Polymers	44
5.3. Precursors to Polyacetylene	46
6. Extensions of these methods in the synthesis of "small-bandgap" polymers	48
7. Conjugated Polymer Matrices.....	51
8. Conclusions and Caveats	55
9. References.....	57

CHAPTER 2: SYNTHESIS AND PRELIMINARY CHARACTERIZATION OF POLYMERS OF MONOSUBSTITUTED CYCLOOCTATETRAENES	79
Introduction	80
A. Ring-Opening Metathesis Polymerization	80
B. General Schemes for the Synthesis of Substituted Cyclooctatetraenes.	85
Results and Discussion	88
A. Monomer Synthesis	88
B. Polymerization	89
C. Polymer Molecular weight.....	96
D. Raman Spectroscopy as Structure Proof for a Polyconjugated Chain.....	102
E. Oxidative Stability	104
Experimental	104
References and Notes.....	118
 CHAPTER 3: PROPERTIES OF POLYMERS OF MONOSUBSTITUTED CYCLOOCTATETRAENES	 122
Introduction	123
A. Intrachain Effects.....	124
Effective Conjugation Length.....	124
Comparison with other Conjugated Polymers.	130
B. Interchain Effects.....	133
Effect upon Electrical Properties.....	133
Effect upon Optical Properties.	135
C. The Solubility/Conjugation Length Tradeoff	136
Results and Discussion	138
A. Visible Absorption Spectra	138
B. Raman Spectra.....	145
C. Relationship between Conjugation Length and Solubility in Polyacetylene.....	146
D. Probes of Film Morphology	152
E. Conductivity	153
F. Nonlinear Optical Properties.....	156
G. Differential Scanning Calorimetry.....	157
H. Isomerization in Solution.....	159
I. Dynamic Cis/trans Isomerization of the Trisubstituted Double Bond	166
Summary	169
Experimental	170
Appendix I. COT Copolymers.....	172
References and Notes.....	175
 CHAPTER 4: COMPUTATIONAL MODELING OF SUBSTITUTED POLYACETYLENE OLIGOMERS	 185
Introduction	186
Results and Discussion	191
A. Chain twisting - static picture	192
B. Dynamic picture of chain twisting	199

C. Cis/Trans Preference for the Trisubstituted Double Bond	204
Summary	207
Experimental	207
Appendix I. Use of phenyl rings to transmit electronic perturbations on the main chain	210
References and Notes.....	212
CHAPTER 5: SOLUBLE, CHIRAL POLYACETYLENES: SYNTHESSES AND INVESTIGATION OF THEIR SOLUTION CONFORMATION	214
Introduction	215
Results and Discussion	218
A. Monomers.....	219
B. Polymers.....	223
C. Electronic transitions and circular dichroism.....	230
Conclusions	238
Experimental	240
References and Notes.....	248

LIST OF TABLES

CHAPTER 2

Table 1. Percentage of conversion and percentage of backbiting product for some soluble poly-RCOT's.....	91
Table 2. Molecular weights (GPC) of cis polymers.	97
Table 3. A comparison of polymerization conditions using s-butylCOT and catalysts 2 and 7.	99
Table 4. Polymer molecular weights after chlorination.....	101
Table 5. Raman Data.	103

CHAPTER 3

Table 1. The effect of side group sterics upon the optical absorption of polymers of substituted acetylenes.	130
Table 2. Visible absorption maxima (in THF).	139
Table 3. Extinction Coefficients of Soluble Polymers.....	143
Table 4. Raman Data.	146
Table 5. Iodine-doped conductivities of polymer films.....	154
Table 6. Isomerization temperature observed for polymer films.....	159

CHAPTER 4

Table 1. Computed twist angles for model compound 1.	197
Table 2. Computed twist angles for model compound 2.	199
Table 3. Number of occurrences of angle Θ_x for various dynamics runs on model compound 1.....	203
Table 4. Energy differences between isomers of 3.....	206

CHAPTER 5

Table 1. ROMP of Chiral COT Monomers.....	226
Table 2. ^1H NMR Chemical Shift Data of Substituted polyRCOTs.....	227
Table 3. Raman Data	230
Table 4. Electronic Transition Data of Poly(COT)'s.....	231

LIST OF FIGURES AND SCHEMES

CHAPTER 1

Figure 1. Structure of the repeat unit of several conjugated polymers including their common abbreviation.	4
Figure 2. Schematic of a π -system including a conformational (rotational) defect and a saturated (sp^3) defect.	5
Figure 3. Common vinyl polymers synthesized by chain-growth polymerization.	10
Figure 4. Modes of polymerization.	11
Figure 5. General scheme for a ring-opening polymerization.	12
Figure 6. Electropolymerization of pyrrole.	15
Figure 7. Possible differences in the linkages in the electrochemical polymerization of pyrrole.	16
Figure 8. Sample monomers that have been oxidatively polymerized either chemically or electrochemically.	17
Figure 9. General formula of polyaniline.	19
Figure 10. Representative formula of counterion affixed polyaniline.	19
Figure 11. Synthesis of "Ryton" (poly(phenylene sulfide)).	20
Figure 12. Nickel-catalyzed polymerization of thiophene.	21
Figure 13. Model for two orthogonally fused conductive polymer chains.	21
Figure 14. Structural variation of poly(alkyl thiophenes)	24
Figure 15. Poly(dibenzothiophene sulfide), polycarbazole, and poly(N-vinylcarbazole)	25
Figure 16. A first step toward the phosphorous analogues of polythiophenes.	26
Figure 17. Syntheses of substituted PPP's.	28
Figure 18. Poly(<i>p</i> -phenylene- <i>co</i> -2,5-pyrazine).	28
Figure 19. Polysilane polymerization via a Wurtz-coupling mechanism.	29
Figure 20. Metal phthalocyanine polymers can be linked via both conjugated and nonconjugated linkages.	31
Figure 21. Stacked dithiolene complexes and linear dithiolene polymer (M = Ni).	32
Figure 22. Polyacene and a representative ladder polymer.	33
Figure 23. Possible events in the pyrolysis of polyacrylonitrile.	33
Figure 24. A "molecular line" 3.06 nanometers long.	34
Figure 25. Poly(<i>p</i> -phenylene-2,6-benzobisthiolediyl) (PBT).	34
Figure 26. Generalized scheme for the topochemical polymerization of diacetylenes.	36
Figure 27. Polymerization of acetylene showing cis and trans isomers.	39
Figure 28. Reduction of conjugation in polyacetylene derivatives that is due to steric effects.	40
Figure 29. Scheme for ring-opening metathesis polymerization.	41
Figure 30. Polymerization and aromatization of cyclohexadiene showing the linkages formed by 1,4- and 1,2-propagation.	43

Figure 31. A low temperature precursor route to PPP.	44
Figure 32. Precursor route to PPV.....	45
Figure 33. Poly(napthalene vinylene), poly(thienylene vinylene) (X=S), and poly(furanylene vinylene) (X=O).	45
Figure 34. Synthesis and conversion of Durham polyacetylene.	46
Figure 35. Polybenzvalene and its conversion to polyacetylene.....	48
Figure 36. The two bond-length alternate forms of polyacetylene and polyparaphenylene.....	49
Figure 37. The two bond-alternate structures of PITN. Both possess some degree of aromaticity.	50
Figure 38. Proposed formation of poly(α -(5,5'-bithiophenediyl)- <i>p</i> -acetoxybenzylidene) (PBTAB). X = S.....	51
Figure 39. Polypyrrole/FeOCl layered complex.	55

CHAPTER 2

Figure 1. The catalytic cycle for ring-opening metathesis polymerization.....	81
Figure 2. Tungsten-based metathesis catalysts.	81
Figure 3. Interesting olefins that have been polymerized by ROMP.....	82
Scheme 1. Cycloextrusion of an aromatic compound during COT polymerization.....	85
Scheme 2. Synthesis of monosubstituted COT's from bromoCOT.	86
Scheme 3. Monosubstituted COT derivatives via COT dianion chemistry.	87
Scheme 4. Synthesis of alkoxyCOT's.	87
Figure 4. ¹ H NMR spectra of (bottom) isopropylCOT, (middle) cis-poly-isopropylCOT, (top) trans-poly-isopropylCOT.....	95
Figure 5. A typical gel permeation chromatogram.	100
Figure 6. Typical Raman spectrum of poly-RCOT.	103
Figure 7. Repeat units contained in the polymers.	116
Figure 8. Typical ¹ H NMR (CDCl ₃) of the olefinic region of poly-RCOT.	117

CHAPTER 3

Figure 1. Steric repulsions in (a) polymers of substituted acetylenes, (b) polymers of substituted cyclooctatetraenes.	128
Figure 2. Steric crowding in (a) polyalkylthiophenes, (b) substituted poly-para-phenylenes.	131
Figure 3. Absorption spectrum for <i>cis</i> - and <i>trans</i> -poly- <i>s</i> -butylCOT.....	142
Figure 4. Visible absorption spectra of NOPF ₆ doped <i>trans</i> -poly- <i>s</i> -butylCOT of molecular formula [(C ₁₂ H ₁₆)(NOPF ₆) _{0.10}] _x	144
Figure 5. Typical DSC exotherm observed upon isomerization of a poly-R-COT film.....	158
Figure 6. Thermal <i>cis</i> / <i>trans</i> isomerization of poly- <i>s</i> -butylCOT in solution.	163
Figure 7. Photochemical <i>cis</i> / <i>trans</i> isomerization of polyneopentylCOT in dilute THF solution.	164
Figure 8. Typical results of <i>cis</i> / <i>trans</i> isomerization kinetics.....	165

Figure 9. Arrhenius plot for thermal cis/trans isomerization of poly- <i>s</i> -butylCOT.....	166
Figure 10. Eyring plot for thermal cis/trans isomerization of poly- <i>s</i> -butylCOT.....	166
Figure 11. NMR resonances of the side groups of poly- <i>s</i> -butylCOT reveal two species in the "trans" polymer.....	168
Figure 12. Potential energy curve for the interconversion of <i>ct</i> and <i>tt</i> diads in poly- <i>s</i> -butylCOT (benzene solution, 50 °C).....	169
Figure 13. Optical-absorption maximum as a function of copolymer feed ratio.....	174

CHAPTER 4

Figure 1. Model compounds used in this study.....	192
Figure 2. An alternative geometry, ruled out (at least for this size regime) by these computations.....	194
Figure 3. Model compound 1 showing the dihedral angles of interest.....	196
Figure 4. Graphical representations of twist angles for different side groups in model compound 1	197
Figure 5. Values of torsion angle Θ_1 at 10 fs intervals accumulated during a 20 ps molecular dynamics run at 300 K (Batchmin) for 1 , R = <i>s</i> -Butyl.....	201
Figure 6. Values of torsion angle Θ_1 at 10 fs intervals accumulated during a 20 ps molecular dynamics run at various temperatures (in K) (Batchmin) for 1 , R = <i>s</i> -butyl.....	201
Figure 7. Average Θ_1 of 1 , R = <i>s</i> -butyl as a function of temperature (in K).....	202
Figure 8. Model tetraenes used to determine heats of formation as a function of side group and isomeric composition.....	205
Figure 9. Relative heats of formation of various isomers of 3 as a function of side group.....	206
Figure 10. Trimer 4 used in molecular mechanics determination of relative energy as a function of phenyl ring twist.....	211
Figure 11. Relative energy of trimer 4 , (0° = phenyl ring is coplanar with backbone).....	212

CHAPTER 5

Figure 1. Chain Twisting in Polyacetylene.....	215
Figure 2. ROMP of COT Derivatives.....	216
Scheme 1. Syntheses of 2 , 3 , 4 , 5	219
Scheme 2. Syntheses of 6 , 7	220
Figure 3. Ring Inversion in Mono-Substituted COT's.....	221
Figure 4. Variable Temperature Circular Dichroism of (9R,10S)- 4	222
Figure 5. Variable Temperature Circular Dichroism of (9R,10S)- 5	223
Figure 6. Possible species formed during isomerization of <i>cis</i> -polyRCOT's.....	229
Figure 7. Circular Dichroism of Poly-trans-(9R,10S)- 4 and Poly-trans-(9R,10S)- 5	233
Figure 8. Variable Temperature Circular Dichroism of Poly- <i>cis</i> -	

(9R,10S)-5.....	234
Figure 9. Variable Temperature Circular Dichroism of Poly- <i>trans</i> -	
(9R,10S)-5.....	235
Figure 10. Variable Temperature Circular Dichroism of Poly- <i>trans</i> -	
(9R,10S)-4.....	236

CHAPTER 1

CONJUGATED POLYMERS: THE INTERPLAY BETWEEN SYNTHESIS, STRUCTURE, AND PROPERTIES

This chapter will appear in *Conjugated Polymers: The Novel Science and Technology of Conducting and Nonlinear Optically Active Materials*,

J. L. Brédas and R. Silbey, eds., Kluwer Academic Publishers,

Dordrecht, The Netherlands.

1. Introduction

Polymers containing loosely held electrons in their backbones, often referred to as conjugated polymers or conducting polymers, have attracted much research effort in the last ten years or so. Many investigations were first motivated by the observation that oxidizing or reducing the backbone (doping) of polyacetylene at a level equivalent to removing/adding an electron, in one out of every 5-15 repeat units, increased the conductivity of the matrix by many orders of magnitude.¹⁻³ Because the electrons in these delocalized systems are also easily polarized by an external electric field such as that found in light, these types of polymers have also attracted interest for their nonlinear optical properties.⁴⁻⁶ These polymers have also been proposed as "molecular wires" for nanotechnology.⁷

It is ironic that one of the lures towards the synthesis of polymers, the ability to produce a material cheaply that is easily cast or molded into the shape of choice either from the melt or from solution, is not commonly achievable with most conjugated polymers. In contrast, a polymer such as polyethylene is synthesized commercially in the amount of some 10 billion pounds a year,⁸ commonly using a titanium-based catalyst system that can produce 10^6 grams of polyethylene per gram of catalyst.⁹ This polymer is practically free of catalyst and can be dissolved, or more commonly, melted and cast into most any shape. The most common synthesis of polyacetylene employs a very similar titanium-based system, but requires a substantial amount of catalyst mixture (> 5% weight catalyst/weight polymer) and is an insoluble polymer that cannot be melted. Moreover, it is difficult, even with repeated washings, to remove the last 1-2% of catalyst residues from the polymer.¹⁰ Although the catalyst systems vary for

other conjugated polymer syntheses, all of the polymers in Figure 1 are insoluble in organic solvents. This insolubility is not surprising since these polymers tend to be conformationally rigid, at least over the length of several monomer units, in order to maintain the conjugation of the electrons in the backbone.

In this chapter, approaches towards the synthesis of conjugated polymers will be discussed with particular emphasis on what control, if any, the method offers over the molecular weight and its distribution for the polymer. Since the form of most conjugated polymers cannot be changed once they are synthesized, several clever procedures have been developed to produce the polymer in a desirable macroscopic form such as a fiber or sheet. Many of the polymers have been derivatized with the goal of controlling their materials properties, most notably their solubility, and strategies and results of synthesizing soluble derivatives of the polymers will be discussed. Many conjugated polymers are synthesized via soluble precursor polymers, and these will be discussed in their own section. These precursors can be cast, coated, etc. and subsequently converted to the conjugated form.

2. Structural features of conjugated polymers

The structure of all conjugated polymers has the same signature. Each atom along the backbone is involved in a π bond, which is much weaker than the σ bonds that hold the atoms in the polymer chain together.[†] Placed side by side (conjugated), these π bonds can delocalize over all the atoms. The extent of

[†] A notable exception is the polysilanes, which are conjugated through their σ (i.e., single-bonded) system.

delocalization of an electron in an extended π system is a matter of some interpretation and debate: Although every electronic wave function is defined for any point in space, most of the electron density is smeared over a relatively small volume.¹¹ Polymers are not completely straight and flat over an infinite distance. Single (i.e., C-C) bonds, even when they are part of a conjugated system, can rotate, given the thermal energy available at room temperature. The rotational potential of a single bond has been calculated to be about 6 kcal/mol in polyacetylene and 3 kcal/mol in polythiophene (gas-phase calculations).¹² These rotations reduce the conjugation (delocalization) of the electrons in the π -system.

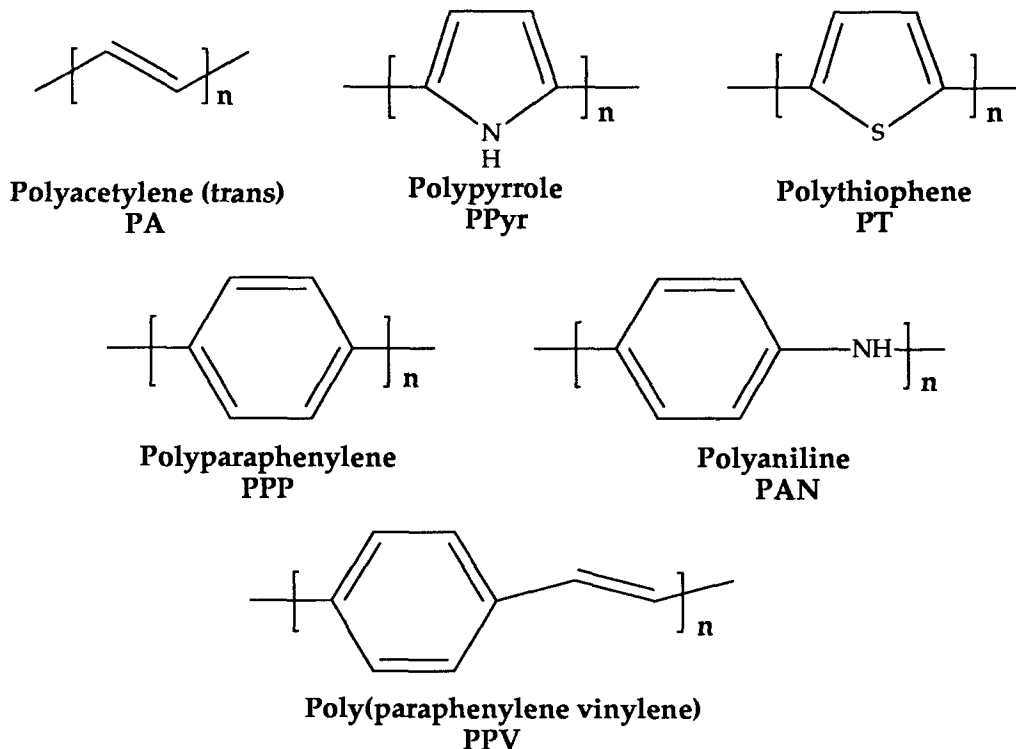


Figure 1. Structure of the repeat unit of several conjugated polymers including their common abbreviation.

This effect can be observed, for example, in the thermochromism of polythiophene derivatives. The lowest energy-optical absorbance in a

conjugated chain typically arises from a $\pi \rightarrow \pi^*$ transition. The more conjugated the double bonds are in the polymer, the lower the energy of this absorption will be. Thus, twisting about the chain will reduce the amount of conjugation and increase the energy (i.e., blue shift) of this absorption.¹³⁻¹⁵ This discussion does not address the problem of chemical (sp^3 , conjugation disrupting) defects that can be formed in the polymer backbone during synthesis or subsequent manipulation.¹⁶⁻¹⁹

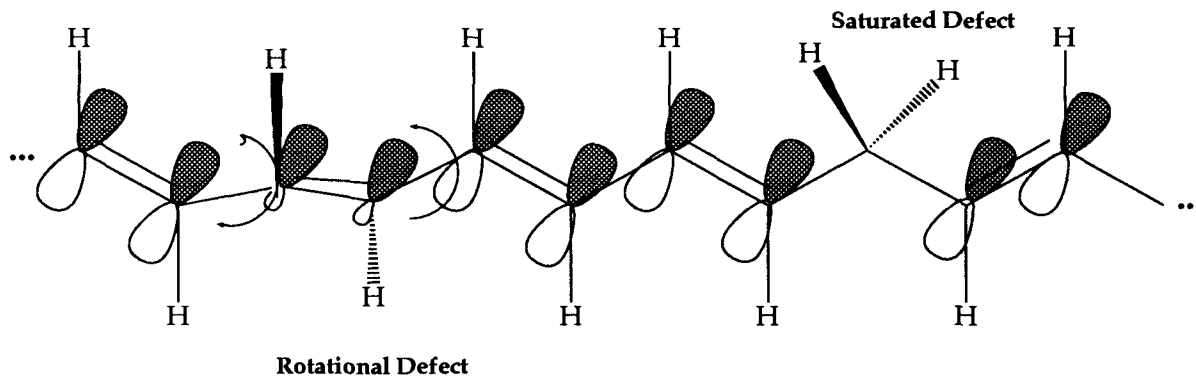


Figure 2. Schematic of a π -system including a conformational (rotational) defect and a saturated (sp^3) defect.

3. Polymer synthesis - Basic methods

This brief treatment is designed to contrast the two basic mechanisms involved in polymer synthesis: step-growth (condensation) or chain-growth (addition). The terms in parenthesis are often used in place of more accurate terms. These terms actually refer to earlier observations about polymerizations and for example, "condensation" is not always appropriate for every step-growth

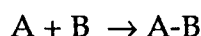
polymerization. The mechanism that a polymerization reaction follows will determine the final molecular weight (M_n)^{††} and the molecular weight distribution of polymer chains in the final product. Unless an experiment is designed to examine the effect of chain length on some physical property of the polymer, it is rarely desirable to have a mixture of short chains in the sample. Optical properties of conjugated polymers such as absorption and Raman scattering will be dependent upon the number of units in the polymer until a relatively high molecular weight has been reached (≈ 50 monomer units is a round number) at which point these properties become much less dependent upon chain length. Particularly the oxidation/reduction potentials for generation of mobile charge carriers (solitons, polarons, bipolarons, etc.) and their spectral properties will vary for short chains and will become relatively invariant for longer chains. Likewise, samples possessing a widely varying collection of chain lengths (i.e., a large polydispersity, defined as M_w/M_n) often have a dispersion of different conjugation lengths, especially when the chain lengths are short, and these complicate characterization of the polymer. In many cases, conjugated polymers are found to possess a bimodal molecular weight distribution. In other words, instead of having a distribution of molecular weights around some average, there is a distribution of high molecular weight chains, and a distribution of lower molecular weight chains, often oligomers. Again, especially when oligomers are present, it is difficult or impossible to determine the physical properties of the high molecular weight polymer, and many experimental efforts have been challenged on this point.

^{††} This is a number average molecular weight. The distribution of molecular weights in the polymer sample can be weighted by their number fraction (M_n), their weight fraction (M_w) their viscosity fraction (M_v), etc.

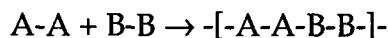
Both polymerization mechanisms can result in high molecular weight polymers with a relatively narrow molecular weight distribution. However, mechanism can be very important. For example, in the synthesis of an insoluble conjugated polymer, one type of polymerization might result in very low molecular weight oligomers precipitating from solution and the other could result in synthesis of high molecular weight polymer before precipitation occurs.

3.1 Step-Growth Polymerization

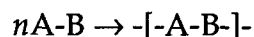
The most general reaction for two molecules can be represented as:



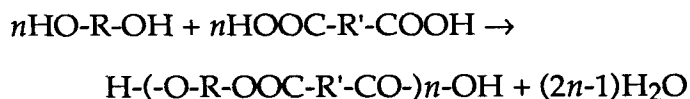
and, in principle, any reaction that links two units together can be used to form a polymer. In general, we can write:



or



A common example of step polymerization is the synthesis of polyesters which takes advantage of the fact that an alcohol and an acid can be condensed together (with the elimination of water, thus the origin of the term "condensation") to form an ester:

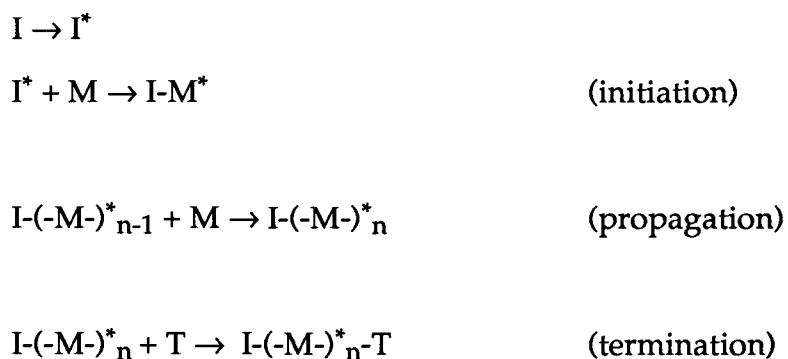


Polyamides, polyurethanes, polycarbonates, and many other polymers are routinely synthesized in this manner. This polymerization, in principle, is general since many synthetic organic reactions can be employed using difunctional units. This reaction takes place in a number of statistical steps and, although the rate of bond formation can be very fast, the rate of molecular weight increase is initially very slow. First, most of the monomers will react to form dimers, and statistically, only after most of the dimers have formed will dimers start to react with monomers or dimers to form trimers or tetramers. Already 50% of the bonds have formed, but the degree of polymerization is only $n=2$. This slow buildup of molecular weight is the primary disadvantage of step-growth polymerization. If an organic reaction has a 50% yield, and it is used in a step-growth polymerization, dimers and trimers will dominate the products. One can show that at 90% conversion, the average degree of polymerization is only 10, at 95% conversion it is 20, and only above 98% conversion (the last 2% of the reaction) do long chains start to reach to form high molecular weight polymer (high polymer). Most organic reactions do not have a 98% yield, so in practice, this method is limited.

Many conjugated polymers are synthesized by step-growth. If the polymer is soluble and the reaction employed is of high yield, high polymer can be expected. However, if oligomers precipitate before they react with one another, or if the yield of the reaction is low, the degree of polymerization can be very low. This problem is often encountered in conjugated polymer synthesis.

3.2 Chain-Growth Polymerization

The second mechanism of polymerization, chain-growth, involves three distinct steps: initiation, propagation, and termination. An initiator reacts with a monomer to produce a new species that can then react with another monomer, and another, until the monomer is depleted or the growing polymer chain undergoes a termination reaction. This procedure is shown schematically below where * refers to a species that can add another monomer. This species is often a radical, cation, anion, or attached transition-metal complex that can insert a monomer between itself and the growing polymer chain.



This reaction is most commonly observed with vinyl monomers, yielding polyethylene, polystyrene, polyacrylates, etc.

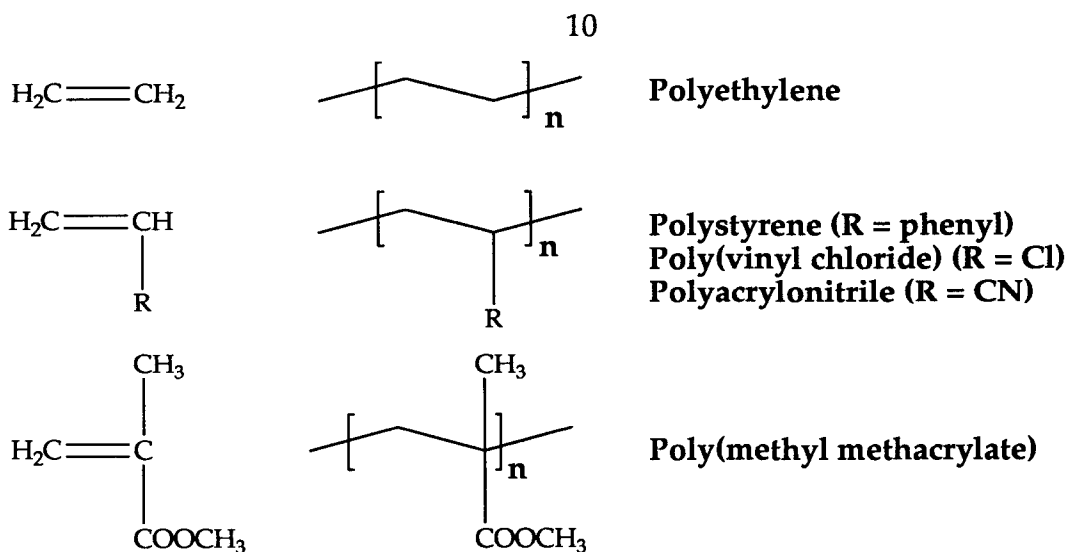


Figure 3. Common vinyl polymers synthesized by chain-growth polymerization.

The rate at which the molecular weight of a chain-growth polymerization increases depends on three rates: the rate of initiation, propagation, and termination (R_i , R_p , R_t). In many cases, once initiated, the polymerization proceeds very quickly, and the propagating chain end "lives" for only a short time before terminating. Usually, the propagating species forms a high polymer during this time. The most noticeable feature in this polymerization ($R_p \gg R_i$) is that high polymer forms very quickly, an advantage if the polymer is insoluble and precipitates quickly from the reaction solution as well.

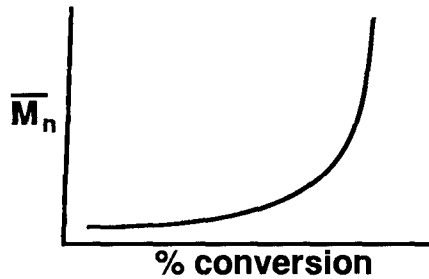
MODES OF POLYMERIZATION

MECHANISM

MOLECULAR WT. CONTROL

$$\bar{M}_n = \bar{X}_n \times \text{Mol. Wt. Monomer}$$

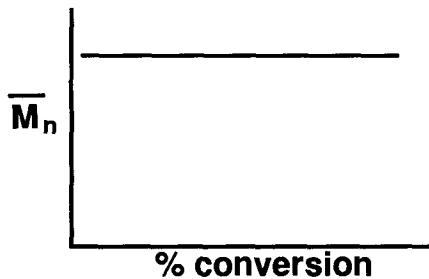
STEP GROWTH



$$\bar{X}_n = \frac{1}{1-\rho}$$

$\rho = \% \text{ functional groups reacted} / 100$

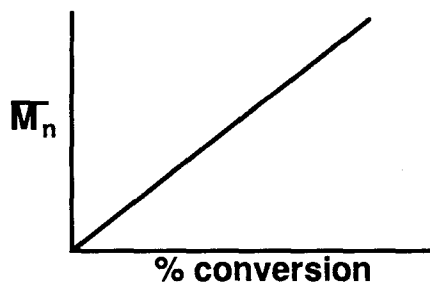
CHAIN GROWTH



$$\bar{X}_n = \frac{1}{1-\rho}$$

$$\rho = \frac{R_p}{R_p + R_t + R_{ct}}$$

LIVING



$$X_n = \frac{\text{moles monomer consumed}}{\text{moles of initiator}}$$

$$R_i \gg R_p; R_t \approx 0$$

Figure 4. Modes of polymerization.

Not much control over molecular weight is available in this scenario. However, if $R_i \gg R_p$, all the chains will initiate at about the same time, and if

there is no chain termination, the molecules will continue to grow until all the monomer is depleted. At this time, since the propagating species is still active at the end of the polymer, a second monomer may be added, which will then polymerize to give a polymer containing two "blocks" (a block copolymer). This special case, referred to as a "living polymerization," allows the ultimate control over molecular weight and provides the most narrow molecular weight distribution available. A common example is the living anionic polymerization of styrene using alkyl lithium reagents.

3.3 Ring-Opening Polymerization

Ring-opening polymerization can follow either a step-growth or chain-growth mechanism and involves the breaking of a bond in a ring to form an open-chain intermediate. In step-growth, these intermediates can react with each other to form polymer. In chain-growth, typically a few monomers ring-open initially, either with or without an initiator, to form a propagating species, which then reacts with another monomer, opening it to form a new propagating species. Several living ring-opening polymerizations are known.

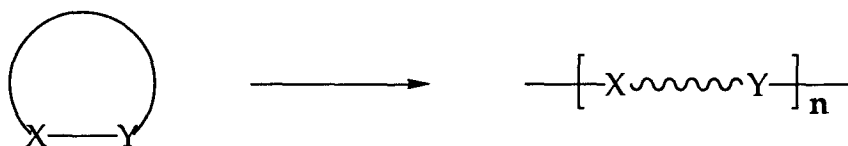


Figure 5. General scheme for a ring-opening polymerization.

4. Direct Synthetic Methods

Since most conjugated polymers cannot be dissolved or melted, they must be synthesized directly in the desired shape and location. This necessity has frustrated many researchers since the form, most importantly the morphology of the conjugated polymer, has one of the greatest influences on many of the properties, most notably the electrical conductivity of the doped polymer. Theory and experiment have placed much emphasis on justifying the formation of mobile, delocalized carriers within the polymer chains (polarons, bipolarons, solitons).^{20, 21} However, since no one polymer strand is long enough to persist over a macroscopic length, the measured conductivity of a polymer sample requires that carriers hop between polymer strands. This hopping is widely believed to limit bulk conductivity.²² Synthesis of highly conductive polymer samples has become an art in some circles since small changes in synthesis, catalyst removal, or doping can dramatically affect sample morphology and result in wide variation in conductivity. Thus, for example, it is important to understand the effects of polymerization conditions on polyacetylene morphology.²³ Deliberate changes in polymer morphology resulting from chain alignment will be reviewed in Section 7.

4.1. Electrochemical Synthesis²⁴

Most conjugated polymers are synthesized by electrochemical means. Pyrrole, thiophene and their derivatives are often polymerized in this manner as are carbazoles, azulenes and pyrenes.²⁵ Typically, this oxidation (2 C-H bonds are converted to a C-C bond plus two H⁺) is accomplished by placing the monomer and electrolyte (e.g., AgClO₄) in a suitable solvent such as acetonitrile

and oxidizing at a mild potential (e.g., 0.5 V). A polymer film grows at the anode in a reaction that is thought to occur as illustrated in Figure 6. An example termination step is shown. In principle, any trace species that can react with the propagating radical cation can terminate one end of the polymer. Any polymer chain that does not re-oxidize is effectively terminated as well. The kinetics of this polymerization is expected to be complex. Among other factors, the reaction occurs in a heterogeneous environment (the electrode surface), and the polymerization is based upon coupling of the radical cations that can occur between the oxidized forms of any combination of monomers and polymer chains.

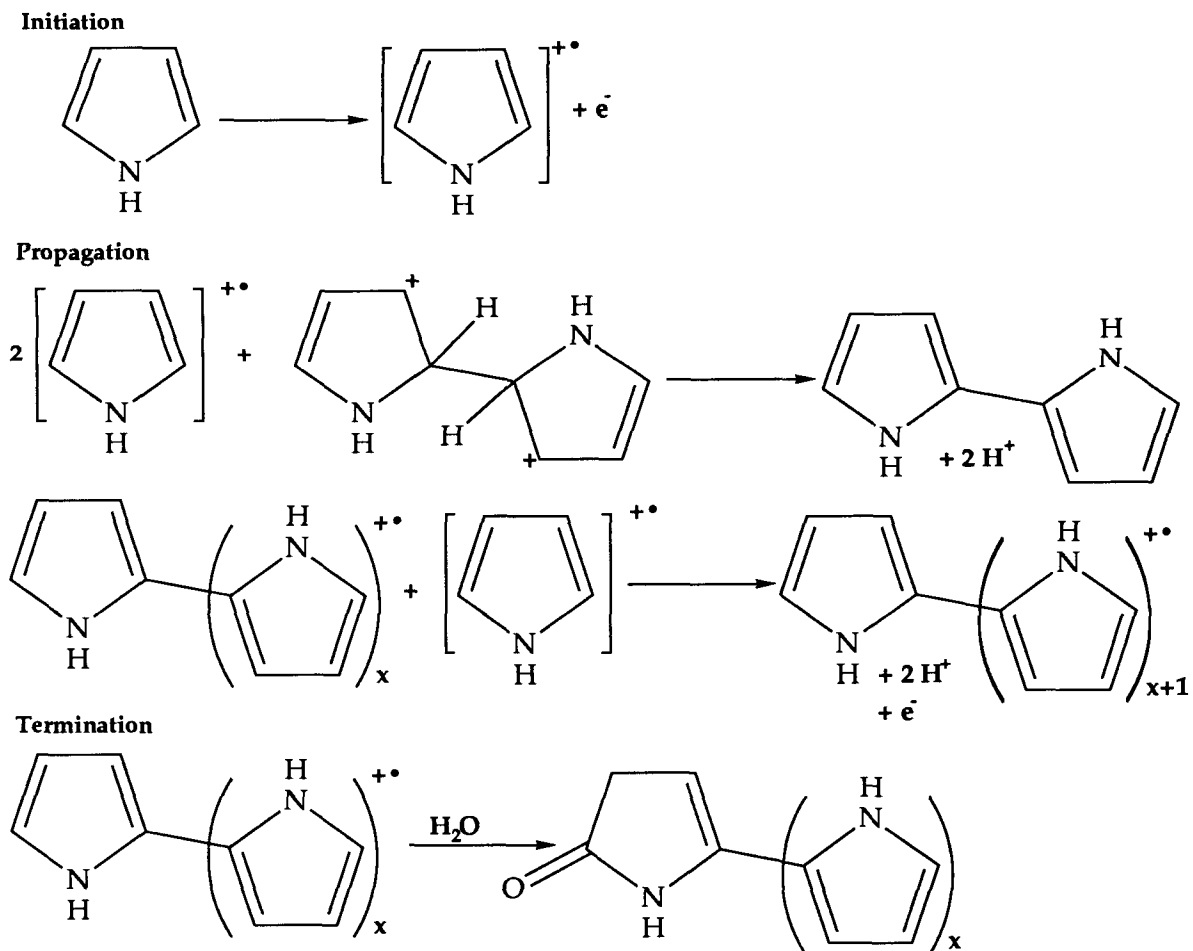


Figure 6. Electropolymerization of pyrrole.²⁶

Although it is thermodynamically favorable for the linkages to be formed at the 2,5 positions of the monomer units as shown above, there is concern that the electrochemical polymerization results in a significant number (perhaps 30%) of linkages that are not of this 2,5 type. 2,3-Couplings do not extend conjugation, in fact, branching of this type actually reduces the conjugation length of the main chain of the polymer.²⁷

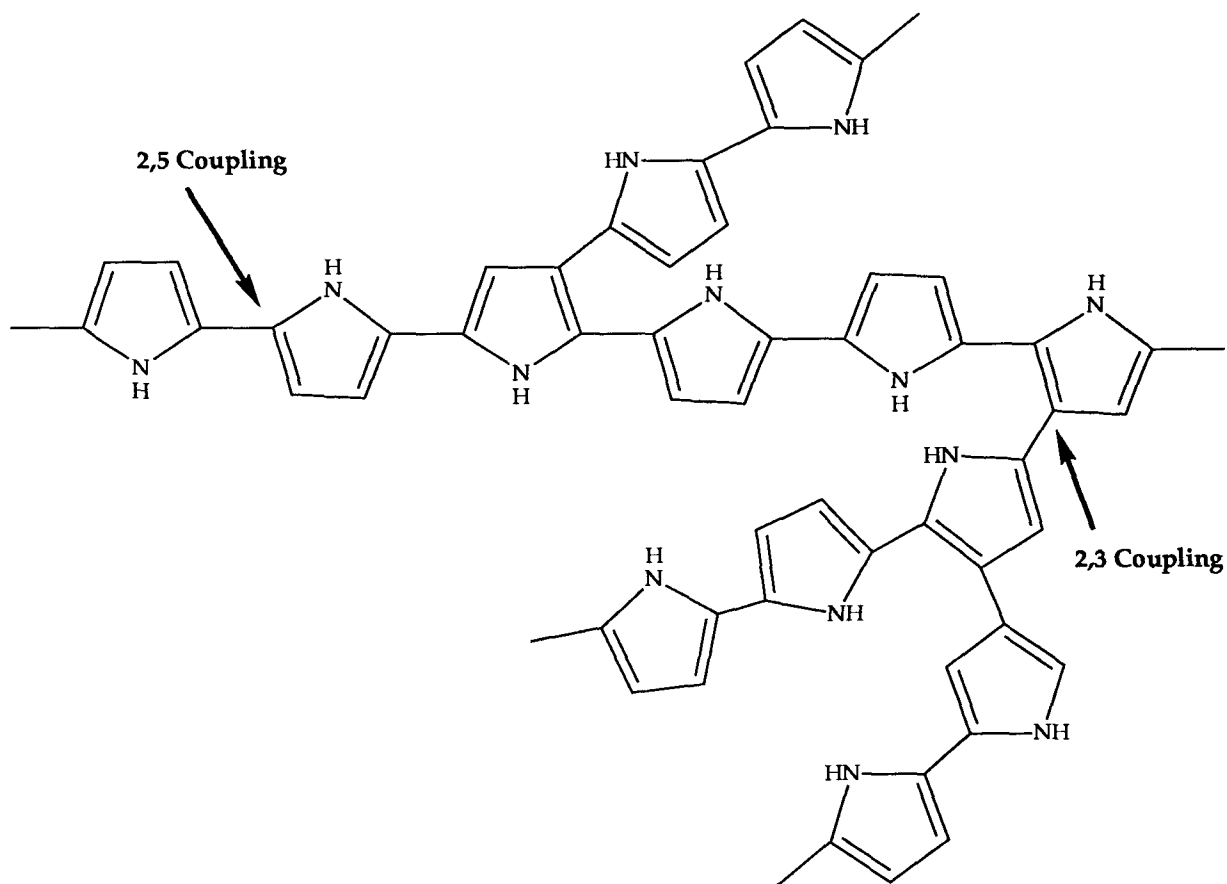


Figure 7. Possible differences in the linkages in the electrochemical polymerization of pyrrole.²⁸

The anodically prepared polymer film is already doped by the excess of charge that is passed in the polymerization reaction and contains the counterion (in this example, ClO_4^-) from the electrolyte solution. The film can usually be compensated (undoped) by passing current in the opposite direction. This method allows for flexibility in the choice of the counterion and has the advantage that the counterion is homogeneously dispersed in the polymer film.²⁹⁻³⁵ Moreover, since the reaction takes place electrochemically, there are methods for exploring the kinetic parameters for doping.³⁶ Nevertheless, the degree of polymerization is generally not known. Some oligomeric material is present.³⁷ By observation of tritium loss from 1,2-tritiated monomers, a degree of

polymerization of about 750 was determined for poly(3,4-dimethyl pyrrole perchlorate).³⁸

New polymers synthesized by this procedure continue to be reported as new oxidizable conjugated units become available. For example, the fused monomers shown in Figure 8 have a higher degree of conjugation and are easier to oxidize than their smaller counterparts.

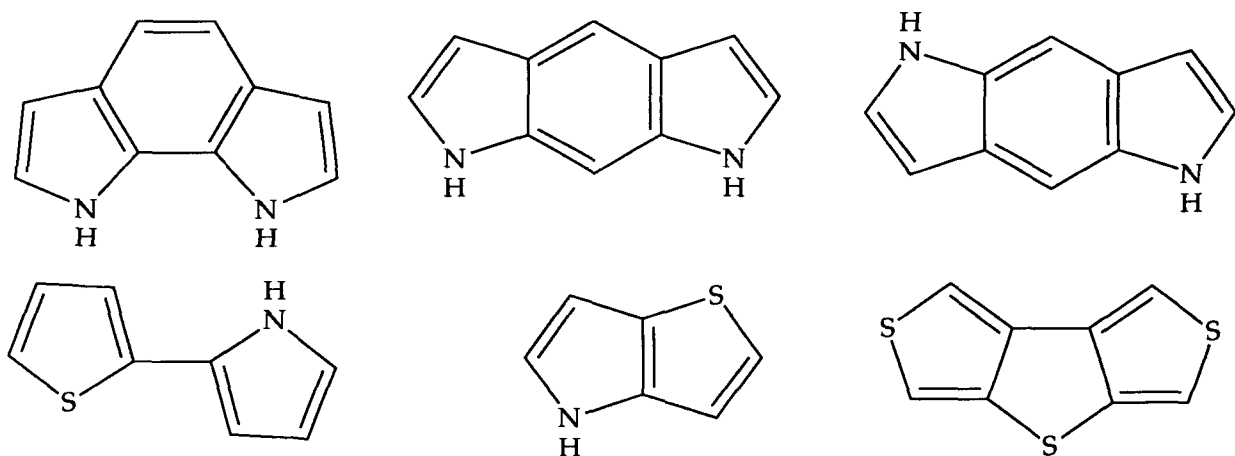


Figure 8. Sample monomers that have been oxidatively polymerized either chemically or electrochemically.³⁹⁻⁴²

Previously, this synthesis had the disadvantage that the size of the film was limited by the size of the anode. However, Naarman has introduced a rotating-drum electrode that allows the continuous synthesis of films.^{43, 44} Other electrode modifications include the use of a needle-to-circle electrode configuration to grow visually striking 2-D and 3-D fractal patterns of polypyrrole,⁴⁵ and precoating of the electrode followed by polymerization to synthesize conducting polymer/plastic polymer composites⁴⁶ or blends.⁴⁷ A polymer-covered electrode with incorporated redox or other catalytic sites can be used as a surface-modified electrode.⁴⁸⁻⁵²

4.2. Synthesis by Step-Growth Polymerization

Probably the most common method of *chemical* synthesis of conjugated polymers is via a step-growth (condensation) polymerization. Before the advent of the continuous electrochemical synthesis (Section 4.1), this method was the only way to make large amounts of polymers such as polythiophene. As mentioned previously, these polymerizations require a high-yield reaction to proceed to a high degree of polymerization. However, in principle, any monomer that can be oxidatively polymerized electrochemically can be polymerized using a chemical oxidant (e.g., FeCl_3) as well.^{53, 54} If the resulting polymer is insoluble, the end of the polymerization may occur in the solid state. This serious limitation is avoided in the synthesis of soluble, conjugated polymers.

4.2.1. *Polyaniline (PAN)* is a unique conjugated polymer because it can exist in a variety of structures depending on the value of y in the general formula of the polymer shown in Figure 9. When y is not equal to 0 or 1, these intermediate forms of polyaniline can be rendered conductive by protonating (proton doping) the imine nitrogens, formally creating radical cations on these sites.⁵⁵ This doping introduces a counterion (e.g., Cl^- if HCl was used as the dopant), and recently, the counterion was affixed to the parent polymer by partially sulfonating the benzene rings in the polymer, resulting in a so-called "self-doped" polymer.⁵⁶ Although aniline⁵⁷ and its derivatives^{58, 59} can be polymerized electrochemically, polymers are often synthesized by step-growth polymerization in an aqueous solution of the monomer, using an oxidant such as $(\text{NH}_4)_2\text{S}_2\text{O}_8$, and HCl .⁶⁰ This polymer is soluble in *N*-methylpyrrolidinone and

97% sulfuric acid^{61, 62} and has a high molecular weight ($\approx 325,000$)⁶³ but shows a bimodal molecular weight distribution by gel permeation chromatography.⁵⁵ The proposed para linkage of the aniline units has been somewhat justified by the favorable comparison of the infrared spectra of polyaniline synthesized as above and polyaniline synthesized via a well-defined precursor polymer.⁶⁴ There is interest in the use of polyaniline in rechargeable batteries,⁶⁵ and repeated doping/undoping of the polymer has been undertaken to change the film morphology, resulting in high selectivities in the separation of gases (O_2/N_2 separation factor = 53).⁶⁶

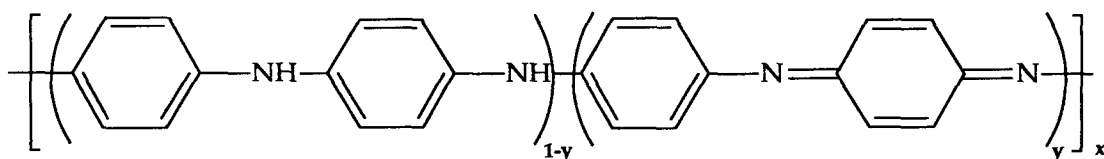


Figure 9. General formula of polyaniline.

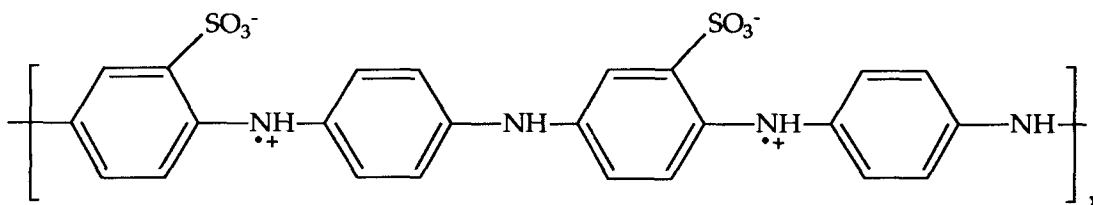


Figure 10. Representative formula of counterion-affixed polyaniline.

4.2.2. *Poly(phenylene sulfide)* is a polymer structurally related to the amine form of polyaniline and is typically made by condensation of dichlorobenzene with sodium sulfide in *N*-methylpyrrolidinone. The polymer precipitates as a white powder that is soluble in high boiling solvents. Although the degree of polymerization is moderate ($M_n = 11,000$), the polymer can be p-doped with SO_3 to a conductivity of 80 S/cm ⁶⁷ and has the advantage of being environmentally stable and easily processable.⁶⁸ It is currently sold by the Phillips Petroleum

Company under the trade name of "Ryton."^{69, 70} The related polymer, poly(phenylene oxide) dopes to a much lower conductivity ($\sigma \approx 10^{-3}$ S/cm) and has been studied much less.⁷¹ Phenylated poly(phenylene sulfide) has been photolyzed to produce a "photo-doped" polymer of modest conductivity ($\sigma \approx 10^{-2}$ S/cm).⁷²

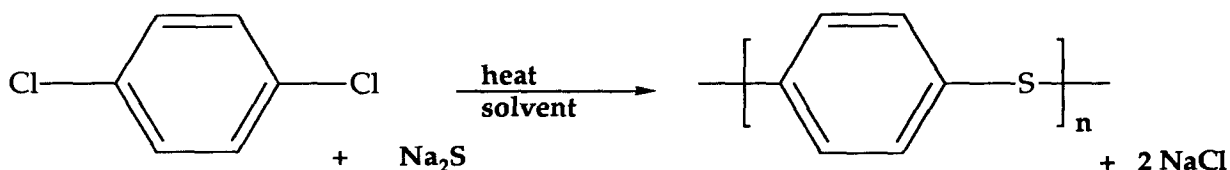


Figure 11. Synthesis of "Ryton" (poly(phenylene sulfide)).

4.2.3. *Polythiophene and its derivatives.* A large amount of work has centered around polythiophene, particularly since many soluble derivatives of the polymer are known (see below). Most workers synthesize polythiophene electrochemically, despite the uncertainty in the structure of electrochemically synthesized polymers (Section 4.1) and concern that the electrochemical synthesis of polythiophene results in overoxidation of the polymer.⁷³ The chemical synthesis of polythiophene is most commonly performed using a nickel-catalyzed coupling of the di-Grignard of thiophene (Figure 12),^{74, 75} although organocuprate couplings,⁷⁶ a polymerization based on Friedel-Crafts alkylation,⁷⁷ coupling of the di-halide using a Ni(0) catalyst,⁷⁸ and direct oxidation with FeCl_3 are employed as well.⁷⁹ The first two (di-halo) coupling schemes are preferred because they ensure that the linkages are of the 2,5 type: Direct chemical coupling does not necessarily guarantee this linkage. All of these syntheses suffer to some extent because it is not easy to remove all of the metal (Ni, Mg, Cu) employed, especially in the synthesis of the parent, insoluble

polymer.

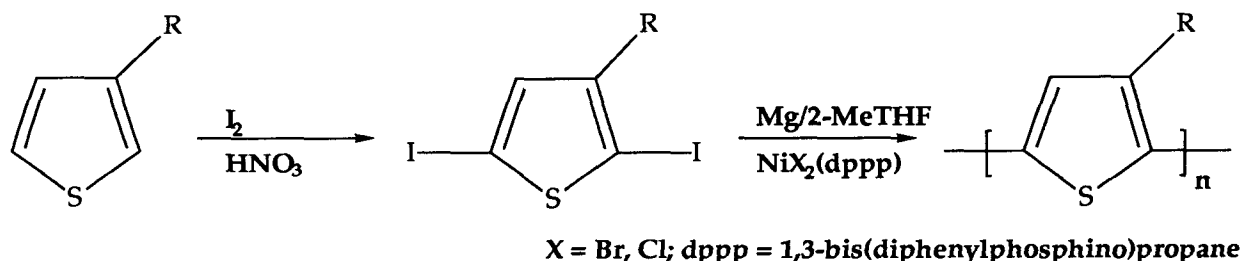


Figure 12. Nickel-catalyzed polymerization of thiophene.

In the area of molecular technology, a switch based on two orthogonally fused polymer chains, one doped (conductive) and the other undoped (insulating) has been proposed,^{80, 81} and an oligomer has been synthesized.⁸² Many tasks remain here, such as incorporating this unit into a device of molecular dimensions and discovering a way to switch the unit selectively.

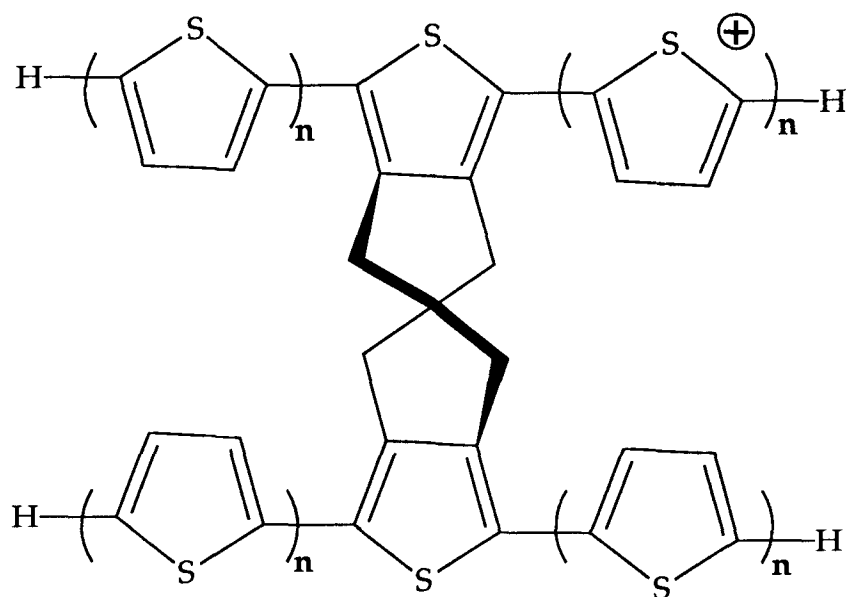


Figure 13. Model for two orthogonally fused conductive polymer chains. An oligomeric form of this model has been synthesized. Oxidation of only one of the two chains has not yet been realized.

As mentioned above, synthesis of an insoluble polymer by this route is not expected to produce a very high degree of polymerization. However, polymerization of a thiophene monomer with a floppy *n*-alkyl tail $[(-\text{CH}_2)_n\text{CH}_3]$ at the 3 position produced a soluble polymer.⁸³⁻⁸⁷ These polymers, particularly with *n*-alkyl tails of 6 or 8 carbons (poly(*n*-hexyl- or *n*-octyl thiophene)) have been well studied and have molecular weights of $M_w = 48,000$ and $M_w/M_n \approx 2$ for poly(*n*-hexyl thiophene) synthesized electrochemically,⁸⁸ and $M_w/M_n = 15,000-30,000/10,000 = 2-3$ for nickel-coupled poly(*n*-octyl thiophene) and $M_w/M_n = 150,000/30,000 = 5$ for FeCl₃ coupled 3-octyl thiophene.⁸⁹ In this study, a high molecular weight shoulder in the FeCl₃ coupled polymer convinced the authors that chain-branching had taken place, and although this observation cast doubt on the exact nature of the material, it did improve its mechanical properties. This strategy has been extended to the synthesis of soluble poly(3-octyl pyrrole), although little subsequent work has been performed on this polymer.⁹⁰

The side groups that solubilize the polymer tend to render the matrix amorphous, and this limitation appears to preclude them from being highly conductive materials ($\sigma > \text{approx. } 10^2 \text{ S/cm}$) even when the polymer is subjected to stretch alignment (Section 7).⁹¹ However, there have been a number of applications such as photocells and antistatic coatings that do not require polymers with extremely high conductivities. Moreover, the presence of the side groups does not appear to reduce the third-order nonlinear susceptibility (χ^3) of the polymer.⁹²⁻⁹⁵ This solubility has also allowed for study of the polymer conformation in solution, using such techniques as light scattering and small-angle neutron scattering, providing an opportunity to link the thermochromism

and solvatochromism of these polymers (Section 2) with changes in the polymer backbone conformation.^{96, 97} These polymers have also been doped in solution and the spectroscopic properties of the doped species studied.⁹⁸ Variation of the group attached at the 3-position of the thiophene monomer has resulted in the synthesis of a variety of derivatives (Figure 14). These include poly(3-alkoxy thiophenes)⁹⁹⁻¹⁰³ which, for reasons that are poorly understood, have slightly reduced bandgaps compared to the poly(3-alkyl thiophenes),¹⁰⁴ ethylmercapto-substituted polythiophenes,^{105, 106} chiral polythiophenes, which can stereoselectively recognize doping agents,¹⁰⁷ a water-soluble derivative, which also contains an attached counterion useful in doping,^{108, 109} polythiophene containing a pendant viologen redox group, which has been used in a microelectrochemical transistor,¹¹⁰ as well as poly(3-(ω -haloalkyl) thiophenes), which can act as a very convenient starting point for further synthetic effort.¹¹¹ Longer side groups ($n = 12$) have also reduced the melting point of the polymer and have allowed for melt-processing.^{89, 112, 113} Several of these soluble derivatives have been used in polymer blends¹¹⁴ with polystyrene^{115, 116} and polyethylene/vinyl acetate.¹¹⁷ Most of these derivatives have been polymerized electrochemically. Their chemical polymerization often produces lower molecular weight materials.

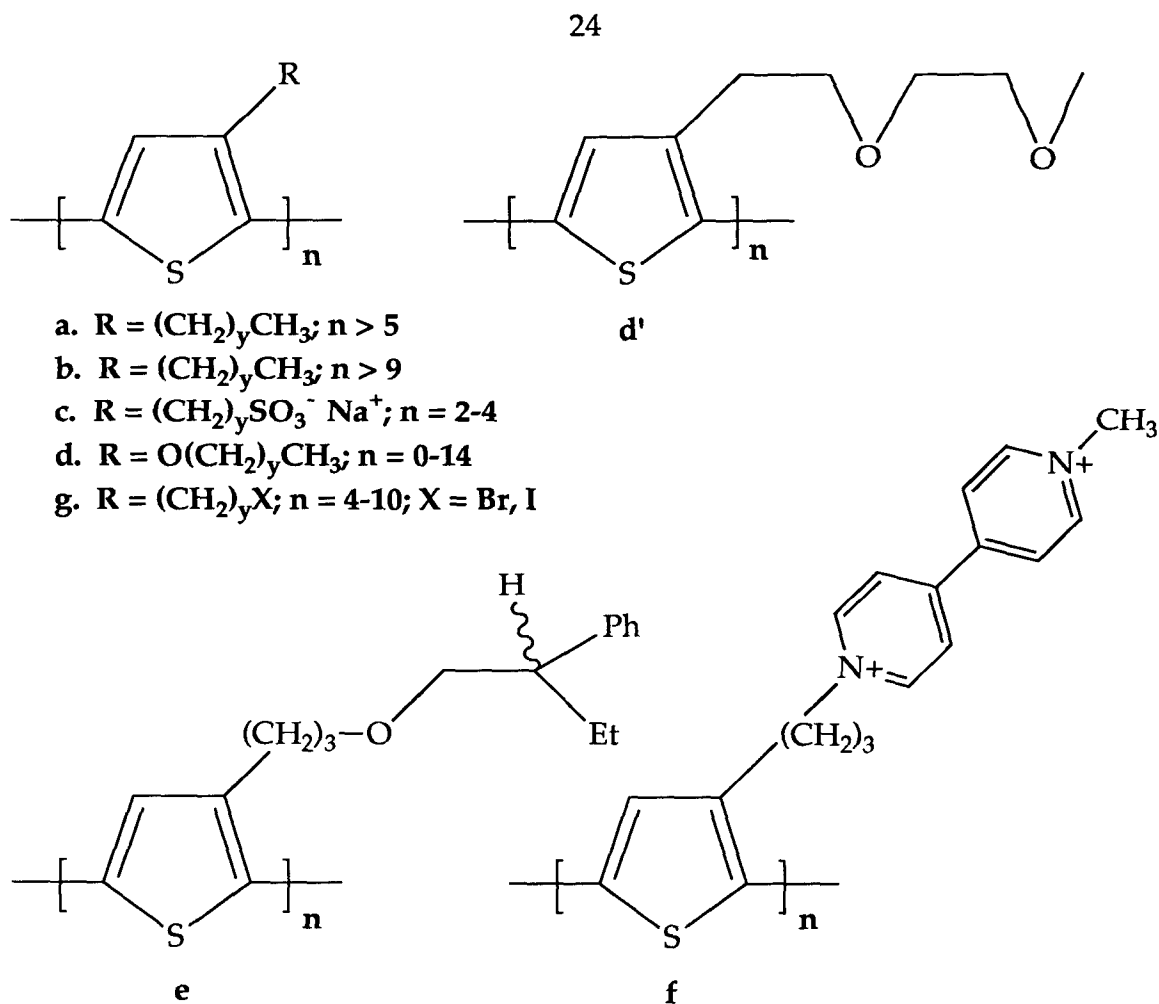


Figure 14. Structural variation of poly(alkyl thiophenes) allows for (a) organic-soluble (b) melt-processible (c) water-soluble (d) reduced bandgap (e) chiral (f) pendant redox-active and (g) synthetically useful derivatives.

4.2.4. Other 5-membered Heterocyclic Derivatives. Several other classes of 5-membered heterocyclic derivatives exist. Most are polymerized via a step-growth mechanism. A dibenzo-fused derivative of polythiophene (Figure 15), which is also partially formed upon doping of poly(phenylene sulfide), can be synthesized by reaction of dibromodibenzothiophene and sodium sulfide. Carbazoles have been polymerized by *in situ* coupling of their Grignards as well as by coupling of diiodocarbazole in molten iodine.^{68, 118, 119} Thin films of carbazole polymers have been prepared by electrochemical oxidation of vacuum-

deposited carbazole.¹²⁰ The most common use of carbazoles, however, is as pendant groups on other polymers. These polymers photoconduct by forming an excited state that can then hop to another, unexcited carbazole moiety in the polymer. This form of energy transfer is not unrelated to electron hopping in conductive, conjugated polymers, and the behavior of these polymers concerns workers in this area, especially when evaluating carrier transport.¹²¹⁻¹²⁴

Recently, the resonant third-order nonlinear optical susceptibility (χ^3) of a composite containing poly(*N*-vinyl carbazole) and an electron acceptor (2,4,7-trinitrofluorenone) has been measured.¹²⁵ Use of this charge-transfer composite is not a recent development, however. In the form of a coated film, it has been used as the photoconductor in reprographic machines marketed by IBM.¹²⁶

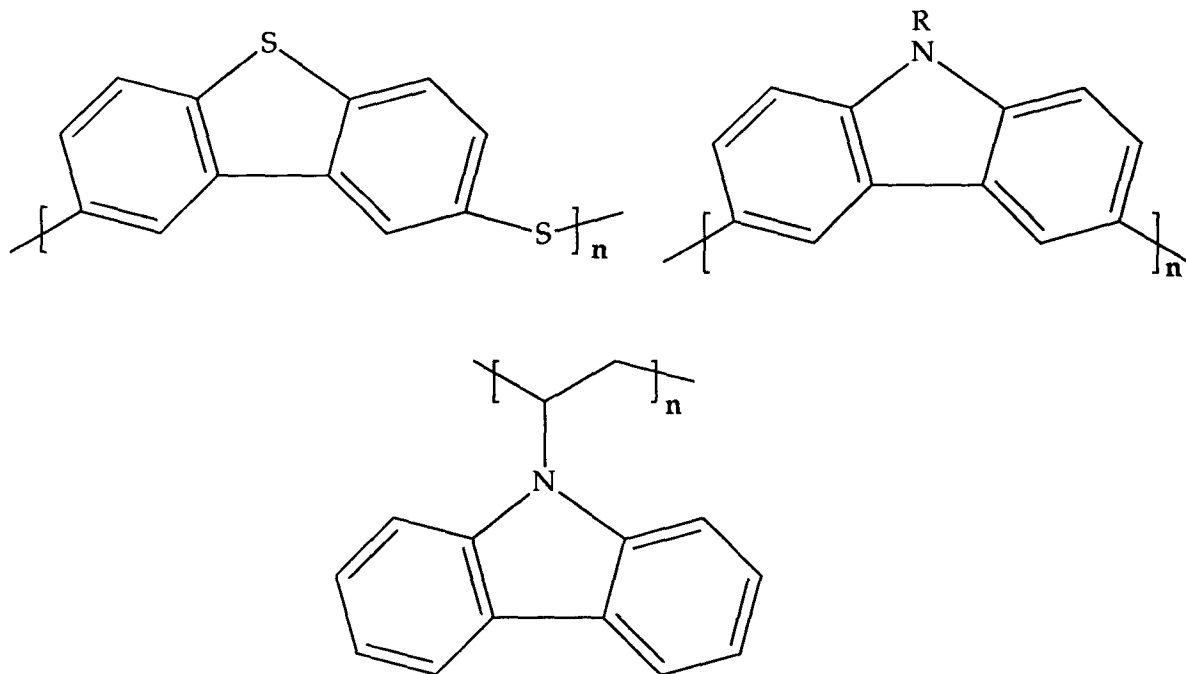


Figure 15. Poly(dibenzothiophene sulfide), polycarbazole, and poly(*N*-vinylcarbazole).

These examples involve pendant groups that interact with each other. There are, of course, several examples of polymers containing pendant chromophores, particularly as liquid crystalline mesogens, that have been investigated as nonlinear optical materials. In these materials, the electronic interaction between chromophores does not generally contribute to the materials' nonlinear optical susceptibility.¹²⁷⁻¹²⁹

There are considerable differences between *cis*-polyacetylene and polythiophene because of the absence/presence of a heteroatom. This heteroatom, in addition to fixing the geometry of some of the bonds in the polymer, influences the electronic structure of the polymer. The changes in properties corresponding to structural variation have been explained in a very intuitive way, using orbital-mixing arguments.^{130, 131} There continues to be a synthetic challenge in the further variation of the heteroatom. For example, substitution by phosphorous is of interest, yet only oligomers of the phosphorous analog of polythiophene have been synthesized.¹³²

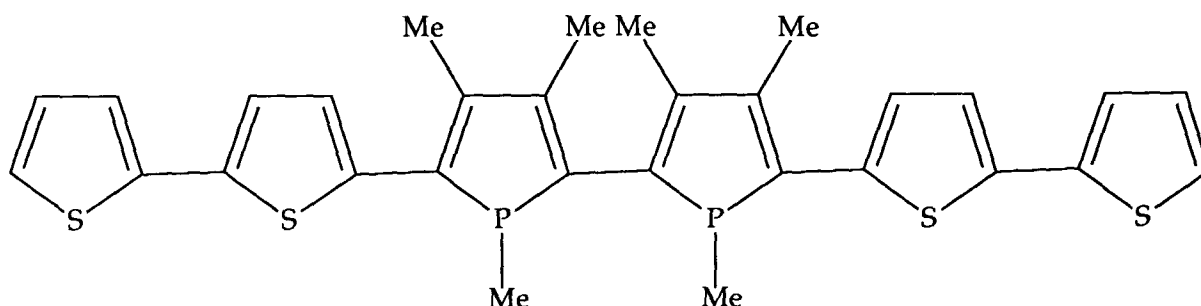


Figure 16. A first step toward the phosphorous analogues of polythiophenes.

4.2.5. *Polyparaphenylene (PPP)*. Despite the high oxidation potential of benzene, polyparaphenylene has been prepared electrochemically, using a variety of solvent systems, most of them highly acidic.²⁵ Although it is often impossible to

comment on the structure of the resulting material, electrochemical syntheses of PPP continue to be reported in such exotic solvents as $\text{SbF}_5\text{-SO}_2$,¹³³ butylpyridinium chloride/ AlCl_3 melt,¹³⁴ and trifluoromethane sulfonic acid.¹³⁵ It is believed that these cations are required to complex or protonate the benzene before it can be oxidized.¹³⁶ PPP can also be prepared in nitrobenzene using potentials as high as 30V. Also, this potential is well above the stability window for the solvent; the films are synthesized before much degradation of the solvent occurs.¹³⁷

Early chemical syntheses of PPP involved the oxidative coupling of benzene using an $\text{AlCl}_3/\text{CuCl}_2$ catalyst.¹³⁸ Like polythiophene, later chemical syntheses involve coupling of benzene para-dihalide or the di-Grignard, or di-lithio derivative formed from it, using a variety of metals or metal salts, mostly based on nickel or copper.¹³⁹ Not unexpectedly, different syntheses produce samples with very different morphologies.¹⁴⁰ This type of synthesis has been extended to the coupling of 2,5-di-*n*-hexylbenzene derivatives to make soluble polyparaphenylenes (Figure 17).¹⁴¹⁻¹⁴³ Although these new polymers are promising, they all still have relatively low degrees of polymerization ($n \leq 30$). Thus, the synthesis of high molecular weight polyparaphenylene via a precursor method has received much attention (Section 5.1).

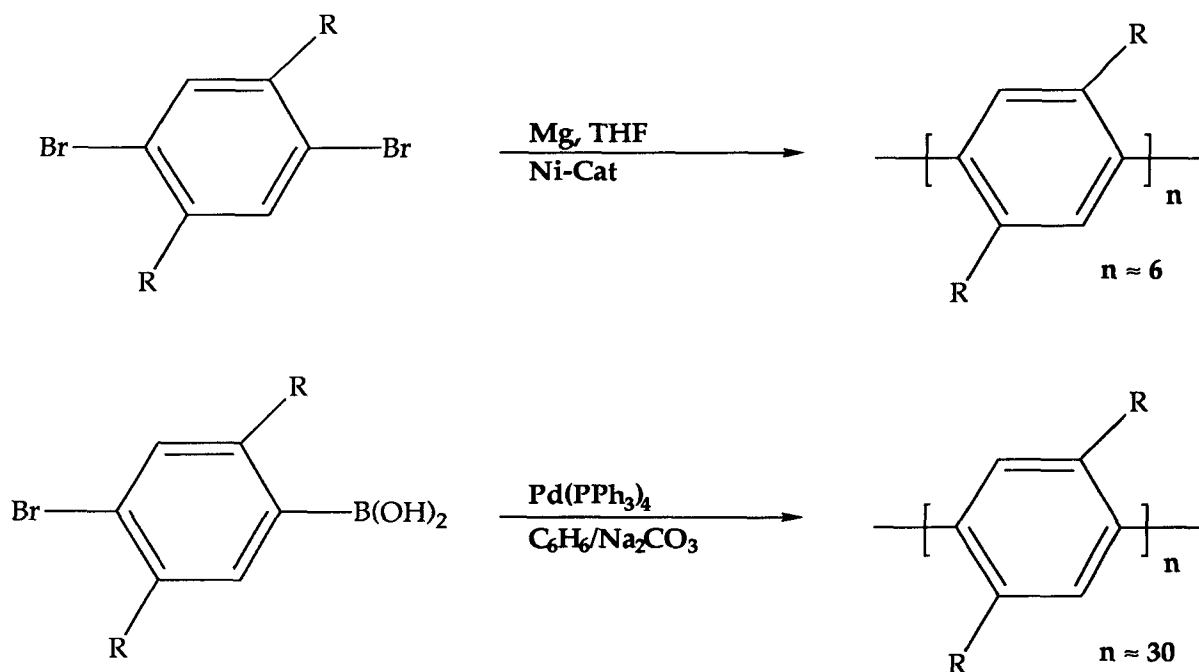


Figure 17. Syntheses of substituted PPP's.

Some heteroatom-substituted derivatives are known. Pyridines^{144, 145} and quinolines¹³⁹ have been polymerized. An example, synthesized by step-growth polymerization, is poly(*p*-phenylene-*co*-2,5-pyrazine) shown in Figure 18.^{146, 147}

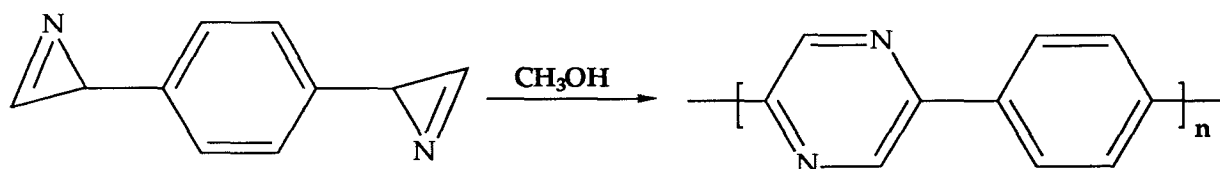


Figure 18. Poly(*p*-phenylene-*co*-2,5-pyrazine).

4.2.6. *Polysilanes*. Polysilanes, in which the conjugation is through the single bonds in the polymer backbone, have attracted much attention because of their interesting UV-spectroscopy and photophysics as well as their photochemistry, photoconduction, nonlinear optical properties and use in microlithography.¹⁴⁸ The backbone of the polymer is "conjugated" (using single or σ bonds in the

polymer) but is still relatively floppy, so these polymers are often soluble and processible. The most common synthesis of polysilanes is a rather brutal Wurtz-coupling of R_2SiCl_2 units with sodium: a step-growth polymerization, although it is complicated by the fact that it takes place in a heterogeneous environment (the sodium surface). This reaction does not tolerate functionality on the polysilane, but several routes for functionalizing the polymer after synthesis have been devised. This synthesis generally produces high molecular weight polymers, although the dispersity of molecular weights is sometimes polymodal, probably reflecting the heterogeneous nature of the reaction.

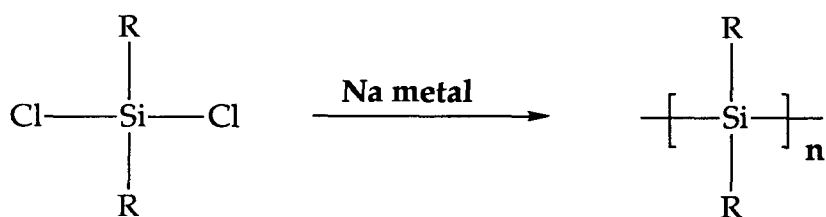
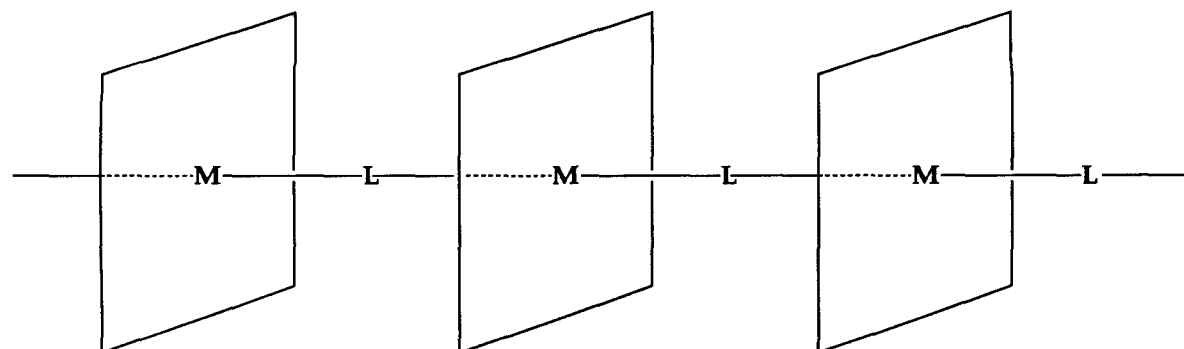


Figure 19. Polysilane polymerization via a Wurtz-coupling mechanism.

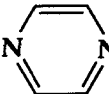
Polysilanes have also been synthesized by dehydrogenative polymerization of silanes (i.e., $SiH_2R_2 \rightarrow -[Si(R)_2]-$), using zirconocene and hafnocene catalysts. So far, these methods have resulted only in oligomers but are still an interesting application of the organometallic " σ bond metathesis" reaction to the synthesis of these main-group polymers.¹⁴⁹⁻¹⁵¹ Further development of this methodology is expected. Anionic ring-opening polymerization, although it does not proceed for several cyclic silanes,¹⁵² has resulted in high polymer for 1,2,3,4-tetramethyl-1,2,3,4-tetraphenylcyclotetrasilane ($M_n \approx 30,000$; $M_w/M_n \approx 2$).¹⁵³ This reaction follows chain-growth kinetics and has the potential of being modified to become a living polymerization (Section 3.2). Silane copolymers with π conjugated units

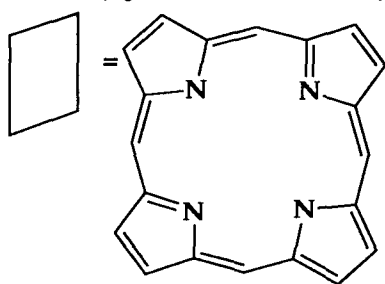
(phenyl¹⁵⁴ and thiophene¹⁵⁵) have also been prepared, allowing for the study of mixed π/σ conjugated systems.

4.2.7. Polymers of Phthalocyanines. A number of investigations of polymers linked through metals have been undertaken. Polymers of phthalocyanines (Figure 20) have been synthesized, using a variety of metals and nonmetals in the center of the macrocyclic ring and a variety of linkages between these rings.^{156, 157} In some cases, the linkage is conjugated with the metal, and there is a delocalized path in the center of the polymer.¹⁵⁸ In many cases, however, the $[-M-X-]$ linkage in the center of the polymer is nonconjugated, and delocalization arises from the overlap of the closely spaced macrocyclic rings.¹⁵⁹⁻¹⁶¹ Partial oxidation of the polymer (doping) increases the conductivity of the material. However, conductivities are generally modest (≤ 1 S/cm). The monomeric macrocycle is typically very insoluble but nevertheless is used commercially for pigments and semiconductor applications. The polymers are also generally insoluble, but molecular weight determinations of some oxygen-linked phthalocyanines (M = Si, Ge, Sn) by end-group analysis and radiotracer techniques find degrees of polymerization of 70-120.¹⁶² These materials are similar to charge-transfer complexes in that they both contain mixed valence stacks of conjugated planar molecules.^{163, 164} However, these polymers are covalently linked. In contrast, charge-transfer complexes can easily dissociate upon dissolution or evaporation, thus losing extended delocalization. Phthalocyanines are only one of a number of macrocycles that can be stacked or polymerized in this manner. Many structurally similar systems can be found in the literature.¹⁶⁵

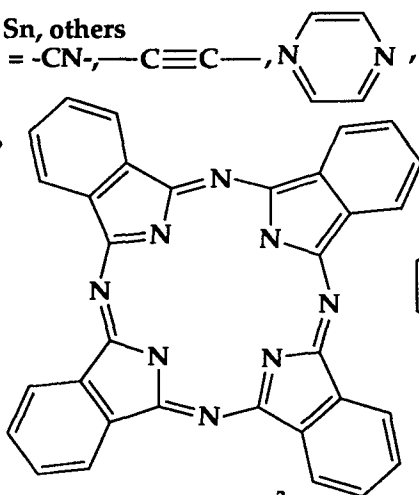


M=Fe, Co, Ru, Mn, Cr, Si, Ge, Sn, others

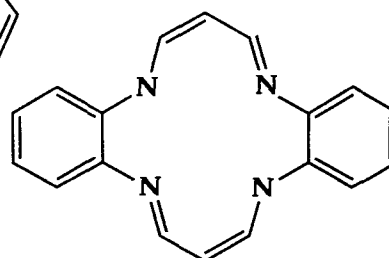
$L_{\text{non-conjugated}}$ = O, S, etc.; L_{conj} = -CN-, $\text{---C}\equiv\text{C---}$, , etc.



Porphyrin²⁻



Phthalocyanine²⁻



dibenzotetraaza-
[14]annulene²⁻

Figure 20. Metal phthalocyanine polymers can be linked via both conjugated and nonconjugated linkages. Only a few of the metals, linkages, and macrocycles are shown here.

4.2.8. Other Conjugated Metal Coordination Polymers. Metals are also incorporated into polymers via conjugated, coordinative linkages such as di-thiolenes. These complexes, originally investigated as monomeric units that stacked to form one-dimensional systems along the stacking direction,¹⁶⁶ have been investigated in polymeric systems, using a variety of counterion ligands.¹⁶⁷⁻¹⁷⁰ Typically, these are synthesized by reacting the conjugated bridge (typically a dianion or tetraanion) with a metal salt (e.g. NiX_2 , X = Cl, Br, etc.). Most of these systems are insoluble and oligomeric in nature and have poor conductivities, even upon doping (values up to 20 S/cm reported). However, these polymers have recently

been synthesized with more flexible linkages, allowing for the study of the effect of this linkage on solubility and electronic properties.^{171, 172} None of the properties of these polymers have rivaled the all-organic, conjugated polymers. They do, however, stand as examples of the role that a transition metal can play as part of a delocalized, conjugated system.

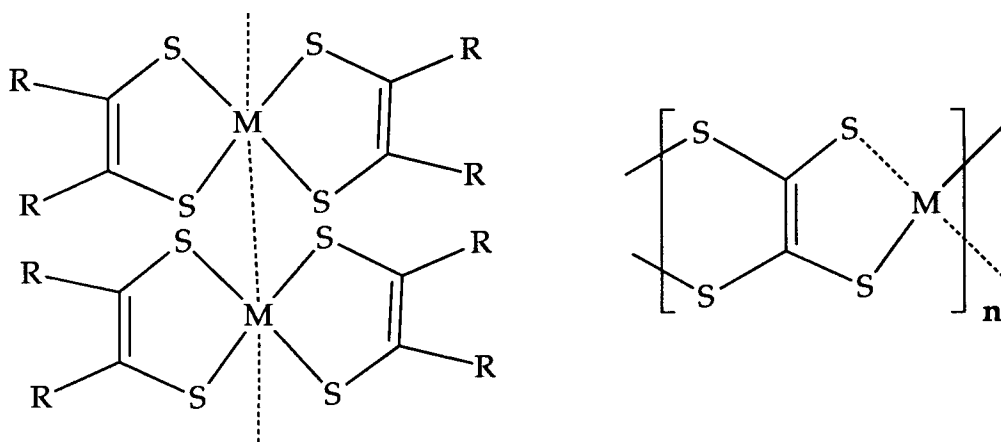


Figure 21. Stacked dithiolene complexes and linear dithiolene polymer (M = Ni). This example illustrates only one of the many conjugated counterions that have been employed.

4.2.9. *Ladder Polymers.* Another important structure in the realm of conjugated polymers is that of the ladder polymer, where monomer units are joined by more than one bond (Figure 22). The parent of this series, polyacene, would be expected to be non-bond-alternate (Section 6) and an intrinsic conductor much like graphite. Although there have been claimed syntheses of this polymer, from the photopolymerization of diacetylenes,¹⁷³ from oxidation of cyclized 1,2-polybutadiene,¹⁷⁴ and from pyrolysis of a phenol-formaldehyde polymer,¹⁷⁵ this system becomes insoluble and very air-sensitive as the number of fused benzene rings increases,¹³¹ and adequate structural characterization is not yet available. Elemental analyses, where given, also suggest that these structures are not

completely fused together as drawn. Since these polymers are linked as ribbons rather than chains, they all tend to suffer from insolubility at low degrees of polymerization.

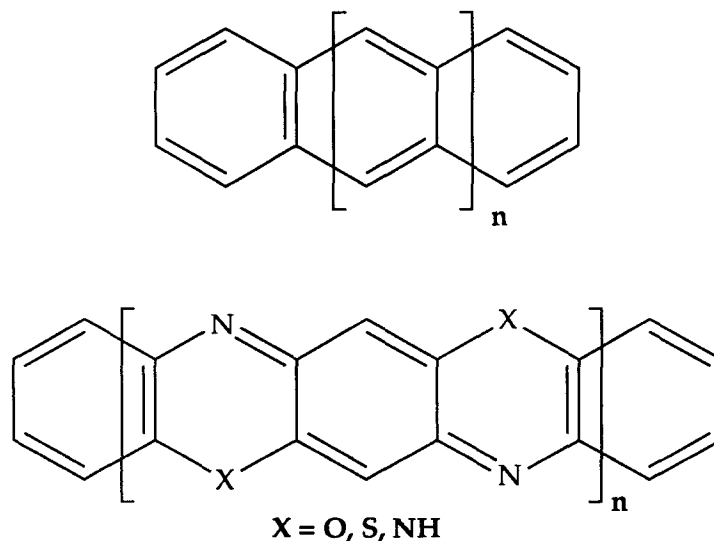


Figure 22. Polyacene and a representative ladder polymer.

Nevertheless, the promise of a thermally stable material prompts continued synthetic endeavor, including pyrolysis of polyacrylonitrile and polycyanoacetylene¹⁷⁶⁻¹⁷⁸ (Figure 23), explorations of electrochemical doping reactions on ladder polymers,¹⁷⁹ and work on the synthesis of ladder polymers with alkyl substituents to enhance solubility.¹⁸⁰ Some of these polymers have been investigated for their nonlinear optical properties.^{181, 182}

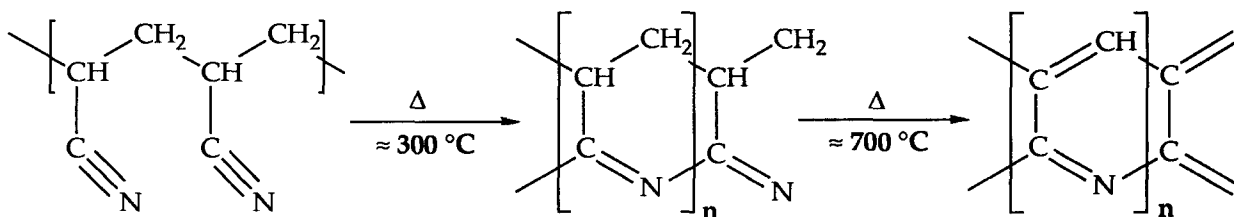


Figure 23. Possible events in the pyrolysis of polyacrylonitrile.¹⁸³

Model compounds of ladder polymers are generally much better characterized and have some unique properties of their own. Oligomers of polyacenequinones have been reported as "molecular lines," since they are so rigid and can be synthesized with well-defined lengths.^{184, 185} Related oligomers have been shown to form oriented Langmuir-Blodgett films,¹⁸⁶ and synthesis of thiol-terminated molecular lines allows them to self-assemble on a gold surface and become electrochemically doped.¹⁸⁷

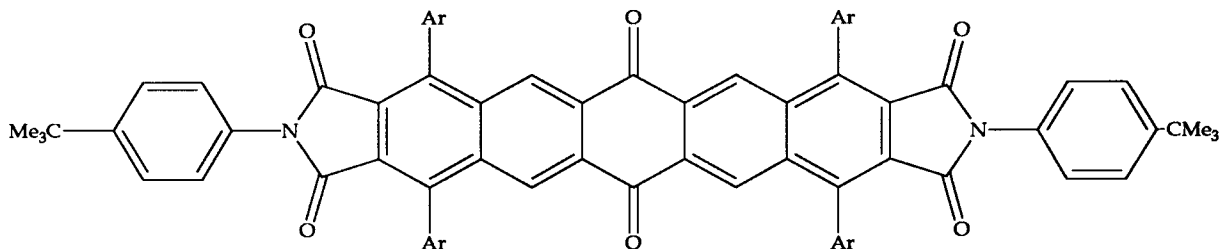


Figure 24. A "molecular line" 3.06 nanometers long.

Loss of some of the ladder-type linkages is found in polymers such as poly(*p*-phenylene-2,6-benzobisthiazole) (PBT, Figure 25). These polymers have been electrochemically doped to a conductivity of 20 ± 10 S/cm,¹⁸⁸ and they are also of interest for their nonlinear optical properties.¹⁸⁹⁻¹⁹² Complexation of these polymers with Lewis acids (e.g., AlCl_3) renders them soluble.¹⁹³

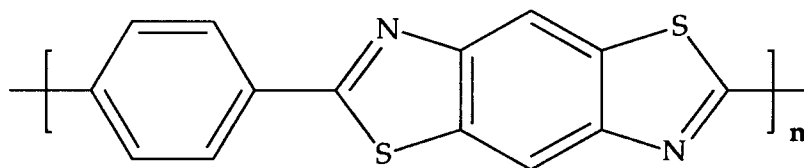


Figure 25. Poly(*p*-phenylene-2,6-benzobisthiazole) (PBT).

This section touches upon the more extensively studied conjugated

polymers formed by step-growth polymerization. There exists substantially more structural variation than is outlined here. The reader is referred to an excellent reference for more examples, including general strategies for synthesis of conjugated polymers.¹⁸³

4.3. The Unusual Topochemical Polymerization to form Polydiacetylenes¹⁹⁴

Single crystals of diacetylenes can be polymerized with light¹⁹⁵ or gamma irradiation¹⁹⁶ to produce crystals of polydiacetylene (Figure 26). Naturally, this reaction requires the reacting units to be oriented in a precise way since molecular motion is limited in the crystalline state. Thus, only certain diacetylene monomers can be polymerized in this manner.¹⁹⁷ However, it has been found that several types of diacetylenes can be polymerized when ordered in multilayers using Langmuir-Blodgett techniques,^{198, 199} and additional work has shown that these polymerizations can take place directly in the Langmuir-Blodgett trough and can be monitored by visible absorption spectroscopy.^{200, 201} They have also been polymerized in lipid vesicles, and the structure of the bilayer is retained after the polymerization.²⁰²⁻²⁰⁶

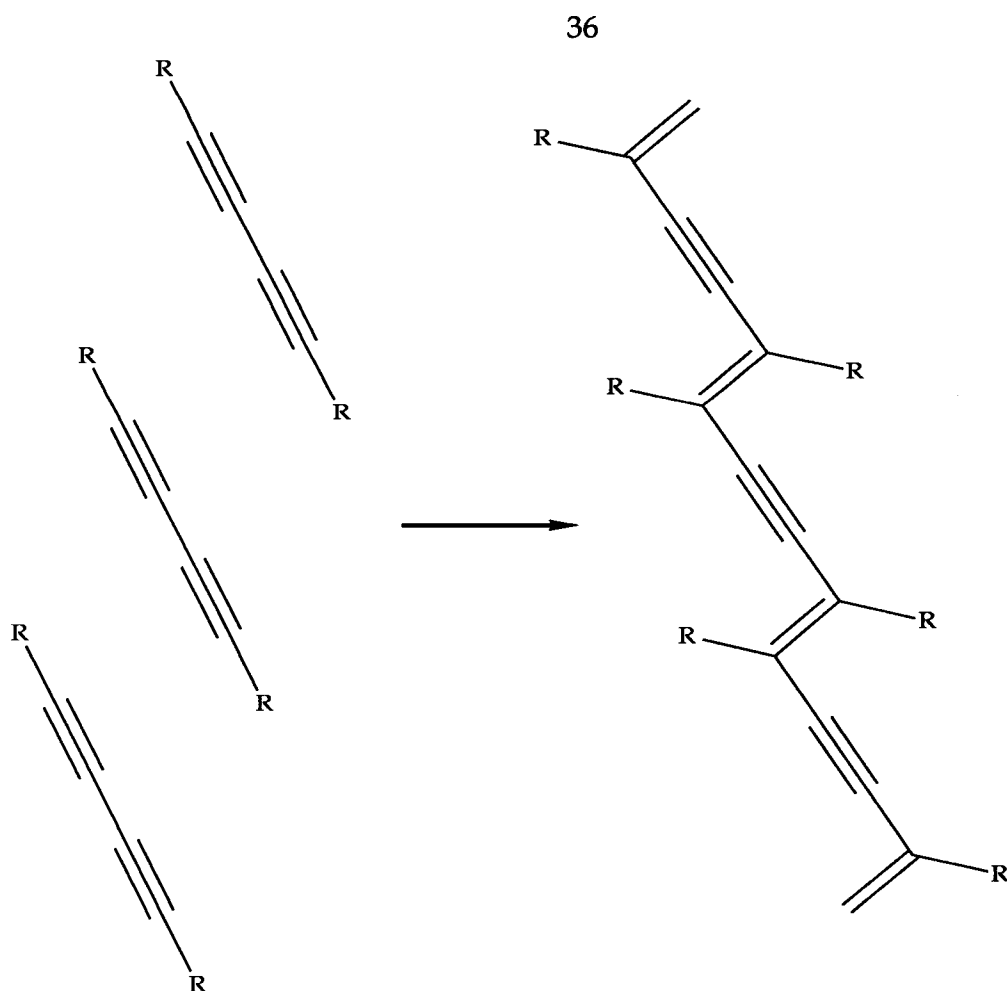


Figure 26. Generalized scheme for the topochemical polymerization of diacetylenes.

Although most of these polymers are insoluble, several soluble polydiacetylenes have been synthesized. The most studied are those containing butoxycarbonylmethyleneurethane (BCMU) groups.^{207, 208} Although not especially good electrical conductors, these polymers are sensitive to changes in environment such as solvent and temperature,²⁰⁹⁻²¹² and mechanical stress ("Mechanochromic Behavior"),²¹³ undergoing conformational changes^{214, 215} and/or aggregation, which lead to striking changes in color. Some of these polymers have large third-order nonlinear optical susceptibilities (χ^3),²¹⁶ leading to interest in their use in devices such as active wave guides.^{217, 218}

4.4. Chain-growth Polymerizations

Chain-growth polymerizations are useful in the synthesis of conjugated polymers because polymer properties can often be tailored by the selection of the catalyst system and because higher molecular weight polymers can be synthesized at a lower degree of conversion of monomer, a point which is particularly attractive when it is necessary to form an insoluble polymer. It has already been pointed out that several conjugated "polymers" are suspected to be oligomers, particularly oxidatively coupled polyparaphenylene, and it is frustrating when the validity of a study must be questioned because it is unclear whether the material under study is really polymeric in nature. Although many would argue that molecular weight has little to do with polymer properties, this premise has little or no experimental verification. Moreover, some of these conjugated polymers are attracting interest as high-strength materials,²¹⁹ and polymer strength is certainly dependent upon molecular weight.

4.4.1. Polyacetylene via Ziegler-Natta polymerization. Acetylene was first polymerized by Natta et al. by bubbling the gas through an organotitanium/trialkylaluminum catalyst mixture, resulting in a black, powdery precipitate.²²⁰ It was not, however, until Shirakawa and co-workers discovered how to produce free-standing films²²¹ and optimized this procedure²²² that it was possible to handle this material easily. These continuous, highly crystalline films made possible the first observations of high conductivity upon exposure to strong oxidants^{1, 2, 3} and later reductants. This development sparked a large amount of subsequent research on polyacetylene and other conjugated polymers. Shirakawa's method continues to be the most

common way to synthesize polyacetylene, and the material produced from this synthesis is often referred to as S-PA (Shirakawa polyacetylene).²²³ A detailed procedure for this synthesis is available,¹⁰ but briefly, the polymer is synthesized by coating the walls of a Schlenk (inert atmosphere) tube with a slurry of $\text{AlEt}_3/\text{Ti}(\text{O}-n\text{-Bu})_4$ (4:1) in toluene followed by admission of acetylene gas, which polymerizes on the surface of the catalyst to produce a shiny silver film that can be pried from the walls of the reaction vessel and washed to remove most of the catalyst residues. Low-temperature (-78°C) synthesis insures the formation of a film with a high content of cis double bonds in the chain. Heating the film to 150°C for an hour or so isomerizes the double bonds to the predominantly trans configuration. This isomerization process has been studied in the solid state and is complicated and dependent on the morphology of the film.^{224, 225} Also, cis-trans isomerization is believed to occur during doping.²²⁶ The single bonds in the polymer can also adopt a cis or trans configuration (termed cisoid and transoid). The barrier for conversion from cisoid to transoid is much lower than for cis/trans isomerization in which the pi (second) bond must be formally broken and reformed. All four combinations of cis/trans single/double bonds in planar²²⁷ as well as nonplanar structures²²⁸ have been considered and a variety of conformations including helical structures^{227, 229, 230} have been proposed. Also, neither *cis*- nor *trans*-polyacetylene contains double bonds of exclusively one type. It has been acknowledged that even after isomerization, residual cis units exist in *trans*-polyacetylene.^{231, 232}

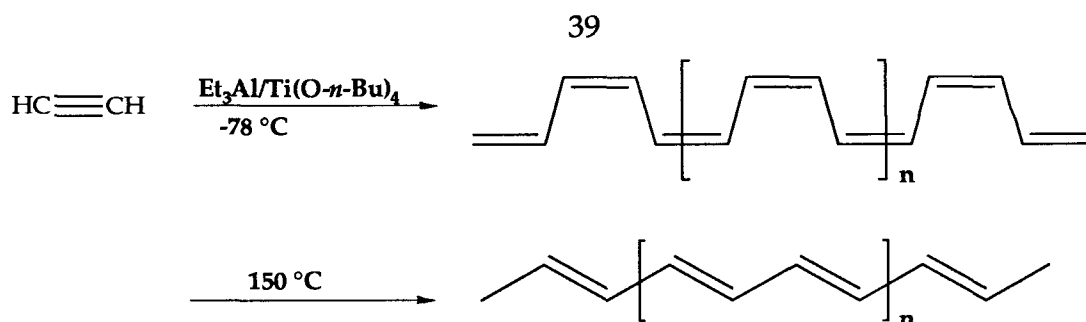


Figure 27. Polymerization of acetylene showing cis and trans isomers.

A number of block and graft copolymers of polyacetylene have been synthesized, generally with the idea of using the second half of the block as a solubilizing tail.²³³ In most cases, this modification rendered the polymer soluble and has allowed a variety of studies of the linear^{234, 235} and nonlinear^{236, 237} optical properties as well as photoinduced absorption studies²³⁸ of polyacetylene segments in solution. There is evidence, however, that the polyacetylene segments in these polymers aggregate in solution,²³⁹ and these studies have not been made in the absence of interchain effects. Some of these block copolymers were observed to phase separate to produce "microdots" of polyacetylene in an insulating matrix and were potentially small enough to observe quantum dot effects.²⁴⁰⁻²⁴²

A very exciting modification of this synthesis has been described by Naarman and others. It involves both the use of an additional reducing agent in the catalyst mixture and mechanical alignment of the polymer by stretching by a factor of 6, which is facilitated by synthesizing the polymer in a mixture of the catalyst and silicone oil.²⁴³⁻²⁴⁵ This new polyacetylene (N-PA) is very well ordered and is believed to have a significantly lower number of nonconjugated (sp^3) defects. The result is extremely high iodine-doped conductivities greater than 100,000 S/cm with values routinely obtained of 10,000-50,000 S/cm. Many have taken this work as evidence that well-ordered organic polymer matrices can

be made as conductive as metals.

Numerous acetylene derivatives have been polymerized with transition metal catalysts, often producing high molecular weight, soluble polyacetylene derivatives.²⁴⁶⁻²⁴⁸ However, the high-energy visible absorptions and low iodine-doped conductivities²⁴⁹⁻²⁵¹ of these polymers indicate that they are much less conjugated than the parent polyacetylene, most likely because of the twisting of the polymer chain that is due to steric repulsions between the closely spaced side groups (Figure 28).²⁵² Polyacetylene derivatives with side groups spaced farther apart have been synthesized and do not have such significantly reduced conjugation (see below).

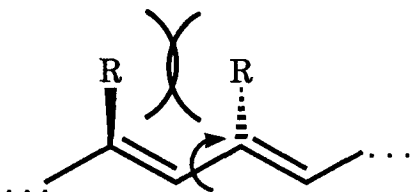


Figure 28. Reduction of conjugation in polyacetylene derivatives that is due to steric effects.

4.4.2. *Ring-Opening Metathesis Polymerization routes to Polyacetylenes.* Ring-opening metathesis polymerization (ROMP) involves the use of a transition-metal carbene complex to cut open a cyclic olefin molecule and "stitch" these molecules back together into a polymer chain (Figure 29).²⁵³ This polymerization is of great interest for the synthesis of conjugated polymers because among other factors, the number of double bonds in the monomer is preserved in the polymer, and because in principle one can take the repeat unit for any conjugated polymer containing an olefin and cyclize it to form a potential new monomer.

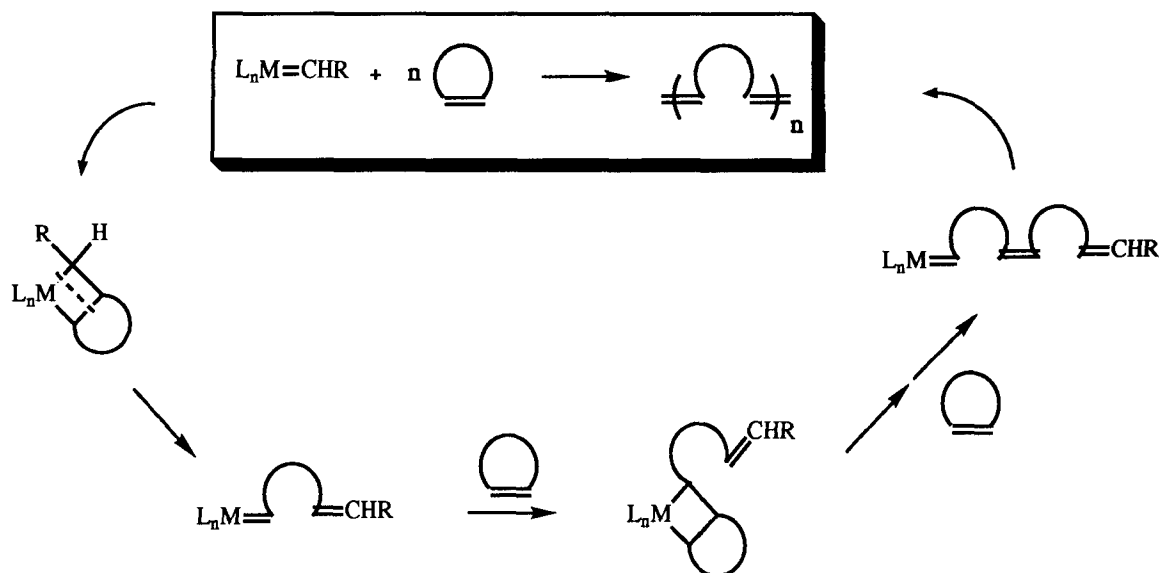


Figure 29. Scheme for ring-opening metathesis polymerization.

This polymerization has been very successfully used to form several precursor polymers, which will be discussed later. However, ROMP has been applied to the direct synthesis of conjugated polymers as well, namely, polyacetylene. In this case, the appropriate monomer is a circle of 4 double bonds: cyclooctatetraene (COT). This monomer, prepared by the tetramerization of acetylene with a nickel catalyst, has been polymerized, first using so-called "classical" but also Lewis-acidic catalysts, which created a number of saturated defects in the polyacetylene,^{254, 255} and more recently using a preformed, non-Lewis-acidic tungsten carbene complex to produce polyacetylene of good quality.²⁵⁶ This method has been extended to the polymerization of mono-substituted COT's which, given the appropriate bulk in the side group, produces soluble, yet highly conjugated, polyacetylene derivatives.²⁵⁷⁻²⁶⁰ The nonlinear optical properties of some of these polymers have been measured,²⁶¹ and these polymers have been exploited in the fabrication of layered structures and efficient solar cells.²⁶² This procedure avoids the harsh, metal-vapor conditions

typically employed when a thin layer of a metal is desired on a surface.

5. Polymers from precursors

Precursor methods can be very advantageous in the synthesis of insoluble, conjugated macromolecules. Most of the insoluble polymers lack adequate characterization data and have low molecular weights. Precursor methods afford a soluble prepolymer that is often of high molecular weight and can be fully characterized. Typically, the best precursors can be converted to the final form under mild conditions that do not disturb the structure of the polymer and with as low a mass loss as possible, although some of the precursors discussed in this section do suffer from the fact that much of the weight of the prepolymer is lost upon conversion.

5.1. Polyparaphenylene (PPP)

Several step-growth routes to PPP have already been described. Despite some clever synthetic ideas, the end product is still a rigid, insoluble polymer, and all the step-growth methods discussed result in a low degree of polymerization. Thus, precursor routes to PPP have taken on much importance.

Early attempts centered around the polymerization and aromatization of cyclohexadiene (Figure 30). This monomer can be polymerized to some degree by Ziegler-type, radical, cationic and anionic initiators.²⁶³⁻²⁶⁶ In several cases, molecular weights were suspected to be low. However, the biggest problem with this scheme is that dehydrogenation of the polymer (precursor conversion)

requires high temperatures and/or strong oxidants and often does not proceed to completion. As an added complication, these polymerizations result in both 1,4- and 1,2-linkages, deviating somewhat from the straight para (1,4) linkages normally drawn. Nevertheless, this precursor route has been employed on several occasions, recently in the synthesis of a soluble polystyrene-PPP block copolymer which was chemically converted from its precursor in solution and could be subsequently doped in solution.²⁶⁷

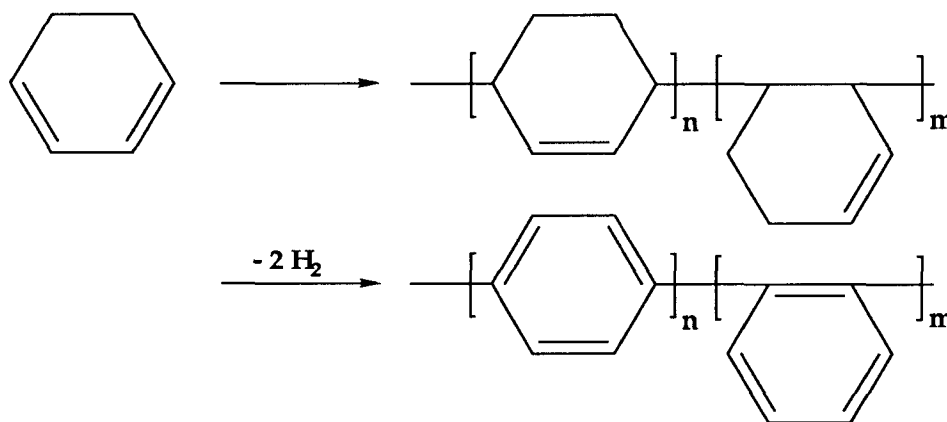


Figure 30. Polymerization and aromatization of cyclohexadiene showing the linkages formed by 1,4- and 1,2-propagation.

More recently, it has been discovered that a *cis*-dihydrocatechol derivative of cyclohexadiene, conveniently produced from the microbial oxidation of benzene, can be converted to a variety of derivatives and polymerized using radical initiators. These polymers can be converted to PPP thermally at much lower temperatures, eliminating alcohol or acetic acid ($T_{\text{conv}} \approx 250\text{-}300\text{ }^{\circ}\text{C}$ for $\text{R} = \text{Me}$, Figure 31).^{268, 269} The concern over 1,2-linkages in the polymer persists with these precursors. However, they have provided a low-temperature route to high molecular weight PPP.

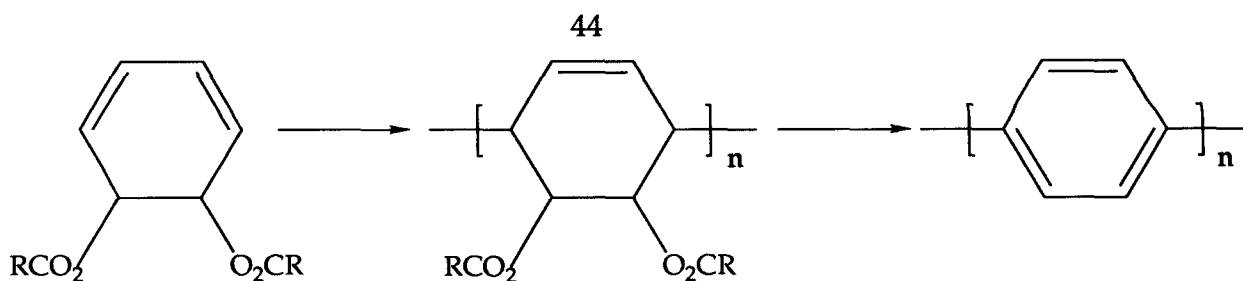
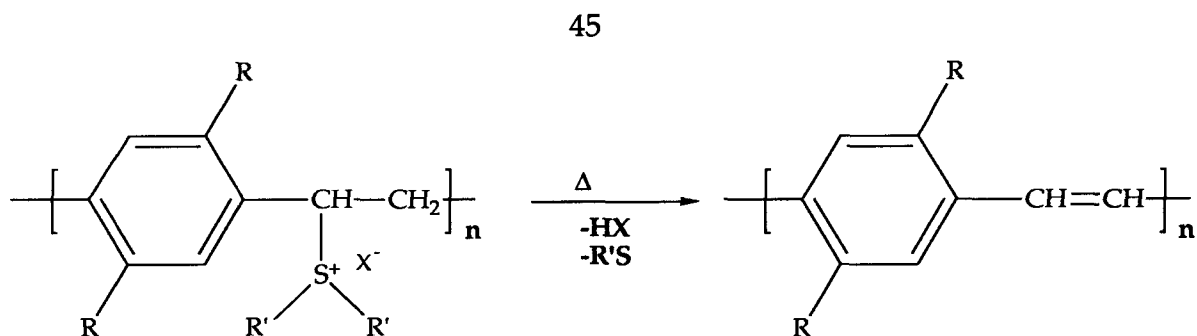


Figure 31. A low-temperature precursor route to PPP. 1,2-Linkages exist in this polymer but are not shown here.

5.2. Poly(Phenylene Vinylene) (PPV) and other Vinylene Polymers

A tremendous amount of interest in PPV was generated upon the invention of a sulfonium salt precursor method by Wessling (Figure 32).²⁷⁰ The precursor polymer, synthesized by adding a base to the *para*-disulfonium salt of the monomer, is thought to form via an anionic-chain mechanism.²⁷¹ Following the process using X-ray scattering, a reduction in the interchain distances as well as an increase in crystallinity has been observed.²⁷² This route has allowed for the preparation of a number of derivatives, including alkoxy (-OR), halogen (Cl, Br) and alkyl-substituted derivatives, typically at the 2,5-positions of the benzene ring.^{273, 274} These substitutions assist in processing the precursors and also modify the bandgap of the polymer to some extent.^{85, 275} A water-soluble 2,5-disubstituted PPV has been reported.²⁷⁶ Substituents can also be placed on the olefin segment of the polymer, resulting in some twisting of the polymer chain that reduces conjugation, but producing soluble, conjugated polymers.²⁷⁷ Subsequent to the demonstration of this route, further efforts have centered on the optimization of the group to be eliminated²⁷⁸ and the effect of polymerization conditions on the molecular weight of the precursor polymer.²⁷⁹ Also, this precursor has been blended with a variety of different types of polymers.^{280, 281}



$R = H, \text{ alkoxy, alkyl, Cl, O(CH}_2)_3\text{SO}_3\text{Na; X = Cl, Br; R}' = \text{alkyl}$

Figure 32. Precursor route to PPV.

Early investigations on this polymer employed it in the formation of graphite intercalation complexes with, for example, potassium²⁸² and FeCl_3 .²⁸³ High conductivities were observed in these materials ($\approx 10^5 \text{ S/cm}$). More recently, however, PPV and its derivatives have been of interest for their third-order nonlinear optical properties,²⁸⁴⁻²⁸⁶ and in optical-recording devices.²⁸⁷ PPV has also found application as a light-emitting diode.²⁸⁸

The sulfonium salt precursor method has also resulted in the synthesis of a variety of other aromatic and heteroaromatic vinylenes. In particular, poly(naphthalene vinylene),²⁸⁹ poly(thienylene vinylene),²⁹⁰⁻²⁹² and poly(furanylene vinylene)²⁹³ and derivatives thereof have been prepared (Figure 33).

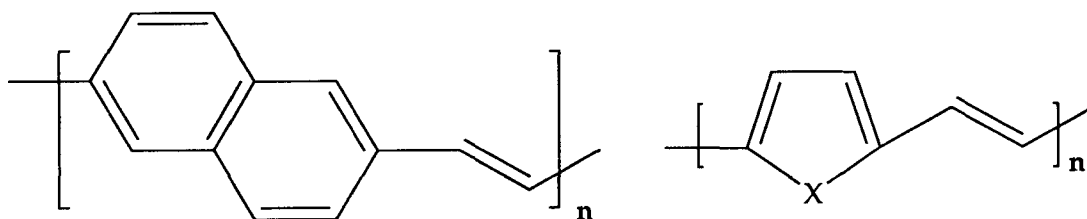


Figure 33. Poly(naphthalene vinylene), poly(thienylene vinylene) ($\text{X}=\text{S}$), and poly(furanylene vinylene) ($\text{X}=\text{O}$).

5.3. Precursors to Polyacetylene

Probably the best known precursor polymer is that developed by Feast and coworkers at the university of Durham.^{294, 295} This polymer is typically referred to as "Feast" or "Durham" polyacetylene and involves the ring-opening metathesis polymerization of cyclobutene derivatives followed by a thermal retro-Diels Alder reaction to perform the conversion (Figure 34). This polymerization is of chain-growth type and the precursor can be easily rid of catalyst residues, a more difficult process with directly synthesized polyacetylene.²⁹⁶ Where $R = CF_3$, this conversion can be performed at a very low temperature ($< 50\text{ }^\circ\text{C}$) and results in a high-quality polyacetylene with relatively low crystallinity. This low crystallinity can be useful, particularly in nonlinear optical applications, where scattering of light off of crystallites becomes a problem. However, crystallinity can be increased, most easily by orienting the material either before²⁹⁷ or as it is converted, and polarized infrared spectroscopy of oriented material revealed a higher anisotropy than observed for a similarly oriented sample of Shirakawa polyacetylene.^{298, 299}

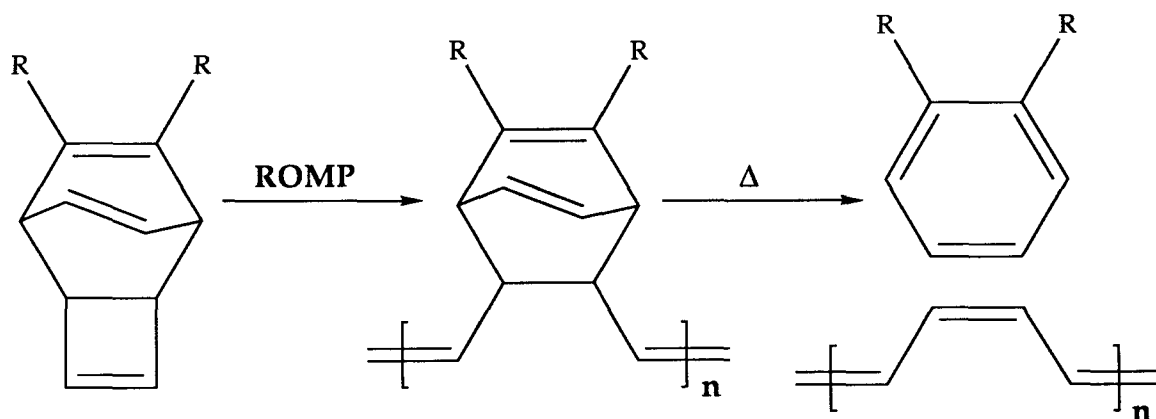


Figure 34. Synthesis and conversion of Durham polyacetylene.

The ring-opening metathesis polymerization (ROMP) employed is subject to a great deal of control, and a controllable polymerization of the Feast monomer has been demonstrated, using metathesis catalysts based on tungsten³⁰⁰ and titanium.³⁰¹ Also, by selecting which starting carbene to employ (which now can be easily varied)³⁰² and taking advantage of the facile, end-capping reaction with an aldehyde or ketone,³⁰³ one can individually control both of the end groups on the polymer. Oligomerization of the monomer followed by conversion produced a series of polyenes, which were separated and characterized. Also, block copolymers were synthesized by polymerizing this monomer and then polymerizing norbornene, a monomer that yields an elastomeric polymer.³⁰⁰ After conversion, the two sections of this block copolymer were observed to phase separate to form well-defined polyacetylene "microdots," as has been noticed for other polyacetylene block copolymers (Section 4.4.1).³⁰⁴

In an effort to reduce the amount of mass loss during conversion, Swager et al. ring-opened benzvalene, also using ROMP. The prepolymer possesses considerable ring strain (the polymer is prone to detonation and can be converted to polyacetylene using mercury salts. This precursor is ideal because it loses no mass upon conversion. However, the polyacetylene produced displays low iodine-doped conductivities and possesses a number of saturated (sp^3) defects as determined by ^{13}C CP-MAS NMR, possibly because of cross-linking induced by residual mercury salts.³⁰⁵

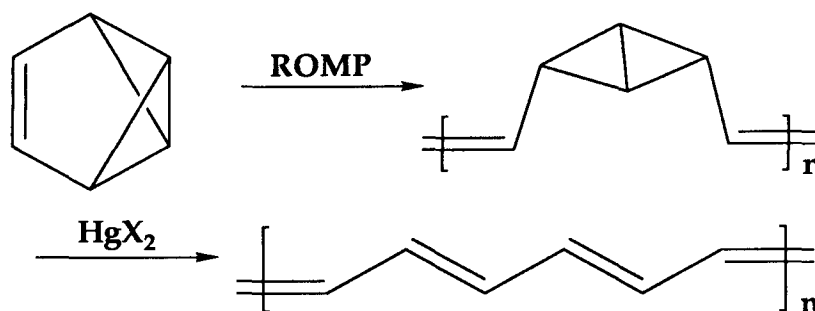


Figure 35. Polybenzvalene and its conversion to polyacetylene.

6. Extensions of these methods in the synthesis of "small-bandgap" polymers

All of this synthetic methodology is designed to establish and exploit the link between structure and properties. In the case of conjugated polymers, one motivation for the synthesis of new structures is the reduction of the bandgap: The energy difference between the highest occupied crystal orbital and the lowest unoccupied crystal orbital of the polymer and, physically, more-or-less the energy of the lowest electronic transition. Briefly, the bandgap of a polymer relates to the ease of generation of carriers. A small bandgap results in easier doping or higher photoconductivities. Ultimately, a polymer with a very small bandgap would be transparent in the visible region of the spectrum and should be easy to dope. A smaller bandgap would also lead to greater mixing between the ground and excited states of the polymer, which could, in principle, lead to larger hyperpolarizabilities (nonlinear optical coefficients).

A very intuitive way of thinking about the bandgaps in conjugated polymers has been advanced by J. L. Bredas.³⁰⁶ Most conjugated organic systems are drawn using single and double bonds, and in the molecule, the single bonds are longer than the double bonds: they have bond-length alternation.

Essentially, one wants to avoid large changes in bond length in going from the ground to the first excited state of the polymer (i.e., jumping its bandgap). In aromatic systems (cyclic arrays of $4n+2$ electrons, which are especially stable, as in benzene), one wants to avoid losing that aromaticity in the excited state, because in the non-aromatic (quinoid, see Figure 36) form, formally long, single bonds are found in the aromatic (short bond) part of the polymer, and the long, single bonds joining the rings become short, double bonds. There is a large change in the bond lengths resulting from this loss of aromaticity, and the large energy cost that is required to go from the aromatic to quinoid form is manifested in a large bandgap (3.2 eV for PPP). If polyacetylene's bonds were all the same length, it would have a zero bandgap and be metallic in nature (elimination of bond-length alternation in one-dimensional systems results in a zero bandgap material). However, polyacetylene is bond-length alternate because of a second-order Peierls distortion that is predicted to occur in all strictly one-dimensional systems, and it has a bandgap (1.8 eV for *trans*-polyacetylene).

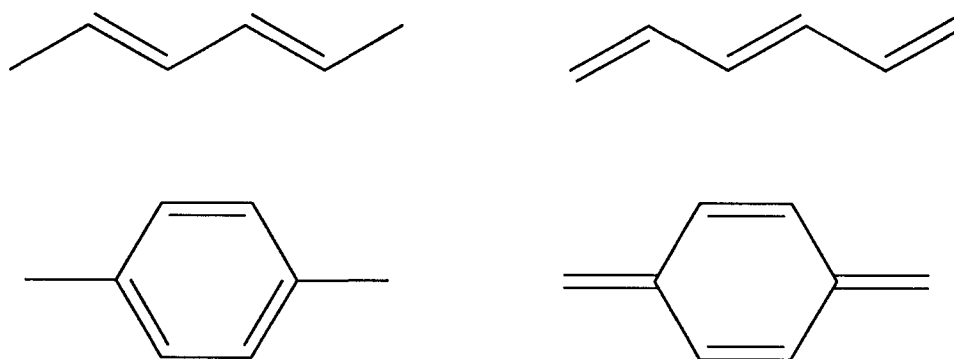


Figure 36. The two bond-length alternate forms of polyacetylene and polyparaphenylene. The aromatic (left) and quinoid (right) forms of PPP are shown.

Wudl and others cleverly exploited this type of reasoning in the design of

a low bandgap polythiophene derivative. As in polyparaphenylene, the quinoid form of polythiophene experiences a loss of aromaticity. By benzannelating polythiophene to give polyisothianaphthene (PITN, Figure 37), Wudl created a polymer where bond-length alternation was reduced since both forms have some aromatic stabilization.³⁰⁷⁻³⁰⁹ In fact, the bandgap for this polymer is approx. 1 eV. More recent theoretical studies have suggested that the bandgap reduction is better explained by orbital-mixing arguments.³¹⁰ However, these very qualitative arguments continue to enjoy success in researchers' design ideas.

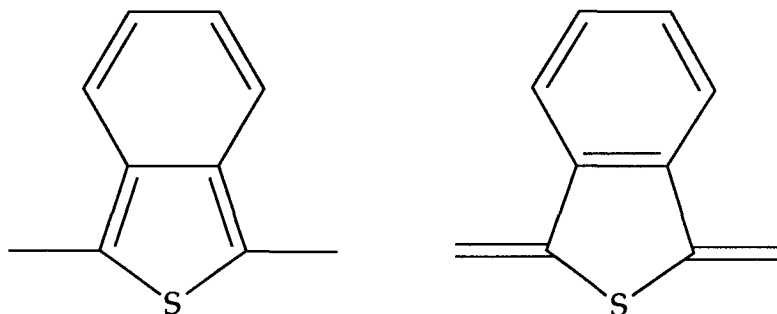


Figure 37. The two bond-alternate structures of PITN. Both possess some degree of aromaticity.

Another approach has been advanced by Jenekhe.^{311, 312} The structure of interest contains alternating aromatic and quinoid units (Figure 38). Reversal of the bonds leads to an identical structure, and bandgaps as low as 0.75 eV have been claimed. The third-order nonlinear optical properties of this polymer have been examined.³¹³ However, these types of low bandgap materials have yet to be definitively synthesized. Here a precursor is converted with bromine (Figure 38), and it has been shown that this reaction step results in bromination of the material, both covalently and ionically.³¹⁴ Since these defects will certainly have an effect on the bandgap of the polymer, further work is warranted. A similar structure was synthesized by reacting 2-pyrrolealdehyde units together using

POCl_3 . The authors note structural irregularities in the polymer such as saturated defects and branched units. Nevertheless, they report a bandgap of about 1 eV.³¹⁵

Alternating quinoid/aromatic polymers containing benzene rings³¹⁶ (and naphthalene and anthracene rings)³¹⁷ have been synthesized as well, although they have a low degree of polymerization. Moreover, their low AsF_5 -doped conductivity ($\approx 10^{-3}$ S/cm), and high-energy optical absorption maxima (3.3 eV) suggest that these polymers contain saturated defects.

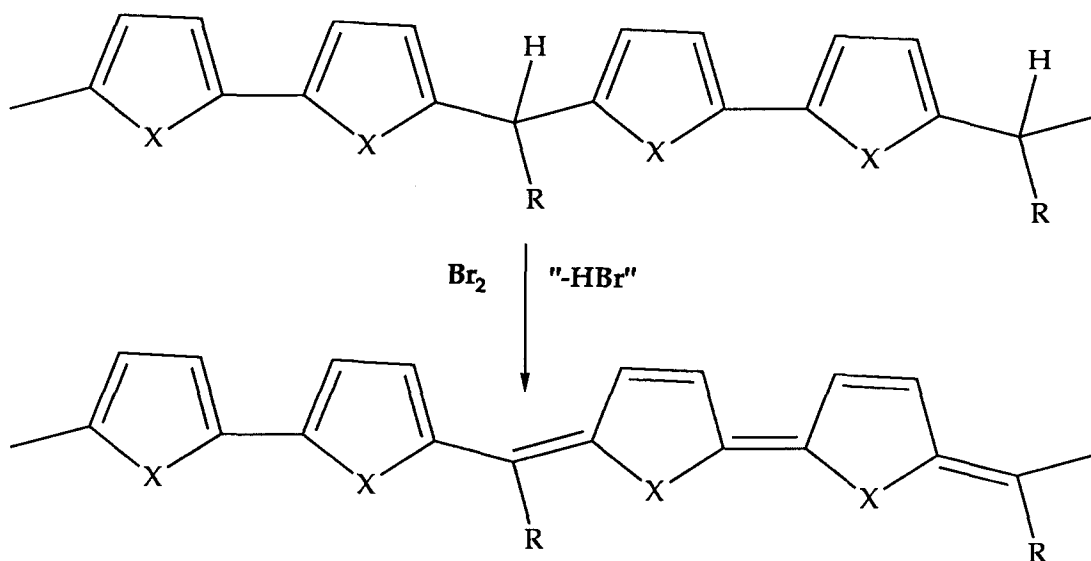


Figure 38. Proposed formation of poly(α -(5,5'-bithiophenediyl)-*p*-acetoxybenzylidene) (PBTAB). X = S; R = *p*-acetoxyphenyl.

7. Conjugated Polymer Matrices

The previous section focused on tailoring the structure of a conjugated polymer. However, several properties of conjugated polymers, including their

optical absorptions, but most notably their doped conductivities are dependent on contacts between polymer chains. Stretch-aligning a fiber or film of a conjugated polymer helps to increase crystallinity, which can easily lead to increases in the doped conductivity of 3-4 orders of magnitude compared to the unoriented material. This increase in conductivity is primarily due to increased carrier mobility associated with the more conjugated (planar) and more closely packed chains found in a crystalline region. Thus, there have been a number of efforts towards organizing a conjugated polymer matrix as well as efforts towards isolating individual polymer strands to study their properties in the absence of neighbors. Conjugated polymers have also been synthesized in matrices that aid in processing.

The first efforts towards synthesizing a conjugated polymer in a matrix were designed to assist in processing. For example, dispersing polyacetylene as a powder in another polymer melt was not useful because of the high loadings required for reasonable conductivity and the realization that these materials were little or no better than the same matrix containing carbon-black as a filler.³¹⁸ A more interesting method employed a Ziegler-Natta catalyst impregnated into a low-density polyethylene matrix. Acetylene gas was admitted and polymerized within the matrix. Relatively high iodine-doped conductivities (≈ 1 S/cm) were obtained for relatively low loadings of polyacetylene (4-6 wt %).³¹⁹ It was also discovered that polyacetylene could be incorporated up to 82% w/w in a polyethylene fiber and drawn and doped to a conductivity of 6000 S/cm.³²⁰ This technique was extended to elastomer composites that were stretched and doped to relatively high conductivities (575 S/cm),³²¹ and polymerization in aramid gels from which strong, oriented conductive fibers could be pulled.³²²

As mentioned before, composites can be prepared electrochemically, typically by polymerizing the monomer on an electrode that had been pretreated with a polymer. This process has been performed with pyrrole, using (with a variety of modifications as well) poly(vinyl alcohol),³²³ poly(vinyl chloride),^{324, 325} polyurethane,³²⁶ and as a graft onto polystyrene functionalized with benzyl chloride side-chains.³²⁷ Pyrrole has been mixed with Kevlar (an ultrahigh modulus polymer) and chemically polymerized to form a very strong "alloy" fiber of polypyrrole and Kevlar.³²⁸

Synthesis in an ordering medium has also resulted in polymer orientation. Aldissi originally discovered that dissolution of a Ziegler-Natta catalyst in a liquid crystalline solvent that was oriented by an external magnetic field followed by polymerization produced an oriented polyacetylene with a very anisotropic doped conductivity of 1235 S/cm ($\rho_{||} / \rho_{\perp} = 4.25$).³²⁹ Later researchers used this technique to achieve conductivities of up to 4800 S/cm.³³⁰ Aldissi has oriented a water-soluble derivative of polythiophene by passing a solution of the polymer through a magnetic field while simultaneously removing the solvent, achieving a conductivity of 10^4 S/cm.²⁸

Porous membranes have also been utilized in the synthesis of oriented conjugated polymers. Polypyrrole and polythiophene have been electrochemically grown in a nucleopore membrane³³¹ to form conjugated polymer microtubules.³³² Polyacetylene, synthesized by allowing catalyst and acetylene to diffuse into the membrane from opposite sides is partially ordered as shown by polarized IR absorption spectra and higher doped conductivities.³³³

Mechanical stretch orientation of polymer films has been one of the most

common methods for achieving higher crystallinity and higher doped conductivities in polymer films. It has been applied successfully to polyacetylene,³³⁴⁻³³⁶ polypyrrole,³³⁷ and polyaniline heated and plasticized with solvent³³⁸ to mention only a few of the many investigations that have been reported. Moreover, polyacetylene synthesized according to the modifications of Naarman (Section 4.4.2) is also stretch-oriented, and this orientation is believed to be one of the reasons that this material displays such a high doped conductivity. A related method involves mechanical orientation during conversion of a precursor polymer. For example, Durham (Feast) polyacetylene has been stretched during conversion by Leising and coworkers, and this material yielded reasonably well-resolved X-ray fiber patterns, which allowed the geometry of the chain to be investigated.³³⁹ The precursor polymers to poly(phenylene vinylene), its 2,5-alkoxy derivatives and poly(thienylene vinylene) have been oriented and then converted to the conjugated polymer, producing films and fibers of mechanically strong material that displays doped conductivities up to 1000 times greater than the unoriented material^{219, 340-343} as well as enhanced and anisotropic nonlinear optical properties.³⁴⁴

Incorporation of conjugated polymeric chains in inorganic host materials has been used to assist polymer ordering and perhaps ultimately to provide a matrix that can be analyzed by X-ray diffraction so as to determine the structure of some of these conjugated polymers. Intercalation of pyrrole in FeOCl results in oxidation of the pyrrole monomers and formation of polypyrrole between FeOCl layers.³⁴⁵ This work has been extended to the intercalation/polymerization of polythiophene in FeOCl,³⁴⁶ and the intercalation/polymerization of polyaniline³⁴⁷ and polythiophene³⁴⁸ in V₂O₅ xerogels. Zeolites have been used as well for the oxidation, entrapment and subsequent spectral characterization of

polyenes³⁴⁹ and for the oxidative polymerization of thiophene and spectral evaluation of the oligomers produced.³⁵⁰ It is of fundamental interest to understand how the spectroscopic properties of these polymers evolve as the chain length increases, and a number of spectra of the radical cations and dications (corresponding to polarons and bipolarons in the polymer) have been obtained in this manner.

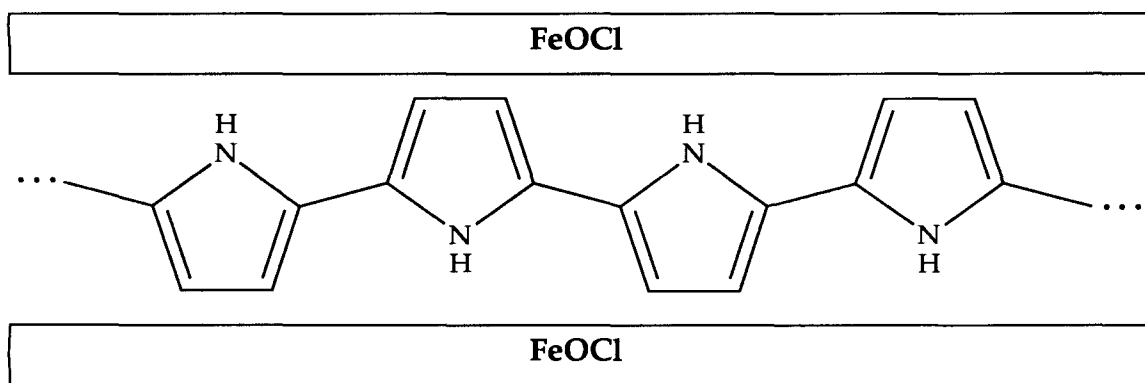


Figure 39. Polypyrrole/FeOCl layered complex.

8. Conclusions and Caveats

This chapter has attempted to give the reader a review of conjugated polymeric materials by outlining the structural variation in both the types of conjugated polymers that have been prepared and in the various methods that have been employed for processing the polymeric matrix. It has categorized this enumeration mostly by the type of synthesis employed for the polymer, making an effort to point out which synthetic methodologies offer the most control over the nature of the resulting material, i.e. how the monomeric units are linked together and what molecular weight and molecular weight distribution can be expected.

Almost all of the research cited here has been performed with the purpose of finding ways to understand and gain control over the properties of these polymeric structures. Few researchers would be willing to admit that they are content in engaging in a "hunt-and-peck" search for that hunk of material that displays the highest figures of merit for whatever electrical or optical property they might be trying to optimize. Nevertheless, with the basic uncertainty in geometry and stoichiometry in many of these solid-state reactions, there is obvious doubt about the relationship between structure and properties that is trying to be elucidated. Many researchers claim to be concerned about properties and not the structure of their materials. However, dramatic examples of physical properties have already been demonstrated, using very simple systems. Controlled pyrolysis of processible resins^{351, 352} and diynes³⁵³ produce materials that although not well-defined structures, are intrinsically conducting because of the large number of free-radical charge carriers that are generated. These materials can be made relatively easily to display conductivities of $\approx 10^2$ S/cm, which are rivalled by relatively few of the structures presented here. Graphite, a cheap, common organic material, can be doped with AsF_5 to a conductivity of approx. 6×10^5 S/cm, comparable with any naturally occurring metal.³⁵⁴ Potassium-doped graphite superconducts at low temperatures.³⁵⁵ These examples are simple, practical realizations of the properties that drive much of this search and are described here to encourage researchers to be critical of the different synthetic techniques and to be aware of possible structural variations in these materials rather than to accept the structure that is drawn on paper. More structural control in the synthesis of materials and acknowledgement of structural flaws in materials should result in a quicker and more correct understanding of their physics and chemistry.

9. References

- (1) Chiang, C. K.; Druy, M. A.; Gau, S. C.; Heeger, A. J.; Louis, E. J.; MacDiarmid, A. G.; Park, Y. W.; Shirakawa, H. *J. Am. Chem. Soc.* **1978**, *100*(3), 1013-1015.
- (2) Chiang, C. K.; C. R. Fincher, J.; Park, Y. W.; Heeger, A. J.; Shirakawa, H.; Louis, E. J.; Gau, S. C.; MacDiarmid, A. G. *Phys. Rev. Lett.* **1977**, *39*(17), 1098-1101.
- (3) Shirakawa, H.; Louis, E. J.; MacDiarmid, A. G.; Chiang, C. K.; Heeger, A. J. *J. Chem. Soc. Chem. Commun.* **1977**, 578-580.
- (4) Heeger, A. J.; Orenstein, J.; Ulrich, D. R., Eds. *Nonlinear Optical Properties of Polymers*; Materials Research Society Symposium Proceedings 109; Materials Research Society, Pittsburgh, 1988.
- (5) Messier, J.; Kajzar, F.; Prasad, P.; Ulrich, D., Eds. *Nonlinear Optical Effects in Organic Polymers*; NATO ASI Series. Series E. Applied Sciences 162; Kluwer Academic Publishers, Dordrecht, The Netherlands, 1989.
- (6) Prasad, P. N.; Ulrich, D. R., Eds. *Nonlinear Optical and Electroactive Polymers*; Plenum Press, New York, 1987.
- (7) Carter, F. L., Ed. *Molecular Electronic Devices*; Marcel Dekker, Inc.: New York, 1982 and 1987; Vol I and II.
- (8) Figure is for low-density polyethylene production for 1990 (est. figure) and does not include 8 billion pounds of high-density polyethylene produced as well: Kiefer, D. M. *Chem. Eng. News* **1990**, *68*(50), 26-28.
- (9) Karol, F. J. in *Organometallic Polymers*; Carraher, C. E.; Sheats, J. E.; Pittman, C. U. Eds.; Plenum Press: New York, 1978; pp. 135-143.
- (10) A remarkably detailed procedure for the most common synthesis of

polyacetylene is available: Gibson, H. W.; Pochan, J. M. in *Encyclopedia of Polymer Science and Engineering*; John Wiley and Sons: New York, 1985; Vol. 1. pp. 87-130.

(11) This principle has been nicely illustrated for a series of soliton model compounds: Tolbert, L. M.; Ogle, M. E. *J. Am. Chem. Soc.* **1990**, *112*(26), 9519-9527.

(12) Bredas, J. L.; Heeger, A. J. *Macromolecules* **1990**, *23*, 1150-1156.

(13) Rughooputh, S. D. D. V.; Hotta, S.; Heeger, A. J.; Wudl, F. *J. Polym. Sci. Polym. Phys.* **1987**, *25*, 1071-1078.

(14) Inganas, O.; Salaneck, W. R.; Osterholm, J.-E.; Laasko, J. *Synth. Met.* **1988**, *22*, 395-406.

(15) Yoshino, K.; Park, D. H.; Park, B. K.; Onoda, M.; Sugimoto, R. *Jap. Journ. Appl. Phys.* **1988**, *27*(9), L1612-L1615.

(16) Clough, S.; Tripathy, S.; Sun, X.-F.; Orchard, B. *Makromol. Chem. Rapid Commun.* **1988**, *9*, 535-538.

(17) Schaefer-Siebert, D.; Roth, S.; Budrowski, C.; Kuzmany, H. *Synth. Met.* **1987**, *21*, 285-291.

(18) Yang, X. Q.; Tanner, D. B.; Arbuckle, G.; MacDiarmid, A. G.; Epstein, A. J. *Synth. Met.* **1987**, *17*, 277-282.

(19) Zuo, F.; Epstein, A. J.; Yang, X.-Q.; Tanner, D. B.; Arbuckle, G.; MacDiarmid, A. G. *Synth. Met.* **1987**, *17*, 433-438.

(20) Heeger, A. J.; Kivelson, S.; Schrieffer, J. R.; Su, W.-P. *Rev. Mod. Phys.* **1988**, *60*(3), 781-850.

(21) Bredas, J. L.; Street, G. B. *Acc. Chem. Res.* **1985**, *18*, 309-315.

(22) Ehinger, K.; Roth, S. in *Electronic Properties of Polymers and Related Compounds*; Kuzmany, H.; Mehring, M.; Roth, S. Eds.; Springer Ser. Solid State Sci. 63; Springer-Verlag: New York, 1985; pp. 67-74.

(23) Abadie, M. J. M.; Boukli, S. M.; Cadene, M.; Rolland, M. *Polymer* **1986**, *27*,

2003-2008.

- (24) A recent review of this topic has appeared: Kaner, R. B. in *Electrochemical Science and Technology of Polymers-2*; Linford, R. G. Ed.; Elsevier Applied Science: Essex, England, 1990; pp 97-147.
- (25) Diaz, A. F.; Bargon, J. in *Handbook of Conducting Polymers*; Skotheim, T. A. Ed.; Marcel Dekker, Inc.: New York, 1986; Vol. 1, pp. 81-115.
- (26) Genies, E. M.; Bidan, G.; Diaz, A. J. *Electroanal. Chem.* **1983**, *149*, 101-113.
- (27) Pfluger, P.; Street, G. B. *J. Chem. Phys.* **1984**, *80*(1), 544-553.
- (28) Kanatzidis, M. G. *Chem. Eng. News* **1990**, *68*(49), 36-54.
- (29) Kaye, B.; Underhill, A. E. *Synth. Met.* **1989**, *28*, C97-C102.
- (30) Winter, H.; Gotschy, B.; Dormann, E. *Synth. Met.* **1990**, *38*(3), 341-352.
- (31) Cheung, K. M.; Bloor, D.; Stevens, G. C. *J. Mat. Sci.* **1990**, *25*(9), 3814-3837.
- (32) Kuwabata, S.; Nakamura, J.; Yoneyama, H. *J. Chem. Soc. Chem. Commun.* **1988**, 779-780.
- (33) Kuwabata, S.; Okamoto, K.; Yoneyama, H. *J. Chem. Soc. Faraday Trans. I* **1988**, *84*, 2317-2326.
- (34) Osaka, T.; Naoi, K.; Ogano, S. *J. Electrochem. Soc.* **1988**, *135*(5), 1071-1077.
- (35) Chao, T. H.; March, J. J. *Polym. Sci. Polym. Chem.* **1988**, *26*(3), 743-753.
- (36) Panero, S.; Prospero, P.; Scorsati, B. *Synth. Met.* **1989**, *28*, C133-C137.
- (37) Yakushi, K.; Lauchlan, L. J.; Clarke, T. C.; Street, G. B. *J. Chem. Phys.* **1983**, *79*(10), 4774-4778.
- (38) Nazzari, A.; Street, G. B. *J. Chem. Soc. Chem. Commun.* **1984**, 83-84.
- (39) Berlin, A.; Ferraccioli, R.; Pagani, G. A.; Sannicolo, F. *Synth. Met.* **1987**, *22*, 89-91.
- (40) Naitoh, S. *Synth. Met.* **1987**, *18*, 237-240.
- (41) Bolognesi, A.; Catellani, M.; Destri, S.; Zamboni, R.; Taliani, C. *J. Chem. Soc. Chem. Commun.* **1988**, 246-247.

- (42) Lazzaroni, R.; Dujardin, S.; Riga, J.; Verbist, J.; Bredas, J. L.; Dehalle, J.; Andre, J. M. in Reference 22; pp. 191-193.
- (43) Naarman, H. *Makromol. Chem. Macromol. Symp.* **1987**, *8*, 1-15.
- (44) Naarman, H. in *Conjugated Polymeric Materials: Opportunities in Electronics, Optoelectronics, and Molecular Electronics*; Bredas, J. L.; Chance, R. R. Eds.; NATO ASI Series. Series E: Applied Sciences 182; Kluwer Academic Publishers: Dordrecht, The Netherlands, 1990; pp. 11-51.
- (45) Fujii, M.; Saeki, Y.; Arie, K.; Yoshino, K. *Jap. Journ. Appl. Phys.* **1990**, *29*(11), 2501-2505.
- (46) Bidan, G. *Mat. Sci. Forum* **1987**, *21*, 21-30.
- (47) Wang, H. L.; Toppare, L.; Fernandez, J. E. *Macromolecules* **1990**, *23*, 1053-1059.
- (48) Faulkner, L. R. *Chem. Eng. News* **1984**, *28*.
- (49) Okabayashi, K.; Ikeda, O.; Tamura, H. *J. Chem. Soc. Chem. Commun.* **1985**, 684.
- (50) Noufi, R. *J. Electrochem. Soc.* **1983**, *130*, 2126.
- (51) Bull, R. A.; Fan, F.-R.; Bard, A. J. *J. Electrochem. Soc.* **1983**, *130*, 1636.
- (52) Ikeda, O.; Okabayashi, K.; Tamura, H. *Chem. Lett.* **1983**, 1821.
- (53) A recent example is given for the chemical synthesis of polypyrrole: Machida, S.; Miyata, S.; Techagumpuch, A. *Synth. Met.* **1989**, *31*, 311-318.
- (54) Mohammadi, A.; Lundstrom, I.; Inganas, O.; Salaneck, W. R. *Polymer* **1990**, *31*, 395-399.
- (55) MacDiarmid, A. G.; Epstein, A. J. *J. Chem. Soc. Faraday Discuss.* **1989**, *88*, 317-332.
- (56) Yue, J.; Epstein, A. J. *J. Am. Chem. Soc.* **1990**, *112*, 2800-2801.
- (57) Diaz, A. F.; Logan, J. A. *J. Electroanal. Chem.* **1980**, *111*, 111-114.
- (58) Wei, Y.; Focke, W. W.; Wnek, G. E.; Ray, A.; MacDiarmid, A. G. *J. Phys.*

Chem. **1989**, *93*, 495-499.

- (59) Leclerc, M.; Guay, J.; Dao, L. H. *Macromolecules* **1989**, *22*, 649-653.
- (60) Chiang, J.-C.; MacDiarmid, A. G. *Synth. Met.* **1986**, *13*, 193-205.
- (61) Andreatta, A.; Cao, Y.; Chiang, J. C.; Smith, P.; Heeger, A. J. *Synth. Met.* **1988**, *26*, 383-389.
- (62) Cao, Y.; Smith, P.; Heeger, A. J. in Reference 44; pp. 171-193.
- (63) Tang, X.; Scherr, E.; MacDiarmid, A. G.; Epstein, A. J. *Bull. Am. Phys. Soc.* **1989**, *34*, 583.
- (64) Vachon, D.; Angus, R. O.; Lu, F. L.; Nowak, M.; Liu, Z. X.; Schaffer, H.; Wudl, F.; Heeger, A. J. *Synth. Met.* **1987**, *18*(1-3), 297-302.
- (65) MacDiarmid, A. G.; Chiang, J.; Halpern, M.; Huang, W. S.; Krawczyk, J. R.; Mammone, R. J.; Mu, S. L.; Somasiri, N. L. D.; Wu, W. *Polym. Prepr.* **1984**, *25*(2), 248-249.
- (66) Anderson, M. R.; Mattes, B. R.; Reiss, H.; Kaner, R. B. *Synth. Met.* **1991**, in Press.
- (67) Schoch, K. F. *Polym. Prepr.* **1984**, *25*(2), 278-279.
- (68) Shacklette, L. W.; Elsenbaumer, R. L.; Chance, R. R.; Eckhardt, H.; Frommer, J. E.; Baughman, R. H. *J. Chem. Phys.* **1981**, *75*(4), 1919-1927.
- (69) Short, J. N.; H. W. Hill, J. *CHEMTECH* **1972**, *2*, 481-485.
- (70) Lenz, R. W.; Handlovits, C. E.; Smith, H. A. *J. Polym. Sci.* **1962**, *58*, 351-367.
- (71) Chance, R. R.; Shacklette, L. W.; Miller, G. G.; Ivory, D. M.; Sowa, J. M.; Elsenbaumer, R. L.; Baughman, R. H. *J. Chem. Soc. Chem. Commun.* **1980**, 348-349.
- (72) Novak, B. M.; Hagen, E.; Viswanathan, A.; Magde, L. *Polym. Prepr.* **1990**, *31*(2), 482-483.
- (73) Krische, B.; Zagorska, M. *Synth. Met.* **1989**, *28*, C263-C268.
- (74) Yamamoto, T.; Sanechika, K.; Yamamoto, A. *J. Polym. Sci. Polym. Lett. Ed.* **1980**, *18*, 9-12.

- (75) Kobayashi, M.; Chen, J.; Chung, T. C.; Moraes, F.; Heeger, A. J.; Wudl, F. *Synth. Met.* **1984**, *9*, 77-86.
- (76) Amer, A.; Zimmer, H.; Mulligan, K. J.; Mark, H. B.; Pons, S.; McAleer, J. F. *J. Polym. Sci. Polym. Lett. Ed.* **1984**, *22*, 77-82.
- (77) Hotta, S.; Soga, M.; Sonoda, N. *Synth. Met.* **1988**, *26*, 267-279.
- (78) Yamamoto, T.; Morita, A.; Maruyama, T.; Zhou, Z.; Kanbara, T.; Sanechika, K. *Polym. J.* **1990**, *22(2)*, 187-190.
- (79) Sugimoto, R.; Takeda, S.; Gu, H. B.; Yoshino, K. *Chemistry Express* **1986**, *1(11)*, 635.
- (80) Farazdel, A.; Dupuis, M.; Clementi, E.; Aviram, A. *J. Am. Chem. Soc.* **1990**, *112(11)*, 4206-4214.
- (81) Aviram, A. *J. Am. Chem. Soc.* **1988**, *110(17)*, 5687-5692.
- (82) Tour, J. M.; Wu, R.; Schumm, J. S. *J. Am. Chem. Soc.* **1990**, *112(14)*, 5662-5663.
- (83) Elsenbaumer, R. L.; Jen, K. Y.; Oboodi, R. *Synth. Met.* **1986**, *15*, 169-174.
- (84) Elsenbaumer, R. L.; Jen, K. Y.; Miller, G. G.; Shacklette, L. W. *Synth. Met.* **1987**, *18*, 277-282.
- (85) Elsenbaumer, R. L.; Jen, K. Y.; Miller, G. G.; Eckhardt, H.; Shacklette, L. W.; Jow, R. in *Electronic Properties of Conjugated Polymers*; Kuzmany, H.; Mehring, M.; Roth, S. Eds.; Springer Ser. Solid State Sci. 76; Springer-Verlag: New York, 1987; pp. 400-406.
- (86) Yoshino, K.; Nakajima, S.; Gu, H. B.; Sugimoto, R. *Jap. Journ. Appl. Phys.* **1987**, *26(8)*, L1371-L1373.
- (87) Kaeriyama, K.; Sato, M.; Tanaka, S. *Synth. Met.* **1987**, *18*, 233-236.
- (88) Hotta, S.; Rughooputh, S. D. D. V.; Heeger, A. J.; Wudl, F. *Macromolecules* **1987**, *20*, 212-215.
- (89) Osterholm, J.-E.; Laakso, J.; Nyholm, P.; Isotalo, H.; Stubb, H.; Inganas, O.;

Salaneck, W. R. *Synth. Met.* **1989**, *28*, C435-C444.

(90) Masuda, H.; Tanaka, S.; Kaeriyama, K. *J. Chem. Soc. Chem. Commun.* **1989**, 725-726.

(91) Higher values of conductivity (up to 720 S/cm) are seen when the film is doped at higher temperatures: Satoh, M.; Imanishi, K.; Yasuda, Y.; Tsushima, R.; Yamasaki, H.; Aoki, S. *Synth. Met.* **1989**, *30*, 33-38.

(92) Prasad, P. in Reference 4; pp 271-282.

(93) Prasad, P. N. in Reference 5; pp 351-363.

(94) Pang, Y.; Prasad, P. N. *J. Chem. Phys.* **1990**, *93*(4), 2201-2204.

(95) Singh, B. P.; Samoc, M.; Nalwa, H. S. *J. Chem. Phys.* **1990**, *92*(5), 2756-2761.

(96) Heffner, G. W.; Rochefort, W. E.; Pearson, D. S. Presented at the 200th National Meeting of the American Chemical Society, Washington, DC.; paper POLY 163.

(97) Aime, J. P.; Bargain, F.; Schott, M.; Eckhardt, H.; Miller, G. G.; Elsenbaumer, R. L. *Phys. Rev. Lett.* **1989**, *62*(1), 55-58.

(98) Nowak, M. J.; Rughooputh, S. D. D. V.; Hotta, S.; Heeger, A. J. *Macromolecules* **1987**, *20*, 965-968.

(99) Feldhues, M.; Kaempf, G.; Litterer, H.; Mecklenburg, T.; Wegener, P. *Synth. Met.* **1989**, *28*, C487-C493.

(100) Kaeriyama, K.; Tanaka, S.; Sato, M.-A.; Hamada, K. *Synth. Met.* **1989**, *28*, C611-C620.

(101) Tanaka, S.; Kaeriyama, K. *Bull. Chem. Soc. Japan* **1989**, *62*, 1908-1912.

(102) Lowen, S. V.; D. MacInnes, J.; Funt, B. L. *J. Polym. Sci. Polym. Chem.* **1989**, *27*, 4087-4097.

(103) Roncali, J.; Marque, P.; Garreau, R.; Garnier, F.; Lemaire, M. *Macromolecules* **1990**, *23*, 1347-1352.

(104) Wudl, F. Presentation at the International Conference on Science and

Technology of Synthetic Metals, Tübingen, FRG, September, 1990.

- (105) Ruiz, J. P.; Nayak, K.; Marynick, D. S.; Reynolds, J. R. *Macromolecules* **1989**, *22*, 1231-1238.
- (106) Ruiz, J. P.; Gieselman, M. B.; Nayak, K.; Marynick, D. S.; Reynolds, J. R. *Synth. Met.* **1989**, *28*, C481-C486.
- (107) Lemaire, M.; Delabouglise, D.; Garreau, R.; Roncali, J. *J. Chim. Phys.* **1989**, *86*(1), 193-198.
- (108) Patil, A. O.; Ikenoue, Y.; Wudl, F.; Heeger, A. J. *J. Am. Chem. Soc.* **1987**, *109*(6), 1858-1859.
- (109) Patil, A. O. *Synth. Met.* **1989**, *28*, C495-C500.
- (110) Shu, C.; Wrighton, M. S. in *Electrochemical Surface Science: Molecular Phenomena at Electrode Surfaces*; Soriaga, M. P. Ed.; ACS Symposium Series 378; American Chemical Society: Washington, DC, 1988; pp. 408-430.
- (111) Baeuerle, P.; Wuerthner, F.; Heid, S. *Angew. Chem. Int. Ed. Engl.* **1990**, *29*(4), 419-420.
- (112) Yoshino, K.; Nakajima, S.; Fujii, M.; Sugimoto, R.-I. *Polymer Commun.* **1987**, *28*, 309-310.
- (113) Yoshino, K.; Nakajima, S.; Sugimoto, R. *Jap. Journ. Appl. Phys.* **1987**, *26*(6), L1038-L1039.
- (114) Laasko, J.; Osterholm, J.; Nyholm, P. *Synth. Met.* **1989**, *28*, C467-C471.
- (115) Hotta, S.; Rughooputh, S. D. D. V.; Heeger, A. J. *Synth. Met.* **1987**, *22*, 79-87.
- (116) Wessling, B. *Synth. Met.* **1988**, *24*, 271-272.
- (117) Isotalo, H.; Stubb, H.; Yli-lahti, P.; Kuivalainen, P.; Osterholm, J.; Laasko, J. *Synth. Met.* **1989**, *28*, C461-C466.
- (118) Wellinghoff, S.; Deng, Z.; Kedrowski, T.; Dick, S.; Jenekhe, S.; Ishida, H. *Mol. Cryst. Liq. Cryst.* **1984**, *106*, 289.
- (119) Jenekhe, S.; Wellinghoff, S.; Reed, J. *Mol. Cryst. Liq. Cryst.* **1984**, *105*, 175.

- (120) Hayashida, S.; Sukegawa, K.; Niwa, O. *Synth. Met.* **1990**, *35*, 253-261.
- (121) Mort, J. *Science* **1980**, *208*(23), 819-825.
- (122) Ito, S.; Katayama, H.; Yamamoto, M. *Macromolecules* **1988**, *21*, 2456-2462.
- (123) Zelent, B.; Messier, P.; Gauthier, S.; Gravel, D.; Durocher, G. *J. Photochem. Photobiol. A.* **1990**, *52*, 165-178.
- (124) Tsujii, Y.; Tsuchida, A.; Onogi, Y.; Yamamoto, M. *Macromolecules* **1990**, *23*, 4019-4023.
- (125) Ghoshal, S.; Chopra, P.; Singh, B. P.; Swiatkiewicz, J.; Prasad, P. N. *J. Chem. Phys.* **1989**, *90*(9), 5078-5081.
- (126) Ellis, J. R. in Reference 25; pp. 489-499.
- (127) DeMartino, R. N.; Choe, E. W.; Khanarian, G.; Haas, D.; Leslie, T.; Nelson, G.; Stamatoff, J.; Stuetz, D.; Teng, C. C.; Yoon, H. in Reference 6; pp. 169-187.
- (128) Griffin, A. C.; Bhatti, A. M.; Hung, R. S. L. in Reference 6; pp. 375-391.
- (129) Griffin, A. C.; Bhatti, A. M.; Howell, G. A. in Reference 4; pp. 115-125.
- (130) Lee, Y.; Kertesz, M. *J. Chem. Phys.* **1988**, *88*(4), 2609-2617.
- (131) Lowe, J. P.; Kafafi, S. A.; LaFemina, J. P. *J. Phys. Chem.* **1986**, *90*(25), 6602-6610.
- (132) Bevierre, M.; Mercier, F.; Ricard, L.; Mathey, F. *Angew. Chem. Int. Ed. Engl* **1990**, *29*(6), 655-657.
- (133) Aeiyaich, S.; Soubiran, P.; Lacaze, P. C.; Froyer, G.; Pelous, Y. *Synth. Met.* **1989**, *32*, 103-112.
- (134) Goldenberg, L. M.; Pelekh, A. E.; Krinichnyi, V. L.; Roshchupkina, O. S.; Zueva, A. F.; Lyubovskaya, R. N.; Efimov, O. N. *Synth. Met.* **1990**, *36*, 217-228.
- (135) Tsuchida, E.; Yamamoto, K.; Asada, T.; Nishide, Y. *Chem. Lett.* **1987**, 1541-1544.
- (136) Ye, J. H.; Chen, Y. Z.; Tian, Z. W. *J. Electroanal. Chem.* **1987**, *229*, 215-222.
- (137) Satoh, M.; Tabata, M.; Kaneto, K.; Yoshino, K. *J. Electroanal. Chem.* **1985**,

195, 203-206.

(138) Kovacic, P.; Kyriakis, A. *J. Am. Chem. Soc.* **1963**, *85*(4), 454-458.

(139) See References 30-39 in: Elsenbaumer, R. L.; Schacklette, L. W. in Reference 25; pp. 213-263.

(140) Pradere, P.; Boudet, A. *J. Mater. Sci.* **1987**, *22*, 4240-4246.

(141) Rehahn, M.; Schlueter, A.; Wegner, G.; Feast, W. J. *Polymer* **1989**, *30*(6), 1054-1059.

(142) Rehahn, M.; Schlueter, A.; Wegner, G.; Feast, W. J. *Polymer* **1989**, *30*(6), 1060-1062.

(143) Rehahn, M.; Schlueter, A.; Wegner, G. *Makrom. Chem.* **1990**, *191*(9), 1991-2003.

(144) Schiavon, G.; Zotti, G.; Bontempelli, G.; LoCoco, F. *Synth. Met.* **1988**, *25*, 365-373.

(145) Laasko, J.; Osterholm, J.; Lindberg, J. J. *Polym. Bull.* **1987**, *18*, 195-201.

(146) Dezotti, M. W. C.; DePaoli, M. A. *Synth. Met.* **1989**, *29*, E41-E45.

(147) Santos, D. A. D.; Galvao, D. S.; Laks, B.; Dezotti, M. W. C.; DePaoli, M. A. *Chem. Phys.* **1990**, *144*, 103-106.

(148) All of the points covered in this section have been recently reviewed: Miller, R. D.; Michl, J. *Chem. Rev.* **1989**, *89*, 1359-1410.

(149) Harrod, J. F. in *Inorganic and Organometallic Polymers*; Zeldin, M.; Wynne, K. J.; Allcock, H. R. Eds.; ACS Symposium Series 360; American Chemical Society: Washington, D. C., 1988; pp. 89-100.

(150) Woo, H.; Tilley, T. D. *J. Am. Chem. Soc.* **1989**, *111*, 8043-8044.

(151) Woo, H.; Tilley, T. D. *J. Am. Chem. Soc.* **1990**, *112*(7), 2843.

(152) Matyjaszewski, K.; Chen, Y. L.; Kim, H. K. in Reference 149; pp 78-88.

(153) Cypryk, M.; Gupta, Y.; Matyjaszewski, K. *J. Am. Chem. Soc.* **1991**, *113*, 1046-1047.

- (154) Nate, K.; Ishikawa, M.; Ni, H.; Watanabe, H.; Saheki, Y. *Organometallics* **1987**, *6*, 1673-1679.
- (155) Chicart, P.; Corriu, R. J. P.; Moreau, J. J. E. *Chem. Mater* **1991**, *3*(1), 8-10.
- (156) Hanack, M.; Datz, A.; Fay, R.; Fischer, K.; Keppeler, U.; Koch, J.; Metz, J.; Mezger, M.; Schneider, O.; Schulze, H. in Reference 25; pp. 133-212.
- (157) Snow, A. W.; Griffith, J. R. in Reference 10, Vol. 11, pp. 212-225.
- (158) Datz, A.; Metz, J.; Schneider, O.; Hanack, M. *Synth. Met.* **1984**, *9*, 31-40.
- (159) Marks, T. J. *Science* **1985**, *227*, 881-889.
- (160) Gaudiello, J. G.; Kellogg, G. E.; Tetrick, S. M.; Marks, T. J. *J. Am. Chem. Soc.* **1989**, *111*(14), 5259-5271.
- (161) Almeida, M.; Gaudiello, J. G.; Kellogg, G. E.; Tetrick, S. M.; Marcy, H. O.; McCarthy, W. J.; Butler, J. C.; Kannewurf, C. R.; Marks, T. J. *J. Am. Chem. Soc.* **1989**, *111*(14), 5271-5284.
- (162) Dirk, C. W.; Inabe, T.; Schoch, K. F.; Marks, T. J. *J. Am. Chem. Soc.* **1983**, *105*(6), 1539-1550.
- (163) Greene, R. L.; Street, G. B. *Science* **1984**, *226*, 651-656.
- (164) Wudl, F. *Acc. Chem. Res.* **1984**, *17*, 227-232.
- (165) Marks, T. J.; Kalina, D. W. in *Extended Linear Chain Compounds*; Miller, J. Ed.; Plenum Press: New York, 1983; Vol. 1, pp. 197-331.
- (166) Alcacer, L.; Novais, H. in Reference 165, Vol. 3, pp. 319-351.
- (167) Dirk, C. W.; Bosseau, M.; Barrett, P. H.; Moraes, F.; Wudl, F.; Heeger, A. J. *Macromolecules* **1986**, *19*, 266-269.
- (168) Vicente, R.; Ribas, J.; Cassoux, P.; Valade, L. *Synth. Met.* **1986**, *13*, 265-280.
- (169) Reynolds, J. R.; Lillya, C. P.; Chien, J. C. W. *Macromolecules* **1987**, *20*, 1184-1191.
- (170) Pittman, C. U.; Carraher, C. E.; Reynolds, J. R. in Reference 10, Vol. 10, pp. 541-594.

- (171) Wang, F.; Reynolds, J. R. *Macromolecules* **1988**, *21*, 2887-2889.
- (172) Wang, F.; Reynolds, J. R. *Macromolecules* **1990**, *23*, 3219-3225.
- (173) Bohlmann, F.; Inhoffen, E. *Chem. Ber.* **1956**, *89*, 1276-1281.
- (174) Kiji, J.; Iwamoto, M. *J. Polym. Sci. Polym. Lett. Ed.* **1968**, *6*, 53-55.
- (175) Tanaka, K.; Ohzeki, K.; Yamabe, T.; Yata, S. *Synth. Met.* **1984**, *9*, 41-52.
- (176) Manassen, J.; Wallach, J. *J. Am. Chem. Soc.* **1965**, *87*(12), 2671-2677.
- (177) Grassie, N.; McNeill, I. C. *J. Polym. Sci.* **1958**, *27*, 207-218.
- (178) Renschler, C. L.; Sylwester, A. P. *Mat. Sci. Forum* **1989**, *52/53*, 301-322.
- (179) Wilbourn, K.; Murray, R. W. *Macromolecules* **1988**, *21*(1), 89-96.
- (180) Blatter, K.; Schlueter, A. *Macromolecules* **1989**, *22*(8), 3506-3508.
- (181) Dalton, L. R. in Reference 5; pp. 123-141.
- (182) Dalton, L. R. in Reference 6; pp. 243-271.
- (183) Feast, W. J. in Reference 25; pp. 1-44.
- (184) Kenny, P. W.; Miller, L. L. *J. Chem. Soc. Chem. Commun.* **1988**, 84-85.
- (185) Dietz, T. M.; Stallman, B. J.; Kwan, W. S. V.; Penneau, J. F.; Miller, L. L. *J. Chem. Soc. Chem. Commun.* **1990**, 367-369.
- (186) Cammarata, V.; Kolaskie, C. J.; Miller, L. L.; Stallman, B. J. *J. Chem. Soc. Chem. Commun.* **1990**, 1290-1292.
- (187) Sum, W.; Kwan, V.; Penneau, J. F.; Miller, L. L. *J. Electroanal. Chem.* **1990**, *291*, 295-299. See also references to the work of Nuzzo and Whitesides contained therein.
- (188) DePra, P. A.; Gaudiello, J. G.; Marks, T. J. *Macromolecules* **1988**, *21*(7), 2295-2297.
- (189) Rao, D. N.; Swiatkiewicz, J.; Chopra, P.; Ghoshal, S. K.; Prasad, P. N. *Appl. Phys. Lett.* **1986**, *48*(18), 1187-1189.
- (190) Wolfe, J. F.; Bitler, S. P. in Reference 6; pp. 401-413.
- (191) Goldfarb, I. J.; Medrano, J. in Reference 5; pp. 93-99.

- (192) Zhao, M. T.; Samoc, M.; Prasad, P. N.; Reinhardt, B. A. *Chem. Mater.* **1990**, 2(6), 670-678.
- (193) Jenekhe, S. A.; Johnson, P. O.; Agrawal, A. K. *Macromolecules* **1989**, 22, 3216-3222.
- (194) For a leading reference, see: Bloor, D.; Chance, R. R., Eds. *Polydiacetylenes*; NATO ASI Series. Series E: Applied Sciences 102; Martinus Nijhoff Publishers: Boston, 1985.
- (195) Wegner, G. *Pure Appl. Chem.* **1977**, 49, 443-454.
- (196) Thakur, M.; Lando, J. B. *Macromolecules* **1983**, 16, 143-146.
- (197) Baughman, R. M. *J. Polym. Sci. Polym. Phys. Ed.* **1974**, 12, 1511-1535.
- (198) Tieke, B.; Lieser, G.; Wegner, G. *J. Polym. Sci. Polym. Chem. Ed.* **1979**, 17, 1631-1644.
- (199) Tieke, B.; Wegner, G. *Makromol. Chem.* **1978**, 179, 1639.
- (200) Day, D. R.; Ringsdorf, H. *Makromol. Chem.* **1979**, 180, 1059.
- (201) Collins, M. A. *J. Polym. Sci. Polym. Phys.* **1988**, 26, 367-387.
- (202) Lopez, E.; O'Brien, D. F.; Whitesides, T. H. *J. Am. Chem. Soc.* **1982**, 104(1), 305-307.
- (203) Johnston, D. S.; Sanghera, S.; Pons, M.; Chapman, D. *Biochim. Biophys. Acta* **1980**, 602, 57-69.
- (204) Pons, M.; Johnston, D. S.; Chapman, D. *J. Polym. Sci. Polym. Chem. Ed.* **1982**, 20, 513-520.
- (205) Pons, M.; Johnston, D. S.; Chapman, D. *Biochim. Biophys. Acta* **1982**, 693, 461-465.
- (206) Leaver, J.; Alonso, A.; Durrani, A. A.; Chapman, D. *Biochim. Biophys. Acta* **1983**, 732, 210-218.
- (207) Patel, G. N.; Chance, R. R.; Witt, J. D. *J. Chem. Phys.* **1979**, 70(9), 4387-4392.
- (208) Biegajski, J. E.; Cadenhead, D. A.; Prasad, P. N. *Macromolecules* **1991**, 24(1),

298-303.

- (209) Wenz, G.; Mueller, M. A.; Schmidt, M.; Wegner, G. *Macromolecules* **1984**, *17*, 837-850.
- (210) Lim, K. C.; Fincher, C. R.; Heeger, A. J. *Phys. Rev. Lett.* **1983**, *50*(24), 1934-1937.
- (211) Lim, K. C.; Kapitulnik, A.; Zacher, R.; Heeger, A. J. *J. Chem. Phys.* **1985**, *82*(1), 516-521.
- (212) Lim, K. C.; Heeger, A. J. *J. Chem. Phys.* **1985**, *82*(1), 522-530.
- (213) Nallicheri, R. A.; Rubner, M. F. *Macromolecules* **1991**, *24*(2), 517-525.
- (214) Peiffer, D. G.; Chung, T. C.; Schulz, D. N.; Agarwal, P. K.; Garner, R. T.; Kim, M. W.; Chance, R. R. in Reference 6; pp. 205-215.
- (215) Allegra, G.; Brueckner, S.; Schmidt, M.; Wegner, G. *Macromolecules* **1986**, *19*, 399-405.
- (216) Sauteret, C.; Herrmann, J. P.; Frey, R.; Pradiere, F.; Ducuing, J.; Baughman, R. H.; Chance, R. R. *Phys. Rev. Lett.* **1976**, *36*, 956-959.
- (217) Thakur, M.; Verbeek, B.; Chi, G. C.; O'Brien, K. J. in Reference 4; pp. 41-64.
- (218) Sandman, D. J.; III, J. W. S.; Jones, M. T. in Reference 6; pp. 367-374.
- (219) Tokito, S. Z.; Smith, P.; Heeger, A. J. *Synth. Met.* **1990**, *36*(2), 183-194.
- (220) Natta, G.; Mazzanti, G. P.; Corrandi, P. *Atti. Naz. Lincei. Cl. Sci. Fis. Mat. Nat. Rend.* **1958**, *25*(8), 3.
- (221) Shirakawa, H.; Ikeda, S. *Polym. J.* **1971**, *2*(2), 231-244.
- (222) Ito, T.; Shirakawa, H.; Ikeda, S. *J. Polym. Sci. Polym. Chem. Ed.* **1974**, *12*, 11-20.
- (223) The synthesis and properties of this material have been reviewed: Chien, J. C. W. *Polyacetylene. Chemistry, Physics, and Materials Science*; Academic Press: San Diego, 1984.
- (224) Gibson, H. W.; Kaplan, S.; Mosher, R. A.; W. M. Prest, J.; Weagley, R. J. J.

Am. Chem. Soc. **1986**, 108(22), 6843-6851.

- (225) Robin, P.; Pouget, J. P.; Comes, R.; Gibson, H. W.; Epstein, A. J. *Journ. de Phys.* **1983**, 44(6), C3-77 to C3-81.
- (226) Hoffman, D. M.; Gibson, H. W.; Epstein, A. J.; Tanner, D. B. *Phys. Rev. B* **1983**, 27(2), 1454-1457.
- (227) Elert, M. L.; White, C. T. *Phys. Rev. B* **1983**, 28(12), 7387-7389.
- (228) Cernia, E.; D'Ilario, L. *J. Polym. Sci. Polym. Chem. Ed.* **1983**, 21, 2163-2176.
- (229) Bozovic, I. *Mod. Phys. Lett. B* **1987**, 1(3), 81-88.
- (230) Rao, B. K.; Darsey, J. A.; Kestner, N. R. *Phys. Rev. B* **1985**, 31(2), 1187-1190.
- (231) Gibson, H. W.; Weagley, R. J.; Mosher, R. A.; Kaplan, S.; W. M. Prest, J.; Epstein, A. J. *Mol. Cryst. Liq. Cryst.* **1985**, 117, 315-318.
- (232) Gibson, H. W.; Weagley, R. J.; Mosher, R. A.; Kaplan, S.; W. M. Prest, J.; Epstein, A. J. *Phys. Rev. B* **1985**, 31(4), 2338-2342.
- (233) Because of the vast number of approaches that have been taken, the reader is referred to an excellent review: Stowell, J. A.; Amass, A. J.; Beevers, M. S.; Farren, T. R. *Polymer* **1989**, 30, 195-201.
- (234) Tubino, R.; Dorsinville, R.; Lam, W.; Alfano, R. R.; Birman, J. L.; Bolognesi, A.; Destri, S.; Catellani, M.; Porzio, W. *Phys. Rev. B* **1984**, 30(11), 6601-6605.
- (235) Piaggio, P.; Cuniberti, C.; Dellepiane, G.; Bolognesi, A.; Catellani, M.; Destri, S.; Porzio, W.; Tubino, R. *Synth. Met.* **1987**, 17, 337-342.
- (236) Dorsinville, R.; Yang, L.; Alfano, R. R.; Tubino, R.; Destri, S. *Solid State Commun.* **1988**, 68(9), 875-877.
- (237) Pflieger, J.; Kminek, I.; Nespurek, S.; Prasad, P. N. *Synth. Met.* **1990**, 37, 255-261.
- (238) Dorsinville, R.; Tubino, R.; Krimchansky, S.; Alfano, R. R.; Birman, J. L.; Bolognesi, A.; Destri, S.; Castellani, M.; Porzio, W. *Phys. Rev. B* **1985**, 32(6), 3377-3380.

- (239) VanNice, F. L.; Bates, F. S.; Baker, G. L.; Carroll, P. J.; Patterson, G. D. *Macromolecules* **1984**, *17*, 2626-2629.
- (240) Bates, F. S.; Baker, G. L. *Macromolecules* **1983**, *16*, 704-707.
- (241) Armes, S. P.; Vincent, B. *Synth. Met.* **1988**, *25*, 171-179.
- (242) Lee, K. I.; Jopson, H. *Makromol. Chem. Rapid Commun.* **1983**, *4*, 375.
- (243) Naarman, H.; Theophilou, N. *Synth. Met.* **1987**, *22*, 1-8.
- (244) Schimmel, T.; Reiss, W.; Gmeiner, J.; Denninger, G.; Schwoerer, M.; Naarman, H.; Theophilou, N. *Solid State Commun.* **1988**, *65(11)*, 1311-1315.
- (245) Basescu, N.; Liu, Z.; Moses, D.; Heeger, A. J.; Naarman, H.; Theophilou, N. *Nature* **1987**, *327*, 403-405.
- (246) Masuda, T.; Higashimura, T. *Acc. Chem. Res.* **1984**, *17*, 51-56.
- (247) Ziegler, J. M. *Polym. Prepr.* **1984**, *25(2)*, 223-224.
- (248) Masuda, T.; Higashimura, T. *Adv. Polym. Sci.* **1987**, *81*, 121-165.
- (249) Petit, M. A.; Soum, A. H.; Leclerc, M.; Prud'homme, R. E. *J. Polym. Sci. Polym. Phys.* **1987**, *25*, 423-433.
- (250) Leclerc, M.; Prud'homme, R. E. *Macromolecules* **1987**, *20*, 2153-2159.
- (251) Furlani, A.; Napoletano, C.; Paolesse, R.; Russo, M. V. *Synth. Met.* **1987**, *21*, 337-342.
- (252) Leclerc, M.; Prud'homme, R. E. *J. Polym. Sci. Polym. Phys. Ed.* **1985**, *23*, 2021-2030.
- (253) Ivin, K. J. *Olefin Metathesis*; Academic Press: San Diego, 1983.
- (254) Tlenkopachev, M. A.; Korshak, Y. V.; Orlov, A. V.; Korshak, V. V. *Dokl. Akad. Nauk SSSR (Engl. Trans.)* **1986**, *291*, 1036-1040.
- (255) Korshak, Y. V.; Korshak, V. V.; Kanischka, G.; Hoecker, H. *Makromol. Chem. Rapid Commun.* **1985**, *6*, 685-692.
- (256) Klavetter, F. L.; Grubbs, R. H. *J. Am. Chem. Soc.* **1988**, *110(23)*, 7807-7813.
- (257) Ginsburg, E. J.; Gorman, C. B.; Marder, S. R.; Grubbs, R. H. *J. Am. Chem.*

Soc. **1989**, *111*, 7621-7622.

(258) Gorman, C. B.; Ginsburg, E. J.; Marder, S. R.; Grubbs, R. H. *Angew. Chem. Adv. Mater.* **1989**, *101*, 1603-1606.

(259) Gorman, C.; Ginsburg, E.; Marder, S.; Grubbs, R. *Polym. Prepr.* **1990**, *31(1)*, 386-387.

(260) Ginsburg, E. J.; Gorman, C. B.; Grubbs, R. H.; Klavetter, F. L.; Lewis, N. S.; Marder, S. R.; Perry, J. W.; Sailor, M. J. in Reference 44; pp. 65-81.

(261) Grubbs, R. H.; Gorman, C. B.; Ginsburg, E. J.; Perry, J. W.; Marder, S. R. in *Materials for Nonlinear Optics: Chemical Perspectives*; Marder, S. R.; Sohn, J. E.; Stucky, G. D. Eds.; ACS Symposium Series 455; American Chemical Society: Washington, DC, 1991; pp. 672-682.

(262) Sailor, M. J.; Ginsburg, E. J.; Gorman, C. B.; Kumar, A.; Grubbs, R. H. *Science* **1990**, *249*, 1146-1149.

(263) Marvel, C. S.; Hartzell, G. E. *J. Am. Chem. Soc.* **1959**, *81*, 448-452.

(264) Lefebvre, G.; Dawans, F. *J. Polym. Sci. A* **1964**, *2*, 3277-3295.

(265) Frey, D. A.; Hasegawa, M.; Marvel, C. S. *J. Polym. Sci. A* **1963**, *1*, 2057-2065.

(266) Cassidy, P. E.; Marvel, C. S.; Ray, S. *J. Polym. Sci. A* **1965**, *3*, 1553-1565.

(267) Zhong, X. F.; Francois, B. *Makromol. Chem. Rapid Commun.* **1988**, *9*, 411-416.

(268) Ballard, D. G. H.; Courtis, A.; Shirley, I. M.; Taylor, S. C. *Macromolecules* **1988**, *21*, 294-304.

(269) McKean, D. R.; Stille, J. K. *Macromolecules* **1987**, *20*, 1787-1792.

(270) Wessling, R. A. *J. Polym. Sci. Polym. Symp.* **1985**, *72*, 55-66.

(271) Lahti, P. M.; Modarelli, D. A.; Denton, F. R.; Lenz, R. W.; Karasz, F. E. *J. Am. Chem. Soc.* **1988**, *110*, 7258-7259.

(272) Moon, Y. B.; Rughooputh, S. D. D. V.; Heeger, A. J.; Patil, A. O.; Wudl, F. *Synth. Met.* **1989**, *29*, E79-E84.

(273) Hoerhold, H.; Helbig, N. *Makromol. Chem. Macromol. Symp.* **1987**, *12*, 229-

258.

(274) Murase, I.; Ohnishi, T.; Noguchi, T.; Hirooka, M. *Synth. Met.* **1987**, *17*, 639-644.

(275) Eckhardt, H.; Shacklette, L. W.; Jen, K. Y.; Elsenbaumer, R. L. *J. Chem. Phys.* **1989**, *91*(2), 1303-1315.

(276) Shi, S.; Wudl, F. in Reference 44; pp. 83-89.

(277) Hörhold, H. Presentation at the International Conference on Science and Technology of Synthetic Metals, Tübingen, FRG, September, 1990.

(278) Lenz, R. W.; Han, C.; Stenger-smith, J.; Karasz, F. E. *J. Polym. Sci. Polym. Chem.* **1988**, *26*, 3241-3249.

(279) Machado, J. M.; III, F. R. D.; Schlenoff, J. B.; Karasz, F. E.; Lahti, P. M. *J. Polym. Sci. Polym. Phys.* **1989**, *27*, 199-203.

(280) Machado, J. M.; Schlenoff, J. B.; Karasz, F. E. *Macromolecules* **1989**, *22*, 1964-1973.

(281) Machado, J. M.; Karasz, F. E.; Lenz, R. W. *Polymer* **1988**, *29*, 1412-1417.

(282) Uneo, H.; Nogami, K.; Yoshino, K. *Phys. Rev. B* **1987**, *36*(15), 8142-8146.

(283) Ueno, H.; Yoshino, K. *Phys. Rev. B* **1987**, *36*(15), 8138-8141.

(284) Singh, B. P.; Prasad, P. N.; Karasz, F. E. *Polymer* **1988**, *29*(11), 1940-1942.

(285) Kaino, T.; Kobayashi, H.; Kubodera, K.; Kurihara, T.; Saito, S.; Tsutsui, T.; Tokito, S. *Appl. Phys. Lett.* **1989**, *54*(17), 1619-1621.

(286) McBranch, D.; Sinclair, M.; Heeger, A. J.; Patil, A. O.; Shi, S.; Askari, S.; Wudl, F. *Synth. Met.* **1989**, *29*(1), 85-90.

(287) Yoshino, K.; Kuwabara, T.; Iwasa, T.; Kawai, T.; Onoda, M. *Jap. Journ. Appl. Phys.* **1990**, *29*(8), L1514-L1516.

(288) Burroughes, J. H.; Bradley, D. D. C.; Brown, A. R.; Marks, R. N.; Mackay, K.; Friend, R. H.; Burns, P. L.; Holmes, A. B. *Nature* **1990**, *347*, 539-541.

(289) Capistran, J. D.; Gagnon, D. R.; Antoun, S.; Lenz, R. W.; Karasz, F. E.

Polym. Prepr. **1984**, 25(2), 282-283.

(290) Murase, I.; Ohnishi, T.; Noguchi, T.; Hirooka, M. *Polymer J.* **1987**, 28(8), 229-231.

(291) Yamada, S.; Tokito, S.; Tsutsui, T.; Saito, S. *J. Chem. Soc. Chem. Commun.* **1987**, 1448-1449.

(292) Jen, K.; Eckhardt, H.; Jow, T. R.; Shacklette, L. W.; Elsenbaumer, R. L. *J. Chem. Soc. Chem. Commun.* **1988**, 215-217.

(293) Jen, K.; Jow, T. R.; Elsenbaumer, R. L. *J. Chem. Soc. Chem. Commun.* **1987**, 1113-1115.

(294) Edwards, J. H.; Feast, W. J. *Polymer* **1980**, 21, 595-596.

(295) Bott, D. C.; Brown, C. S.; Chai, C. K.; Walker, N. S.; Feast, W. J.; Foot, P. J. S.; Calvert, P. D.; Billingham, N. C.; Friend, R. H. *Synth. Met.* **1986**, 14, 245-269.

(296) Edwards, J. H.; Feast, W. J.; Bott, D. C. *Polymer* **1984**, 25, 395-398.

(297) Kahlert, H.; Leising, G. *Mol. Cryst. Liq. Cryst.* **1985**, 117, 1.

(298) Bott, D. C.; Brown, C. S.; Winter, J. N.; Barker, J. *Polymer* **1987**, 28, 601-616.

(299) Brown, C. S.; Vickers, M. E.; Foot, P. J. S.; Billingham, N. C.; Calvert, P. D. *Polymer* **1986**, 27, 1719-1724.

(300) Schrock, R. R. *Acc. Chem. Res.* **1990**, 23(5), 158-165.

(301) Klavetter, F. L.; Grubbs, R. H. *Synth. Met.* **1988**, 26, 311-319.

(302) Johnson, L. K.; Virgil, S. C.; Grubbs, R. H.; Ziller, J. W. *J. Am. Chem. Soc.* **1990**, 112(13), 5384-5385.

(303) Schrock, R. R.; DePue, R. T.; Feldman, J.; Schaverien, C. J.; Dewan, J. C. *J. Am. Chem. Soc.* **1988**, 110, 1423-1435.

(304) Steltzer, F.; Leitner, O.; Leising, G.; Pressl, K.; Grubbs, R. H. *Synth. Met.* **1991**, in press.

(305) Swager, T. M.; Dougherty, D. A.; Grubbs, R. H. *J. Am. Chem. Soc.* **1988**, 110(9), 2973-2974.

- (306) Bredas, J. L. *J. Phys. Chem.* **1985**, *82*, 3808-3811.
- (307) Wudl, F.; Kobayashi, M.; Heeger, A. J. *J. Org. Chem.* **1984**, *49*, 3382-3384.
- (308) Kobayashi, M.; Colaneri, N.; Boysel, M.; Wudl, F.; Heeger, A. J. *J. Chem. Phys.* **1985**, *82*(12), 5717-5723.
- (309) Bredas, J. L.; Heeger, A. J.; Wudl, F. *J. Chem. Phys.* **1986**, *85*(8), 4673-4678.
- (310) Pranata, J.; Grubbs, R. H.; Dougherty, D. A. *J. Am. Chem. Soc.* **1988**, *110*(11), 3430-3435.
- (311) Jenekhe, S. A. *Nature* **1986**, *322*, 345-347.
- (312) Jenekhe, S. A. *Macromolecules* **1986**, *19*, 2663-2664.
- (313) Jenekhe, S. A.; Lo, S. K.; Flom, S. R. *Appl. Phys. Lett.* **1989**, *54*(25), 2524-2526.
- (314) Patil, A. O.; Wudl, F. *Macromolecules* **1988**, *21*(2), 540-542.
- (315) Becker, R.; Bloechl, G.; Braeunling, H. in Reference 44; pp. 133-139.
- (316) Al-Jumah, K.; Fernandez, J. E. *Macromolecules* **1987**, *20*(6), 1177-1180.
- (317) Al-Jumah, K.; Fernandez, J. E. *Macromolecules* **1987**, *20*(6), 1181-1183.
- (318) Wnek, G. E. in Reference 25; Vol 1, pp. 205-211.
- (319) Galvin, M. E.; Wnek, G. E. *Polym. Commun.* **1982**, *23*, 795.
- (320) Chiang, J. C.; Smith, P.; Heeger, A. J.; Wudl, F. *Polymer Commun.* **1988**, *29*, 161-163.
- (321) Rubner, M. F.; Tripathy, S. K.; J. Georger, J.; Cholewa, P. *Macromolecules* **1983**, *16*, 870-875.
- (322) Smith, P.; Heeger, A. J.; Wudl, F.; Chiang, J. in Reference 4; pp. 283-290.
- (323) Lindsey, S. E.; Street, G. B. *Synth. Met.* **1984/85**, *10*, 67-69.
- (324) Niwa, O.; Kakuchi, M.; Tamamura, T. *Macromolecules* **1987**, *20*(4), 749-753.
- (325) DePaoli, M. A.; Waltman, R. J.; Diaz, A. F.; Bargon, J. J. *Polym. Sci.* **1985**, *23*, 1687-1698.
- (326) Bi, X.; Pei, Q. *Synth. Met.* **1987**, *22*, 145-156.
- (327) Nazzal, A. I.; Street, G. B. *J. Chem. Soc. Chem. Commun.* **1985**, 375-376.

- (328) Nemoto, H.; Marks, T. J.; Groot, D. C. D.; Kannewurf, C. R. *Chem. Mater.* **1990**, *2*, 349-351.
- (329) Aldissi, M. *J. Polym. Sci. Polym. Lett. Ed.* **1985**, *23*, 167-170.
- (330) Akagi, K.; Katayama, S.; Shirakawa, H.; Araya, K.; Mukoh, A.; Narahara, T. *Synth. Met.* **1987**, *17*, 241-246.
- (331) Cai, Z.; Martin, C. R. *J. Am. Chem. Soc.* **1989**, *111*(11), 4138-4139.
- (332) Martin, C. R.; Dyke, L. S. V.; Cai, Z.; Liang, W. *J. Am. Chem. Soc.* **1990**, *112*(24), 8976-8977.
- (333) Liang, W.; Martin, C. R. *J. Am. Chem. Soc.* **1990**, *112*(26), 9666-9668.
- (334) Druy, M. A.; Tsang, C.; Brown, N.; Heeger, A. J.; MacDiarmid, A. G. *J. Polym. Sci. Polym. Phys. Ed.* **1980**, *18*, 429-441.
- (335) Lugli, G.; Pedretti, U.; Perego, G. *J. Polym. Sci. Polym. Lett. Ed.* **1985**, *23*, 129-135.
- (336) Park, Y. W.; Park, C.; Lee, Y. S.; Yoon, C. O.; Shirakawa, H.; Suezaki, Y.; Akagi, K. *Solid State Commun.* **1988**, *65*(2), 147-150.
- (337) Hagiwara, T.; Hirasaka, M.; Sato, K.; Yamaura, M. *Synth. Met.* **1990**, *36*, 241-252.
- (338) MacDiarmid, A. G.; Epstein, A. J. in Reference 44; pp. 53-63.
- (339) Kahlart, H.; Leitner, O.; Leising, G. *Synth. Met.* **1987**, *17*, 467-472.
- (340) Gagnon, D. R.; Karasz, F. E.; Thomas, E. L.; Lenz, R. W. *Synth. Met.* **1987**, *20*, 85-95.
- (341) Jen, K.; Shacklette, L. W.; Elsenbaumer, R. *Synth. Met.* **1987**, *22*, 179-183.
- (342) Jin, J.; Park, C. K.; Shim, H.; Park, Y. *J. Chem. Soc. Chem. Commun.* **1989**, 1205-1206.
- (343) Machado, J. M.; Masse, M. A.; Karasz, F. E. *Polymer* **1989**, *30*(11), 1992-1996.
- (344) Swiatkiewicz, J.; Prasad, P. N.; Karasz, F. E. *Appl. Phys. Lett.* **1990**, *56*(10), 892-894.

- (345) Kanatzidis, M. G.; Tonge, L. M.; Marks, T. J.; Marcy, H. O.; Kannewurf, C. R. *J. Am. Chem. Soc.* **1987**, *109*(12), 3797-3799.
- (346) Kanatzidis, M. G.; Hubbard, M.; Tonge, L. M.; Marks, T. J.; Marcy, H. O.; Kannewurf, C. R. *Synth. Met.* **1989**, *28*, C89-C95.
- (347) Kanatzidis, M. G.; Wu, C.; Marcy, H. O.; Kannewurf, C. R. *J. Am. Chem. Soc.* **1989**, *111*(11), 4139-4141.
- (348) Kanatzidis, M. G.; Wu, C.; Marcy, H. O.; DeGroot, D. C.; Kannewurf, C. R. *Chem. Mater.* **1990**, *2*, 222-224.
- (349) Ramamurthy, V.; Caspar, J. V.; Corbin, D. R. *J. Am. Chem. Soc.* **1991**, *113*(2), 594-600.
- (350) Caspar, J. V.; Ramamurthy, V.; Corbin, D. R. *J. Am. Chem. Soc.* **1991**, *113*(2), 600-610.
- (351) Keller, T. M. *CHEMTECH* **1988**, *October*, 635-639.
- (352) Keller, T. M.; Gatz, R. F. *Polymer Commun.* **1987**, *28*, 334-336.
- (353) Hopf, H.; Kretschmer, O.; Naarman, H. *Angew. Chem. Int. Ed. Engl. Adv. Mater.* **1989**, *28*(12), 1745-1746.
- (354) Foley, C. M. T.; Zeller, C.; Falardeau, E. R.; Vogel, F. L. *Solid State Commun.* **1977**, *24*, 371-375.
- (355) Kobayashi, M.; Tsujikawa, I. *J. Phys. Soc. Japan* **1979**, *46*(6), 1945-1946.

CHAPTER 2

SYNTHESIS AND PRELIMINARY CHARACTERIZATION OF POLYMERS OF MONOSUBSTITUTED CYCLOOCTATETRAENES

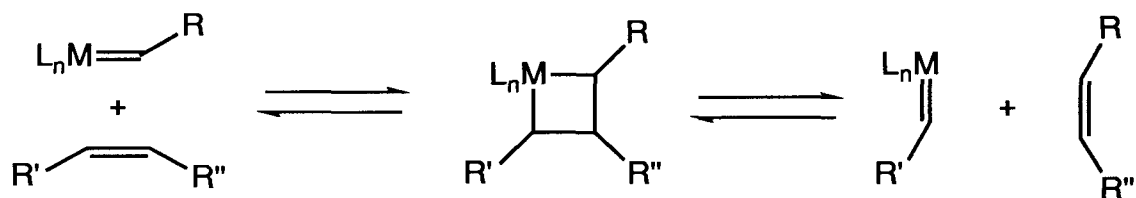
Introduction

A. Ring-opening metathesis polymerization

Ring-opening metathesis polymerization (ROMP) has been used to polymerize a number of cyclic olefins.¹⁻⁵ The accepted mechanism of this reaction is shown in Figure 1 and involves a metallocarbene, either preformed or generated in situ. The driving force for the reaction is the release of ring strain in the cyclic olefin. A variety of metathesis catalysts are known, and they display great diversity in their catalytic activity as well as tolerance of functional groups. There has been a considerable effort in tailoring these properties in preformed metathesis catalysts by varying the steric and electronic environment at the catalytic center.⁶

Some catalysts, such as **1**, do not catalyze ROMP when there is only a small thermodynamic driving force. In the case of olefins with substantial ring-strain, however, the relative rates of initiation and propagation are much faster and can be controlled. In the absence of chain-termination or chain-transfer steps, if the rate of propagation is slowed relative to the rate of initiation, all the catalytic centers can initiate at about the same time. This set of conditions results in the smallest statistical variation in polymer chain lengths (polydispersity) and is termed a "living" polymerization.⁷ Living polymerizations have been realized using **1** and various strained cyclic olefins such as norbornene (**3**),^{8,9} cyclobutene (**4**),¹⁰ and Feast's monomer (**5**),¹¹⁻¹³ a precursor to polyacetylene (Figure 3).^{14, 15}

Acyclic Olefins:



Cyclic Olefins:

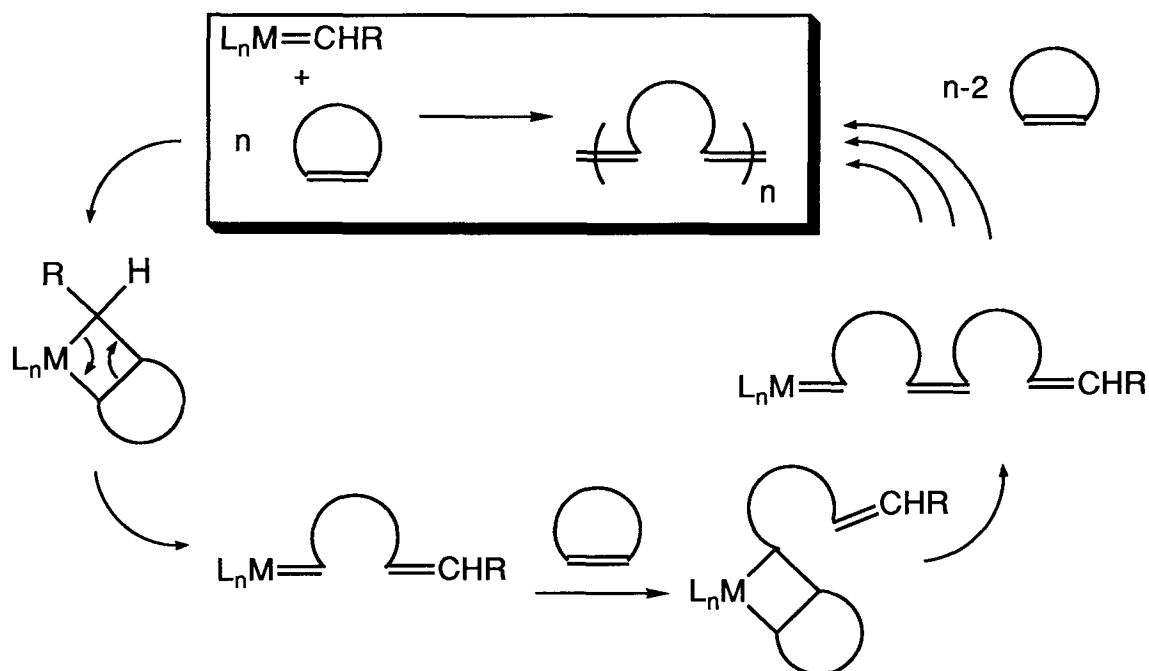


Figure 1. The catalytic cycle for ring-opening metathesis polymerization.

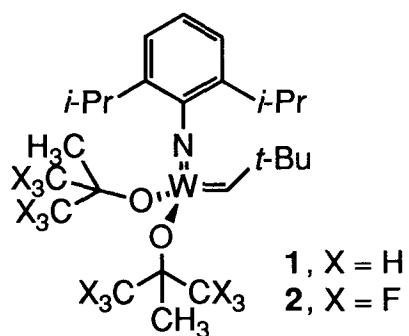


Figure 2. Tungsten-based metathesis catalysts.⁶

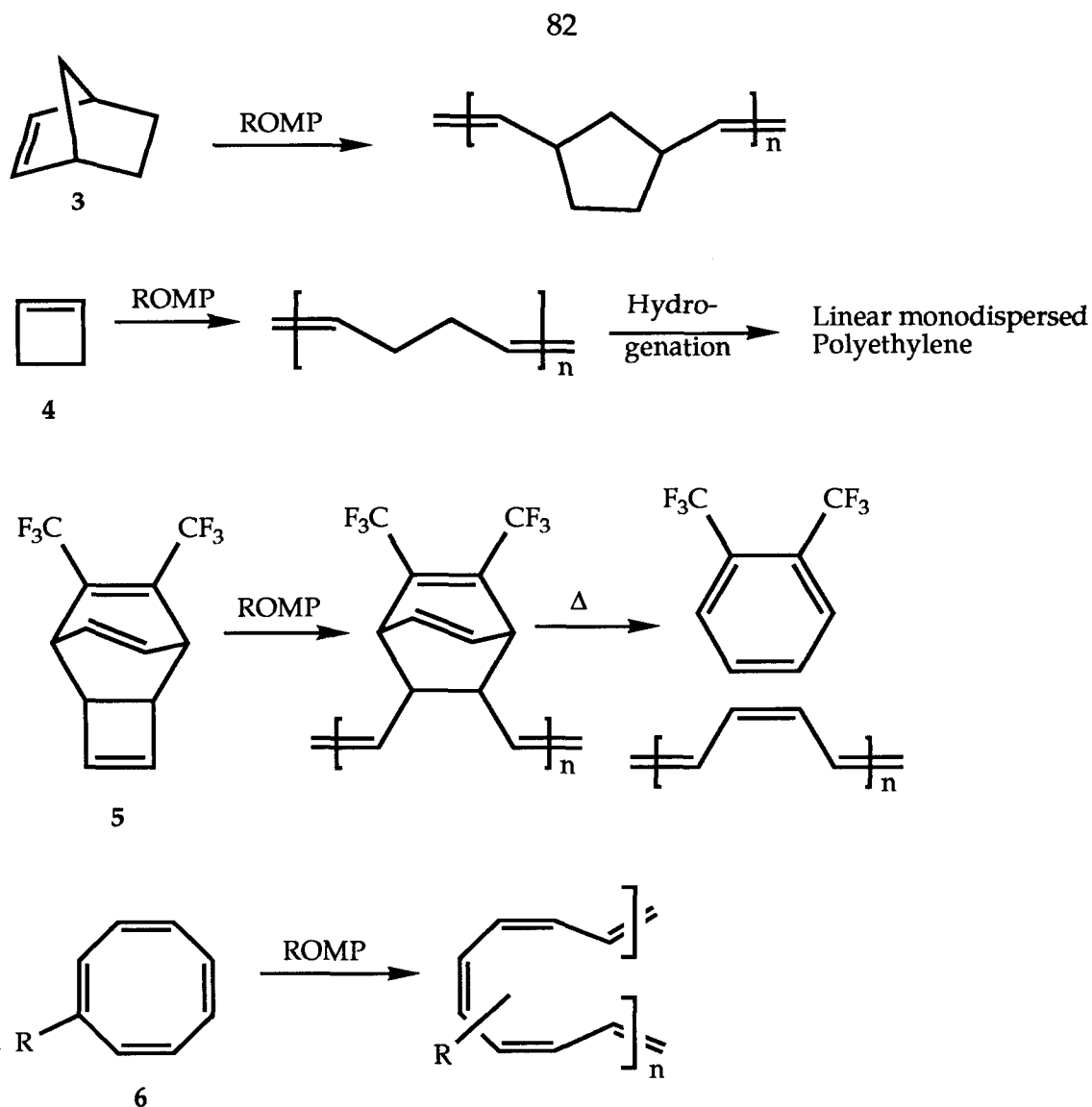


Figure 3. Interesting olefins that have been polymerized by ROMP. **3**, **4**, and **5** contain a considerable amount of ring strain and lead to living polymers. COT (**6**) contains much less ring strain and requires a more active catalyst for polymerization.

More active metathesis catalysts are known. For example, **2**, in which the *t*-butoxy groups of **1** have been replaced with the more electron-withdrawing hexafluoro-*t*-butoxy groups, will polymerize olefins with much less ring strain.⁶ This catalyst displays a very high metathesis activity. It will metathesize acyclic olefins such as 2-pentene to a mixture of 2-butene and 3-hexene, a reaction in

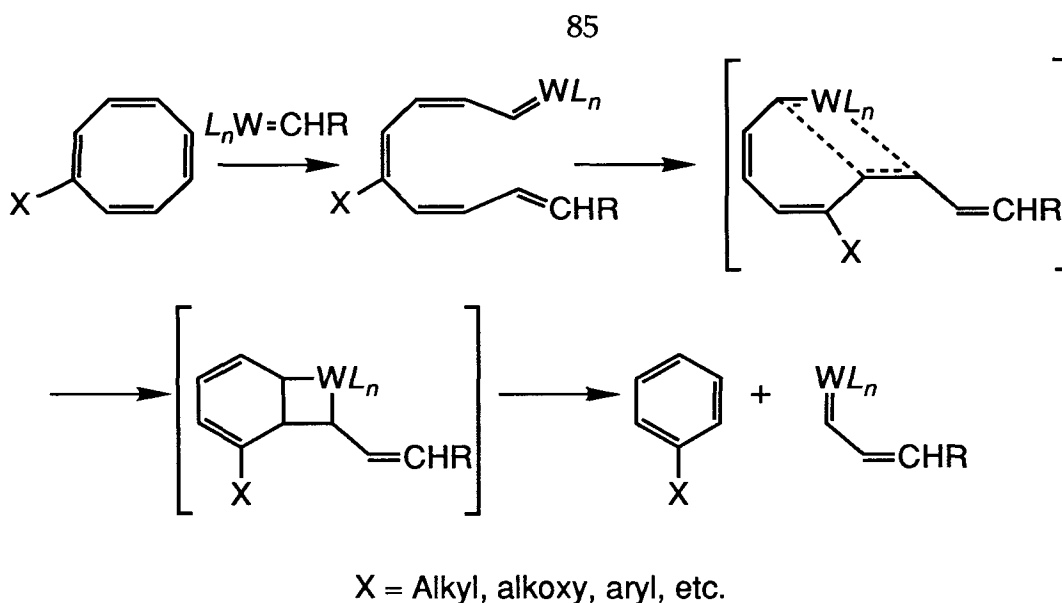
which entropy is probably the principal driving force.⁶ Cyclooctatetraene (COT, **6**), the cyclic olefin in this study, is estimated to contain only about 2.5 Kcal/mol of ring strain.¹⁶ It will polymerize to form polyacetylene with only a very active metathesis catalyst such as **2**.

Around 1986, the ROMP of cyclooctatetraene (COT, **6**) was reported simultaneously by two groups: Korshak et al.^{17, 18} using a "classical" metathesis catalyst $W[OCH(CH_2Cl)_2]_nCl_{6-n}/AlEt_2Cl$ ($n = 2$ or 3) generated in situ, and Klavetter and Grubbs¹⁹ using catalyst **2**. The classical catalyst is known to be Lewis-acidic, and there was concern that it could further react with the nascent polyacetylene to form saturated (sp^3) defects in the polymer chain. This point is important since these defects reduce the conjugation of the chain and thus can easily affect the electrical^{20, 21} and optical²²⁻²⁴ properties of the polymer. Polymerization of COT using **2** produced a polyacetylene with no detectable sp^3 defects. This catalyst and derivatives thereof were employed to form the polymers described here.

The polymerization of COT and its derivatives produces polyacetylenes that can be shown to be of "high quality." This term, frequently used by workers in the conjugated polymer community, indicates that the polymer does not contain any detectable chemical defects and that the polymerization reaction has deposited the polymer in a convenient form, generally a homogeneous film of more or less controllable thickness. Nevertheless, the polymerization does suffer from several undesirable features. First of all, use of **2** offers little control over molecular weight and molecular weight distribution of the synthesized polymers. It appears that only a small amount of the catalyst initiates and that the resulting species propagates very quickly. Varying the monomer to catalyst

ratio in the polymerization under these conditions offers little control over polymer molecular weight. In principle, however, the relative rates in any chain-growth polymerization can be tailored. In particular, it is known that Lewis bases reversibly bind to the catalyst, slowing the rate of propagation considerably.²⁵ The rate of initiation may be slowed as well. Addition of several equivalents of tetrahydrofuran per equivalent of catalyst will slow the polymerization down to a manageable rate.

The polymerization also suffers from a side reaction. At any propagation step, the very active metathesis catalyst can undergo acyclic metathesis with the growing polymer chain, producing benzene or a substituted benzene. Formation of an aromatic ring is a strong driving force for this side reaction. This side reaction, termed cycloextrusion or "back-biting," does not terminate the polymerization, but it does reduce the molecular weight of the polymer. In dilute solution, it has been shown that this side reaction resulted in the production of a substantial amount of benzene, and subsequently little polymer was formed.¹⁹



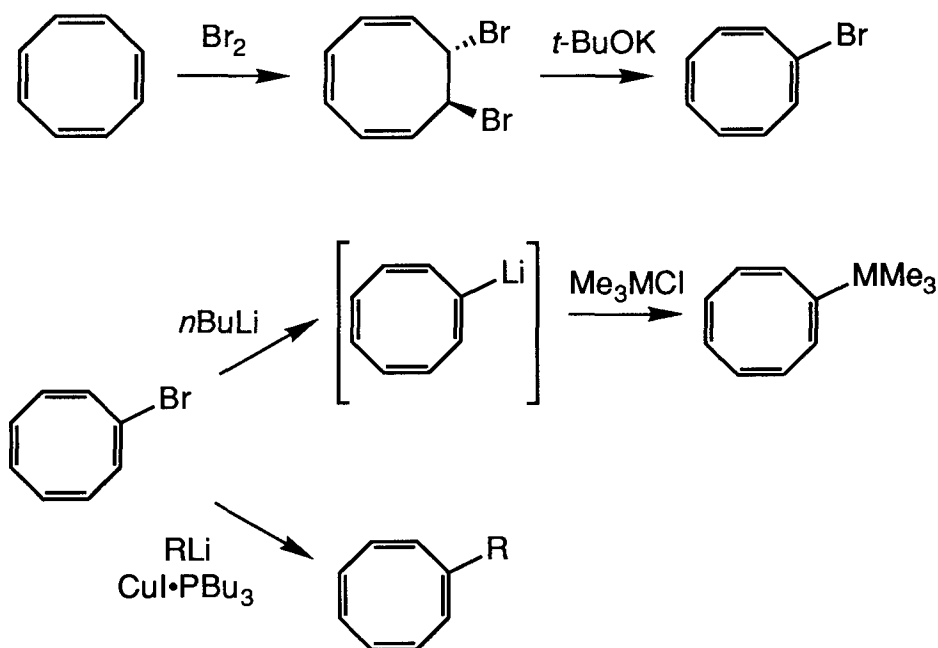
Scheme 1. Cycloextrusion of an aromatic compound during COT polymerization.

B. General schemes for the synthesis of substituted cyclooctatetraenes

This work involves the polymerization of monosubstituted COT's and began with a review of the literature of COT synthesis. Much synthetic effort has centered around COT because of its intriguing physical properties. These include its reduction to the aromatic 10 electron dianion (which can be used as a ligand), its cycloaddition and rearrangement products, and the dynamic processes such as ring-inversion and bond-shifting that have been observed for COT derivatives. All of these, as well as accounts of the many synthetic efforts related to this molecule have been detailed,^{26, 27} and the study of these properties continues.²⁸⁻³¹

Most of the literature concerning the synthesis of monosubstituted COT's involve bromoCOT,³² synthesized by bromination/dehydrobromination of COT. This compound should be stored at low temperature to avoid rearrangement to

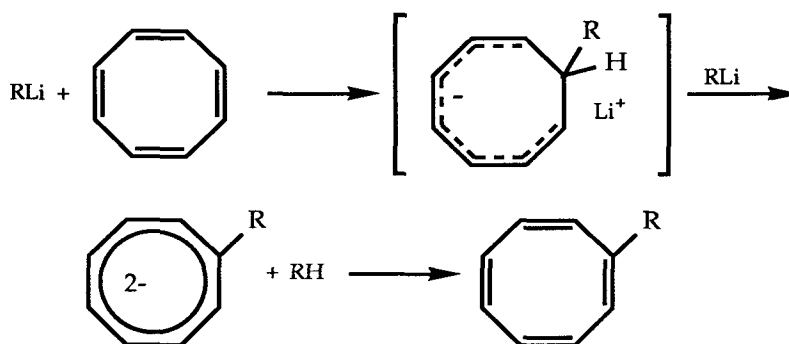
β -bromostyrene.³³⁻³⁵ BromoCOT can be treated with *n*-butyl lithium at $-78\text{ }^\circ\text{C}$ to form lithioCOT over the course of 1-2 hours. This species can then be quenched with a suitable electrophile to form a monosubstituted derivative. The series trimethylsilyl-, trimethylgermyl-, trimethylstannylCOT was prepared in this manner by Ginsburg,³⁶ following literature procedures.³⁷ Epoxides can also be used as electrophiles. LithioCOT ring-opens ethylene oxide to form β -cycloocta-tetraenylethanol.³⁸ 2-Butene oxide can also be opened, but the addition of a Lewis acid ($\text{BF}_3 \cdot \text{Et}_2\text{O}$) is required.³⁹



Scheme 2. Synthesis of monosubstituted COT's from BromoCOT.

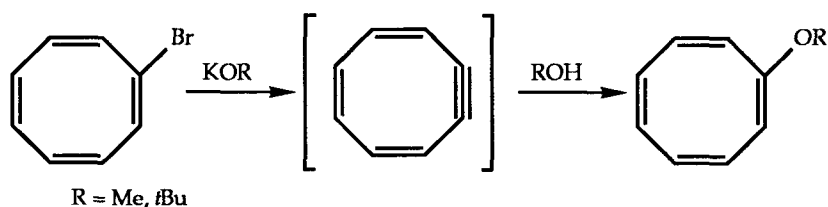
Alkyl and aryl derivatives of COT can be synthesized by generation of the alkyl/aryl organocuprate in situ at $-70\text{ }^\circ\text{C}$ followed by addition of BromoCOT and stirring for several hours at low temperature.^{32, 40} This reaction generally proceeds in an acceptable yield but requires a fourfold excess of the cuprate ($\text{R}_2\text{CuLi} \cdot \text{PBU}_3$) and thus an eightfold excess of the lithium reagent. This

requirement is undesirable when the lithium reagent must be prepared. Initially a more attractive route was via the COT dianion. Addition of two equivalents of alkyl lithium to COT generated the monosubstituted COT dianion by a reaction thought to proceed as shown in Scheme 3.^{41, 42} Oxidation of the dianion to the neutral species was reported to yield the monosubstituted derivative. This route uses COT instead of bromoCOT, which has to be prepared, and requires only two equivalents of lithium reagent as opposed to eight.



Scheme 3. Monosubstituted COT derivatives via COT dianion chemistry.⁴¹

Alkoxy derivatives of COT are also synthesized from bromoCOT. In this reaction, an alkoxide acts as a base, generating the triene-yne of COT. The alcohol formed is then thought to re-add across the triple bond (Scheme 4).⁴³



Scheme 4. Synthesis of alkoxyCOT's.

Results and Discussion

The purpose of this chapter is to discuss the synthesis of different polymers. Later chapters will be devoted to the discussion of the effect of the side group on properties such as conductivity, crystallinity, solubility, and the optical properties of the polymer. As a result, the discussion here will be restricted to the characterization of the polymer only as it relates to the synthesis. This includes polymer molecular weight and structural characterization that provides evidence that the polymerization reaction produced the desired product. The full structure-property study includes some additional polymers such as poly-*t*-butylCOT and poly-trimethylsilylCOT. Their syntheses and a full discussion of their properties are described elsewhere.³⁶

A. Monomer synthesis

Monomers were synthesized using procedures based upon those discussed in the introduction. Several modifications were necessary before these syntheses were successful in our hands. The organocuprate route was by far the most reliable. It was effective for all the syntheses attempted except for that of isopropylCOT, which failed for unknown reasons. Because of the large excess of cuprate and thus lithium reagent required in this synthesis, the dianion route was attempted whenever possible, as in the synthesis of cyclopentylCOT. However, this route also did not work exactly as described in the literature. Closer examination of the procedure⁴¹ revealed that all syntheses were performed on a small (4.4 mmol) scale and the products purified by preparative VPC. The oxidation was accomplished in the literature using air. The authors specifically claim not to have observed cyclooctatrienes upon workup. However,

we found that this route did not give complete oxidation before hydrolysis and resulted in the formation of cyclooctatrienes, an unacceptable side product since ROMP of this species along with COT would produce a polyacetylene containing undesirable sp^3 defects. Moreover, the authors noted that air oxidation resulted in a lowered yield of product as evidenced by higher yields of cyclooctatrienes if the mixture was hydrolyzed before oxidation. Thus, we preferred to use a small excess of ethereal iodine to oxidize the dianion and produced certain COT derivatives, most notably *sec*-butylCOT, in moderate yield, but also on a large scale. In some cases, this reaction failed to generate a dianion, most notably when R = cyclopropyl. In others (R = isopropyl), a small amount of triene was detected by GC/MS even after careful oxidation. This impurity could be removed, however, by treatment of the mixture with dicyano dichloroquinone (DDQ). Since the organocuprate route can not be readily performed on a large scale, dianion chemistry has recently been used in larger-scale syntheses.

Synthesis of alkoxy-substituted COT derivatives also proceeded as detailed before. Although the original synthesis was reported using dimethylsulfoxide as a solvent, it was found that the use of tetrahydrofuran provided higher yields and a much easier workup.

B. Polymerization

In all cases described here, polymerization was readily achieved, provided that the monomer was a liquid. In the case of *p*-methoxyphenylCOT, a solid, it was necessary to dissolve the monomer in a minimum of solvent (toluene). Despite efforts, it was difficult to obtain reproducible polymerization results. In some trials, a black-tacky material was recovered and was shown by ^1H NMR to

be almost completely composed of what appeared to be back-biting product (anisole) and residual monomer suspended in a small amount of polymer. In others, a free standing film was produced, but it was almost completely insoluble, even in the mostly cis form. Similar results were obtained using another solid monomer, $\text{Cp}_2\text{Fe-CH}_2\text{O-COT}$ (Cp_2Fe = ferrocenyl, side group is bound to one of the Cp rings).⁴⁴

To avoid the back-biting reaction, the polymerization was performed in neat liquid monomer whenever possible. This procedure provided the highest possible effective monomer concentration at the catalyst center. Even under these conditions, a small amount of cycloextrusion product was detected. Since tri-substituted olefins undergo metathesis much more slowly, if at all,⁴⁵ it is assumed that they will not react, and any cycloextrusion process will produce only substituted benzene. Based upon this assumption, the percentage of conversion as well as percentage of back-biting product can be calculated from NMR integration as described in the experimental section. Many of the polymers in this study were found to be mostly soluble in the predominantly cis form. When NMR solutions were prepared, however, enough insoluble material remained that filtration was necessary to reduce severe broadening in the ^1H NMR spectrum. Removal of this polymeric material prohibited an accurate calculation of either of these quantities. Thus, these data are presented in Table 1 only for completely soluble polymers.

Table 1. Percentage of conversion and percentage of back-biting product for some soluble poly-RCOT's.

R	% Conversion	% Back-biting
s-Butyl	89	16
Isopropyl	91	2
Cyclopentyl	86	4

As a result of this back-biting side reaction, elemental analysis data for an as-synthesized polymer film reveals only that no monomer or catalyst was lost to the environment during the polymerization. It is possible to wash the film to remove the catalyst,¹⁹ but this act also removes the R-benzene, thus changing the side-chain/main-chain mass ratio of the mixture in an unpredictable way. While the amount of back-biting in the polymer can be determined by ¹H NMR integration, this procedure is not sufficiently accurate to calculate a meaningful elemental composition.

Two catalysts were employed in this study: catalyst 2, first synthesized by Schrock and co-workers,⁶ and catalyst 7, synthesized by Lynda Johnson in the Grubbs group.⁴⁶ Both show qualitatively the same metathesis activity under the conditions described in the experimental section. Molecular weights of the resulting polymers are similar for each of the two catalysts.

In all cases, polymers were obtained as films. These films were generally strong and flexible. They could be folded in half without breaking. As mentioned before, initially synthesized, predominantly cis polymer films were black. After isomerization, the predominantly trans polymer films were green-gold and shiny. The simplest evidence for this cis/trans isomerization comes

from the optical-absorption spectra. Optical-absorption maxima in the visible for dilute solutions of these polymers are similar to those for polyacetylene in the solid state.

Polymers containing *n*-alkyl side chains, even with a length of 18 carbons (poly-octadecylCOT) were found to be mostly soluble in the *cis* form, but almost completely insoluble in the *trans* form. It appears that the steric bulk of the side chain at the position adjacent (α) to the double bond determines the polymer's solubility. Thus, poly-neopentylCOT and poly-2-ethylhexylCOT ($R_\alpha = -CH_2-$) have a solubility behavior much like the poly-*n*-alkylCOT polymers ($R_\alpha = -CH_2-$ also). Basically, the same behavior is observed for alkoxy ($R_\alpha = -O-$) and phenyl-substituted derivatives. Polymers containing a secondary ($R_\alpha = -CHR'R''$) or tertiary ($R_\alpha = -CR'R''R'''$) substituent adjacent to the double bond are soluble in both the predominantly *cis* and predominantly *trans* form. These polymers could be fully characterized in solution.

The solubility of the first class of polymers (e.g. $R_\alpha = -CH_2-$) is by no means clear-cut. They are "mostly soluble" in the *cis* form. This solubility ranges from *cis*-poly-*n*-butylCOT, where the majority of the material remains behind when a suspension containing 1 mg of polymer per mL of solvent (THF or toluene) was filtered to *cis*-poly-neopentylCOT, where almost all of the material dissolved. In all cases, samples were difficult to filter (0.5 μm filter). All contained some insoluble material. No major differences in solubility were observed when polymer samples were placed into toluene, THF, or methylene chloride. Samples tended to isomerize and precipitate or aggregate in solution. Thus, it was important to obtain molecular weight data as quickly as possible after synthesis and dissolution since this isomerization/precipitation could be

unpredictable. For example, in two trials under identical conditions, neopentylCOT was polymerized using catalyst 7. In the first trial, after one hour, polymer films were dissolved in THF and found to be quite insoluble. Black solutions filtered to give an orange-black material that had a low molecular weight by GPC ($M_n = 4000-5000$). In the second trial, after one hour, polymer films were dissolved in THF and found to be almost completely soluble. Black solutions filtered to give a green-black solution containing a much higher molecular weight material (reported in Table 2 below). This solution isomerized under inert atmosphere within a day to form a blue suspension, which could not be filtered through a 0.5 μm filter. Solutions of cis polymer can be stored for months in the dark at $-50\text{ }^\circ\text{C}$ without isomerization or loss of solubility. Thus, they do serve as soluble "precursors" for trans polymer and are of interest in their own right as soluble, conjugated polymers.

Although Ginsburg has determined that little isomerization occurs in the solid state in poly-trimethylsilylCOT,³⁶ it was found that films of poly-RCOT's containing an α -methylene group become much less soluble over the course of 1-2 days. These films eventually become almost completely insoluble except for a small amount of purple or blue material that leaches out of the film. A week after synthesis differential scanning calorimetry of these films reveals no exotherm assigned to cis/trans isomerization. Thus, isomerization does appear to occur in the solid state in these polymers.

Proton NMR data could be collected for all of the polymers in the cis form. Residual monomer and back-biting product can be identified (vide supra). For the side-chain protons, resonances similar to those of the monomer are observed but are shifted slightly downfield. A broad series of resonances between 5.6 and

7.0 ppm (C_6D_6) is observed, corresponding to protons on the main chain. All of these resonances shift downfield as the polymer isomerizes from *cis* to *trans*. This shift corresponds with the increased electron delocalization expected upon isomerization. Two resonances are observed for each of the side-chain protons in the *trans* form. These are thought to correspond to *cis-trans* and *trans-trans* diads in the polymer and are discussed more thoroughly in the next chapter. All of this NMR behavior is illustrated for R=isopropyl in Figure 4. Proton NMR spectra of isopropylCOT, *cis*-polyisopropylCOT and *trans*-polyisopropylCOT are shown for comparison. Comparison of the *cis* and *trans* NMR spectra for other soluble polymers is possible but is more difficult for more complicated side chains because of overlapping resonances, etc. In all cases, the methine proton (e.g., -CHRR') in the side chain is the best resolved. NMR spectra for the insoluble-*trans* polymers display similar features to those observed in *cis*-polyisopropylCOT and are otherwise unremarkable.

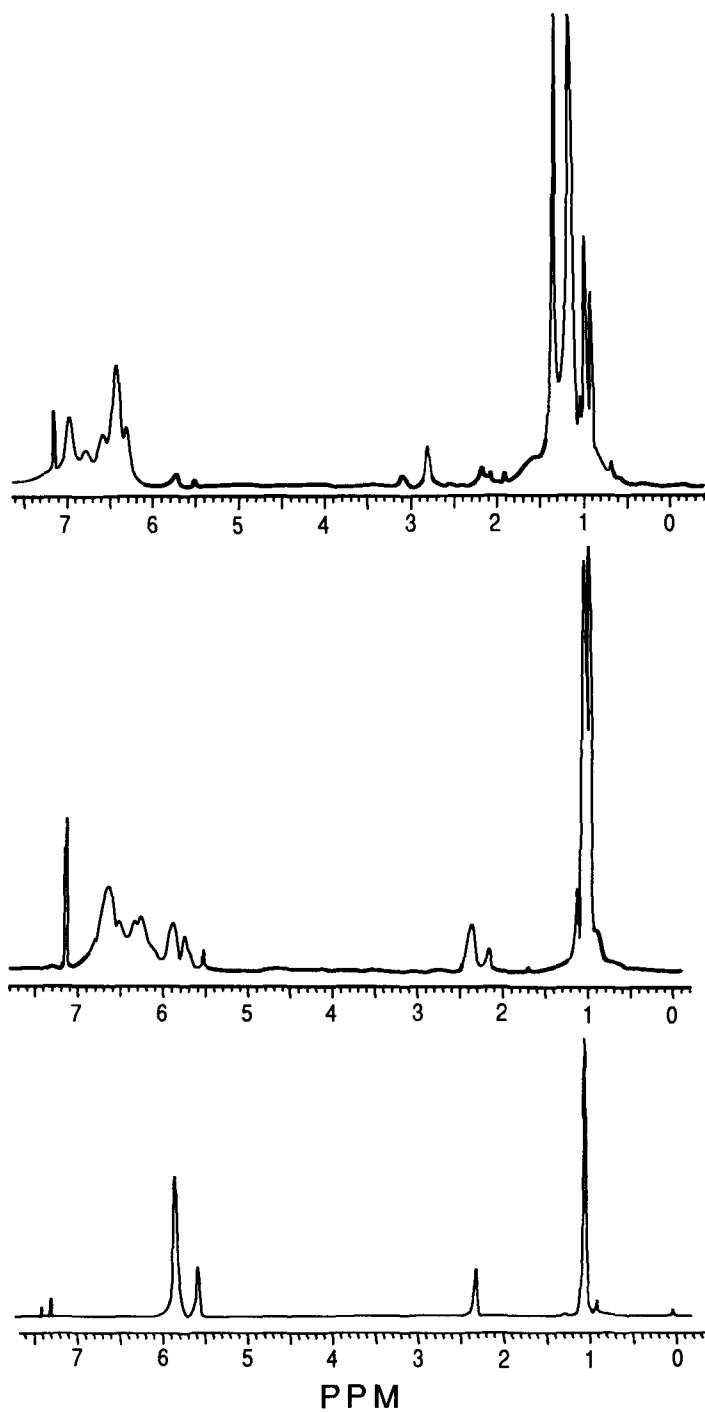


Figure 4. ^1H NMR spectra of (bottom) isopropylCOT, (middle) *cis*-poly-isopropylCOT, (top) *trans*-poly-isopropylCOT.

C. Polymer molecular weight

At a monomer/catalyst ratio of 150:1, it was always possible to synthesize a high molecular weight polymer appropriate for use in this study. Number average (M_n) and weight average (M_w) molecular weights as determined by GPC⁴⁷ are listed in Table 2. These molecular weights are versus polystyrene standards and are thus relative molecular weights. However, even for a large correction factor (for example, 0.2 times polystyrene), the determined molecular weights are high enough to suggest strongly that these samples are not oligomeric in nature. Polymers with small side groups (R = methyl, R = methoxy) were not sufficiently soluble for GPC. These molecular weight data are reported for polymers synthesized with catalyst 7 at a monomer/catalyst ratio of 150:1.

Table 2. Molecular weights (GPC) of cis polymers.

R	M _n (x 10 ³)	M _w (x 10 ³)	PDI
<i>n</i> -Butyl	2.9	13.8	4.7
<i>n</i> -Octyl	47	111	2.5
<i>n</i> -Octadecyl	14	46	3.2
Neopentyl	93	132	1.4
2-Ethylhexyl	238	360	1.5
<i>t</i> -Butoxy	252	341	1.4
Phenyl	233	345	1.5
<i>s</i> -Butyl	24.8	49.5	2.0
Isopropyl	10.0	58.0	5.7
Cyclopentyl	16.0	121.7	7.6
Cyclopropyl	20.4	52.4	2.6

Several of these molecular weights are different from those reported in the literature.^{48, 49} It was determined that the amount of material that can be solubilized was dependent upon the age of the polymer sample. For example, if a sample of *cis*-poly-*n*-octylCOT remained in the drybox at room temperature for one week, much of the resulting material was insoluble. This behavior will be attributed to facile isomerization to the insoluble trans isomer, even in the solid state, rather than to cross-linking, since a copolymer synthesized from 50% trimethylsilylCOT/50% *n*-octylCOT was found to be soluble as long as it remained under inert atmosphere (Appendix I, Chapter 3). For polymers that were soluble in both the cis and trans forms, an increase molecular weight versus polystyrene was observed upon isomerization. Presumably, the polymer chains became more rigid upon isomerization, and the subsequent increase in

hydrodynamic radius is reflected as an increase in apparent molecular weight. In order to be as consistent as possible, the molecular weights reported here are for polymer samples dissolved in the chromatography solvent within one hour after synthesis. Thus, they are presumed to be mostly cis in configuration.

In order to determine the effect of catalyst and monomer/catalyst ratio upon the molecular weight and distribution of the resulting polymer, *s*-butylCOT was polymerized with both **2** and **7** at various monomer/catalyst ratios. The results of this experiment are displayed in Table 3. In this experiment, ultraviolet absorption (UV) detection at 360 nm was employed, as it was much more sensitive to low and high molecular weight tails in the chromatogram. Simultaneous refractive index (RI) detection showed a much less sensitive response to molecular weight, higher values for M_n , lower values for M_w , and substantially smaller polydispersities. The data indicate that molecular weight is generally insensitive to monomer/catalyst ratio. However, at low ratio, polydispersities are generally broader, perhaps because depletion of monomer (or at least the local concentration of monomer at the propagating center) effectively terminates the polymerization. Large polydispersities suggest a slow initiation rate relative to propagation rate. However, competing cycloextrusion should be more facile as the monomer depletes, and this effect will also influence polydispersity. Catalyst **2** produced polymers with lower polydispersities. However, THF was added to this catalyst before polymerization and not to catalyst **7**, so conclusions on the relative initiation rates of the two different carbenes are not warranted. This statement applies to relative amounts of back-biting and conversion as well. On the basis of observations of a number of polymerizations, differences of $\pm 10\%$ in these numbers are probably in the range of experimental error. Catalyst **7**, with a molecule of THF precoordinated to the

metal center, was preferred since it reacted at a reasonable and generally reproducible rate. Catalyst 2 reacts too quickly without added THF to be convenient. Overall, under these conditions, neither catalyst offers control over molecular weight. With the use of various Lewis bases, it may be possible to tailor relative rates of initiation and propagation and effect some control.

Table 3. A comparison of polymerization conditions using *s*-butylCOT and catalysts 2 and 7.

Catalyst	M/Ca	M _n ^{b,c}	M _w ^{b,c}	PDI ^b	% Conv ^d	% BB ^{d,e}
7	50:1	15.6	221.4	14.2	95	15
7	100:1	15.8	473.0	29.9	95	11
7 ^f	150:1	14.7	174.6	11.9	89	16
7	200:1	13.9	160.3	11.5	92	11
2	50:1	7.7	68.2	8.8	88	8
2	100:1	10.5	81.5	7.7	72	16
2	150:1	14.0	71.5	5.1	98	7
2	200:1	13.1	54.8	4.2	98	8

^aMonomer to catalyst ratio (mol/mol) ^bFor as-synthesized, high-cis polymer
^c(MW × 10³) ^dBy ¹H NMR (vide supra) ^ePercentage of back-biting product.
^fMolecular weight values here are different from those in Table 2, possibly because of the difference in the mode of detection.

GPC traces were rarely Gaussian in shape. Often the trace contained a low molecular weight fraction. If this distribution is bimodal, molecular weights are close together. Also, hydrodynamic radius (stiffness) of the polymer chain will have an effect on the calculated molecular weight versus polystyrene. It is noticeable that the apparent molecular weight increases upon cis/trans isomerization (e.g., for R = *s*-butyl), suggesting an increase in hydrodynamic radius. Also, aggregation behavior of these polymers remains unexplored,

although aggregation is strongly indicated upon isomerization for some of the polymers. This uncertainty could be addressed by light scattering measurements. Light scattering on *cis*-poly-*t*-butylCOT³⁶ indicated that the polymer had a weight average molecular weight of approximately 20,000 (120 monomer units). However, this polymer is relatively nonconjugated and displays poor electrical properties. It also does not absorb the light used in the light scattering experiment (632.8 nm). All of the polymers described here absorb in this region and attempts to perform light scattering measurements upon them failed for this reason. This singular molecular weight measurement does confirm the conclusion from GPC results that the COT ring system can be polymerized by ROMP to give a high molecular weight polymer.

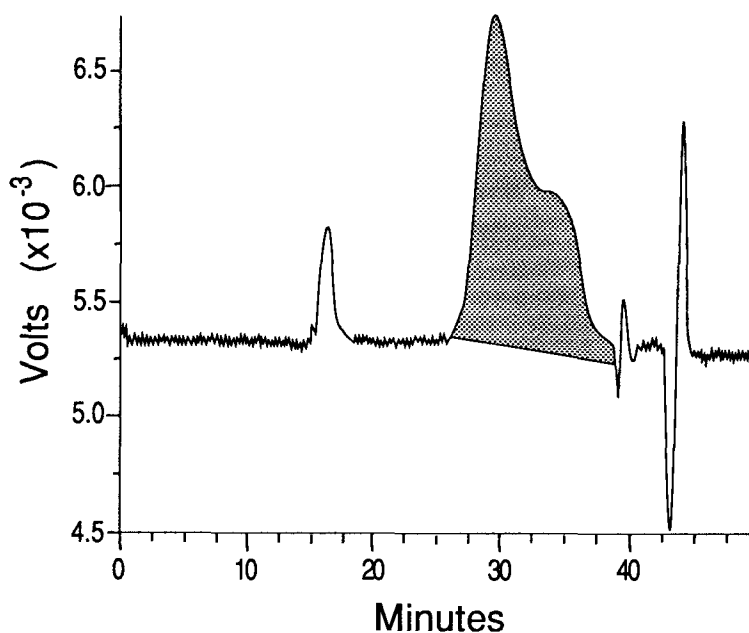


Figure 5. A typical gel permeation chromatogram. The molecular weight distribution is often bimodal although often not reproducibly so. The high molecular weight peak has been shown to be an artifact of the instrument employed.

For sufficiently high molecular weight samples ($M_n > 10000$ versus polystyrene standards), no observed polymer property had any noticeable dependence upon molecular weight. In some cases (*trans*-poly-*n*-alkylCOT polymers, especially R = *n*-butyl and *n*-octyl) extremely small amounts of oligomers could be separated out by column chromatography (THF eluent) that differed in color and showed molecular weights of $M_n < 5000$ versus polystyrene (UV detection @ 560 nm). However, much less than 0.1 mg of material was collected and further characterization ($^1\text{H NMR}$) was attempted but was not successful.

Some of the polymers with unusual solubility behavior were chlorinated and chromatographed. Chlorination is expected to reduce the stiffness of the poly-olefin chain somewhat, but it will also increase the actual molecular weight of the polymer. These results indicate that these polymers contain a substantial number of monomer repeat units. Unfortunately, chlorination of poly-COT (i.e., R = H), did not result in dissolution of the polymer, although the suspended polymer turned almost completely white in color.

Table 4. Polymer molecular weights after chlorination.

R	$M_n (\times 10^3)$	$M_w (\times 10^3)$	PDI
<i>n</i> -Butyl	14.3	120	8.4
<i>n</i> -Octyl	32.3	146	4.5
Neopentyl	38.0	104	2.7

Again, nonuniform molecular weight distributions with low molecular weight fractions were observed. The molecular weight of poly-*n*-butylCOT is

much higher after chlorination. Presumably, the high molecular weight fraction of this polymer was originally insoluble and has been solubilized. In the case of poly-*n*-octylCOT and poly-neopentylCOT, molecular weights versus polystyrene actually decreased.

D. Raman spectroscopy as structure proof for a polyconjugated chain

A *trans* polyene or *trans*-polyacetylene chain possesses local C_{2h} symmetry. Two strongly resonance-enhanced symmetric stretches are observed in the Raman spectrum, and these were found in Raman spectra of all of the polymers described here. These stretches are assigned as $A_g(\text{C-C}) (\nu_1)$ and $A_g(\text{C=C}) (\nu_2)$.⁵⁰ They are the best obtainable evidence for a conjugated chain since NMR resonances are typically broad and inconclusive and IR stretches, observed at 740 cm^{-1} for *cis*-polyacetylene and 1015 cm^{-1} for *trans*-polyacetylene⁵¹ are obscured by stretches in the side groups of most of these polymers. The exact position of these Raman bands can be influenced by the degree of conjugation of the polymer and the excitation wavelength employed. At this stage of characterization, it is enough to point out that the bands are in the correct region to conclude that these polymers contain highly conjugated polyacetylene backbones. These Raman bands are for the *trans*-polyacetylene chain. We have not observed a Raman spectrum for *cis*-polyacetylene. It is thought that the light and/or heating that is due to the laser isomerizes the samples. Attempts at obtaining low-temperature (77 K) Raman spectra have so far been unsuccessful for experimental reasons. Also, Raman spectra for poly-phenylCOT are inconclusive and are not reported since they contain several stretches that are due to the phenyl ring in the region of interest.

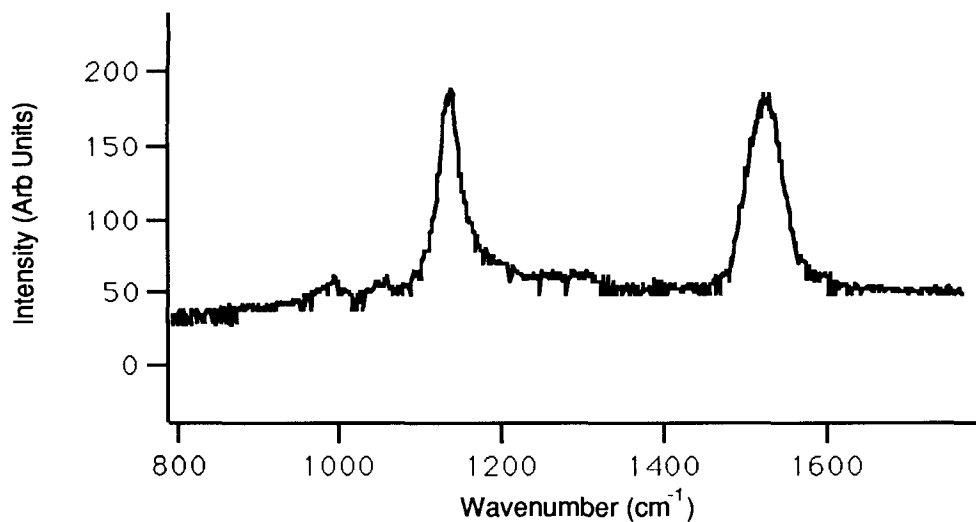


Figure 6. Typical Raman spectrum of poly-RCOT.

Table 5. Raman Data.

R	$\nu_1 A_g(\text{C-C}) (\text{cm}^{-1})$	$\nu_2 A_g(\text{C=C}) (\text{cm}^{-1})$
Methyl	1126-1132	1516
<i>n</i> -Butyl	1132	1514
<i>n</i> -Octyl	1114-1128	1485
Neopentyl	1131	1509
2-Ethylhexyl	1128	1507
Methoxy	1126-1128	1530
<i>t</i> -Butoxy	1121	1507
<i>s</i> -Butyl	1125-1128	1512
Isopropyl	1129	1527
Cyclopentyl	1131	1533
Cyclopropyl	1125 ^a	1515 ^a
<i>t</i> -Butyl	1147	1539-1547
TMS	1132	1532

^aOnly a very weak signal was observed.

E. Oxidative Stability

Polyacetylene is known to be unstable towards air oxidation.^{52, 53} Some increase in stability has been achieved by encapsulating polyacetylene films,⁵⁴ or by the addition of antioxidants,⁵⁵ but these efforts have not achieved long-term (months to years) stability. The polyacetylenes in this study were also found to be unstable. Nevertheless, the rigorous exclusion of air in samples was not found to be necessary when performing routine characterization such as GPC or measuring absorption spectra. Dilute polymer solutions were observed to lose their color over the course of 6-12 hours, so no characterization was performed on samples exposed to the air for more than a few minutes.

Experimental

Instrumentation. All syntheses are air- and moisture-sensitive and were performed using standard Schlenk techniques under argon purified by passage through columns of BASF RS-11 (Chemalog) and Linde 4Å molecular sieves. Polymerizations and subsequent handling of polymer films and preparation of polymer solutions were done in a nitrogen-filled Vacuum Atmospheres drybox. NMR spectra were recorded with either a JEOL FX-90Q (89.60 MHz ¹H; 22.51 MHz ¹³C), a Bruker AM-500 (500.14 MHz ¹H, 125.13 MHz ¹³C) or a JEOL GX-400 (399.65 MHz ¹H, 100.40 MHz ¹³C) spectrometer. Chemical shifts were referenced to the chemical shift of the residual protons of the solvent with respect to tetramethylsilane. Ultraviolet-visible absorption spectroscopy was performed on either an HP 8451A or an HP 8452A diode array spectrophotometer. Low-temperature optical spectra were obtained by placing a solution in an NMR tube

into the window of a clear-quartz finger Dewar flask filled with a dry ice/acetone slurry. Gas chromatography analyses (VPC) were performed on a Shimadzu GC-Mini-2 flame-ionization instrument with a 50 m capillary column and a Hewlett-Packard model 339A integrator. Low-resolution mass spectra were obtained on a Hewlett-Packard Series 5970 mass selective detector in conjunction with a Series 5890 GC equipped with a 15 m SE-30 capillary column. Preparative VPC was performed on a Varian 920 Aerograph with a thermal conductivity detector equipped with a Hewlett Packard 7127A strip recorder. Thin-layer chromatography (TLC) was performed on precoated TLC plates (silica gel 60 F-254, EM Reagents). Flash chromatography was by the method of Still et al.,⁵⁶ using silica gel 60 (230-400 mesh ATM, EM Reagents). Elemental analysis was determined at the analytical facilities of the California Institute of Technology. Gel permeation chromatography was performed on one of two instruments: a homemade instrument employing three Shodex size exclusion columns, model numbers KF-803, KF-804, and KF-805 (70,000, 400,000, and 4,000,000 MW polystyrene exclusion limit, respectively), an Altex model 110A pump and a Knauer differential refractometer and a Kratos UV detector (detection at the visible absorption maximum of the polymer sample), with CH_2Cl_2 as an eluant at a flow rate of 1.5 mL/min, or a Waters GPC-120C with THF as an eluant. Molecular weights are reported relative to narrow molecular weight polystyrene standards. GPC samples (0.5 wt%) were filtered through a 0.5 μm filter prior to injection. Static light scattering data were obtained by Glen Heffner and Dale Pearson (UC Santa Barbara). Resonance Raman spectra were obtained using 488 nm excitation from an argon-ion laser source using two different setups. The first setup employed a SPEX monochromator, a power source of 300-330 mW, and each sample was referenced to the known absorption frequencies of a CCl_4 or silicon sample. Data on the second setup were collected

by Hyun Chae Cynn in Dr. Malcom Nicol's group at UC Los Angeles. This setup employed a Princeton Instrument IRY 1024/G optical multichannel analyzer that was sensitive enough to permit employment of a much lower incident power (≈ 50 mW). In this setup, the wavelength scale of the detector was calibrated using diamond and calcite samples. In both cases, samples were polymer films enveloped between two thin glass plates (biological cover slips) or were polymer films on a glass substrate. It was found that scattering the light directly off the polymer films gave consistently higher signal-to-noise ratios. No attempt was made to cool the sample during analysis.

Materials: Pentane, tetrahydrofuran, toluene and diethyl ether were distilled from sodium benzophenone ketyl. Methylene chloride and chloroform were vacuum-transferred from calcium hydride. COT was purchased from Strem or was received as a gift from BASF and was distilled from calcium hydride before use. All reagents were purchased from Aldrich unless otherwise noted.

Monomer Syntheses:

Bromocyclooctatetraene and methyl cyclooctatetraene were synthesized by the method of Gasteiger et al.³² $[n\text{-Bu}_3\text{P}\cdot\text{CuI}]_4$ ⁵⁷ was synthesized as described in the literature. MethoxyCOT and *t*-butoxyCOT were synthesized as described in the literature⁴³ except that THF was used as the solvent for the reaction instead of DMSO. *p*-MethoxyphenylCOT and cyclopropylCOT were synthesized as described in the literature.⁴⁰ The tungsten metathesis catalyst, $\text{W}(\text{CH}(t\text{-Bu}))(\text{N}(2,6\text{-}(i\text{-Pr})_2\text{C}_6\text{H}_3)(\text{OCMe}(\text{CF}_3)_2)_2$, (2) was prepared by E. J. Ginsburg and S. R. Marder using literature methods.⁶ Their generous gift of catalyst is appreciated and S. C. Virgil is gratefully acknowledged for the

preparation of catalyst precursors. The Tungsten catalyst $W(\text{CH}(o\text{-MeOPh}))(\text{NPh})(\text{OCMe}(\text{CF}_3)_2)_2 \cdot \text{THF}$, (7) was a generous gift by L. K. Johnson, and its preparation is described in the literature.⁴⁶

AlkylCOT derivatives (except for methylCOT) and phenylCOT were synthesized from the appropriate alkyl or aryl lithium, $[n\text{-Bu}_3\text{P} \cdot \text{CuI}]_4$, and bromocyclooctatetraene in a procedure described below. *n*-Butyl lithium, *s*-butyl lithium, and phenyl lithium were purchased from Aldrich as 1-2 M solutions in diethyl ether. *n*-octyl lithium, *n*-octadecyl lithium, 2-ethyl hexyl lithium and cyclopropyl lithium were prepared from the corresponding alkyl bromide and lithium metal in a procedure similar to that described by Brandsma and Verkruijsse⁵⁸ for the preparation of *n*-butyl lithium, except that after reaction is complete, the solution was filtered through a pad of Celite into a flask equipped with a sidearm stopcock, and the volume of the solution was not adjusted. Neopentyl lithium was synthesized as described in the literature,⁵⁹ and secondary alkyl lithiums (isopropyl lithium, cyclopentyl lithium were synthesized in the same manner using the appropriate alkyl chloride.

A representative procedure for the synthesis of an alkylCOT is as follows: At -30 °C, 230 mL (0.313 moles) of a 0.66 M solution of octyl lithium in diethyl ether was added via cannula with stirring to 60.4 g (39.1 mmol) of $[n\text{-Bu}_3\text{P} \cdot \text{CuI}]_4$ that had been dissolved in ca. 100 mL of diethyl ether. This mixture was stirred for ca. 1 hour. A solution of 7.04 g (39.1 mmol) of bromocyclooctatetraene dissolved in ca 50 mL of diethyl ether was added dropwise. This solution was stirred overnight at -40 °C. The flask was then allowed to warm over the course of ca. 2 hours to -10 °C. Upon reaching this temperature, the flask was cooled to -78 °C and oxygen was bubbled through the solution for 5 minutes. Solution was

rewarmed to $-10\text{ }^{\circ}\text{C}$ and carefully hydrolyzed with a saturated ammonium chloride solution. The blue aqueous layer was separated from the yellow-green organic layer, washed with diethyl ether, and the organics were dried (MgSO_4) and concentrated. A substantial amount of material remained. The organics were collected by Kugelrohr distillation and consisted primarily of the product and R-R (in this case, $n\text{-C}_{16}\text{H}_{34}$, GC/MS m/z 226) plus a small amount of residual $n\text{-Bu}_3\text{P}$ (GC/MS m/z 202). Pure octylCOT was obtained by distillation ($75\text{-}85\text{ }^{\circ}\text{C}$, 0.02 mm) followed by flash chromatography over silica, petroleum ether eluent 5.83 g (70 %).

A representative procedure for synthesis via the COT dianion as is follows: COT (2.1 g, 20 mmol), was dissolved in 100 mL of diethyl ether and cooled to $0\text{ }^{\circ}\text{C}$. 2.5 g (50 mmol) of isopropyl lithium were transferred to a flask in the drybox and dissolved in 50 mL of diethyl ether and cooled to $0\text{ }^{\circ}\text{C}$. The solution of isopropyl lithium was added via cannula to the COT solution over the course of 10 minutes or so. A reddish color indicative of dianion formation was noticed in the flask but did not persist. After the addition was complete, the reaction flask was stirred at $0\text{ }^{\circ}\text{C}$ for 30 minutes. After approximately 10 minutes of this time, the reddish color reappeared. Meanwhile, iodine crystals (4.8 g, 1.5 equiv) were placed into a flask that was evacuated at $-196\text{ }^{\circ}\text{C}$ and refilled with argon. The iodine was then dissolved in 100 mL of diethyl ether. The dianion solution was then added at $0\text{ }^{\circ}\text{C}$ via cannula. Near the end of the addition, the dark-brown to black solution turned yellow-orange in color. The solution was warmed to room temperature, poured cautiously into water. The layers were separated and the aqueous layer was extracted with fresh diethyl ether. The organic layers were combined, dried (MgSO_4), and concentrated. Distillation ($49\text{ }^{\circ}\text{C}/250\text{ mtorr}$) produced a material that was shown to have a small amount of

isopropylcyclooctatriene by GC/MS (m/z 148 [parent], 105 [base]). This procedure did not always yield a monosubstituted COT with this contamination, however.

A representative procedure for removal of a triene impurity from a monosubstituted COT derivative is as follows: A mixture of *i*-propylCOT and *i*-propylcyclooctatriene (approx 3 g) was added to a slurry of dicyano-dichloroquinone (DDQ) in 50 mL of dry benzene. This mixture was stirred under argon at room temperature for 2 hours. The mixture was then poured onto a flash chromatography column and eluted with petroleum ether. The resulting solution was concentrated and redistilled to produce a product that showed little or no triene (< 1 %) by GC/MS (total ion count integration).

***n*-ButylCOT** ^1H NMR (400 MHz, CDCl_3) δ 5.67 (br, 6H, COT), 5.43 (s, 1H, COT), 1.93 (t, $J = 7.0$ Hz, COT- CH_2), 1.26 (br, 4H - CH_2CH_2 -), 0.79 (t, $J = 7.1$ Hz, 3H, - CH_3); $^{13}\text{C}\{^1\text{H}\}$ NMR (22.5 MHz, CDCl_3) δ 144.72, 134.64 (br), 131.85, 131.32 (br), 128.28, 126.13, 37.42, 30.73, 22.22, 13.90; MS m/z 160 [parent], 131, 117 [base], 103, 91, 78; m/e calcd 160.1252, found 160.1246, $\Delta = -3.8$ ppm.

OctylCOT ^1H NMR (500 MHz, CDCl_3) δ 5.74 (br, 6H, COT), 5.53 (s, 1H, COT), 2.02 (t, $J = 7.4$ Hz, 2H, COT- CH_2 -), 1.38 (br, 2H), 1.30 (br, 10H, - CH_2 -), 0.88 (t, $J = 6.8$ Hz, 3H, CH_3); $^{13}\text{C}\{^1\text{H}\}$ NMR (22.5 MHz, CDCl_3) δ 144.72, 134.32 (br), 131.85, 131.27 (br), 126.72, 126.07, 37.75, 31.90, 29.43, 29.30, 29.17, 28.52, 22.67, 14.03; MS m/z 216 [parent], 187, 159, 131, 117 [base], 103, 91, 78; m/e calcd 216.1878, found 216.1870, $\Delta = -3.7$ ppm.

OctadecylCOT ^1H NMR (500 MHz, CDCl_3) δ 5.74 (br, 6H, COT), 5.53 (s, 1H,

COT), 2.02 (t, $J = 7.3$ Hz, 2H, COT-CH₂), 1.37 (br, 2H), 1.26 (br, 30H, -CH₂-), 0.88 (t, $J = 6.8$ Hz, 3H, -CH₃); ¹³C{¹H} NMR (22.5 MHz, CDCl₃) δ 144.72, 134.32 (br), 131.85, 131.33 (br), 126.13 (br), 37.75, 31.97, 29.76, 29.69 (sh), 29.50, 29.37, 29.17, 28.52, 22.67, 14.03; MS m/z 357 [parent], 159, 131, 118 [base], 117, 103, 91, 78; m/e calcd 356.3443, found 356.3449, $\Delta = 1.7$ ppm.

***s*-ButylCOT** ¹H NMR (500 MHz, CDCl₃) δ 5.79 (br, 6H, COT), 5.53 (s, 1H, COT), 2.10 (sex, $J = 7.0$ Hz, 1H, COT-CH), 1.30 (br, 2H, -CH-CH₂-CH₃), 1.00 (d, $J = 7.0$ Hz, 3H, -CH-CH₃), 0.87 (br, 3H, -CH₂CH₃); ¹³C{¹H} NMR (125 MHz, CDCl₃) δ 148.58, 132.33, 131.85, 131.74, 131.59, 131.53, 130.52, 125.26, 43.63, 28.21, 19.84, 12.01; MS m/z 160 [parent], 131 [base], 115, 104, 91, 77; m/e calcd 160.1252, found 160.1250, $\Delta = -1.3$ ppm. Anal. Calcd. for C₁₂H₁₆: C, 89.94; H, 10.06. Found: C, 89.75, H, 9.98.

NeopentylCOT ¹H NMR (500 MHz, CDCl₃) δ 5.77 (br, 6H, COT), 5.47 (s, 1H, COT), 1.90 (s, 2H, COT-CH₂), 0.94 (s, 9H, -C(CH₃)₃); ¹³C{¹H} NMR (125 MHz, CDCl₃) δ 142.28, 137.13, 132.34, 132.25, 132.16, 131.30, 130.10, 129.82, 51.89, 31.41, 30.03; MS m/z 174 [parent], 159, 143, 129, 117 [base], 103, 91, 78; m/e calcd 174.1409, found 174.1404, $\Delta = -2.6$ ppm. Anal. Calcd. for C₁₃H₁₈: C, 89.59; H, 10.41. Found: C, 89.29; H, 10.35.

2-EthylhexylCOT Normal separation by column chromatography of the product from the dimer (5,8-diethyldodecane) was not possible. Purification was effected by preparative gas chromatography on a 15% SE-30 on HP chromasorb column using a column/injector/detector temperatures of 160/210/195 °C, respectively (53x50 μ L injections). ¹H NMR (500 MHz, CDCl₃) δ 5.76 (br, 6H, COT), 5.50 (s, 1H, COT), 1.94 (br, 2H, COT-CH₂), 1.25 (br, 9H, -CH₂- + -CH-), 0.87 (t, $J = 6.3$ Hz,

3H, -CH₃), 0.82 (t, J = 7.2 Hz, 3H, -CH₃); ¹³C{¹H} NMR (22.5 MHz, CDCl₃) δ 143.74, 134.77, 131.92, 131.14 (br), 127.43, 42.43, 37.62, 32.36, 28.85, 25.60, 23.06, 14.16, 10.72; MS *m/z* 216 [parent], 187, 159, 131, 117 [base], 103, 91; *m/e* calcd 216.1878, found, 216.1882, Δ = 1.8 ppm.

IsopropylCOT ¹H NMR (500 MHz, CDCl₃) δ 5.83 (br, 6H, COT), 5.55 (s, 1H, COT), 2.30 (sep, J = 6.8 Hz, 1H, COT-CH-), 1.03 (d, J = 6.9 Hz, 6H, -CH₃); ¹³C{¹H} NMR (22.5 MHz, CDCl₃) δ 150.50, 133.02, 131.53 (br), 130.62, 123.47, 33.61 & 35.15 (-CH-, ring inv. isomers), 22.22, 21.57 (-CH₃, ring inv. isomers); MS *m/z* 146 [parent], 131 [base], 116, 103; *m/e* calcd 146.1096, found 146.1097, Δ = 1.0 ppm.

CyclopentylCOT ¹H NMR (500 MHz, CDCl₃) δ 5.81 (br, 6H, COT), 5.55 (s, 1H, COT), 2.46 (m, 1H, COT-CH-), 1.73 (m, 2H), 1.63 (m, 2H), 1.53 (m, 2H), 1.39 (m, 2H); ¹³C{¹H} NMR (22.5 MHz, CDCl₃) δ 147.97, 133.34, 132.37, 131.59 (br), 131.01, 130.49, 47.30, 31.71, 25.27; MS *m/z* 172 [parent], 157, 143, 129 [base], 117, 104; *m/e* calcd 172.1252, found 172.1251, Δ = -0.6 ppm.

Polymer Syntheses:

All polymerizations were carried out in the drybox at ambient temperature. All polymerizations were accomplished using 150 molar equivalents of monomer to 1 molar equivalent of catalyst unless stated otherwise. In a typical polymerization, 2-3 mg of catalyst (**2** or **7**) were weighed into a tared vial and dissolved in a minimum of pentane (2-3 drops). One drop of THF was added to catalyst **2** to slow the rate of polymerization. Lewis bases will reversibly bind to the catalyst, slowing the rate of propagation considerably.²⁵ Catalyst **7** already has a molecule of THF precoordinated to the metal center, so

further addition was not deemed necessary. To this mixture, 150 ± 10 molar equivalents (≈ 150 - $250 \mu\text{L}$ depending on the monomer employed) of monomer (in all cases described here, a yellow liquid) were added, and the contents of the vial were mixed. The mixture typically began to turn a darker and darker orange-brown color within 15 seconds, signifying the onset of polymerization. Over the next minute or so, the mixture could be transferred by pipette to a glass slide or other noninteracting substrate such as a KBr die or polyethylene film. Here, the mixture hardened into a black film, which could then be removed from the substrate with a razor blade. To terminate the polymerization, a small amount of the polymer was dissolved and 50 equivalents of benzaldehyde or isovaleraldehyde were added immediately. Samples could then be filtered for study by NMR or GPC. Alternatively, films were rinsed repeatedly at 0°C with dry pentane and methanol under argon in order to remove soluble components such as residual monomer, catalyst decomposition products, and substituted benzene produced by back-biting during the polymerization. After rinsing, the films were subject to dynamic vacuum to remove solvent until a vacuum of < 1 mtorr was achieved. By rinsing at low temperature and protecting the films from light, the highest possible cis content was insured.

Procedure for chlorination of a polymer sample

A sample of the polymer (20-50 mg) was placed into approximately 30 mL of carbon tetrachloride. The polymer did not dissolve but typically was suspended as small black pieces in the solvent. Chlorine gas was bubbled through the solution with vigorous stirring at a rate sufficient to keep the solution a pale yellow-green color. The black pieces turned white at the edges and then dissolved. After dissolution, the flask was kept under a slight pressure

of argon. The color disappeared from the solution within 2-3 minutes. The solvent was removed under vacuum and the polymer sample was isolated as a white powder and used immediately for GPC.

Procedure for cis/trans isomerization

Isomerization of the polymer from a predominantly cis configuration to a predominantly trans configuration could be accomplished either thermally, photochemically, or over time by allowing polymer solutions to remain in the light at room temperature under inert atmosphere. Thermal isomerization was accomplished by heating the sample in benzene or THF at 60-80 °C (THF was superheated above its boiling point) in a tube sealed with a Kontes screw top until the visible absorption spectrum showed no change. Kinetic measurements of the rate of this isomerization as well as more detailed experiments on the isomeric composition of the polymer in the "cis" and "trans" forms are described in the next chapter.

Photochemical isomerization was accomplished at 0 °C (monitored by thermocouple and external meter in the bath) by exposure of the sample dissolved in THF or benzene to light from a Pyrex-filtered, 350 watt, medium-pressure mercury Hanovia lamp again, until no change in the visible absorption spectrum was observed (approx 6-12 hours for a ≈ 1 mg/mL sample). Overexposure resulted in a decrease in color, indicating decomposition of the material in solution. THF, toluene and benzene were suitable solvents for this experiment, but chlorinated solvents were not acceptable.

Solutions of predominantly cis polymer were found to isomerize when

permitted to sit under inert atmosphere under ambient conditions for 2-4 weeks. Decreases in optical-absorption maximum (λ_{\max}) or absorption intensity because of photodegradation were not observed when the sample was isomerized in this manner. Solutions could be stored in ambient light under inert atmosphere for months with no change.

These isomerized solutions could be recast into films that were shiny and green-gold in color. As will be described in detail in the structure-property section of this study, isomerization rendered many polymers almost completely insoluble. Nevertheless, the inhomogeneous, partially precipitated suspensions that resulted from isomerization could be recast into shiny green-gold films as well, allowing for investigation of some of the properties of completely isomerized insoluble material.

Procedure for calculation of % Conversion and % Back-biting by NMR

Figure 8 shows the olefinic region of the ^1H NMR spectrum of the product of a typical polymerization.[†] This spectrum is of the predominantly cis form of the polymer in the mixture, and although the shape of the olefinic polymer peak changes during isomerization to the predominantly trans form, it does not change the calculation shown here. The olefin region here is similar for any soluble polyacetylene derivative reaction mixture, and the calculation of percent conversion and percent cycloextrusion is done in an identical manner for all polymers.

[†] This spectrum is of polymer derived from monomer 5 in Chapter 5.

One can identify three resolved integrals in Figure 8: I_1 , I_2 , and I_3 . They are the integration of the following:

I_1 : Cycloextrusion product (5H). We do not consider the contribution by the phenyl imido group in the catalyst or the ortho-methoxy benzylidene group on the tail of the polymer, which also displays resonances in this region. Thus, we get a higher estimate of percent cycloextrusion.

I_2 : Integration of all protons on the polymer backbone plus six protons of the residual monomer (sharp peaks upfield).

I_3 : One proton of the residual monomer, based on comparison with the ^1H NMR spectrum of the monomer.

We define three variables:

X = moles of unreacted monomer

Y = moles of monomer that reacted with the catalyst

Z = moles of cycloextrusion product.

Thus, the polymers in this study are effectively copolymers of the repeat units shown in Figure 7. In this figure, repeat units are shown in the all-*trans* form. The isomeric content of the polymers is irrelevant for the calculations shown here.

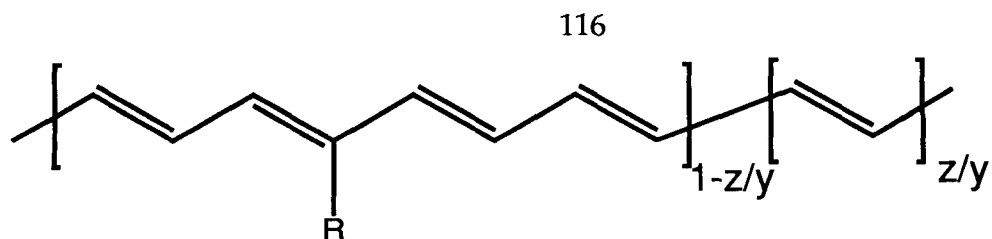


Figure 7. Repeat units contained in the polymers.

Now, we can express the three integrals in terms of X, Y, and Z:

$$I_1 = 5Z \quad I_2 = 6X + (7Y - 5Z) \quad I_3 = X$$

In the treatment above, the quantity $7Y - 5Z$ is all the olefin protons in the polymer, i.e. all the olefin protons in the monomer minus those lost to cycloextrusion product.

Given I_1 , I_2 , and I_3 , we can solve for X, Y, and Z. Then,

$$\% \text{ conversion} = \frac{Y}{Y+X}$$

$$\% \text{ back-biting} = \frac{Z}{Y}$$

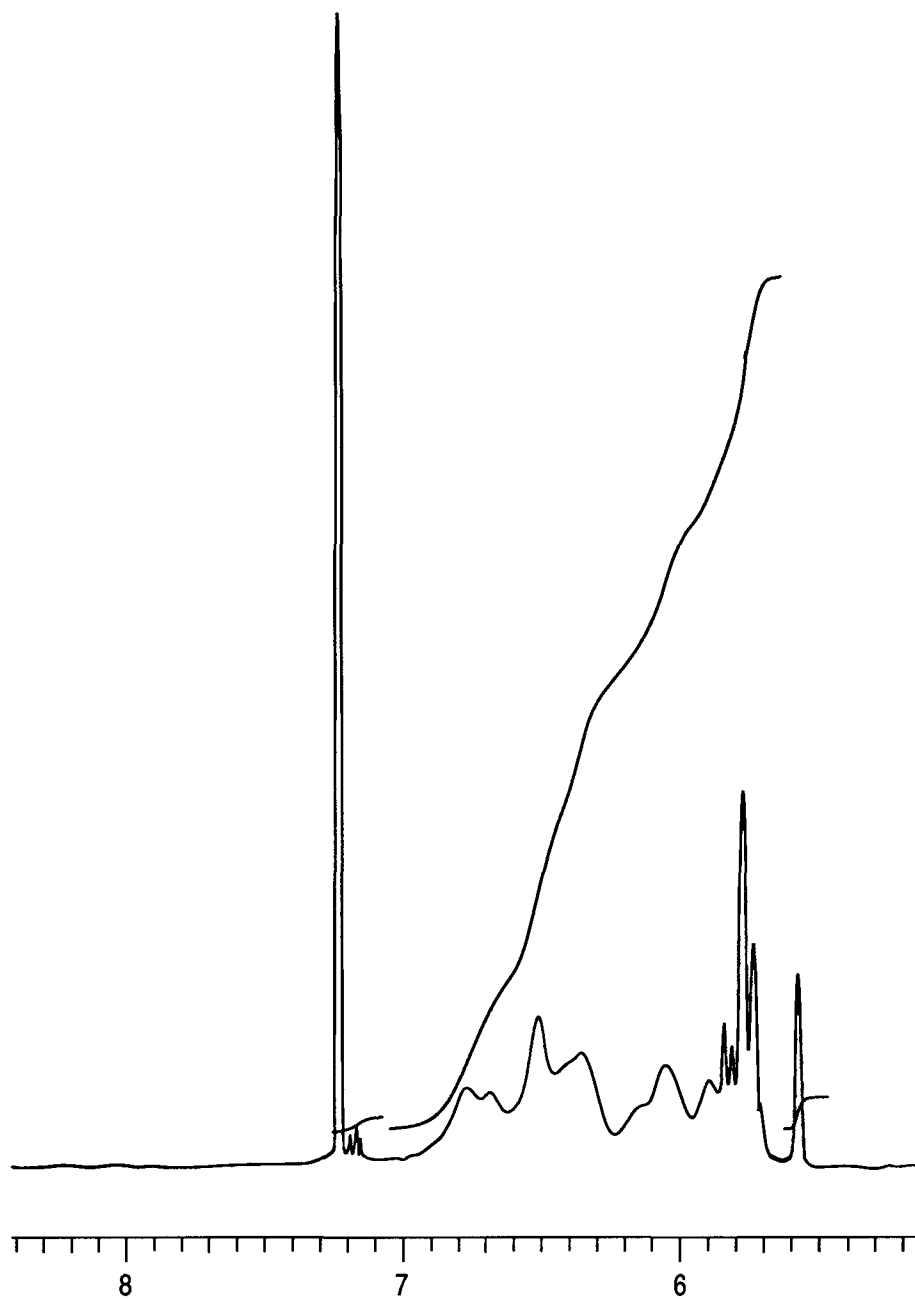


Figure 8. Typical ^1H NMR (CDCl_3) of the olefinic region of poly-R-COT.

References and Notes

- (1) Ivin, K. J. *Olefin Metathesis*; Academic: London, 1983.
- (2) Grubbs, R. H. in *Comprehensive Organometallic Chemistry*; Wilkinson, G. Ed.; Pergamon: New York, 1982; Vol. 8, pp. 499-551.
- (3) Gilliom, L. R., Ph. D. Thesis, California Institute of Technology, 1986.
- (4) Swager, T. M., Ph. D. Thesis, California Institute of Technology, 1988.
- (5) Novak, B. M., Ph. D. Thesis, California Institute of Technology, 1989.
- (6) Schrock, R. R.; DePue, R. T.; Feldman, J.; Schaverien, C. J.; Dewan, J. C.; Liu, A. H. *J. Am. Chem. Soc.* **1988**, *110*(5), 1423-1435.
- (7) For a more complete discussion, see: Grubbs, R. H.; Tumas, W. *Science* **1989**, *243*, 907-915.
- (8) Schrock, R. R.; Feldman, J.; Cannizzo, L. F.; Grubbs, R. H. *Macromolecules* **1987**, *20*, 1169-1172.
- (9) A living polymerization of norbornene has also been claimed using a tantalum-based metathesis catalyst: Wallace, K. C.; Schrock, R. R. *Macromolecules* **1987**, *20*(2), 448-450.
- (10) Wu, Z.; Grubbs, R. H. Submitted for publication in *J. Am. Chem. Soc.*
- (11) Knoll, K.; Krouse, S. A.; Schrock, R. R. *J. Am. Chem. Soc.* **1988**, *110*, 4424-4425.
- (12) Knoll, K.; Schrock, R. R. *J. Am. Chem. Soc.* **1989**, *111*(20), 7989-8004.
- (13) Klavetter, F. L.; Grubbs, R. H. *Synth. Met.* **1988**, *26*, 311-319.
- (14) Edwards, J. H.; Feast, W. J. *Polymer* **1980**, *21*, 595-596.
- (15) Bott, D. C.; Brown, C. S.; Chai, C. K.; Walker, N. S.; Feast, W. J.; Foot, P. J. S.; Calvert, P. D.; Billingham, N. C.; Friend, R. H. *Synth. Met.* **1986**, *14*, 245-269.
- (16) Schleyer, P. v. R.; Williams, J. E.; Blanchard, K. R. *J. Am. Chem. Soc.* **1970**, *92*, 2377-86.

- (17) Korshak, Y. V.; Korshak, V. V.; Kanischka, G.; Höcker, H. *Makromol. Chem., Rapid Commun.* **1985**, *6*, 685-692.
- (18) Tlenkopachev, M. A.; Korshak, Y. V.; Orlov, A. V.; Korshak, V. V. *Doklad. Akad. Nauk, Eng. Transl.* **1987**, *291*, 1036-1040.
- (19) Klavetter, F. L.; Grubbs, R. H. *J. Am. Chem. Soc.* **1988**, *110*, 7807-7813.
- (20) Schäfer-Siebert, D.; Roth, S.; Budrowski, C.; Kuzmany, H. *Synth. Met.* **1987**, *21*, 285-291.
- (21) Zuo, F.; Epstein, A. J.; Yang, X.; Tanner, D. B.; Arbuckle, G.; MacDiarmid, A. G. *Synth. Met.* **1987**, *17*, 433-438.
- (22) Eckhardt, H. *J. Chem. Phys.* **1983**, *79*(4), 2085-2086.
- (23) Yang, X. Q.; Tanner, D. B.; Arbuckle, G.; MacDiarmid, A. G.; Epstein, A. J. *Synth. Met.* **1987**, *17*, 277-282.
- (24) The previous papers involve studies on polyacetylenes in which defects are selectively introduced. A comment as to whether these defects have been placed randomly or nonrandomly has been made: Clough, S.; Tripathy, S.; Sun, X.-F.; Orchard, B.; Wnek, G. *Makromol. Chem., Rapid Commun.* **1988**, *9*, 535-538.
- (25) Klavetter, F. L., Ph. D. Thesis, California Institute of Technology, 1989.
- (26) Fray, G. I.; Saxton, R. G. *The Chemistry of Cyclo-octatetraene and its Derivatives*; Cambridge University: Cambridge, 1978.
- (27) Schroder, G. *Cyclooctatetraen*; Verlag Chemie: Weinheim, 1965.
- (28) Paquette, L. A.; Trova, M. P.; Luo, J.; Clough, A. E.; Anderson, L. B. *J. Am. Chem. Soc.* **1990**, *112*(1), 228-239.
- (29) Paquette, L. A.; Wang, T.-Z. *J. Am. Chem. Soc.* **1988**, *110*(24), 8192-8197.
- (30) Paquette, L. A.; Trova, M. P. *J. Am. Chem. Soc.* **1988**, *110*(24), 8197-8201.
- (31) Paquette, L. A.; Wang, T.-Z.; Cottrell, C. E. *J. Am. Chem. Soc.* **1987**, *109*(12), 3730-3734.
- (32) Gasteiger, J.; Gream, G.; Huisgen, R.; Konz, W.; Schnegg, U. *Chem. Ber.*

1971, 104, 2412-2419.

- (33) Huisgen, R.; Konz, W. E. *J. Am. Chem. Soc.* **1970**, 92(13), 4102-4104.
- (34) Konz, W. E.; Hechtel, W.; Huisgen, R. *J. Am. Chem. Soc.* **1970**, 92(13), 4104-4105.
- (35) Huisgen, R.; Konz, W. E.; Gream, G. E. *J. Am. Chem. Soc.* **1970**, 92(13), 4105-4106.
- (36) Ginsburg, E. J., Ph. D. Thesis, California Institute of Technology, 1990.
- (37) Cooke, M.; Russ, C. R.; Stone, F. G. A. *J. Chem. Soc., Dalton Trans.* **1975**, 256-259.
- (38) Paquette, L. A.; Henzel, K. A. *J. Am. Chem. Soc.* **1975**, 97(16), 4649-4658.
- (39) Moore, J. S.; Gorman, C. B.; Grubbs, R. H. *J. Am. Chem. Soc.* **1991**, 113(5), 1704-1712.
- (40) Harmon, C. A.; Streitwieser, A., Jr. *J. Org. Chem.* **1973**, 38(3), 549-551.
- (41) Miller, J. T.; Dekock, C. W.; Brault, M. A. *J. Org. Chem.* **1979**, 44, 3508-3510.
- (42) Alternate conditions were reported for the synthesis of *t*-butylCOT:
Miller, M. J.; Lyttle, M. H.; Streitwieser, A., Jr. *J. Org. Chem.* **1981**, 46, 1977-1984.
- (43) Oth, J. F. M.; Merényi, R.; Martini, T.; Schröder, G. *Tet. Lett.* **1966**, (27), 3087-3093.
- (44) Marder, S. R.; Tiemann, B. G. Unpublished results.
- (45) Reference 1, pp. 139.
- (46) Johnson, L. K.; Virgil, S. C.; Grubbs, R. H. *J. Am. Chem. Soc.* **1990**, 112, 5384-5385.
- (47) Odian, G. *Principles of Polymerization*; John Wiley and Sons: New York, 1981; p. 20.
- (48) Gorman, C. B.; Ginsburg, E. J.; Marder, S. R.; Grubbs, R. H. *Angew. Chem. Adv. Mater.* **1989**, 101, 1603-1606.
- (49) Gorman, C.; Ginsburg, E.; Marder, S.; Grubbs, R. *Polym. Prepr.* **1990**, 31(1),

386-387.

- (50) Kuzmany, H. *Pure and Appl. Chem.* **1985**, *57*(2), 235-246.
- (51) Gibson, H. W.; Kaplan, S.; Mosher, R. A.; W. M. Prest, J.; Weagley, R. J. *J. Am. Chem. Soc.* **1986**, *108*(22), 6843-6851.
- (52) Pochan, J. M.; Pochan, D. F.; Rommelmann, H.; Gibson, H. W. *Macromolecules* **1981**, *14*(1), 110-114.
- (53) Müller, H. K.; Hocker, J.; Menke, K.; Ehinger, K.; Roth, S. *Synth. Met.* **1985**, *10*, 273-280.
- (54) Deits, W.; Cukor, P.; Rubner, M.; Jopson, H. *Synth. Met.* **1982**, *4*, 199-210.
- (55) Benni, P.; D'Ilario, L.; Schwarz, M. *J. Mat. Sci. Lett.* **1988**, *7*, 1124-1125.
- (56) Still, W. C.; Kahn, M.; Mitra, A. L. *J. Org. Chem.* **1978**, *43*, 2923-2925.
- (57) Kauffman, G. B.; Teter, L. A. *Inorg. Synth.* **1963**, *7*, 10-11.
- (58) Brandsma, L.; Verkruijsse, H. *Preparative Polar Organometallic Chemistry*; Springer-Verlag: New York, 1987; pp. 17-18.
- (59) Schrock, R. R.; Feldman, J. D. *J. Am. Chem. Soc.* **1978**, *100*, 3359.

CHAPTER 3

PROPERTIES OF POLYMERS OF MONOSUBSTITUTED CYCLOOCTATETRAENES

Introduction

A "hunk" of polymer can be described on several different levels, ranging from macroscopic to microscopic. When "zooming in" on a polymer sample, one is first concerned with the bulk form (powder, film, etc.), then the nature of microscopic regions (bulk crystalline, microcrystalline, amorphous), and then the nature of individual polymer chains (rodlike, wormlike). The terms mentioned above are gross simplifications of what occurs in a polymer matrix. Almost all crystalline polymers contain amorphous regions, and physical properties can vary dramatically as the size of a crystalline region changes or as the degree of crystallinity of a polymer sample changes. Likewise, in discussing a conjugated polymer, it is often necessary to refer to chains as "rodlike" since these samples must be straight and flat to some extent in order to display extended conjugation. However, if one steps back and looks at a larger segment of the polymer chain, one will see that these chains are twisted on this larger size-scale. On the smallest scale, bonds can rotate or isomerize from cis to trans, angles can bend, and any of these perturbations can and will be reflected in the behavior of the polymer. Moreover, if a polymer is amorphous or dissolved in solution, it can move, and this dynamic picture must also be considered when discussing the physical properties of a sample.

Conjugated polymers are generally of interest for their unusual optical properties (linear and nonlinear) and for their ability to become good conductors, typically when oxidized or reduced. The relationship between conjugation and the nature of a polymer matrix upon these properties is the central question in this field.¹ It will be shown that the effective conjugation of monomer units in a chain, and thus these physical properties, can be influenced by features on many

size regimes. Interchain effects can be concluded to affect physical properties as well. In particular, conductivity is a property that clearly must arise from a bulk sample, since no electron or hole can traverse macroscopic dimensions travelling on only one polymer chain. Thus, the subject of this thesis, the effects of structural variation upon a polyacetylene chain, will be explored in several size regimes and under static and dynamic conditions wherever possible.

A. Intrachain Effects

Effective conjugation length.

The first issue at hand is developing a workable, useful definition of what is meant by "conjugation" in a conjugated polymer. The simplest and obviously inaccurate view of a conjugated polymer chain is that it is an infinite series of coplanar monomer units joined end-to-end. This ideal model would describe the most conjugated molecule. Now that we have the most conjugated molecule, we can consider various perturbations upon the chain and come to some conclusions about what perturbations most dramatically reduce conjugation. Any polymer molecule will not be infinitely long. What is the effect of reducing the length (or molecular weight) of a polymer upon the conjugation? Moreover, no polymer molecule is perfectly flat. Twisting the chain will reduce the conjugation as well.

In the case of polyacetylene, it has been convenient to define a quantity, typically referred to as the effective conjugation length, which relates a physical property of a sample to the degree of conjugation in that sample. It has long been observed that the lowest energy optical absorption of a polyene chain (assigned most simply as $\pi \rightarrow \pi^*$, although configuration interaction is required to most accurately describe the states in this transition) decreases in energy as the

length of the polyene increases.²⁻⁹ It has been shown¹⁰⁻¹³ that a plot of this optical-absorption maximum (λ_{\max} , nm) versus $1/n$ where n is the number of double bonds in the polyene gives a linear plot. Thus, conjugation length, n (more appropriately termed effective conjugation length) of a sample is the number of double bonds in an unsubstituted all-*trans*-polyene with the same λ_{\max} as the sample.

There are problems with this definition. The optical-absorption maximum of a polyene is somewhat dependent upon the solvent in which the spectrum is recorded. It can be dependent upon the end groups on the polyene, and this quantity is typically defined for polymer samples in which end groups probably have little effect. The best data for this definition come from *t*-butyl capped polyenes in which the endcap has a minimal electronic effect upon the π -system. Definitions based upon phenyl capped polyenes are less satisfying since the phenyl groups are conjugated with the polyene. Cyanines, in which there are heteroatoms conjugated with the ends of the polyene, are completely different molecules.¹⁴ The two heteroatoms can perturb the geometry of the entire chain. Moreover, the quantity n , as with any defined quantity, can and is easily misused. It is often stated that *cis*-polyacetylene is less conjugated than *trans*-polyacetylene. In principle, 5 *cis* double bonds can be coplanar, and if their optical absorption is of higher energy, it is unclear that they are de facto less conjugated since their topology differs from the comparable polyene of 5 *trans* double bonds. Actually, the optical-absorption maximum of a polyene with the isomeric composition (ct)_x is not very different from the same polyene of isomeric composition (tt)_x for a given chain length.¹⁵ Comparison of the absorption spectra of *cis* and *trans* isomers of other conjugated molecules reveals similar trends.¹⁶⁻¹⁸ The lowest energy optical absorption of *cis*-polyacetylene is

100 nm lower (i.e., higher in energy) than that of *trans*-polyacetylene.¹⁹ Thus, although there is still controversy in the the literature,²⁰⁻²² it is quite possible that *cis*-polyacetylene is significantly more nonplanar than *trans*-polyacetylene and the comment that *cis* is less conjugated than *trans* is accurate. Comparison of conjugation lengths between two different polymers is obviously invalid.

The functional form of this definition addresses one of the issues mentioned above. The optical-absorption maximum, since it varies with $1/n$, will asymptotically approach some limiting value as n gets large. Thus, conjugation, especially as defined here, will become less and less dependent upon chain length as that chain length increases. Interestingly enough, the infinite chain value of the optical-absorption maximum for polyenes is of lower energy than the optical-absorption maximum observed for polyacetylene. Several workers^{10, 23} have taken this observation to suggest that conformational or other defects limit the conjugation in polyacetylene to an effective conjugation length of approximately 30 double bonds. Thus, in the solid state, polyacetylene is typically not flat enough to display the lowest energy optical absorption possible.

The issue of effective conjugation length has also been addressed for polyacetylene by observing the position of the $A_g(\text{C}=\text{C})$ stretch in the Raman spectrum of the polymer. This stretch is also observed in biopolyenes²⁴ and in polymers of monosubstituted acetylenes.²⁵ Recently, Raman data have been tabulated for a number of polyenes of differing lengths,¹⁰ but before this time, workers were making arguments about the distribution of conjugation lengths in polyacetylene, given selective resonance enhancement of the polymer sample, using different excitation wavelengths in the Raman experiment.²⁶⁻³⁰ Basically, a

higher energy excitation wavelength will resonance-enhance lower conjugation-length segments in the polymer sample. By changing this wavelength and observing the change in the position of the $A_g(\text{C}=\text{C})$ stretch (and making some assumptions about the variation of the resonance-enhanced scattering cross section as a function of n), it was concluded that there is a distribution of conjugation lengths in a polyacetylene sample.³¹⁻³⁴ Furthermore, it appears that this distribution is bimodal with a population centered around 10 double bonds (thought to be the average conjugation in an amorphous region) and another population centered around 50 double bonds (thought to be the average conjugation in a crystalline region). The effective conjugation differences between crystalline and amorphous regions can be attributed to increased planarity that is due to packing in the crystalline regions. However, the optical-absorption change that is due to packing (*vide infra*) may also have an effect and could be included in an analysis as well.

The decreasing optical-absorption maximum with increasing n applies for other conjugated polymers such as polythiophene³⁵ and poly-*para*-phenylene.³⁶ In fact, much recent work has probed the evolution of properties such as oxidation/reduction potential of oligomers and conductivity and spectral signatures of carriers in oxidized or reduced oligomers as the chain length increases.³⁷⁻⁴² Many of the electrical and optical properties of relatively short oligomers ($n=6-10$) are found to be close to those in the polymer.

An appropriate and useful place for effective conjugation length to be studied is in polymers of substituted acetylenes.⁴³⁻⁴⁵ The polymerization of these monomers will result in polymers in which there is a side group attached to every other carbon on the main chain. In all cases, the effective conjugation

length of the resulting polymer is lower than that observed for polyacetylene. The cis/trans composition of these polymers is rarely probed despite the fact that it is expected to affect the optical-absorption maximum.^{46, 47} The overriding effect, however, is believed to be the steric repulsions between the side groups, resulting in twisting of the chain and lowering of the conjugation.

Deplanarization of a polyacetylene chain should not be particularly difficult. Recent calculations have suggested a barrier for complete rotation in the unsubstituted polymer to be on the order of 6 kcal/mol.⁴⁸ In most cases, conjugation length is noticeably diminished as evidenced by high-energy optical absorptions (e.g., poly-*t*-butyl acetylene is white).⁴³ In some cases, iodine-doped conductivities have been measured and were found to be many orders of magnitude lower than those found for polyacetylene ($\sigma \approx 10^{-3}$ to 10^{-5} Ω^{-1}/cm).⁴⁹⁻⁵¹

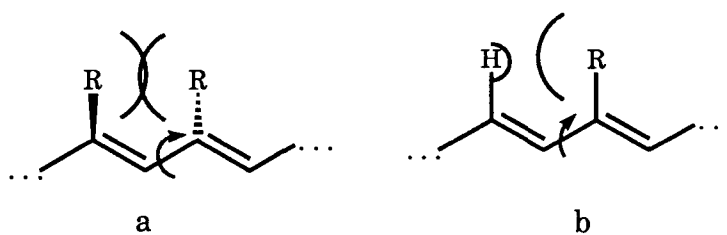
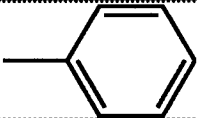
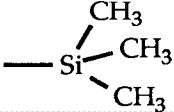
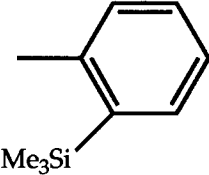

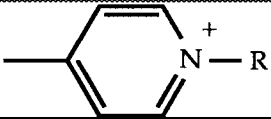


Figure 1. Steric repulsions in (a) polymers of substituted acetylenes, (b) polymers of substituted cyclooctatetraenes.

Most polymers of monosubstituted acetylenes are soluble, and a current topic of interest is the exploration of this solubility/conjugation length tradeoff. It will be demonstrated that the polymerization of monosubstituted COT derivatives produces polyacetylenes that are substituted only on the average at one of every eight carbons on the backbone. This strategy leads to a much less significant steric crowding and has resulted in soluble, substituted

polyacetylenes with the highest effective conjugation lengths measured. In fact, observation of unusual solubility behavior as the steric bulk of the side groups is systematically decreased suggests that this family of polymers reaches the limiting case of solubility in the tradeoff of conjugation length. Nevertheless, three notable efforts have recently produced polymers of substituted acetylenes that have significant conjugation lengths and are still soluble. It appears that pendant aromatic groups can turn 90° with respect to the main chain of the polymer, resulting in a minimal steric perturbation. Poly-phenylacetylene has been found to be soluble in most cases and is a red material with the highest effective conjugation length of any polymer in the family, although it is still low.⁵² Recently, it has been shown that poly-*ortho*-R-phenylacetylene (R = CF_3 ⁵³ or TMS⁵⁴) is soluble and highly conjugated.⁵⁵ Poly-4-ethynyl pyridinium salts are soluble in water or polar organics, depending upon the counterion.⁵⁶ Polyacetylene in which the side group is an acetylene displays a minimal steric perturbation upon the main chain and is reported to confer solubility while still maintaining an appreciable conjugation.⁵⁷ Further optical and electrical properties have not been reported for these polymers.

Table 1. The effect of side-group sterics upon the optical absorption of polymers of substituted acetylenes.

R	λ_{\max} (nm)	Solvent	Ref
H	≈ 650	Solid state	19
—CH ₃	290	heptane	25
	325-350	CHCl ₃	52
	292	THF	53
<i>n</i> -hexyl	290-300	hexane	56
	542	THF	57
	510	CHCl ₃	58
	450	EtOH	59

Comparison with other conjugated polymers.

An effective conjugation length can be defined for other polymers by extrapolating optical-absorption data of model oligomers of the polymer. The sensitivity of effective conjugation towards chain twisting is not as dramatically

observed with most other conjugated polymers, however. Although the solubility/conjugation length tradeoff has been discussed with respect to polymers of substituted phenylene-vinylenes, no significant reduction of conjugation has been observed upon substitution of polythiophenes (PT) or poly-*para*-phenylenes (PPP). One simple reason is that these topologies are significantly different and that the side groups can more easily stay out of each other's way.

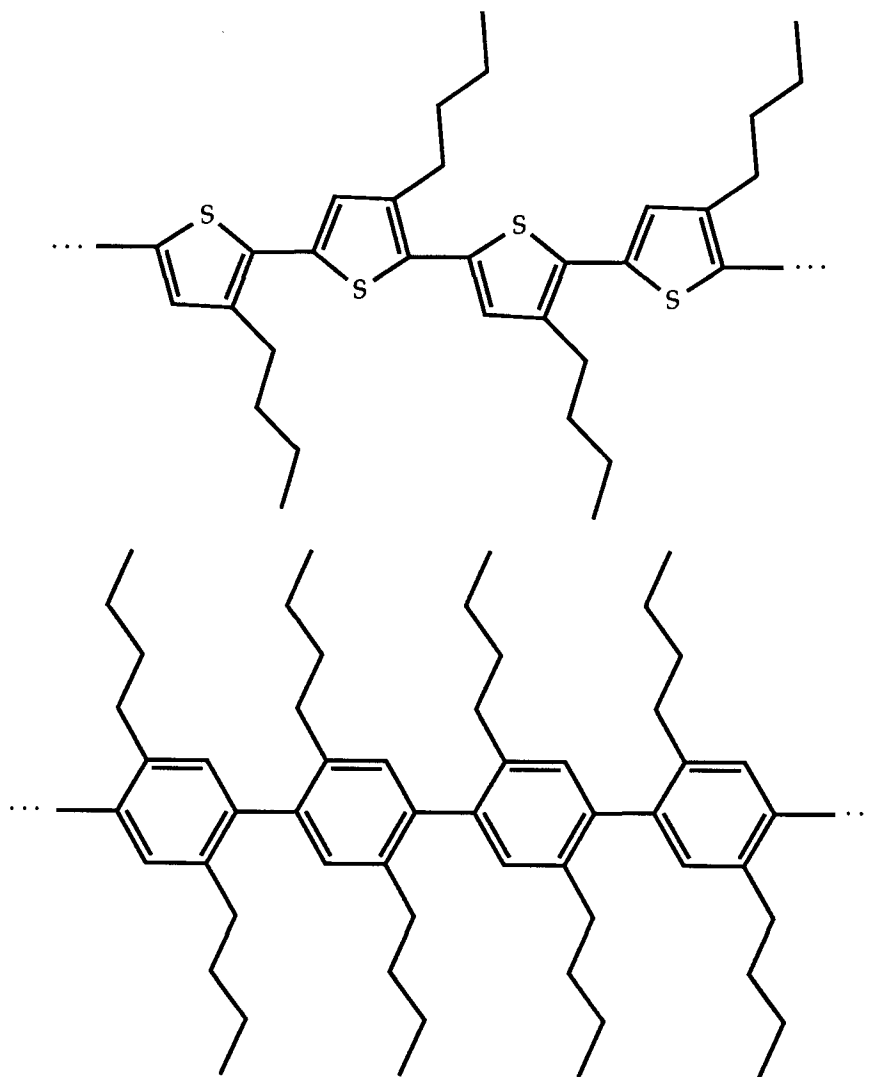


Figure 2. Steric crowding in (a) polyalkylthiophenes, (b) substituted poly-*para*-phenylenes.

Nonetheless, the coupling between monomer units in a PT or PPP chain is much less than the coupling between double bonds in polyacetylene. This coupling can be represented qualitatively by the Hückel parameter, β , the coupling between unit cells in the polymer. In polyacetylene, $\beta_{\text{intracell}}$ would be $\beta_{\text{C=C}}$ and $\beta_{\text{intercell}}$ would be $\beta_{\text{C-C}}$. As has been discussed at length, were these two β 's equal (i.e., if the single and double bond in polyacetylene were equal in length (no bond-length alternation)) polyacetylene would be a metal. However, they are not, and polyacetylene is a semiconductor. They are not so dramatically different, however, that intercell coupling is negligible. This intercell coupling is reflected in the lowering of the optical-absorption energy in polyacetylene compared to the monomer (ethylene), the existence of a large single bond rotational potential (≈ 6 kcal/mol) in butadiene^{60, 61} compared to the rotation barrier (4.5 kcal/mol)⁶² in the nonconjugated and more sterically congested analogue, butane, and a dramatic increase in the energy of the visible absorption maximum when the polymer chain is deplanarized.

Since the unit cells in PT and PPP are aromatic, $\beta_{\text{intercell}}$ is much less than $\beta_{\text{intracell}}$. Here, $\beta_{\text{intercell}}$ can be defined as the $\beta_{\text{C-C}}$ between thiophene/benzene rings. The other quantity, $\beta_{\text{intracell}}$ is introduced for comparison to polyacetylene and can be regarded as the coupling between any two atoms within the unit cell (i.e. ring) of PT or PPP. This larger difference in coupling is most dramatic in PPP. It is manifested by a smaller change in the optical-absorption energy in PPP³⁶ compared to benzene and the existence of a much lower single-bond rotational potential (calculated to be 2-3 kcal/mol in PPP)^{63, 64} This lower rotational potential is also illustrated by the nonplanarity of biphenyl in the gas phase, although in the crystal, biphenyl is planar.⁶⁵ Although no specific

experiments have been performed to explore the torsions in substituted derivatives of PT and PPP, theoretical studies have been performed,^{66, 67} and it follows from this analogy that there would be a much less dramatic decrease in the observed conjugation length when the polymer chain is deplanarized. These ring torsions have been discussed with respect to electronic structure in polyaniline,⁶⁸ and intrachain conformational changes have been postulated⁶⁹ as being responsible for so-called memory effects^{70, 71} upon doping this polymer, although a satisfactory argument against changes in polymer morphology as the result of charging/discharging has not been advanced.

B. Interchain Effects

Inherent in the discussion of isomerization is the importance of crystallinity. In this section, the role of interchain effects upon the electrical and optical properties of polyenes and polyacetylene will be enumerated. Specific conditions for the synthesis of polyacetylene have been of concern, since different synthetic methods, or even small differences in conditions for a given method, can change the morphology of polyacetylene and properties as well.⁷² Given that this study concerns itself with the effect of the primary structure of the polymer upon physical properties, it is prudent to keep in mind that some properties (notably, conductivity) are influenced by these interchain effects as well.

Effect upon electrical properties.

The conductivity of a sample is proportional to the concentration of free-carriers, n , and the carrier mobility, μ ,

$$\sigma = en\mu \quad (1)$$

where e is the unit electronic charge (1.6×10^{-19} C).⁷³ In conjugated polymers, carriers are created by "doping." This term is somewhat inaccurate and not directly comparable to doping processes in semiconductors. It is so commonly used, however, as to be unavoidable. When doping a conjugated polymer, the chain is formally oxidized or reduced. Creation of cations and anions in the chain is accompanied by some important geometry changes in the polymer and the creation of a continuum of states in what was originally the forbidden energy gap in the undoped semiconducting polymer. The process of carrier generation, including a full theoretical description^{74, 75} and the physical properties of carrier states (spectral,⁷⁶ magnetic⁷⁷ signatures, etc.) have been discussed in tutorial form in the literature. The carrier is simply a cation or anion that is somewhat delocalized over the polymer chain. Once carriers have been created, they have to move through the sample in order for bulk conductivity to be observed. Initially, this process involves escaping the Coulombic attraction of the counterion formed during the redox process. Then, the carrier can move along the polymer chain. The extent of delocalization of the particle and its ability to move its carrier density along the chain have been issues of great interest to researchers, prompting studies of carrier delocalization⁷⁸ and mobility in the presence of an electric field.

No polymer chain extends from one end of a sample to another, so bulk conductivity cannot be propagated solely by intrachain processes. In fact, there are those who argue that intrachain processes are unimportant for carrier mobility.⁷⁹ Extended delocalization lowers the energy of carriers, thus assisting in carrier generation, but polymer chains are not long enough freeways to be important for transport. The necessity of extended delocalization for carrier

generation is actually under debate, given that reasonably high conductivities ($\sigma \approx 10^{-2} \Omega^{-1}/\text{cm}$) have been observed in iodine-doped polyisoprene.^{80, 81} Most importantly, carriers must hop from one chain to another. Taking a step back and viewing a polymer as a group of crystalline regions separated by amorphous sections, carriers must hop from one crystalline region to another. It is reasonable to believe that hopping from one chain to another is easier when the chains are packed together as in a crystalline region. Thus, a high degree of crystallinity in a sample is widely believed to be important for high conductivity. Models based upon hopping between crystalline islands of high conductivity are popular for the description of conductivity in highly conductive samples. Other models are invoked for more amorphous samples of lower conductivity. The ease of doping a crystalline versus an amorphous region and the change in conductivity as the sample is progressively doped to a greater and greater degree has implications about the effects of interchain contacts upon carrier generation and mobility. All in all, very detailed models⁸²⁻⁸⁴ are required to interpret correctly the conductivity of a sample as a function of doping level, temperature,^{85, 86} and electric-field frequency (AC conductivity),⁸⁷ but interchain effects are undoubtedly central to an accurate description.

Effect upon optical properties.

The effect of interchain interactions upon polyacetylene's optical properties is much less discussed, yet it deserves some mention in this context. Polymer crystallinity will scatter infrared light, and this scattering will reduce the efficiency of nonlinear optical processes.⁸⁸ Perhaps a less incidental concern is the different optical absorption between polyacetylene in the solid state and in solution. Specifically, a red shift in the lowest energy visible absorption maximum has been observed in β -carotene (a biopolyene) upon aggregation in

the bilayers of lipid vesicles⁸⁹ and in polyenes in comparing their solution and solid-state spectra.¹⁰ Also, the lowest energy absorption peak in polyacetylene red-shifts when pressure is applied to the sample, presumably because of increased interchain interactions.⁹⁰ This red shift can be attributed in part to increased planarity of the chains in this medium, but it is also rationalized by the fact that the solid polyenes are a more polarizable medium than typical organic solvents. Neither ground nor excited states of polyenes have a dipole moment, and it has been noted that polyene spectra are not very sensitive to solvent polarity but rather to solvent polarizability.⁹¹ Optical absorptions were observed to red-shift in more polarizable solvents. Polarizability and interchain interactions are important to consider in the interpretation of conjugated polymer optical spectra. In particular, the band gap of *trans*-polyacetylene is generally reported to be about 1.4 eV,⁹² based upon the position of the absorption edge of a thin film of the polymer. Not only does this determination of bandgap not take into account Frank-Condon factors (i.e., it assumes that the lowest energy that the polymer absorbs at directly gives the energy difference between the highest-occupied orbital and the lowest-unoccupied orbital), but it does not concern itself with interchain effects. Presumably the true bandgap for *trans*-polyacetylene is somewhat higher in energy (between 1.4 and 1.8 eV is commonly accepted), and computations that claim to predict "correctly" the bandgap of *trans*-polyacetylene at 1.4 eV should be re-examined.⁹³

C. The solubility/conjugation length tradeoff

The issue of how to preserve a long conjugation length without sacrificing solubility has been discussed with respect to polymers of substituted acetylenes. However, other methods of solubilizing polyacetylene have been employed. One

might copolymerize a substituted acetylene with acetylene to produce a copolymer that is only partially substituted and perhaps more conjugated. This approach has been tried using methyl acetylene and acetylene,⁵⁸ and using phenyl acetylene and acetylene.⁹⁴ In the first study, intermediate conductivities between polyacetylene and polymethylacetylene were observed, but no optical-absorption data were presented to determine the effect on conjugation length. Methyl acetylene was observed to react somewhat faster than acetylene. In the second, phenyl acetylene was observed to react much faster than acetylene under the experimental conditions, leading possibly to blocky copolymers and definitely to much reduced doped conductivities. Optical-absorption data were also not presented here. More work is called for in this field, although most substituted acetylenes are liquids at room temperature, and mixing them with acetylene (a gas) might make accurate determinations of relative reactivities difficult. Polymers containing highly conjugated units as in polyacetylene can also be derived from elimination reactions on polymers such as polyvinylchloride²⁷ or polyvinylalcohol^{†,28} or by the rearrangement of poly(1,3-butadiene)⁹⁵ or poly(acetylene-co-1,3-butadiene).⁹⁶

A number of block and graft copolymers of polyacetylene have been synthesized, generally with the idea of using the second half of the block as a solubilizing tail.⁹⁷ In most cases, this modification rendered the polymer soluble and has facilitated a variety of studies of the linear^{98, 99} and nonlinear^{100, 101} optical properties as well as photoinduced absorption studies¹⁰² of polyacetylene segments in solution. There is evidence, however, that the polyacetylene segments in these polymers aggregate in solution,^{103, 104} and these studies have

[†] The material obtained from this process is commercially available as Polaroid K, a polarizing sheet.

not been made in the absence of interchain effects.

Results and Discussion

A number of experiments have been undertaken to explore both the intrachain and interchain effects in polymers of monosubstituted COT derivatives. Often it is not possible to sort one out from the other. In the case of visible absorption spectra in dilute solution, it is believable that these results accurately reflect an intramolecular phenomenon. Wide-Angle X-ray scattering results will reflect a bulk phenomenon. Conductivity and differential scanning calorimetry results are much more difficult to interpret, and particularly the latter relies upon consideration of both intrachain and interchain phenomena. In assessing all of this data, however, it is possible to arrive at a consistent interpretation in terms of what is occurring both within and between polymer chains.

A. Visible Absorption Spectra

All of the polymers display intense absorptions ($\epsilon \approx 10^3$) in the visible. The absorption maxima for both the predominantly cis and trans forms of the polymer are tabulated in Table 2. Here, the assignments to these isomers are based on the similarity in absorption maxima of these polymers in solution to polyacetylene in the solid state. These do not rule out other phenomena such as aggregation. However, results from NMR and electrochemistry,¹⁰⁵ presented both here and in previous work,¹⁰⁶ support this assignment.

Table 2. Visible absorption maxima (in THF).

R	λ_{cis} (nm)	λ_{trans} (nm)
<i>n</i> -Butyl	462	614 ^a
<i>n</i> -Octyl	480	632 ^a
<i>n</i> -Octadecyl	538	630 ^a
Neopentyl	412	634 ^a
2-Ethylhexyl	--- ^b	616 ^a
<i>t</i> -Butoxy	496 ^c	594 ^a
Phenyl	522	620 ^a
<i>s</i> -Butyl	360	556
Isopropyl	306, 366	556
Cyclopentyl	302, 365	550
Cyclopropyl	--- ^b	586 ^a
<i>t</i> -Butyl	302	432
TMS	380	540

^aThere is evidence that this material is not a homogeneous solution. Most of this material cannot be filtered through a 0.5 μm filter. ^bNot recorded. ^cA typical (mean) value.

Optical-absorption spectra of the *cis* polymers are difficult to interpret. Often they were broad, and partial isomerization caused the observed absorption maximum to move. In particular, the value of λ_{cis} for poly-*s*-butylCOT was previously reported to be 418 nm.¹⁰⁷⁻¹⁰⁹ Spectra of material taken within an hour after synthesis showed a λ_{cis} of 360 nm. A second absorption maximum around 300 nm was not resolved from this peak as was observed in *cis*-poly-isopropylCOT and *cis*-polycyclopentylCOT. Although it appeared almost completely soluble, *cis*-poly-*t*-butoxyCOT displayed an optical-absorption maximum that varied from ≈ 300 nm to ≈ 500 nm. It is suspected that facile

isomerization and possibly aggregation may play a role in confusing this determination.

In the trans form, many of the polymers were almost completely insoluble. Most spectral data reported here are from dilute solutions, isomerized by allowing the material to sit under inert atmosphere at room temperature for anywhere from 6 hours to several days. Vibronic coupling was not observed in the cis or trans polymers at room temperature, although it was found in biopolyenes,⁹¹ synthetic polyenes,¹⁵ and in random COT/COD (COD=cyclooctadiene, a nonconjugated monomer) copolymers.¹¹⁰ At -78 °C, however, fine structure was observed in *trans*-polytrimethylsilylCOT.¹⁰⁶ No thermochromic effects were observed in dilute solutions of *trans*-poly-*n*-octylCOT, which is not surprising if the polymer is aggregated in solution. The absorption maximum of (aggregated?) dilute solutions of insoluble polymers, however, was generally reproducible within 30 nm. Filtration of these solutions typically resulted in a purple material ($\lambda_{\text{max}} = 580 \pm 10$ nm) that has been shown to be of low molecular weight (Chapter 2). No significant solvatochromic effect was observed as solvent polarity changed (e.g., spectra in THF, CH₂Cl₂, benzene). However, a 30 nm red shift was observed in the absorbance maximum of *trans*-poly-*s*-butylCOT dissolved in CS₂ ($\lambda_{\text{max}} = 586$ nm) versus THF ($\lambda_{\text{max}} = 556$ nm). This solvent is not polar but is very polarizable (i.e., the solvent electron cloud can respond to the high-frequency, transient dipole induced by an electronic transition) and stabilizes the transition in the polymer, presumably because it is also very polarizable. The effect of solvent polarizability upon optical transitions in biopolyenes has been noted,⁹¹ and the possible effect of polymer polarizability upon polymer solubility will be discussed shortly.

Effective conjugation length has been discussed in the introduction of this chapter and defined for polyenes. Since optical-absorption data, and thus conjugation length scale, are affected by end groups, solvent, etc., ranges of values will be presented here. Based upon the scale, λ_{trans} for the different polymers suggests that those with methylene units adjacent to the main chain have an effective conjugation length of 25-30 double bonds. Even the low molecular weight, purple material resulting from filtration of these polymers (Chapter 2) is in this range. All of these polymers display broader but slightly red-shifted absorption spectra in the solid state. For example, *trans*-poly-*n*-octylCOT has a broad absorption centered around 650 nm in the solid state, comparable to the absorption energy of polyacetylene. Thus, the effective conjugation length of these polymers is similar to that observed for polyacetylene. The polymers with more bulky substituents, especially adjacent to the main chain, have slightly blue shifted λ_{trans} (R = isopropyl, *s*-butyl, cyclopentyl, TMS), implying a slightly reduced effective conjugation length of 20-25 double bonds. The bulky side group in *trans*-poly-*t*-butylCOT severely limits conjugation to perhaps 10 double bonds (directly comparable to the most intense transition recorded in dichloromethane of an all *trans*-polyene with 10 double bonds).¹⁵ These trends in effective conjugation are consistent with all of the other data reported here. Overall, neglecting the small electronic perturbation of the alkyl side groups (expected to change the optical absorption by less than 10 nm),¹¹¹ a polymer such as *trans*-poly-*s*-butylCOT displays the highest effective conjugation length for a *soluble* polyacetylene.

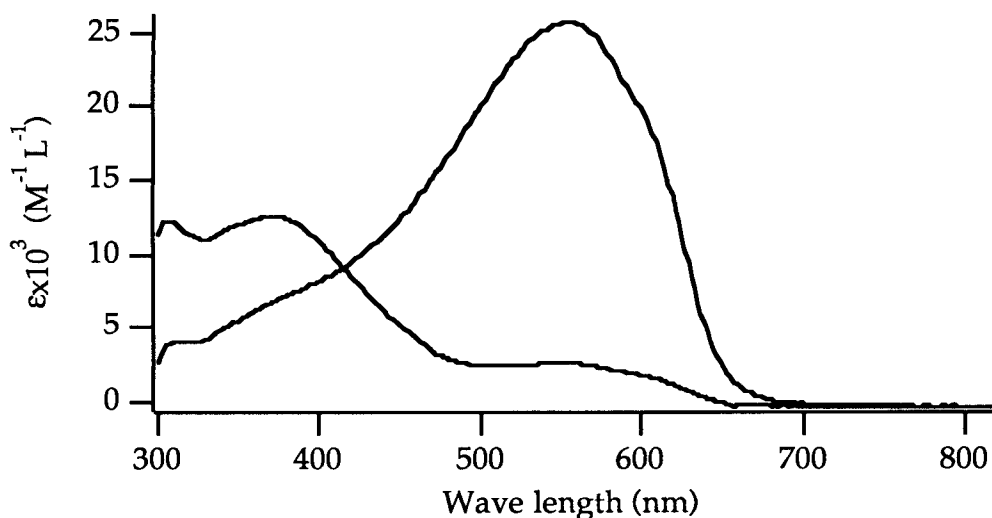


Figure 3. Absorption spectrum for *cis*- and *trans*-poly-*s*-butylCOT. Some isomerization from *cis* to *trans* is noticeable in the spectrum of the *cis* polymer.

As can be observed in Figure 3, absorption spectra are quite broad. Moreover, *trans*-poly-*s*-butylCOT absorbs below 500 nm, tailing into the ultraviolet region of the spectrum. This absorption may indicate that the distribution of effective conjugation lengths in the sample may contain some relatively nonconjugated segments. The nature of these segments (i.e. whether they are due to very twisted regions of the polymer chain or perhaps due to chemical (sp^3) defects cannot be determined from this spectrum. Moreover, transitions to higher energy states also cannot be ruled out.

Extinction coefficients are reported only for soluble polymers. The low value for *trans*-polycyclopentylCOT remains unexplained since a similarly low value was not observed for the same sample in the *cis* form. It is possible that more subtle steric effects would affect the extinction coefficient more dramatically than the optical-absorption maximum. Extinction coefficients are based upon moles of repeat unit (e.g., $[C_8H_7R]$) and are not corrected for the

percent conversion of the reaction. Also, cis polymer absorption spectra often have a small absorption in the region where the trans polymer absorbs (Figure 3), and extinction coefficients are not corrected for whatever small amount of isomerization may have occurred during synthesis and dissolution. Overall, one can see an increase in extinction coefficient upon isomerization, not unexpected given the polyene data cited before, and a high final value for the trans polymers.

Table 3. Extinction Coefficients of Soluble Polymers.

R	$\epsilon_{\text{cis}}^{\text{a}}$	$\epsilon_{\text{trans}}^{\text{a}}$
s-Butyl	12.6	25.6
Isopropyl	12.9, 12.1	28.9
Cyclopentyl	14.0, 12.3	19.3

^a $\times 10^3 \text{ mol}^{-1}$. Values are given at the wavelengths reported in Table 2.

Efforts have been undertaken to observe the spectral signature of so-called "mid-gap states" in doped polymers. It was mentioned in the introduction that much recent work has been undertaken to generate and observe oxidized or reduced forms of oligomers,³⁷⁻⁴² and absorption spectra of both photogenerated⁷⁶ and chemically generated⁹² states have been obtained, including work on soluble block copolymers containing polyacetylene^{98, 99} and on soluble poly-alkylthiophenes.¹¹² A substantial amount of work has centered around the electrochemical oxidation of some of the polymer films, and this work, including optical spectra, is described elsewhere.¹⁰⁶ It was of interest to obtain a spectrum of soluble, doped polymer in the visible and near infrared. Initial experiments using a diode-array spectrophotometer in the visible confirmed that the doped species, recognizable as an instantaneous change in color from purple to blue as

the dopant (NOPF₆), was added to the polymer (*trans*-poly-*s*-butylCOT), decomposed to an unidentified brown species over the course of 5-10 minutes at room temperature (Figure 4).

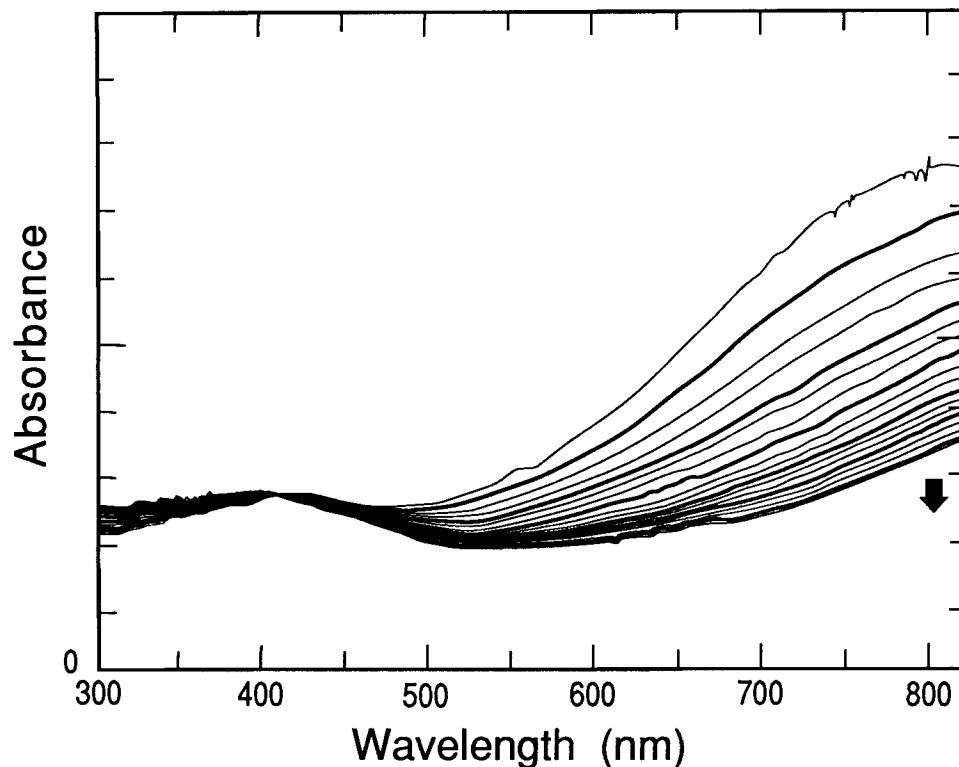


Figure 4. Visible absorption spectra of NOPF₆ doped *trans*-poly-*s*-butylCOT of molecular formula [(C₁₂H₁₆)(NOPF₆)_{0.10}]_x. The arrow indicates that the absorbance tailing out into the near infrared is decreasing over time. Presumably the absorption maximum of the doped species is in the near infrared.

The doped species does not form, at least over the course of 5-10 minutes, at -78 °C as suggested by the lack of change in the color of the solution. However, at -20 °C, the species forms, and sealed tubes of the doped *trans*-poly-*s*-butylCOT can be kept at -50 °C for 3-4 weeks. This species is intensely colored in the late visible and near infrared. Dilution to a reasonable concentration for spectroscopy ($\approx 10^{-4}$ to 10^{-5} M) unfortunately resulted in decomposition,

probably because the sample was sensitive to trace impurities. Use of a 1mm cell permitted the collection of a spectrum at $-30\text{ }^{\circ}\text{C}$ (CHCl_3 bath), although very little absorption was observed, possibly because of partial decomposition.

Nevertheless, a weak, broad absorption centered around 880 nm was observed.

Much better results have been obtained by T. Jozefiak et al. on thin films.¹⁰⁵

B. Raman Spectra

The existence of two peaks in the Raman spectra of the polymers has been used as evidence that all of these polymers are highly conjugated (Chapter 2). As was mentioned in the introduction, Raman can be used to explore the different effective conjugation lengths in a polyacetylene sample. With these samples, the position of the $A_g(\text{C}=\text{C})$ stretch is not noted to be very sensitive to the different effective conjugation lengths observed by visible light absorption. This observation is not surprising since the visible absorption spectra of all of these samples (with the exception of *trans*-poly-*t*-butylCOT) suggest that they all contain conjugated segments, which should be resonance enhanced at an excitation wavelength of 488 nm. It would be interesting to fit the Raman spectra recorded at a variety of wavelengths to the conjugation length distribution model developed by Kuzmany³¹ and Fitchen and Lichtmann.²⁹ These models suggested a bimodal distribution of conjugation lengths in polyacetylene that was due to amorphous and crystalline regions of the polymer. Presumably a polymer in solution would not have this bimodal distribution. The visible absorption maximum identifies only the most predominant effective conjugation length in solution (weighted by extinction coefficient, which is known to increase as conjugation length increases). This experiment, although it does rely on some assumptions, would map out the distribution of effective conjugations in the

polymer. Of course, using these models as a guide, a model could be developed to fit the absorption spectrum as well.

Table 4. Raman Data.

R	$\nu_1 A_g(\text{C-C}) (\text{cm}^{-1})$	$\nu_2 A_g(\text{C=C}) (\text{cm}^{-1})$
Methyl	1126-1132	1516
<i>n</i> -Butyl	1132	1514
<i>n</i> -Octyl	1114-1128	1485
Neopentyl	1131	1509
2-Ethylhexyl	1128	1507
Methoxy	1126-1128	1530
<i>t</i> -Butoxy	1121	1507
<i>s</i> -Butyl	1125-1128	1512
Isopropyl	1129	1527
Cyclopentyl	1131	1533
Cyclopropyl	1125 ^a	1515 ^a
<i>t</i> -Butyl	1147	1539-1547
TMS	1132	1532

^aOnly a very weak signal was observed.

C. Relationship between Conjugation Length and Solubility in Polyacetylene

Observations regarding the solubility of both *cis* and *trans* polymers were made in the last chapter. Some of the behavior was difficult to obtain reproducibly, especially because facile isomerization was converting a soluble polymer into an insoluble polymer. The observations, however, correlate with the notion that there is a tradeoff between conjugation and solubility in

substituted polyacetylenes.

The first group of polymers to be discussed here is that group in which there is a methylene (-CH₂-) unit immediately adjacent to the main chain of the polymer. These include polymers with *n*-alkyl side chains as well as polymers with neopentyl (i.e. -CH₂(CH₃)₃) and 2-ethylhexyl (i.e. -CH₂CH(C₂H₅)(C₄H₉)) side groups. All of these polymers have an effective conjugation length similar to polyacetylene. The side chain solubilizes the polymer when it is in the *cis* form, although these polymers are almost completely insoluble in the *trans* form. The material remaining in solution cannot be easily filtered and is thus probably not homogeneously dispersed. Polyenes containing *cis* double bonds have been observed to be more soluble than all *trans* polyenes,¹⁵ although this insolubility was attributed to cross-linking by these workers. If cross-linking does occur here, it does not severely interrupt conjugation, and the previous conclusion would imply that *trans*-polyacetylene must be cross-linked in the solid state. Simple aggregation also would explain the observed phenomena. There is clearly room for more investigation here.

A secondary or tertiary group adjacent to the main chain does reduce the conjugation, but it affords solubility in both the *cis* and *trans* forms of the polymer. Two points are noted here. First, only steric effects immediately adjacent to the main chain affect conjugation and solubility. *trans*-PolyneopentylCOT, in which a *t*-butyl group is spaced one unit away from the main chain, behaves like *trans*-poly-*n*-alkylCOT. There is some room to tailor the steric effect. *Trans*-poly-*t*-butylCOT is soluble, but not highly conjugated. Pulling this bulky group back a small amount (as in *trans*-polytrimethylsilylCOT: a Si-C bond is longer than a C-C bond)¹⁰⁶ increases the conjugation considerably.

Use of a secondary group (as in *trans*-poly-*s*-butylCOT) has so far provided the highest possible conjugation length without loss of solubility. Tying back the groups, as in *trans*-poly-cyclopropylCOT, afforded a polymer more or less like *trans*-poly-*n*-alkylCOT. This abrupt loss of solubility suggests that there is a rather sharp transition between highly conjugated, insoluble polyacetylene and somewhat less conjugated, soluble polyacetylene. The overall effect in this system is that the steric effect of the side group reduces the conjugation of the polymer. The simplest explanation would be that the side group causes the polymer chain to twist, and this deplanarization is supported by computations reported in the next chapter.

Why are polyacetylenes with long conjugation lengths insoluble? Knoll and Schrock argue, given the data on discrete polyenes¹⁵ and block copolymers containing polyacetylene,¹⁰⁴ that molecules containing greater than 20 double bonds in conjugation aggregate (via cross-links) to limit the conjugation length and the solubility of a polyene. The exact limit of conjugation length can be debated on the basis of optical absorption¹⁹ and Raman³¹ data for polyacetylene. Indeed, we seem to be able to solubilize higher effective conjugation length polymers, perhaps because the side groups help to stabilize the polymer against cross-linking. We also seem to have found a limit of an effective conjugation of about 30 double bonds, somewhat different from Schrock and Knoll's value. Aggregation phenomena (or cross-linking) appear to set in on any polyacetylene with an optical absorption above 580 nm or so. More, albeit preliminary, data on copolymers of monosubstituted COT's support this conclusion and will be presented in Appendix I.

The line between soluble and insoluble is difficult to probe. Certainly the

inability to filter some solutions suggests that this line exists, but this simple determination does not address the cis/trans content of the polymer when it aggregates, nor does it address molecular weight effects, if any. Light scattering would normally identify a large increase in particle size upon aggregation. It has been used to probe the absolute molecular weight of poly-*t*-butylCOT.¹¹³ However, the technique relies upon the scattering of visible light, and all of the other polymers absorb too much visible light for any appreciable signal to be detected. Use of infrared light is a possibility, but scattering efficiency is wavelength-dependent, falling off proportionally as $1/\lambda^4$ (λ = wavelength).¹¹⁴ Light scattering on highly conjugated polyacetylene has been achieved using resonance-enhanced light scattering and observing the excess depolarized (HV) Rayleigh scattering.¹⁰³ Small-Angle X-ray scattering (SAXS) also remains an unexplored possibility. It has been used in the analysis of polymers and in aggregation phenomena in dyes.¹¹⁵

Can this solubility behavior be rationalized in terms of molecular interactions? In discussing this issue, let us choose to assume that in polyacetylene and highly conjugated polyacetylene derivatives, chains aggregate in a way that does not include cross-linking. Thus, this discussion will bypass the simple and perhaps valid argument that highly conjugated molecules cross-link and are thus insoluble.¹⁵ A number of models exist for describing the relationship between structure and solubility, and the merits of two of them will be discussed.

The simplest view of polyacetylene as a generally insoluble polymer is that it is flat and stiff, a requirement for conjugation. Thus, its insolubility can be rationalized entirely upon considerations of entropy.¹¹⁶ Flexible chains can

dissolve and assume many new conformations, with a substantial increase in entropy. A stiff-chain polymer must break a number of intermolecular contacts to become soluble (as must a flexible-chain polymer), but the polymer is stiff and cannot assume many new conformations. Thus, the minor gain in entropy does not make the process favorable. This rationalization has been successfully applied to the prediction of phase behavior and properties of stiff-chain molecules such as rigid polyesters. It also prescribes some methods for solubilizing some of these polymers, such as the synthesis of polymer with long, flexible tails to increase the entropy gain upon dissolution. This strategy works for polyalkylthiophenes, but even the attachment of *n*-octadecyl (C₁₈) chains to *trans*-polyacetylene does not solubilize it. A more comprehensive model is required.

A second rationalization is in terms of interaction between polymer chains. A Flory-Huggins model encompasses both entropic and enthalpic contributions and simply states that the overall free energy of mixing ($\Delta G_m = \Delta H_m + T\Delta S_m$) must be negative for polymer dissolution to occur.^{117, 118} Polymer behavior here suggests that highly conjugated chains must have a positive enthalpy of mixing, and this behavior can be rationalized. The electrons in these chains are very polarizable, presumably leading to large Van der Waals interactions which, after all, hold these molecules together. Sometimes Van der Waals forces can be small, allowing the enthalpy of mixing to be small. It is understood, however, that these conjugated polymers are very polarizable^{119, 120} (as well as hyperpolarizable,¹²¹ leading to nonlinear optical effects), so the strength of intermolecular Van der Waals interactions may be extreme in this particular class of polymers.

It has been calculated that linear polarizability increases with conjugation length.¹¹⁹ Thus, it is possible that a reduction in conjugation length can result in a reduction in polarizability, leading to a reduction in intermolecular forces.¹²² This rationalization would explain the observed solubility trends in this class of polymers. Large polarizabilities in polyenes and polyacetylene have been inferred on the basis of solvatochromism in the optical-absorption spectra of these species. For example, the spectrum of an all *trans*-polyene containing 13 double bonds in highly polarizable CS₂ is red shifted by 46 nm relative to the spectrum in pentane.¹⁵ As mentioned before, the spectrum of *trans*-poly-*s*-butylCOT is red shifted by 30 nm in CS₂ versus THF ($\lambda_{\text{CS}_2} = 586 \text{ nm}$, $\lambda_{\text{CH}_2\text{Cl}_2} = 556 \text{ nm}$). Naturally, a twist in the chain that is due to the steric perturbation of the side group has an effect on entropy as well, and the relative contributions to the energy of dissolution by the enthalpic and entropic terms are unclear.

The effect of torsions upon conjugation in other conjugated polymers has been discussed in very qualitative terms in the introduction of this chapter. This discussion is also applicable in the rationalization of polymer-polymer interactions. Why are polyalkylthiophenes soluble but polyacetylenes with long, alkyl tails are not? This difference may arise from differing polarizabilities of the two chains. If polyacetylene is more polarizable than polythiophene, a comparison not addressed so far in the literature to the author's knowledge, polyacetylene should have a stronger polymer-polymer interaction parameter and thus not be dissolved as easily.

D. Probes of Film Morphology

Scanning electron microscopy (SEM), wide-angle X-ray scattering and infrared scattering all show these samples to be amorphous. SEM's of both the surface of the films and in freeze-fracture cross sections showed them to be completely smooth, with no detectable fibrillar morphologies or other features of size 1 μm or larger. This observation is in contrast to that of films of polyCOT, which have smooth surfaces but fibrillar interiors.¹²³

Polyacetylene synthesized by the Shirakawa or Naarman routes (Chapter 1) is highly crystalline. PolyCOT has also been reported to be highly crystalline.¹²³ In contrast, films of poly-R-COT (except for R = methyl, which still appears somewhat crystalline) show only an amorphous halo by wide-angle X-ray scattering. This observation is in contrast to polyCOT, in which lattice spacings could be determined from several sharp lines observed.

Absorption spectra of polyCOT films show high optical density (1-3 for 20 μm thick films) even below the true absorption edge⁸⁸ in the near IR. The apparent absorption decreases with increasing wavelength but extends out beyond 2000 nm. This apparent absorption is actually due to scattering as shown by laser light scattering observations. As an example, the loss coefficient of such films is estimated to be $> 500 \text{ cm}^{-1}$ at 1500 nm. The origin of this scattering is certainly due to internal, optical inhomogeneities in the polymer associated with the semicrystalline, fibrillar morphology. In contrast, films of poly-*n*-butylCOT show very clean transmission in the near IR. Films 100 μm thick show a sharp absorption edge at $\sim 900 \text{ nm}$ and very little absorption beyond 1000 nm. For poly-*n*-butylCOT films, the loss coefficient is estimated to be $< 0.2 \text{ cm}^{-1}$ at 1500

nm. The greatly reduced scattering loss indicates that partial substitution of polyacetylene with butyl groups has resulted in a more homogeneous morphology, approaching that of an amorphous polymer. This low scattering will be important if polyacetylene is to be used in optical applications.

E. Conductivity

Determining trends in the iodine-doped conductivities of films is generally difficult. None of the substituted polymers has an improved conductivity over the parent (i.e., R = H). This fact is hardly surprising since side groups should reduce both intrachain and interchain carrier transport, presumably by reducing conjugation that is due to twisting and interchain hopping, via destruction of crystallinity and separation of chains by the side groups. Overall, more conjugated polymers tend to be more conductive. This statement represents an empirical observation and not a conclusion about the predominant influence of the side group upon intra- versus intermolecular interactions. Indeed, some comparisons cannot be rationalized by simple ideas about conjugation or interchain interactions. For example, even though it would be logical that side-group interference with electron hopping would be higher in poly-*n*-octylCOT than in poly-*n*-butylCOT, the former has a reproducibly higher conductivity by two orders of magnitude. There is no evidence that the conjugation in poly-*n*-butylCOT is reduced compared to poly-*n*-octylCOT, either. It is also not clear that the low conjugation length of poly-*t*-butylCOT should result in such a poor iodine-doped conductivity. Nonconjugated polymers such as polyisoprene⁸⁰ have been doped to much higher conductivities, and polyenes with lower effective conjugation lengths produce the spectral signature of a bipolaron when oxidized.¹²⁴ Thus, the low iodine uptake and low conductivity

are not consistent with the rationalization that poly-*t*-butylCOT has insufficient conjugation to sustain some type of charge carrier. It is possible that either poor diffusion of iodine and/or poor interchain communication that is due to the bulky side groups was a limiting factor in this case. In contrast, poly-*t*-butoxyCOT absorbed a substantial amount of iodine, yet it too displayed a low conductivity after doping.

Table 5. Iodine-doped conductivities of polymer films.

R	σ (Ω^{-1}/cm)	y^a
H ^f	50-350	0.17
Methyl	15-44	---b
<i>n</i> -Butyl	0.25-0.7	0.10-0.13
<i>n</i> -Octyl	15-50	0.11-0.19
<i>n</i> -Octadecyl	0.60-3.65	0.14-0.16
Neopentyl (1) ^c	0.2-1.5	0.10-0.18
Neopentyl (2) ^d	15-21	0.13-0.17
Methoxy	$3.6-3.9 \times 10^{-3}$	---b
<i>t</i> -Butoxy	$\approx 10^{-7}$	0.11-0.12
Phenyl	0.3-0.6	0.19-0.28
<i>s</i> -Butyl (cis)	$1.0-2.0 \times 10^{-4}$	0.33
<i>s</i> -Butyl (trans) ^e	0.03	0.31
<i>t</i> -Butyl	$< 10^{-8}$	≈ 0.03
TMS ^e	0.2	0.12

^aBased upon the molecular formula $(\text{C}[\text{H}/\text{R}]\text{I}_y)_x$. ^bNot recorded. ^cAs synthesized film. ^dAfter a blue, trans suspension was recast from solution. ^eFilm recast from solution. ^fFrom reference 123.

Since variation was often observed in the conductivity, ranges are often reported. No observations definitively revealed the reason for the variation, but some possibilities are suggested by the data. First, the relative proportion of *cis* and *trans* double bonds may play a role. These polymer samples were doped and their conductivities were measured within a week after synthesis. However, facile isomerization behavior has been noticed for several of these polymers. Polyacetylene is known to isomerize upon doping,^{125, 126} and *cis*-polyacetylene is reported to have a higher iodine-doped conductivity than *trans*-polyacetylene.¹²⁷ However, the substantial increase in conductivity in poly-neopentylCOT and poly-*s*-butylCOT if the polymer was isomerized in solution (even if it then precipitated) and was then recast before doping suggests the reverse. Isomerization in solution is perhaps a more gentle process than thermal isomerization in the solid state, resulting in less destruction to the film.

Sample thickness may also play a role. Although in the calculation of the conductivity, sample thickness is taken into account, it has been suggested that thinner samples of conjugated polymers display higher doped conductivities.¹²⁸ Higher conductivities have been observed in thin films of some of these polymers. For example, although it is not reported in Table 5, a thin (< 10 μm) film of poly-*n*-octylCOT displayed a conductivity an order of magnitude higher than that of thicker films.¹²⁹ Inhomogeneous doping is not the cause, either. A profile of iodine concentration obtained by energy-dispersive spectroscopy (EDS) through a cross section of a 200 μm -thick film showed that iodine was homogeneously distributed throughout the thickness of the film.

Stretching is known to increase the conductivity of doped polymer samples, particularly in the stretch direction.¹³⁰⁻¹³² This increase is thought to

occur because of partial alignment of polymer chains. Poly-*n*-octylCOT could be stretched up to 15 times its length within a few hours after synthesis. However, conductivities were determined to fall inside the range of unstretched films. No increase in crystallinity of the films was observed by wide-angle X-ray scattering, either.¹³³ Residual monomer in the film may plasticize it, allowing chains to slip past each other during stretching without enough friction to cause alignment. The best conditions for future attempts would probably involve the prior removal of impurities from the film followed by stretching (and perhaps isomerization) at the lowest possible temperature. It may be advantageous to admit solvent (e.g., THF) vapor to slightly swell and plasticize the film if it is found that large forces are necessary to induce stretching. Stretching under some of these conditions has been attempted. The right combination of force and temperature was not successfully achieved.

F. Nonlinear Optical Properties

These measurements were made by Dr. Joseph Perry at the Jet Propulsion Laboratory. Third harmonic generation (THG) measurements on poly-*n*-butylCOT films, referenced to a bare, fused silica plate, were made using 1064 nm pulses. These measurements showed that the $|\chi(3)|$ of films of poly-*n*-butylCOT, $\sim 1 \times 10^{-10}$ esu were comparable to that for unoriented polyacetylene at the same wavelength.¹³⁴ However, comparison of the linear transmission spectra of these materials in the near infrared shows that the partially substituted polyacetylene has greatly improved optical quality.

Films of polytrimethylsilylCOT were also examined. As discussed above, this polymer is completely soluble and can be converted to a fully trans

conformation in solution. Films of the trans form of the polymer are then easily produced from solution by casting or spin-coating. THG measurements at 1064 nm give $|\chi(3)| = 2 \pm 1 \times 10^{-11}$ esu for this polymer. This value is somewhat lower than that of poly-*n*-butylCOT or polyacetylene, consistent with the reduced effective conjugation length inferred from the energy of the absorption maximum, as discussed earlier. These films prepared from solution are of good optical quality and show low scattering losses at least as low as the poly-*n*-butylCOT films.

G. Differential Scanning Calorimetry

All films display an irreversible exotherm between 100-165 °C that does not correspond to any weight loss as shown by thermal gravimetric analysis (Table 6). This exotherm is attributed to cis/trans isomerization as is observed in polyacetylene. Most of the films isomerize below 150 °C, the cis/trans isomerization temperature reported for polyacetylene¹³⁵ and observed for poly-COT (i.e., R = H). Since any side group on the polymer appears to render it amorphous, it appears that crystalline polyacetylene is more difficult to isomerize than amorphous polyacetylene. This conclusion is supported by the DSC of the amorphous polyacetylene produced by the precursor route of Feast and Edwards.¹³⁶ This form of polyacetylene is reported to have an isomerization temperature of 117 °C.¹³⁷ The soluble polymers with a reduced conjugation length, however, have higher isomerization temperatures than the less-twisted derivatives. This behavior is understandable since a longer conjugation length polyene sequence should be easier to isomerize than a shorter conjugation length sequence. Thus, it is required to take both intrachain and interchain effects into account when attempting to understand the solid-state isomerization behavior of these polymer

films.

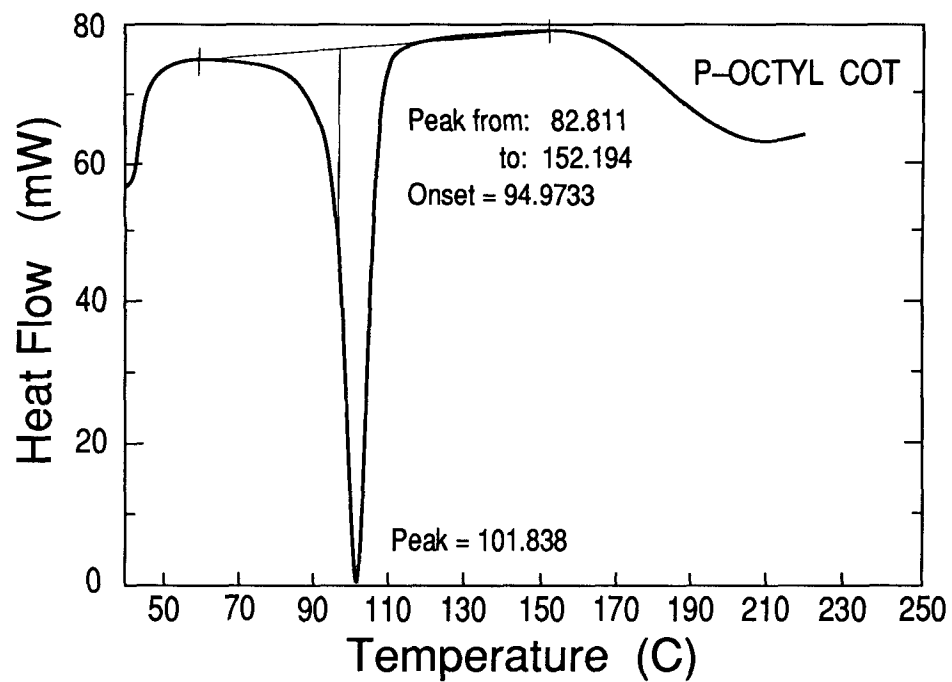


Figure 5. Typical DSC exotherm observed upon isomerization of a poly-R-COT film.

Table 6. Isomerization temperature observed for polymer films.

R	T _{isom}
H	150
Methyl	103
<i>n</i> -Butyl	107
<i>n</i> -Octyl	102
<i>n</i> -Octadecyl	102
Neopentyl	110
Methoxy	131
<i>t</i> -Butoxy	116
Phenyl	114
<i>s</i> -Butyl	122
Isopropyl	122
Cyclopentyl	119
Cyclopropyl	115
<i>t</i> -Butyl	164
TMS ^e	150

H. Isomerization in Solution

Polyacetylene not only has single-bond torsions. The double bonds in the polymer can be in one of two configurations, *cis* or *trans*. Although increased conjugation length does not appear to have an effect upon the single-bond torsional potential,^{48, 138} it does have a notable effect upon double-bond isomerization potential as suggested by DSC measurements.

In polyacetylene, it is accepted that the *trans* configuration is more stable than the *cis* configuration by approximately 0.85 kcal/mol of CH units (based upon calorimetry measurements).¹³⁵ Isomerization can be induced using heat¹³⁹⁻¹⁴¹ or upon doping.^{125, 126} Photochemical isomerization has not been

reported for polyacetylene in the solid state, but it can be accomplished in solution with some of these substituted polymers (see below). The thermal isomerization of polyacetylene has been studied in the solid state and is complicated, following no discrete reaction order. It is accepted that isomerization in crystalline regions and amorphous regions will proceed with different activation energies.¹⁴² At early stages of isomerization (presumably in the amorphous regions where chains are more free to move), the process is activated by about 17 kcal/mol, although barriers as low as 11 kcal/mol have been claimed.¹⁴³ At higher conversion (presumably in the crystalline regions of the polymer), this activation barrier increases considerably. This relatively low isomerization barrier is not surprising since the biradicals created in the twisted transition state would be stabilized by delocalization within the π -system. Lowering of cis/trans isomerization barriers because of biradical delocalization has been observed for stilbenes ($\Delta G^\ddagger = 55.1$ kcal/mol at 723K), cumulenes ($\Delta G^\ddagger = 30, 27.5,$ and 20 kcal/mol at 373K, 298K, and 393K for 4, 5, and 6 carbon cumulenes, respectively), and many other delocalized systems as compared to a 65 kcal/mol barrier at 723K for ethylene ($\text{CHD}=\text{CHD}$).¹⁴⁴ Since the twisted, biradical transition state can be thought of not just as two localized spins but as a pair of mobile, delocalized solitons, this transition state is an ultimate example of stabilization that is due to delocalization. It is only recently, however, that rational model compounds to investigate the isomerization barrier in a polyene as a function of conjugation length have been synthesized and studied.¹⁴⁵

In the last chapter, the isomerization of soluble polymers in solution either thermally, photochemically, electrochemically¹⁰⁵ or over time under conditions of ambient temperature and light was described. These mild conditions are of interest compared to the comparably more brutal thermal conditions used to

isomerize polyacetylene. It is believed that chemical defects can be created during thermal isomerization of polyacetylene in the solid state.¹⁴⁰ We observed no evidence of this phenomenon (by NMR) when soluble polyacetylenes were isomerized in solution. Overoxidation during electrochemical doping/isomerization may have produced some defects as evidenced by a drop in current as a polymer film was electrochemically cycled.¹⁰⁵

In the completely (cis and trans) soluble polymers, the chromophores that are due to each isomer are well separated in energy, allowing Ginsburg et al. to follow the photochemical cis/trans isomerization of poly-trimethylsilylCOT in solution.¹⁴⁶ Interestingly, an isosbestic point was observed, suggesting that an entire chromophore of olefins (the equivalent of 15-20 double bonds) was isomerizing simultaneously in solution without detectable intermediates. Tanaka has observed an isosbestic point in the visible absorption spectrum upon thermal cis/trans isomerization of polyacetylene in the solid state.¹⁴³ Simultaneous isomerization of multiple double bonds in polyenes^{147, 148} and other conjugated molecules¹⁴⁹ is also preceded in the literature. Proposed trajectories in which more than one double bond is isomerized at a time are often constructed with the minimum motion of atoms, and multiple isomerization trajectories often allow for less motion than separate single isomerization trajectories. This isomerization in polyenes is postulated to be via an excited state surface in which barriers to rotation (isomerization) are low (< 1 kcal/mol).¹⁴⁷ Furthermore, it is suggested that this state can be thermally populated and is the isomerization pathway for long polyenes.¹⁴⁰

The thermal isomerization of poly-*s*-butylCOT in solution was monitored by visible absorption spectroscopy (Figure 6). An isosbestic point was observed

throughout most of the reaction. Near the end of the reaction, large increases in extinction coefficient were observed with a concomitant loss of the isosbestic point. Upon further examination of the reported data on the isomerization of poly-trimethylsilylCOT, it was realized that this reaction was observed in its early stages. These new data suggest that new changes take place near the end of the reaction. The most likely explanation is a large conformational change allowing for a larger transition dipole moment (and thus the observed large increase in extinction coefficient). This conformational change is presumably not required for the polymer chain to be flat enough (on the small scale) to display an effective conjugation length of roughly 20 double bonds.

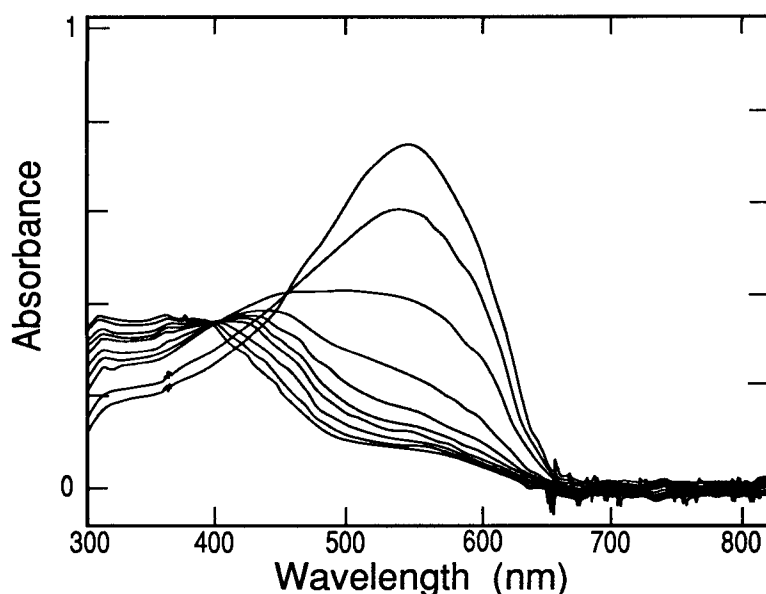


Figure 6. Thermal cis/trans isomerization of poly-*s*-butylCOT in solution.

Photochemical isomerization of polyneopentylCOT displayed an isosbestic point when monitored by visible absorption spectroscopy even though the *trans* form of the polymer is expected to be insoluble (Figure 7). This isosbestic point appears to persist even at the later stages of the reaction. Moreover, the absorption maximum that is due to the *trans*-chromophore was observed at 565 nm instead of approximately 600 nm observed if the isomerization took place over a longer time period. It is postulated that two processes occur here, isomerization and aggregation, and that the second does not immediately occur after the first. Thus, the initial spectrum might contain some isomerized/aggregated material (which is red shifted in energy), and the isomerization produces a new material that is not yet aggregated in dilute solution. The final absorption maximum (≈ 565 nm) suggests that this may be the effective conjugation of *trans*-polyneopentylCOT in the absence of aggregation effects. If this is the case, it is remarkably similar to that of *trans*-poly-*s*-butylCOT. It does not appear that *cis*-polyneopentylCOT is going to a mixture of

aggregated and unaggregated *trans*-polyneopentylCOT since the reaction ($A \rightarrow B + C$, where B and C have different absorption spectra) is not expected to display an isosbestic point.

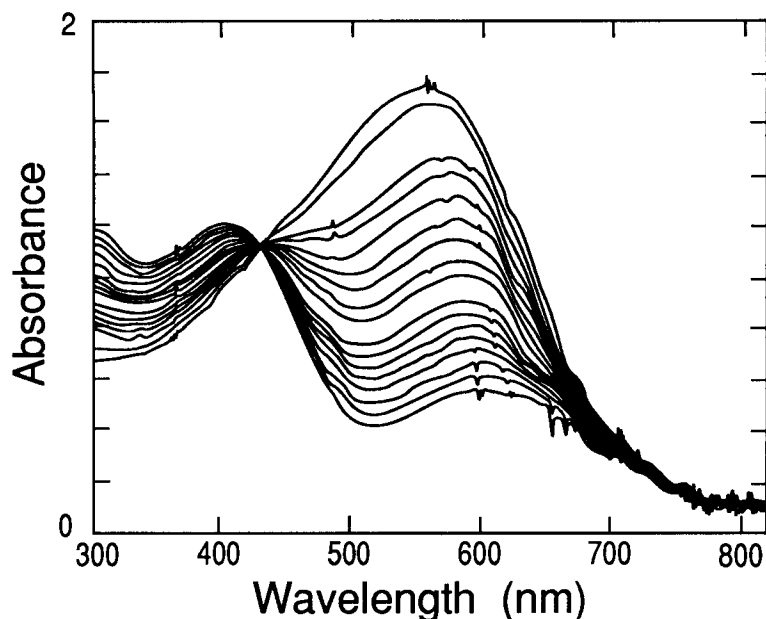


Figure 7. Photochemical *cis*/*trans* isomerization of polyneopentylCOT in dilute THF solution. Spectra are taken after 30-second increments of photolysis.

It was possible to determine rates of isomerization by monitoring the change in absorbance of the *cis* and *trans* chromophores of poly-*s*-butylCOT. The increase in absorption at 560 nm that was due to the *trans*-chromophore was used to calculate rates. Since there is some absorption of the *trans*-chromophore in the region where the *cis*-chromophore absorbs, plots of the decrease in absorbance of the *cis*-chromophore were not valid for rate determination. First-Order kinetics was obeyed. An Arrhenius plot of rate at four temperatures varying from 45-75 °C gave an energy of activation $E_a = 21.3 \pm 0.4$ kcal/mol with $A = 2.4 \times 10^{10}$. An Eyring plot gave activation parameters of $\Delta H^\ddagger = 20.6 \pm 2.1$ kcal/mol and $\Delta S^\ddagger = -13.3 \pm 4.5$ cal/mol•K. These parameters are in the range reported for

polyacetylene in the solid state and as discussed above, represent a stabilized barrier for olefin isomerization. In this case, the molarity refers to moles of "chromophores," a vacuous designation, but as suggested by the isosbestic point in the absorption spectrum, it is the species under study.

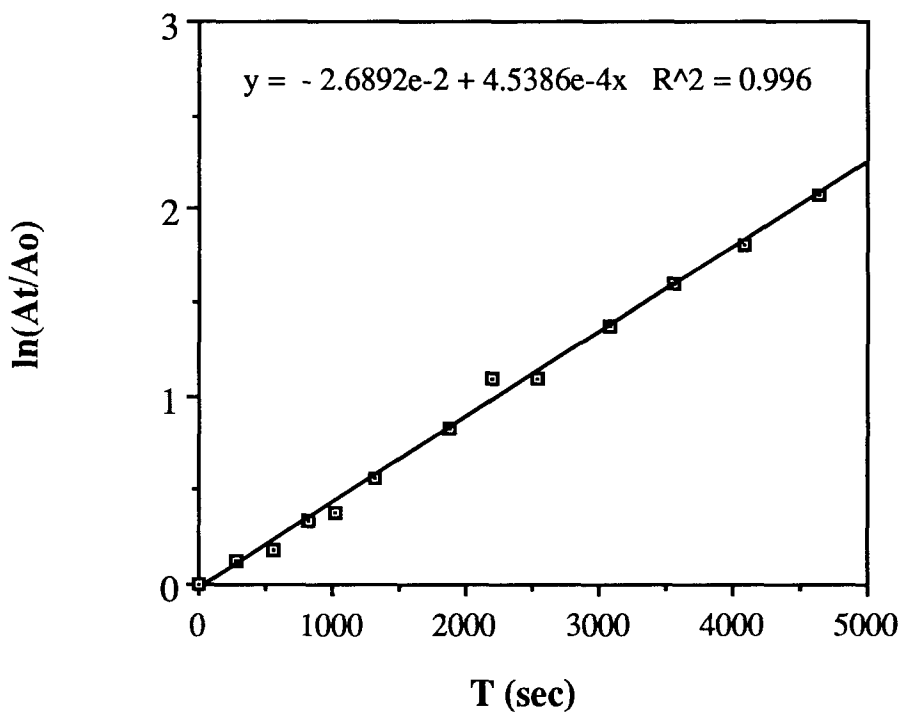


Figure 8. Typical results of cis/trans isomerization kinetics of poly-*s*-butylCOT at 65 °C, monitored by absorbance at 560 nm.

These experiments are reported for benzene solutions of the polymer. Kinetics was also run at 70 °C and 56 °C in THF, and isomerization rates were observed to be similar to those in benzene. No pronounced solvent effect was observed, suggesting a nonpolar transition state. Photochemical quantum yields for isomerization were not determined but would be of interest, both with and without added triplet sensitizers.

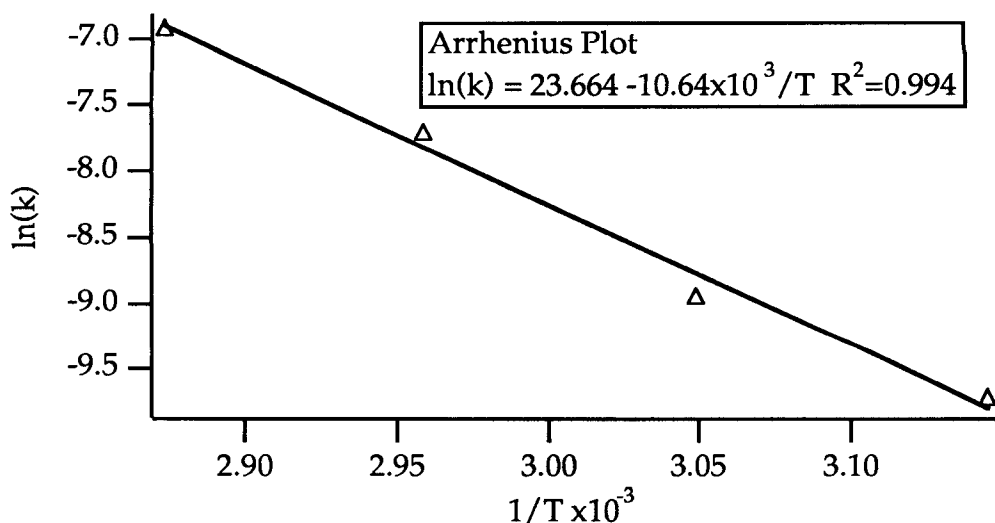


Figure 9. Arrhenius plot for thermal cis/trans isomerization of poly-s-butylCOT.

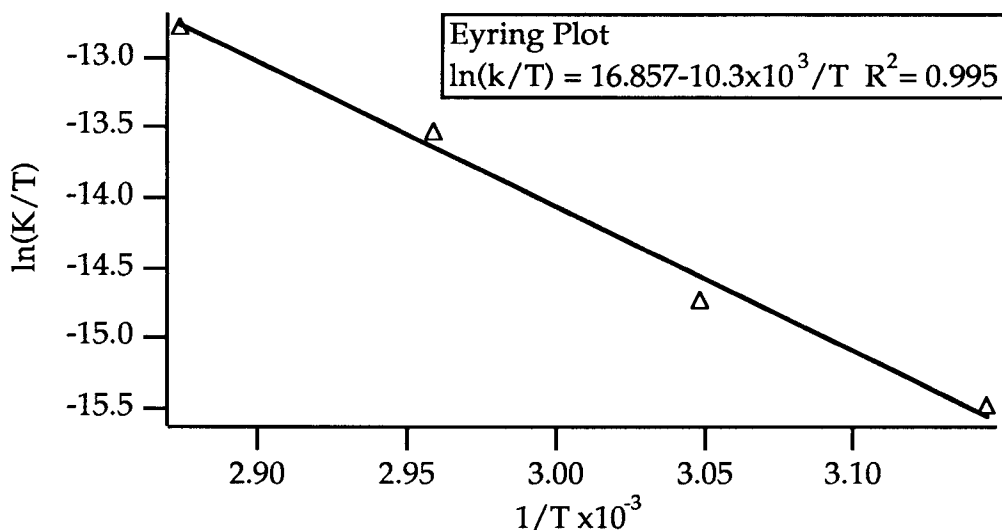


Figure 10. Eyring plot for thermal cis/trans isomerization of poly-s-butylCOT.

I. Dynamic Cis/trans Isomerization of the Trisubstituted Double Bond

Despite the energetic preference for a double bond to be trans, residual cis units are observed in "fully" isomerized polyacetylene. These units comprise an estimated 5-7% of *trans*-polyacetylene,¹⁴² and their effect upon carrier (soliton) formation has been discussed.¹³⁹ This observation coupled with the low barrier

for isomerization illustrates that the isomeric content of polyacetylene is not a clear-cut issue, and that the designations of *cis* and *trans* refer to polymer containing predominantly that isomer. Residual *cis* units in *trans*-polyacetylene (and *trans* units in *cis*-) will undoubtedly influence the physical properties of the polymer and are not often accounted for when interpreting the data.

The existence of residual *cis* units in the so-called "all *trans*" polymer became an issue when NMR spectra of soluble polymers in the *cis* and *trans* form were compared. As was mentioned in the last chapter, resonances that were due to main-chain protons were broad and generally uninformative. However, it was noticed that there were two resonances for each of the side-chain protons in the *trans* polymer, yet only one resonance in the *cis* polymer. These resonances are well separated and particularly easy to observe for the methine (e.g., -CH-) proton of the side group in the spectrum of *trans*-poly-*s*-butylCOT. The three resonances are assigned to *cis/cis*, *cis/trans* and *trans/trans* diads in the polymer. Integration of the two resonances at 50 °C determines the relative energy differences of the two diads to be small (0.8 kcal/mol). A spectrum of the methine region of the polymer in an intermediate stage of isomerization is shown in Figure 11. In the next chapter, it will be shown that semiempirical computations predict that trisubstituted double bonds in polyenes do not necessarily have the strong energetic preference to be *trans* versus *cis* with respect to the main chain. Side groups in polymers of substituted acetylenes also appear to increase the *cis* content (again with respect to the main chain) of the polymer.⁴⁶

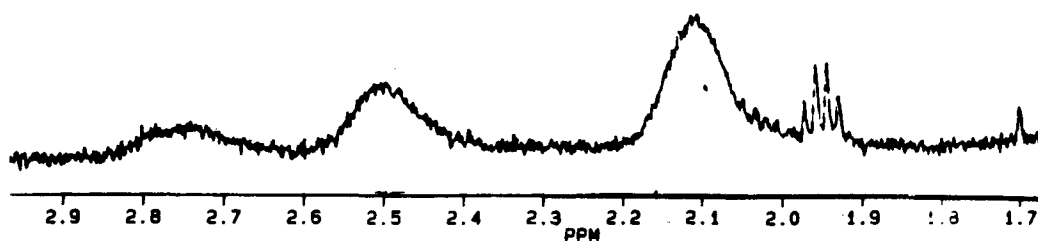


Figure 11. NMR resonances of the side groups of poly-*s*-butylCOT reveal two species in the "trans" polymer.

It was of interest to determine if *cis*/*trans* and *trans*/*trans* diads could interconvert. A magnetization transfer experiment on *trans*-poly-*s*-butylCOT revealed that these two species do interconvert, and $\Delta G^\ddagger = 18.9 \pm 0.4$ kcal/mol was measured at 50 °C in benzene. This activation energy corresponds to an interconversion rate of ≈ 1 s⁻¹ at this temperature.

Presumably a single double-bond isomerization does not produce a dramatic change in the absorbance of the chromophore (i.e., some length of polymer with an effective conjugation of ≈ 20 double bonds must contain at least two of these trisubstituted double bonds), since two species are not observed in the visible absorption spectrum. The spectrum of *trans*-poly-*s*-butylCOT is broad and is assumed to contain overlapping absorptions that are due to all of these species. Comparing visible absorbance data¹⁵ on alternating *cis*/*trans* polyenes (e.g., [ct]_x) with that of all *trans* polyenes (e.g., [tt]_x) suggests that these absorptions differ by perhaps 10-20 nm. In polymers of substituted acetylenes in which every double bond is trisubstituted, this dynamic isomerization may play an important role in the description of the conjugation of the polymer. Despite much synthetic work on polymers of substituted acetylenes (vide infra), even the acknowledgment of isomerization from *trans* to *cis* has been mentioned only

the data accumulated here and the modeling studies in the next chapter, we have been able to explore the entire range of effective conjugations for a polyacetylene chain. The tradeoff between conjugation and solubility and the maximum effective conjugation in polyacetylene that is still soluble have been illustrated.

Experimental

Instrumentation. Magnetization transfer was performed on a Bruker AM-500 (500.14 MHz ^1H) spectrometer. Chemical shifts were referenced to the chemical shift of the residual protons of the solvent with respect to tetramethylsilane. Ultraviolet-visible absorption spectroscopy was performed on either an HP 8451A or an HP 8452A diode-array spectrophotometer. Absorption spectra in the near infrared were collected on a Cary 14 UV/VIS/NIR as modified by Online Instruments. Resonance Raman spectra were obtained using 488 nm excitation from an argon ion laser source using two different setups. The first setup employed a SPEX monochromator, a power source of 300-330 mW, and each sample was referenced to the known absorption frequencies of a CCl_4 or silicon sample. Data on the second setup were collected by Hyun Chae Cynn in Dr. Malcom Nicol's group at UC Los Angeles. This setup employed a Princeton Instrument IRY 1024/G optical multichannel analyzer, which was sensitive enough to permit employment of a much lower incident power (≈ 50 mW). In this setup, the wavelength scale of the detector was calibrated using diamond and calcite samples. In both cases, samples were polymer films enveloped between two thin glass plates (biological cover slips) or were polymer films on a glass substrate. It was found that scattering the light directly off the polymer films gave consistently higher signal-to-noise ratios. No attempt was made to cool the sample during analysis. Scanning electron microscopy of gold-coated

samples (10 nm coating, sputtered deposition) was performed using 20 KeV electrons (micrographs taken in back-scattering mode). X-ray diffraction was measured by wide-angle scattering from a Guinier camera employing monochromatic Cu K α radiation. The third-order susceptibilities of polymer films were determined by Dr. Joseph Perry of the Jet Propulsion Laboratory using wedged-cell, third harmonic generation (THG) techniques.^{150, 151} THG measurements on poly-*n*-butylCOT and poly-trimethylsilyl films, referenced to a bare, fused silica plate, were made using 1064 nm pulses from a Q-switched Nd:YAG laser. Wedge THG interference fringes were observed by translating the cell normal to the laser beam. Thermal analysis was performed under a nitrogen purge on a Perkin Elmer DSC-7 differential scanning calorimeter and a Perkin Elmer TGS-2 thermogravimetric analyzer both at a scanning rate of 20 °C/min.

Doping and Conductivity measurements

Doping was accomplished by exposing the polymer films to iodine vapor for 3 to 6 hours in a previously evacuated chamber followed by pumping (< 0.01 torr) for approximately one hour or longer to remove any excess iodine. Films immediately became blue-black in color but remained flexible. Conductivities were measured using a four-point probe in a nitrogen drybox or a four-wire probe attached to a Schlenk line.¹⁵² Similar conductivities were observed using both methods. Film thicknesses were measured either with Fowler Digitrix II digital calipers or a Dektak 3030a profilometer. A JEOL 733 electron microprobe equipped with wavelength-dispersive X-ray detectors was used for energy-dispersive spectroscopy (EDS).

A solution of *trans*-poly-*s*-butylCOT was doped with NOPF₆ as was reported for solution-doped poly-alkylthiophenes.¹¹² The appropriate amount of a 4 mg/mL solution of NOPF₆ in CH₃CN was added to a 2 mg/mL solution of *trans*-poly-*s*-butylCOT in CHCl₃ to give doping levels between $y = 0.05$ and $y = 0.20$ ((C₁₂H₁₆)(NOPF₆)_y). Solutions were observed to decompose (e.g., turn from deep-blue to brown in color) over the course of 5-10 minutes at room temperature but were stable over the course of weeks at -50 °C under inert atmosphere.

Kinetic Measurements on *trans*-poly-*s*-butylCOT

Rates for *cis*/*trans* isomerization of poly-*s*-butylCOT were determined by observing the rate of appearance of the peak at 560 nm of a 4×10^{-5} M solution of the polymer in either THF or benzene. Temperature was controlled via a constant temperature bath (error ± 2 °C). Construction of Arrhenius and Eyring plots and subsequent determination of ΔH^\ddagger and ΔS^\ddagger are described in the literature.¹⁵³ Magnetization transfer was accomplished using a 180_A- τ -90_B pulse sequence at 50 °C in C₆D₆ as described in the literature.¹⁵⁴ The *ct* resonance at 2.5 ppm (A) was irradiated, and both this resonance and the *tt* resonance at 2.8 ppm (B) were integrated. An ethylene glycol temperature standard was used to calibrate the probe temperature (error ± 1 °C). T₁ values were obtained using a standard inversion-recovery sequence (180_A- τ -90_A).

Appendix I. COT Copolymers

It has already been demonstrated that COT can be copolymerized with COD to give a random copolymer containing segments of reduced conjugation

length and with norbornene to give a block copolymer containing highly conjugated segments.¹⁵⁵ Both of these types of polymers are interesting, but neither is soluble and highly conjugated. By copolymerizing two monosubstituted COT derivatives, one that homopolymerizes to give a soluble polymer and one that homopolymerizes to give an insoluble polymer (both in the trans form), it should be possible to "tailor" the effective conjugation length of the resulting polymer by adjusting the ratio of the two monomers. Preliminary results on copolymers of *n*-octylCOT or *n*-butylCOT with trimethylsilylCOT reveal that the effective conjugation length of the resulting copolymer increases monotonically with the amount of the *n*-octylCOT or *n*-butylCOT in the monomer feed (Figure 13). These results are preliminary because of the difficulty in obtaining adequate characterization data. As the absorption maximum of the polymer reaches approximately 580 nm, the polymer solutions behave strangely, giving swirling suspensions that take a minute or longer to become homogeneous to the eye when poured into an excess of solvent, finally becoming completely insoluble. It is hypothesized that solubility decreases as the polymer in the solution isomerizes over the course of time. The data in Figure 13 correspond to the optical-absorption maximum of very dilute copolymer solutions. Although copolymers derived from 40% or 50% trimethylsilylCOT in the monomer feed appeared completely soluble in concentrated (≈ 1 mg/mL) solutions in both the cis and trans forms, copolymers synthesized with a smaller ratio of this monomer may be aggregated in the trans form, much like *trans*-poly-*n*-butylCOT or *trans*-poly-*n*-octylCOT.

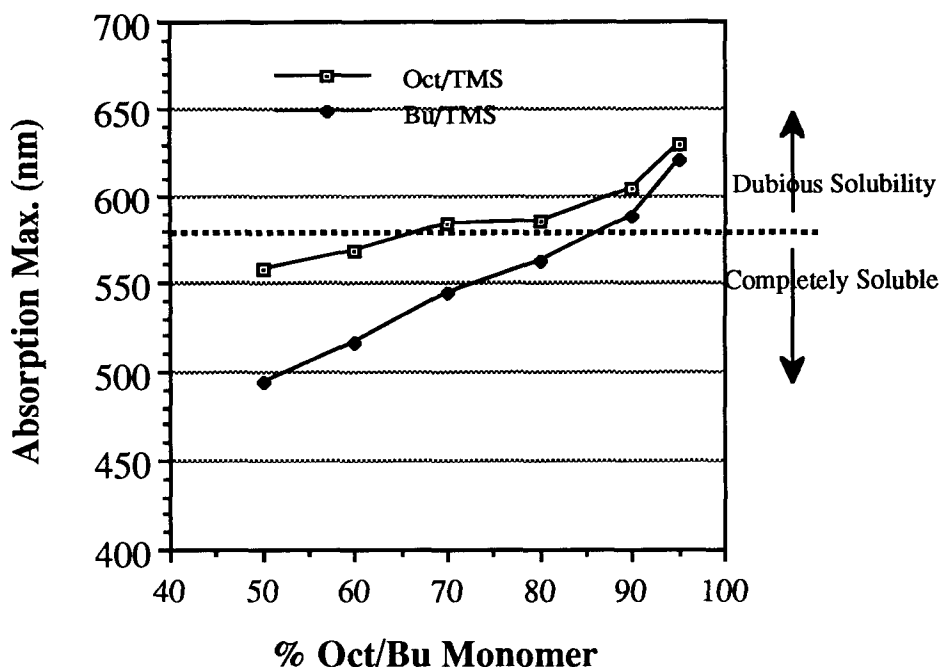


Figure 13. Optical-absorption maximum as a function of copolymer feed ratio. Has the soluble polyacetylene with the highest conjugation length been synthesized?

It is interesting to note that as the optical-absorption maximum of a polyacetylene increases to around 580 nm (in a common, organic solvent), the polymer becomes insoluble. This phenomenon has been observed in polyacetylene block copolymers (see discussions in Chapters 1 and 3) and has been attributed to aggregation and/or cross-linking, either of which could conceivably be facilitated as the effective conjugation of the chain increases. Although it would be more definitive if there were more structural characterization data and more information as to which polymers were soluble and which were aggregated (perhaps via small-angle X-ray scattering), these data do support the contention that there is a maximum, soluble conjugation

length possible for polyacetylene. Experimental conditions could be optimized such that in the language of the solid state physicist, the bandgap of the polymer could be tailored by the introduction of weak defects (e.g., cis linkages or twists in the chain) as opposed to strong defects (e.g., chemical defects).

References and Notes

- (1) For a recent, general discussion of various effects upon polymer conjugation, see: Batchelder, D. N. *Contemp. Phys.* **1988**, *29*(1), 3-31.
- (2) Bohlmann, F. *Chem. Ber.* **1952**, *85*(5), 386-389.
- (3) Bohlmann, F. *Chem. Ber.* **1953**, *86*(1), 63-69.
- (4) Bohlmann, F.; Kieslich, K. *Chem. Ber.* **1954**, *87*(9), 1363-1372.
- (5) Nayler, P.; Whiting, M. C. *J. Chem. Soc. Chem. Comm.* **1955**, , 3037-3046.
- (6) Sondheimer, F.; Ben-Efraim, D. A.; Wolovsky, R. J. *Am. Chem. Soc.* **1961**, *83*, 1675-1681.
- (7) Karrer, P.; Eugster, C. H. *Helv. Chim. Acta* **1951**, *34*, 1805-1814.
- (8) D'Amico, K. L.; Manos, C.; Christensen, R. L. *J. Am. Chem. Soc.* **1980**, *102*(6), 1777-1782.
- (9) Winston, A.; Wichacheewa, P. *Macromolecules* **1973**, *6*(2), 200-205.
- (10) Schaffer, H. E.; Chance, R. R.; Knoll, K.; Schrock, R. R.; Silbey, R. in *Conjugated Polymeric Materials: Opportunities in Electronics, Optoelectronics, and Molecular Electronics*; Bredas, J. L.; Chance, R. R. Eds.; NATO ASI Series. Series E: Applied Sciences 182; Kluwer Academic Publishers: Dordrecht, The Netherlands, 1990; pp. 365-376.
- (11) Kohler, B. E. in *Electronic Properties of Polymers and Related Compounds*; Kuzmany, H.; Mehring, M.; Roth, S. Eds.; Springer Ser. Solid State Sci. 63; Springer-Verlag: New York, 1985; pp. 100-106.

- (12) Kohler, B. E.; Pescatore, J., J. A. in Reference 10, pp. 353-364.
- (13) Also for a good review of polyene spectroscopy, see: Hudson, B.; Kohler, B. E. *Synth. Met.* **1984**, *9*, 241-253.
- (14) Suzuki, H. *Electronic Absorption Spectra and Geometry of Organic Molecules*; Academic Press: New York, 1967; pp. 364-377.
- (15) Knoll, K.; Schrock, R. R. *J. Am. Chem. Soc.* **1989**, *111*(20), 7989-8004.
- (16) Rao, C. N. R. *Ultra-Violet and Visible Spectroscopy*; Plenum Press: New York, 1967; pp. 95-97.
- (17) Reference 14, pp. 357-363.
- (18) Fueno, T.; Yamaguchi, K. *Bull. Chem. Soc. Jpn.* **1972**, *45*(11), 3290-3300.
- (19) Eckhardt, H. *J. Chem. Phys.* **1983**, *79*(4), 2085-2086.
- (20) Baughman, R. H.; Hsu, S. L.; Pez, G. P.; Signorelli, A. J. *J. Chem. Phys.* **1978**, *68*(12), 5405-5409.
- (21) Elert, M. L.; White, C. T. *Phys. Rev. B* **1983**, *28*(12), 7387-7389.
- (22) Rao, B. K.; Darsey, J. A.; Kestner, N. R. *Phys. Rev. B* **1985**, *31*(2), 1187-1190.
- (23) Kohler, B. E. Personal communication.
- (24) Rimai, L.; Heyde, M. E.; Gill, D. J. *Am. Chem. Soc.* **1973**, *95*(14), 4493-4501.
- (25) Berréher, J.; Lapersonne-Meyer, C.; Schott, M.; Le Postollec, M. *Chem. Phys.* **1983**, *77*, 11-19.
- (26) Vardeny, Z.; Ehrenfreund, E.; Brafman, O.; Horovitz, B. *Phys. Rev. Lett.* **1983**, *51*(25), 2326-2329.
- (27) Baruya, A.; Gerrard, D. L.; Maddams, W. F. *Macromolecules* **1983**, *16*(4), 578-580.
- (28) Lichtmann, L. S.; Fitchen, D. B.; Temkin, H. *Synth. Met.* **1979/1980**, *1*, 139-149.
- (29) Lichtmann, L. S., Ph. D. Thesis, Cornell University, 1981.
- (30) Schügerl, F. B.; Kuzmany, H. *J. Chem. Phys.* **1981**, *74*(2), 953-958.

- (31) Kuzmany, H. *Pure and Appl. Chem.* **1985**, *57*(2), 235-246.
- (32) Iwahana, K.; Kuzmany, H. in Reference 11, pp. 145-147.
- (33) Ehrenfreund, E.; Vardeny, Z.; Brafman, O. in Reference 11, pp. 137-143.
- (34) Kuzmany, H.; Knoll, P. in Reference 11, pp. 114-121.
- (35) Sease, J. W.; Zechmeister, L. *J. Am. Chem. Soc.* **1947**, *69*, 270-273.
- (36) See References 30-39 in: Elsenbaumer, R. L.; Schacklette, L. W. in *Handbook of Conducting Polymers*; Skotheim, T. A. Ed.; Marcel Dekker, Inc.: New York, 1986; Vol. 1, pp. 213-263.
- (37) Schenk, R.; Gregorius, H.; Meerholz, K.; Heinze, J.; Müllen, K. *J. Am. Chem. Soc.* **1991**, *113*(7), 2634-2647.
- (38) Caspar, J. V.; Ramamurthy, V.; Corbin, D. R. *J. Am. Chem. Soc.* **1991**, *113*(2), 600-610.
- (39) Ramamurthy, V.; Caspar, J. V.; Corbin, D. R. *J. Am. Chem. Soc.* **1991**, *113*(2), 594-600.
- (40) Spangler, C. W.; Rathunde, R. A. *J. Chem. Soc., Chem. Commun.* **1989**, 26-27.
- (41) Andrews, L.; Lurito, J. T. *Tetrahedron* **1986**, *42*(22), 6343-6349.
- (42) Fichou, D.; Horowitz, G.; Garnier, F. *Synth. Met.* **1990**, *39*, 125-131.
- (43) Masuda, T.; Higashimura, T. *Adv. Polym. Sci.* **1986**, *81*, 121-165.
- (44) Masuda, T.; Higashimura, T. *Acc. Chem. Res.* **1984**, *17*, 51-56.
- (45) Gibson, H. W. in Reference 36, pp. 405-439.
- (46) Cis/trans content has been probed for some polymers, and it appears that bulkier side groups increase the cis content of the polymer: Leclerc, M.; Prud'homme, R. E.; Soum, A.; Fontanille, M. *J. Polym. Sci. Polym. Phys. Ed.* **1985**, *23*, 2031-2041.
- (47) The few studies on the cis/trans content of polymers of substituted acetylenes are contained in this reference and References 10-13 therein: Costa, G.; Grosso, A.; Sacchi, M. C.; Stein, P. C.; Zetta, L. *Macromolecules* **1991**, *24*(10), 2858-

2861.

- (48) Brédas, J. L.; Heeger, A. J. *Macromolecules* **1990**, *23*(4), 1150-1156.
- (49) Furlani, A.; Napoletano, C.; Paolesse, R.; Russo, M. V. *Synth. Met.* **1987**, *21*, 337-342.
- (50) Petit, M. A.; Soum, A. H.; Leclerc, M.; Prud'homme, R. E. *J. Polym. Sci. Polym. Phys.* **1987**, *25*, 423-433.
- (51) Leclerc, M.; Prud'homme, R. E. *Macromolecules* **1987**, *20*(9), 2153-2159.
- (52) Ehrlich, P.; Anderson, W. A. in Reference 36, pp. 441-488.
- (53) Masuda, T.; Hamano, T.; Higashimura, T.; Ueda, T.; Muramatsu, H. *Macromolecules* **1988**, *21*(2), 281-286.
- (54) Masuda, T.; Hamano, T.; Tsuchihara, K.; Higashimura, T. *Macromolecules* **1990**, *23*(5), 1374-1380.
- (55) Masuda, T.; Higashimura, T. in *Silicon-based Polymer Science: A Comprehensive Resource*; Ziegler, J. M.; Fearson, F. W. Eds.; Advances in Chemistry Series 224; American Chemical Society: Washington, D. C., 1990; pp. 641-661.
- (56) Subramanyam, S.; Blumstein, A. *Macromolecules* **1991**, *24*(10), 2668-2674.
- (57) Yamaguchi, M.; Torisu, K.; Hiraki, K.; Minami, T. *Chem. Lett.* **1990**, 2221-2222.
- (58) Chien, J. C. W.; Wnek, G. E.; Karasz, F. E.; Hirsch, J. A. *Macromolecules* **1981**, *14*(3), 479-485.
- (59) Zeigler, J. M. *Polym. Prepr.* **1984**, *25*(2), 223-224.
- (60) Hudson, B. S.; Kohler, B. E.; Schulten, K. in *Excited States*; Lim, E. C. Ed.; Academic Press: New York, 1982; Vol. 6, p 27.
- (61) Lasaga, A. C.; Aerni, R. J.; Karplus, M. J. *Chem. Phys.* **1980**, *73*(10), 5230-5243.
- (62) Pine, S. H. *Organic Chemistry*, Fifth Edition; McGraw-Hill: San Francisco,

1987; p. 140.

- (63) Rao, B. K.; Kestner, N. R.; Darsey, J. A. *Z. Phys. D.* **1987**, *6*, 17-20.
- (64) Brédas, J. L.; Street, G. B.; Thémans, B.; André, J. M. *J. Chem. Phys.* **1985**, *83*, 1323.
- (65) Brock, C. P.; Minton, R. P. *J. Am. Chem. Soc.* **1989**, *111(13)*, 4586-4593.
- (66) Brédas, J. L. in Reference 11, pp. 166-171.
- (67) Cui, C. X.; Kertesz, M. *Phys. Rev. B.* **1989**, *40(14)*, 9661-9670.
- (68) Ginder, J. M.; Epstein, A. J. *Phys. Rev. B.* **1990**, *41(15)*, 10674-10685.
- (69) Brédas, J. L.; Quattrocchi, C.; Libert, J.; Meyers, F. Poster TH 2.3, International Conference on the Science and Technology of Synthetic Metals (ICSM), Tübingen, Germany, August, 1990.
- (70) Villeret, B.; Nechtschein, M. *Phys. Rev. Lett.* **1989**, *63(12)*, 1285-1287.
- (71) Jozefowicz, M. E.; Laversanne, R.; Javadi, H. H. S.; Epstein, A. J.; Pouget, J. P.; Tang, X.; MacDiarmid, A. G. *Phys. Rev. B.* **1989**, *39(17)*, 12958-12961.
- (72) Abadie, M. J. M.; Boukli, S. M.; Cadene, M.; Rolland, M. *Polymer* **1986**, *27*, 2003-2008.
- (73) Frommer, J. E.; Chance, R. R. in *Encyclopedia of Polymer Science and Engineering*; Wiley & Sons: New York, 1986; Vol. 5, pp. 462-507.
- (74) Brédas, J. L.; Street, G. B. *Acc. Chem. Res.* **1985**, *18*, 309-315.
- (75) Heeger, A. J.; Kivelson, S.; Schrieffer, J. R.; Su, W.-P. *Rev. Mod. Phys.* **1988**, *60(3)*, 781-850.
- (76) Heeger, A. J. *Polym. J.* **1985**, *17(1)*, 201-208.
- (77) Ikehata, S.; Kaufer, J.; Woerner, T.; Pron, A.; Druy, M. A.; Sivak, A.; Heeger, A. J.; MacDiarmid, A. G. *Phys. Rev. Lett.* **1980**, *45(13)*, 1123-1126.
- (78) This principle has been nicely illustrated for a series of soliton model compounds: Tolbert, L. M.; Ogle, M. E. *J. Am. Chem. Soc.* **1990**, *112(26)*, 9519-9527.
- (79) Ehinger, K.; Roth, S. in Reference 11, pp. 67-74.

- (80) Thakur, M. *Macromolecules* **1988**, *21*(3), 661-664.
- (81) See also a recent write-up surrounding this controversy: Borman, S. *Chem. Eng. News* **1990**, *68*(19), 53-55.
- (82) Bott, D. C. in Reference 36; Vol 2, pp. 1192-1232.
- (83) Baughman, R. H.; Shacklette, L. W. *Phys. Rev. B.* **1989**, *39*(9), 5872-5886.
- (84) Baughman, R. H.; Shacklette, L. W. *J. Chem. Phys.* **1989**, *90*(12), 7492-7504.
- (85) Chiang, C. K.; Park, Y. W.; Heeger, A. J.; Shirakawa, H.; Louis, E. J.; MacDiarmid, A. G. *J. Chem. Phys.* **1978**, *69*(11), 5098-5104.
- (86) Mihály, G.; Vanscó, G.; Pekker, S.; Jánossy, A. *Synth. Met.* **1979/80**, *1*, 357-362.
- (87) Epstein, A. J. in Reference 82, pp. 1041-1098.
- (88) Weinberger, B. R.; Roxlo, C. B.; Etemad, S.; Baker, G. L.; Orenstein, J. *Phys. Rev. Lett.* **1984**, *53*(1), 86-89.
- (89) Kolev, V. D. *J. Mol. Struct.* **1984**, *114*, 257-260.
- (90) Moses, D.; Feldblum, A.; Ehrenfreund, E.; Heeger, A. J.; Chung, T.-C.; MacDiarmid, A. G. *Phys. Rev. B.* **1982**, *26*(6), 3361-3369.
- (91) Sklar, L. A.; Hudson, B. S.; Petersen, M.; Diamond, J. *Biochemistry* **1977**, *16*(5), 813-819.
- (92) Patil, A. O.; Heeger, A. J.; Wudl, F. *Chem. Rev.* **1988**, *88*, 183-200.
- (93) This paper involves valence-effective Hamiltonian (VEH) calculations on various conjugated polymers. In particular, this author has noted that small changes in geometry will noticeably affect bandgap calculations in independently performed VEH computations: Brédas, J. L.; Chance, R. R.; Baughman, R. H. *J. Chem. Phys.* **1982**, *76*(7), 3673-3678.
- (94) Deits, W.; Cukor, P.; Rubner, M.; Jopson, H. *Synth. Met.* **1982**, *4*, 199-210.
- (95) Dias, A. J.; McCarthy, T. J. *Macromolecules* **1985**, *18*(5), 869-871.
- (96) Tolbert, L. M.; Schomaker, J. A.; Holler, F. J. *Synth. Met.* **1986**, *15*, 195-199.

- (97) Because of the vast number of approaches that have been taken, the reader is referred to an excellent review: Stowell, J. A.; Amass, A. J.; Beevers, M. S.; Farren, T. R. *Polymer* **1989**, *30*, 195-201.
- (98) Tubino, R.; Dorsinville, R.; Lam, W.; Alfano, R. R.; Birman, J. L.; Bolognesi, A.; Destri, S.; Catellani, M.; Porzio, W. *Phys. Rev. B* **1984**, *30(11)*, 6601-6605.
- (99) Piaggio, P.; Cuniberti, C.; Dellepiane, G.; Bolognesi, A.; Catellani, M.; Destri, S.; Porzio, W.; Tubino, R. *Synth. Met.* **1987**, *17*, 337-342.
- (100) Dorsinville, R.; Yang, L.; Alfano, R. R.; Tubino, R.; Destri, S. *Solid State Commun.* **1988**, *68(9)*, 875-877.
- (101) Pflieger, J.; Kminek, I.; Nespurek, S.; Prasad, P. N. *Synth. Met.* **1990**, *37*, 255-261.
- (102) Dorsinville, R.; Tubino, R.; Krimchansky, S.; Alfano, R. R.; Birman, J. L.; Bolognesi, A.; Destri, S.; Castellani, M.; Porzio, W. *Phys. Rev. B* **1985**, *32(6)*, 3377-3380.
- (103) VanNice, F. L.; Bates, F. S.; Baker, G. L.; Carroll, P. J.; Patterson, G. D. *Macromolecules* **1984**, *17(12)*, 2626-2629.
- (104) Krouse, S. A.; Schrock, R. R. *Macromolecules* **1988**, *21(6)*, 1885-1888.
- (105) Jozefiak, T. H.; Lewis, N. S.; Grubbs, R. H. Unpublished results.
- (106) Ginsburg, E. J., Ph. D. Thesis, California Institute of Technology, 1990.
- (107) Gorman, C.; Ginsburg, E.; Marder, S.; Grubbs, R. *Polym. Prepr.* **1990**, *31(1)*, 386-7.
- (108) Grubbs, R. H.; Gorman, C. B.; Ginsburg, E. J.; Perry, J. W.; Marder, S. R. in *Materials for Nonlinear Optics: Chemical Perspectives*; Marder, S. R.; Sohn, J. E.; Stucky, G. D. Eds.; ACS Symposium Series 455; American Chemical Society: Washington, DC, 1991; pp. 672-682.
- (109) Gorman, C. B.; Ginsburg, E. J.; Sailor, M. J.; Moore, J. S.; Jozefiak, T. H.; Lewis, N. S.; Grubbs, R. H.; Marder, S. R.; Perry, J. W. *Synth. Met.* **1991**, *41(3)*,

1033-1038.

(110) Marder, S. R.; Perry, J. W.; Klavetter, F. L.; Grubbs, R. H. *Chem. Mater.* **1989**, *1*(2), 171-173.

(111) Based upon the Fieser-Kuhn rules for polyene optical spectra. For a good description, see: Silverstein, R. M.; Bassler, G. C.; Morrill, T. C. *Spectrometric Identification of Organic Compounds*, Fourth Ed.; John Wiley & Sons: New York, 1981; Chapter 6.

(112) Nowak, M. J.; Rughooputh, S. D. D. V.; Hotta, S.; Heeger, A. J. *Macromolecules* **1987**, *20*(5), 965-968.

(113) Heffner, G.; Pearson, D. Unpublished results.

(114) Wyatt, P. J.; Jackson, C.; Wyatt, G. K. *Am. Laborat.* **1988**, *20*(5), 86.

(115) Glatter, O.; Kratky, O. *Small Angle X-ray Scattering*; Academic Press: San Diego, 1982; Chapters 1, 12 and 15.

(116) Ballauff, M. *Angew. Chem. Int. Ed. Engl.* **1989**, *28*, 253-267.

(117) This theory of polymer mixing is well described by a text on polymer science: Rudin, A. *The Elements of Polymer Science and Engineering*; Academic Press, Inc.: San Diego, 1982; Chapter 12.

(118) Paul, D. R.; Barlow, J. W.; Keskkula, H. in *Encyclopedia of Polymer Science and Engineering*; John Wiley and Sons, New York, 1985; Vol. 12, pp. 399-461.

(119) de Meio, C. P.; Silbey, R. J. *Chem. Phys.* **1988**, *88*(4), 2558-2566.

(120) Soos, Z. G.; Hayden, G. W. *Phys. Rev. B.* **1989**, *40*(5), 3081-3089.

(121) de Meio, C. P.; Silbey, R. J. *Chem. Phys.* **1988**, *88*(4), 2567-2571.

(122) DeGennes, P. J. Discussion with R. H. Grubbs communicated to the author.

(123) Klavetter, F. L.; Grubbs, R. H. *J. Am. Chem. Soc.* **1988**, *110*, 7807-7813.

(124) Spangler, C. W.; Rathunde, R. A. *J. Chem. Soc., Chem. Commun.* **1989**, 26-27.

(125) Francois, B.; Bernard, M.; Andre, J. J. *J. Chem. Phys.* **1981**, *75*(8), 4142-4152.

- (126) Hoffman, D. M.; Gibson, H. W.; Epstein, A. J.; Tanner, D. B. *Phys. Rev. B.* **1983**, 27(2), 1454-1457.
- (127) Chien, J. C. W. *Polyacetylene: Chemistry, Physics, and Material Science*; Academic: Orlando, FL, 1984; p. 634.
- (128) Heeger, A. J. Presentation (MAT I, T1) International Conference on the Science and Technology of Synthetic Metals (ICSM), Tübingen, Germany, August, 1990.
- (129) Sailor, M. J.; Lewis, N. S.; Grubbs, R. H. Unpublished results.
- (130) Druy, M. A.; Tsang, C.-H.; Brown, N.; Heeger, A. J.; MacDiarmid, A. G. *J. Polym. Sci. Polym. Phys. Ed.* **1980**, 18, 429-441.
- (131) Lugli, G.; Pedretti, U.; Perego, G. *J. Polym. Sci. Polym. Lett. Ed.* **1985**, 23, 129-135.
- (132) Park, Y. W.; Park, C.; Lee, Y. S.; Yoon, C. O.; Shirakawa, H.; Suezaki, Y.; Akagi, K. *Solid State Commun.* **1988**, 65(2), 147-150.
- (133) Kahlert, H.; Leitner, O.; Leising, G. *Synth. Met.* **1987**, 17, 467-472.
- (134) Kajzar, F.; Etemad, S.; Baker, G. L.; Messier, J. *Synth. Met.* **1987**, 17, 563-567.
- (135) Ito, T.; Shirakawa, H.; Ikeda, S. *J. Polym. Sci. Polym. Chem. Ed.* **1975**, 13, 1943.
- (136) Edwards, J. H.; Feast, W. J.; Bott, D. C. *Polymer* **1984**, 25, 395-398.
- (137) Bott, D. C. *Polym. Prepr.* **1984**, 25(2), 219-220.
- (138) Clough, S. B. *CHEMTRACTS-Macromol. Chem.* **1990**, 1, 307-309.
- (139) Gibson, H. W.; Weagley, R. J.; Mosher, R. A.; Kaplan, S.; Prest, J., W. M.; Epstein, A. J. *Phys. Rev. B.* **1985**, 31(4), 2338-2342.
- (140) Kohler, B. E. *J. Chem. Phys.* **1988**, 88(4), 2788-2792.
- (141) Robin, P.; Pouget, J. P.; Comés, R.; Gibson, H. W.; Epstein, A. J. *Journal de Physique* **1983**, 44(6), C3-77.
- (142) Gibson, H. W.; Kaplan, S.; Mosher, R. A.; W. M. Prest, J.; Weagley, R. J. J.

Am. Chem. Soc. **1986**, *108*(22), 6843-6851.

(143) Tanaka, M.; Yasuda, H.; Tanaka, J. *Bull. Chem. Soc. Jpn.* **1982**, *55*(11), 3639-3640.

(144) Oki, M. *Applications of Dynamic NMR Spectroscopy to Organic Chemistry; Methods in Stereochemical Analysis*; VCH Publishers: Deerfield Beach, Florida, 1985; Vol. 4, pp. 106-139.

(145) Doering, W. v. E.; Birladeanu, L.; Cheng, X.; Kitagawa, T.; Sarma, K. *J. Am. Chem. Soc.* **1991**, *113*(12), 4558-4563.

(146) Ginsburg, E. J.; Gorman, C. B.; Marder, S. R.; Grubbs, R. H. *J. Am. Chem. Soc.* **1989**, *111*, 7621-7622.

(147) Kohler, B. E.; Mitra, P.; West, P. *J. Chem. Phys.* **1986**, *85*(8), 4436-4440.

(148) Ohmine, I.; Morokuma, K. *J. Chem. Phys.* **1981**, *74*(1), 564-569.

(149) Sandros, K.; Sundahl, M.; Wennerström, O.; Norinder, U. *J. Am. Chem. Soc.* **1990**, *112*(8), 3082-3086.

(150) Meredith, G. R.; Buchalter, B.; Hanzlik, C. *J. Chem. Phys.* **1983**, *78*, 1543.

(151) Kajzar, F.; Messier, J. *J. Opt. Soc. Am. B.* **1983**, *4*, 1040.

(152) Sze, S. M. *Physics of Semiconductor Devices*; Wiley & Sons: New York, 1981; p. 30.

(153) Sandström, J. *Dynamic NMR Spectroscopy*; Academic Press: San Diego, 1982.

(154) Mann, B. E. in *Annual Reports on NMR Spectroscopy*; Webb, G. A. Ed.; Academic Press: San Diego, 1982; Vol. 12, p. 272.

(155) Klavetter, F. L., Ph. D. Thesis, California Institute of Technology, 1989.

CHAPTER 4

COMPUTATIONAL MODELING OF SUBSTITUTED POLYACETYLENE OLIGOMERS

This work was performed in close collaboration with Eric J. Ginsburg

Introduction

As computers and computer programs become more sophisticated, computer modeling of molecules has been increasingly used to determine their relative energies, possible conformations and physical properties. Programs containing a variety of methods are now available, and an increasing number of synthetic chemical research groups are employing them to rationalize physical observations and to aid in the design of new molecules. The use of these computer programs is not without caveats and limitations. The workings of the world are not simply stated in program text, and the scientist must determine and justify the validity of a particular model in the prediction of molecular properties. However, the literature is filled with notable successes. Particularly in the field of polymer science, where NMR signals are blobs and the likelihood of obtaining X-ray diffraction data, let alone a "crystal structure," is often slim, these computational methods can often help to paint a picture of polymer conformation and dynamics that is more concrete than a qualitative rationalization.

In the last chapter, experimental data were presented for a number of polymers of monosubstituted cyclooctatetraenes (COT's) that suggested a connection between side-group sterics, reduction of effective conjugation length, and polymer solubility. Also, NMR data suggested that unlike conjugated disubstituted olefins, the trisubstituted olefins to which the side groups are attached do not display a preference to be trans with respect to the main chain. The explanation was advanced that the side group twisted the polymer main chain and also created some cis units in the polymer main chain. Both of these

effects would influence the effective conjugation length of the polymer, and both empirical and semiempirical methods will be used here to support and illustrate these phenomena.

A number of computational methods are available to complete these tasks, and the first step is to evaluate and select the method that will give the most meaningful results in some reasonable amount of time. The most unassuming view of a molecule is as a collection of nuclei with electrons whizzing around them. One can then fix the nuclei in space and calculate the electronic state wave function and the energy for the molecule. By moving the nuclei and repeating this calculation, the full potential energy surface of the molecule can be mapped out. This type of calculation, termed *ab initio*, is the most "high level" computation commonly used, but the number of interactions to take into account is large and the solution must be computed iteratively and often takes many steps before it is found. Currently, *ab initio* calculations can be performed on molecules with perhaps ten heavy (non-hydrogen) atoms at an appreciable computational cost (days to weeks of CPU time).

By parameterizing some of the interactions and neglecting certain calculation-intensive multicenter integrals, the amount of time for a computation can be decreased, allowing for computations on larger molecules. These methods, termed semiempirical, still calculate electronic state wave functions and use them to determine molecular energies. However, they rely on some empirical data, and this reliance forces the scientist to make some judgements on which values for parameters such as atomic orbital sizes and values of certain overlap or resonance integrals are appropriate for the specific system under study. The integrals are parameterized so that the method correctly predicts

molecular geometries and heats of formation in as many cases as possible. Typically, if a similar system has been successfully modelled with the method of interest (EHT, CNDO, MNDO, AM1), there is a reasonable basis for its use. Sometimes failures of various methods are noted in the literature and can be used to guide the selection.

In an empirical method, no calculations are typically performed to determine electronic-state wave functions. Indeed, in the most common empirical method, force field calculations, the program is blissfully unaware of electrons at all. Basically, a force field calculation treats a molecule as a set of balls and springs. The total energy expression of a molecule is arbitrarily broken down into a set of functions that describe energy as a function of bond stretch (E_b), bond angle (E_Θ), torsion (E_ϕ), through space interactions (E_{VDW}), hydrogen-bonding interactions (E_{HB}), etc.

$$E_{\text{total}} = E_b + E_\Theta + E_\phi + E_{VDW} + E_{HB} \dots \quad (1)$$

These functions all contain variable parameters that are parameterized for each atom and/or bond type. Thus, for instance, a bond-stretch function might look like

$$E_b = \frac{1}{2} K_b (R - R_0)^2 [1 + d(R - R_0)]. \quad (2)$$

For the C-H bond in methane (or more generally, any sp^3 hybridized carbon bonded to a hydrogen), K_b , R_0 and d are constants that are tabulated and inserted by the program. Note that K_b and R_0 can be thought of as a bond-force

constant ($\text{kcal/mol} \cdot \text{\AA}^2$) and a mean-bond distance (\AA). However, they are best viewed as numbers that are selected so that when this energy expression is combined with all of the others, correct energies are obtained for molecules containing C-H bonds. The correction factor, d , is merely another parameter that assists in getting correct energies. Thus, no parameter by itself is necessarily meaningful. One can set up a force field that underestimates bond stretching but increases Van der Waals interactions and gets the same energies. The only criterion for a parameter is that it correctly predicts the energy of the molecule when employed in its energy expression. A number of force fields are available (MM2, AMBER, OPLS, and others) and many are parameterized to be accurate for one particular class of molecules (e.g., proteins). Here, it is important that the force field be chosen to reflect interactions that occur in the molecule of interest. A force field is unlikely to render benzene as planar and non-bond-alternate if it doesn't specifically recognize and treat the system as "aromatic." For all of these caveats, force field calculations can be done quickly. Computational power now allows empirical calculations to be performed on substantial (thousands of atoms) macromolecules and also allows us to take solvent interaction into account. The previously discussed semiempirical and *ab initio* methods are generally only suitable only for calculations on a lone molecule (noninteracting, gas phase).

Most commonly, a computation is performed to find the energy (heat of formation) and optimum geometry for a molecule. Of course, molecules are not motionless, and the real picture of a molecule would show it in motion and perhaps in several accessible conformations. Since molecular mechanics is capable of calculating an energy as a function of position, potential energy surfaces can be sketched out. Naturally, the creator of the force field would have

to parameterize it so that it calculated barrier heights as well as energy minima correctly. A potential energy surface is useful for examining the energy of a molecule as a function of one or two geometric parameters (e.g., as a function of the twist around one or two bonds). However, to get a picture of all types of geometry changes that can occur in the entire molecule, one may perform a dynamic force field calculation.¹ A force field provides analytical expressions for the forces on a molecule in a given conformation. From these, velocities of atoms can be derived. The static molecule is allowed to move at these velocities for some small time, and then the new geometry can be used to calculate new velocities. This procedure can be used to generate molecular conformations at regular time steps, and the examination of these conformations allows for a dynamic view of the molecule. In many computational packages that perform force field calculations, one can specify a temperature (used to calculate available energies and then velocities), a time step, and a time length for a simulation, and the program can provide an animated sequence of the molecule and/or monitor various conformational parameters (bond lengths, angles, etc.) as a function of time. This method, among others, facilitates the exploration of the conformational space of the molecule. Larger barriers are often "hopped" by performing dynamics at elevated temperatures and then reducing the temperature to a reasonable value, a process called simulated annealing.

A number of computational efforts have been undertaken on conjugated polymers. Many of them center around the prediction of polymer bandgap, bandwidth and oxidation and reduction potentials based upon a well-defined repeat unit. Other efforts compute the electronic and geometric effects of the creation of charge carriers (solitons, polarons, bipolarons). Realizing that the geometry of a polymer chain will have an effect upon its electrical and optical

properties, exploration of the conformation of a polymer chain is also of interest. Thémans et al. examined 3-alkyl derivatives of oligothiophenes using MNDO.² They found little perturbation of the backbone geometry or electronic properties by the substituent, although this result is questionable since the failure of MNDO to treat torsions correctly has been noted.³ Polymers of substituted acetylenes were modeled by Leclerc and Prud'homme, using a molecular mechanics approach.⁴ The backbone of polymethylacetylene was found to be much less twisted than that of poly-*t*-butylacetylene.⁵ They concluded that their results, along with the experimental results of Ciardelli et al.,⁶ imply that chain geometry is most affected by substitution at the first carbon of a substituent. The polymers to be discussed here are much less substituted and more highly conjugated than polymers of substituted acetylenes (Chapter 3). However, the force field parameters used in this study are applicable in this system, and similar steric effects are observed as well. The role of ring torsions on the bandgaps and bandwidths of polyparaphenylene,^{7, 8} polypyrrole,^{9, 10} polythiophene^{9, 10} and polyaniline¹¹ have been explored. Most recently, *ab initio* calculations on the gas-phase torsion potentials of oligomers representative of polyacetylene, polydiacetylene and polythiophene have been reported.¹²

Results and Discussion

A model for local polymer conformation can be developed with the aid of both empirical and semiempirical calculations on model oligomers of type 1 and 2 (Figure 1). Both solvent and larger size regimes (entire polymer chains, groups of polymer chains, and larger) influence physical properties. However, these computations will show that there is a convincing correlation between many of the polymer's physical properties and conformation on this smallest-size regime.

At the current level of computational power available, empirical calculations on model molecules of this size are feasible. A geometry optimization can be performed within an hour. Semiempirical calculations are also feasible: a geometry optimization requires approximately 10 hours of CPU time. So-called "higher level" calculations (e.g., *ab initio*) would be impossible or prohibitively expensive in terms of time. Naturally, as time and computer technology progress, the window of feasibility will widen to include more rigorous methods for a molecule of some given complexity.

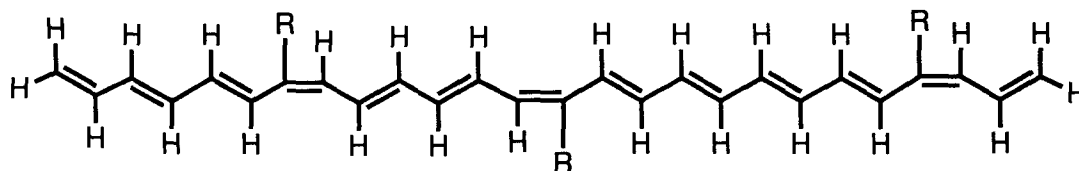
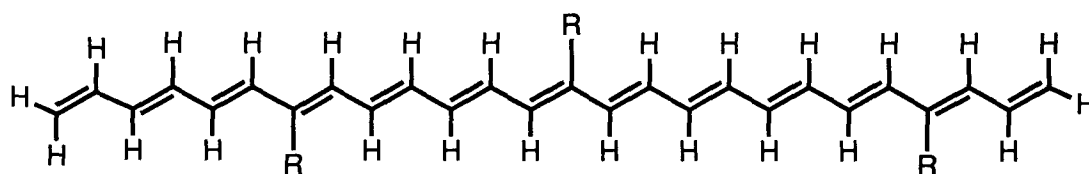


Figure 1. Model compounds used in this study.

A. Chain twisting - Static Picture

This section is concerned with the description and justification of the results of geometry optimization of model oligomers. Two methods have been employed. The empirical method involves a force field calculation, using the force field MM2. This force field has been subject to several modifications, and

full details are included in the experimental section. The semiempirical method employs the AM1 Hamiltonian. This parameterization is the most recent one commonly available and is believed to account for known deficiencies in previous methods, most notably the correct determination of torsion angles corresponding to energy minima, a weakness of its predecessor, MNDO.³

Since the model compounds employed are obviously not identical to the polymers they are designed to represent, some justification of the chosen structure is required. It has already been mentioned that these oligomers represent one of the smallest-size regimes for the polymer, and this fact should be kept in mind when assessing the validity of the experiment. Side-group placement on the polyene is 7 and 9 carbons apart, respectively. Polymerization of a monosubstituted COT will give side groups spaced, on the average, every eight carbons apart. Assuming that the trisubstituted olefins in the monosubstituted COT do not react in the polymerization, these side groups could get as close as 4 carbons apart. The steric effects of side groups spaced this closely have not been explored specifically. However, since these two side groups are not directly attached to each other, a force field calculation will recognize their interaction only through the Van der Waals energy term, and especially for small (second row) atoms, this term rapidly becomes negligible for increasing distance.¹³ Most force field calculations have a "cut-off" distance and do not consider Van der Waals interactions for atoms spaced farther apart than this distance. Finally, a trimer was selected to determine whether there were any unusual ways for sterics to be relieved that would not be possible in a smaller compound. It was expected that some combination of torsion potential and Van der Waals interactions would create twists around single bonds in the main chain, probably adjacent to the side group. This description turned out to be

accurate. However, it is possible that the force field could have, for example, kept the chain flat and bent it to relieve sterics through 3-point angle deformations (Figure 2).

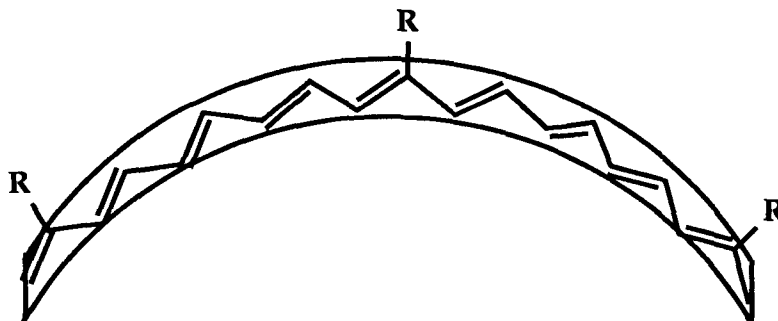


Figure 2. An alternative geometry, ruled out (at least for this size regime) by these computations.

A second concern is the justification of the methods employed. Early force field calculations did not treat bonding in a very sophisticated way, and for example, would assume that an oxygen bonded to one carbon was a carbonyl and an oxygen bonded to two carbons was an ether. This treatment is acceptable for many molecules. However, treating all C_{sp^2} - C_{sp^2} interactions identically in a polyene is not acceptable. It is well documented in the literature on polyenes that there is bond-length alternation (i.e., C-C is $\approx 1.48 \text{ \AA}$ and C=C is $\approx 1.34 \text{ \AA}$). Many force fields concern themselves only with atom types. This is not the case in the version of MM2 employed here. Interactions are tabulated for atoms bonded in specific ways. Thus, the single-bond torsion potential in a polyene is specifically tabulated (e.g., $C_{sp^2} = C_{sp^2} - C_{sp^2} = C_{sp^2}$). Torsion potentials are expressed as a three-term Fourier series, e.g.,

$$E_{tors} = \frac{1}{2}[B(1 + \cos(\omega)) + C(1 - \cos(2\omega)) + D(1 + \cos(3\omega))]. \quad (3)$$

The force field used to calculate the results¹⁴ uses the values $B = 1.25$ and $C = 8.0$; MM2(85) uses -0.93 and 8.0 .¹⁵ In each case, the threefold term, D , was not employed (i.e., $D = 0$). Brédas and Heeger have used ab initio routines to calculate the gas-phase torsion potential of polyacetylene oligomers to be about 6 kcal/mol. This value is comparable to the barrier calculated around the single bond in butadiene, in the oligomers discussed here and in the rotation barrier used in previous calculations on *cis*- and *trans*-polyacetylene.¹⁶ Again, one cannot compare experimental data with just one term in the full energy expression. However, Ginsburg¹⁷ has explored the effects on the geometry when B and C are changed, if only to show that small changes in these values do not dramatically change the twists around the single bonds observed in the results.

Both MM2 and AM1 give qualitatively similar pictures. Two single bonds are twisted in the model compounds (Table 1). These twists are found in the main-chain single bonds adjacent to all three substituents and are reported for those around the center substituent. Instead of reporting the dihedral angle, the absolute value of its supplement is reported in order to better indicate the relative deviation from planarity (i.e., $0^\circ = \text{planar}$) of the chain. Thus, the data reported do not indicate the direction of twist, only the magnitude. No bond lengths or angles are dramatically different from those reported for polyenes. Furthermore, dihedral angles around single bonds farther removed from the substituent as well as dihedral angles about all double bonds deviate less than 5° from 180° (i.e., planarity). Empirically, it is observed that twists in both Θ_1 and Θ_2 are large in the models of soluble polymers. In contrast, in the model of poly-*t*-butoxyCOT, Θ_1 is large, but Θ_2 is not, and experimentally, the polymer is not soluble. Given the good correlation between polymer solubility and chain twist, one can place a thick (to indicate some uncertainty) line across the bar graph of

twist angles. If both Θ_1 and Θ_2 are sufficiently large, the polymer is predicted to be soluble. This use of the model, in fact, prompted the synthesis of *trans*-polyisopropylCOT and *trans*-poly-cyclopentylCOT. Although the twist angles here are different, the optical-absorption maximum for these two polymers are more or less identical. Moreover, although *trans*-polycyclopropylCOT appeared as if it could be soluble, it was not. Note, however, that *trans*-polytrimethylsilylCOT has a different optical-absorption maximum than *trans*-poly-*s*-butylCOT. Overall, this "two-twist" picture empirically correlates well with solubility as illustrated by the bar that can be drawn in Figure 4. The twists, however, correlate less with optical-absorption maximum.

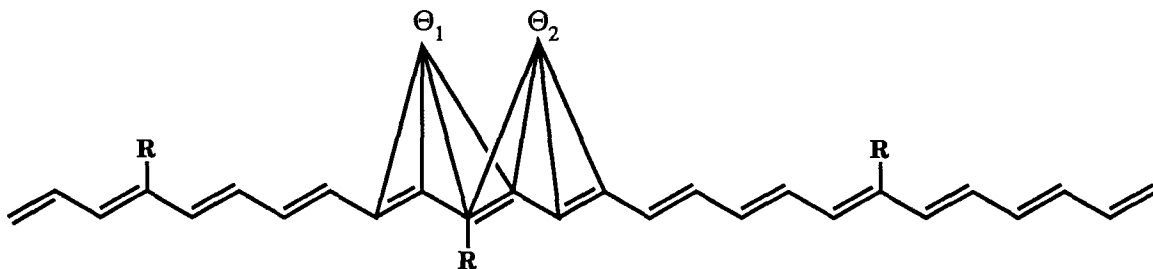


Figure 3. Model compound 1 showing the dihedral angles of interest. The same angles are reported for compound 2.

Table 1. Computed twist angles for model compound 1.^a

R	MM2 Θ_1	MM2 Θ_2	AM1 Θ_1	AM1 Θ_2
<i>n</i> -Bu	5.03	6.50	6.95	7.10
<i>s</i> -Bu	21.95	12.41	26.49	15.95
<i>t</i> -Bu	52.74	14.40	64.66	19.18
MeO	16.48	0.88	18.86	1.01
<i>t</i> -BuO	27.77	2.67	31.12	1.01
TMS	28.35	13.26	37.71	10.31
Phenyl	7.03 ^b	4.04 ^b	5.08 ^c	2.06 ^c
Neopentyl	15.72	3.10	15.49	0.71
Cyclopentyl	25.35	12.51	25.96	17.76
Isopropyl	35.83	10.02	24.27	19.12
Cyclopropyl	14.74	8.74	28.96	11.95

^aAngles reported are the absolute value of the supplement of the corresponding dihedral angle. ^bThe phenyl group is twisted 65° out of the plane of the backbone. ^cThe phenyl group is twisted 64° out of the plane of the backbone

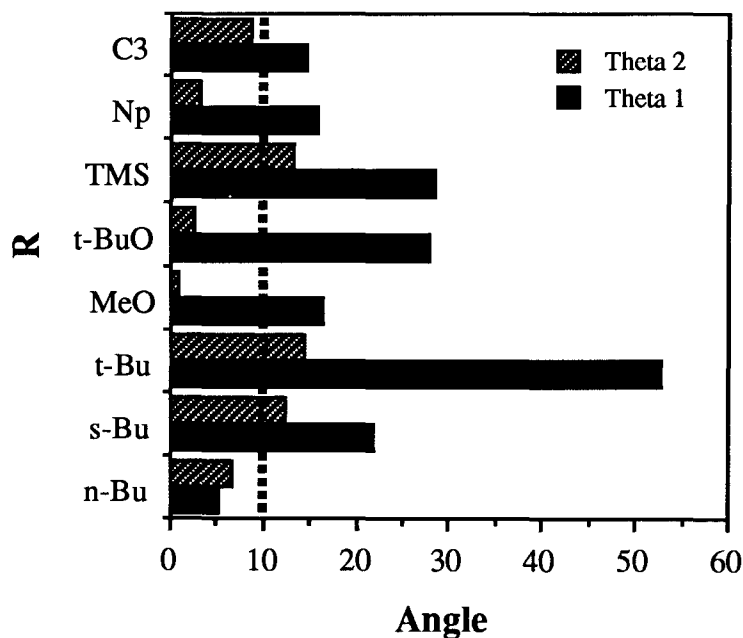


Figure 4. Graphical representations of twist angles for different side groups in model compound 1. (MM2 results, C3 = cyclopropyl, Np = neopentyl).

It is noteworthy that MM2 and AM1 results are similar. MM2 treats each single bond independent of conjugation length, whereas AM1 performs a full Hartree-Fock calculation on the molecule, which should be dependent on chain size. Similar twist angles are found for an arbitrary conjugation length. Thus, this computation agrees qualitatively with previous geometry optimizations on polyenes and polyacetylenes. Conjugation length does not affect single-bond rotation potentials, although it does affect double-bond isomerization potentials, since these motions do not occur solely via the ground electronic state of the molecule.

Results on the model compound **2** are important because of the evidence in the last chapter, and in Section C here, that the trisubstituted double bonds in the polymer can often be cis with respect to the main chain. These cis linkages certainly will have an effect on the determination of effective conjugation length and upon polymer solubility. However, twisting plays a role here as well. The polymer is not some combination of planar cis linkages and twisted trans segments. Indeed, twists around single bonds adjacent to cis double bonds appear even larger than those adjacent to trans double bonds. Overall, the real polymer is best thought of as some combination of these two models illustrated above.

Table 2. Computed twist angles for model compound 2.^a

R	MM2 Θ_1	MM2 Θ_2	AM1 Θ_1	AM1 Θ_2
<i>n</i> -Bu	32.50	11.68	50.80	35.31
<i>s</i> -Bu	36.66	7.92	42.05	32.46
<i>t</i> -Bu	64.81	3.52	40.67	23.55
MeO	28.25	6.81	32.70	23.67
<i>t</i> -BuO	35.36	6.76	40.16	28.34
TMS	25.46	10.43	25.65	11.61
Phenyl	19.14 ^b	7.51 ^b	20.99 ^c	7.59 ^c
Np	49.43	11.82	36.32	28.33
Cyclopentyl	32.84	7.85	47.61	28.65
Isopropyl	63.55	2.43	42.47	22.68
Cyclopropyl	18.01	8.14	24.86	17.10

^aAngles reported are the absolute value of the supplement of the corresponding dihedral angle. ^bThe phenyl group is twisted 49° out of the plane of the backbone. ^cThe phenyl group is twisted 48° out of the plane of the backbone.

B. Dynamic Picture of Chain Twisting

One issue that has not yet been addressed is the extent to which the solubility-inducing kink is a static or a dynamic phenomenon (see the discussion of solubility in Chapter 3). The question remains: Are the substituted polycyclooctatetraenes rigid, but kinked, molecules, or does the attachment of substituents make the backbone flexible by providing hinge points about which the polymer rotates? In the absence of experimental data, molecular dynamics calculations, which are used to explore the evolution of molecular motion over time,^{1, 18} can provide some insight. Molecular dynamics simulations of the model compound 1 have been conducted. The structures were held at 300 K for a simulated 20 picoseconds. The torsion angle, Θ_1 , was sampled every 20 femtoseconds. Figure 5 shows the total distribution of torsion angles sampled

over 20 ps in molecular dynamics simulations at 300 K of three different polycyclooctatetraene trimers. In general, the dihedral angles remain close to transoid planarity (180°), rocking from side to side during the run. The single bond in the *n*-butyl oligomer spends more time in a nonplanar conformation than the unsubstituted (i.e., R = H) oligomer. The single bond in the *s*-butyl oligomer samples even more nonplanar conformations. The single bond in the *t*-butyl oligomer, however, is found in both transoid ($|180^\circ| \leq \theta_1 \leq |90^\circ|$) and cisoid ($|90^\circ| \leq \theta_1 \leq |0^\circ|$) conformations. During the run tabulated in Figure 5, the *t*-butyl substituent was never coplanar with the main chain. Thus, it was found on only one side of the chain, and Θ_1 assumed only negative values. In longer runs or at higher temperatures, the *t*-butyl substituent should eventually move to the other side. Overall, in going from *n*-butyl to *s*-butyl to *t*-butyl, the dynamics indicates that the model spends more and more time in more varied conformations. Thus, floppiness increases with the steric bulk of the substituent.

Different conformations can also be discovered by Monte Carlo methods, where a number of conformations are generated and then minimized with the intention of finding structures corresponding to local minima in the potential energy surface.¹ This method was employed here to insure that the optimized geometries reported in the last section corresponded to the lowest energy conformation of the molecule and not a local minimum energy. The potential energy surface can also be sampled by running dynamics at higher temperatures, although this procedure tends to favor the entropic portion of the free energy ($\Delta G = \Delta H - T\Delta S$).¹ The relative number of structures found as a function of angle for **1**, R = *s*-butyl at a number of different temperatures is shown in Figure 6.

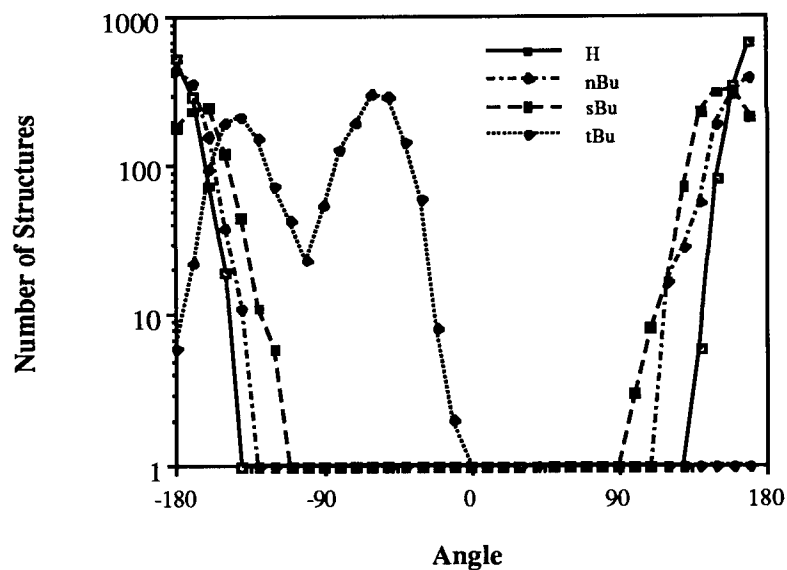


Figure 5. Values of torsion angle Θ_1 at 10 fs intervals accumulated during a 20 ps molecular dynamics run at 300 K (Batchmin) for **1**, R = *s*-Butyl.¹⁴

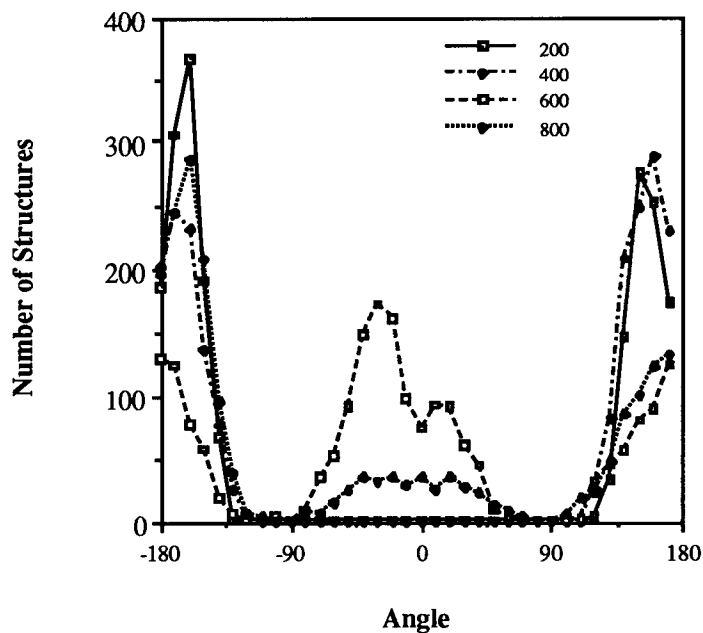


Figure 6. Values of torsion angle Θ_1 at 10 fs intervals accumulated during a 20 ps molecular dynamics run at various temperatures (in K) (Batchmin) for **1**, R = *s*-butyl.¹⁴

One can see that more and more nonplanar conformations are sampled as the temperature of the simulation increases. However, this travel over the potential energy surface is limited by the fact that sufficient velocity is required to get over a given energy barrier in one step. Otherwise, forces will be recomputed and the molecule will slide back down the surface in the next step. This event occurred in the 600K dynamics run, but did not occur in the 500K or 700K dynamics runs. Keeping this caveat in mind, if one looks at the average angle Θ_1 as a function of temperature, it does decrease as expected.

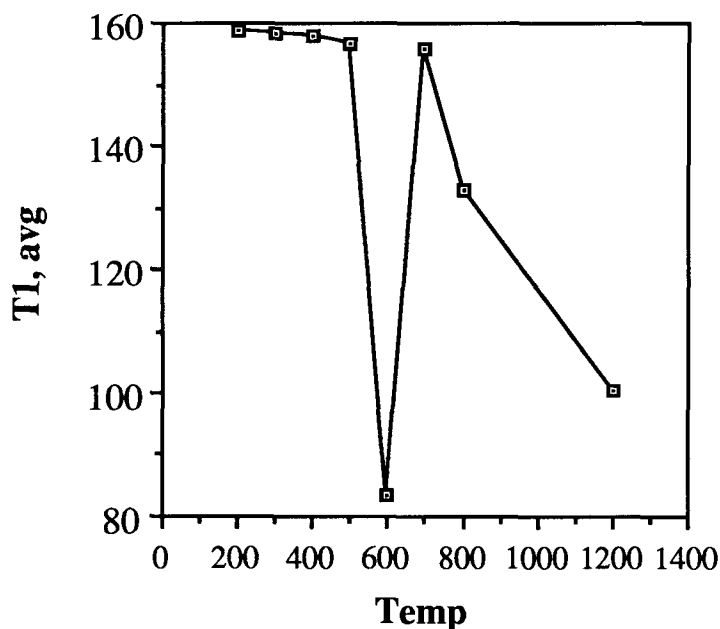


Figure 7. Average Θ_1 of 1, R = *s*-butyl as a function of temperature (in K).

Table 3. Number of occurrences of angle Θ_X for various dynamics runs on model compound 1.

R	<i>n</i> -Bu	<i>s</i> -bu	<i>t</i> -bu	TMS	TMS	<i>s</i> -bu	<i>s</i> -bu	TMS	<i>s</i> -bu	<i>s</i> -bu
T (°C)	300	300	300	300	400	400	200	200	1200	1200
Θ	Θ_1	Θ_1	Θ_1	Θ_1	Θ_1	Θ_1	Θ_1	Θ_1	Θ_1	Θ_2
-180	446	179		35	87	195	186	25	111	247
-170	355	234	6	109	228	245	305	67	101	257
-160	158	251	22	233	408	231	367	205	62	155
-150	38	120	94	186	451	137	190	177	59	123
-140	11	44	197	56	201	77	66	74	46	64
-130		11	214	21	59	27		6	43	44
-120		6	152	3	26	5			22	24
-110			74		5				41	13
-100			43		7				31	4
-90			23						26	8
-80			54						25	8
-70			128						35	
-60			192						44	
-50			301						62	
-40			288						76	
-30			143						66	
-20			59						75	
-10			8						70	
0			2						61	
10									38	
20									42	
30									57	
40									48	
50									33	1
60									28	2
70									23	7
80									21	6
90									32	17
100		3							25	28
110		8			8				48	34
120	16	16		33	23	27	4	10	69	56
130	28	71		122	85	82	34	114	71	97
140	56	228		354	133	208	146	509	86	153
150	187	304		470	151	248	275	520	107	208
160	311	312		299	78	288	253	239	105	212
170	394	213		79	50	230	174	54	111	232

Table 3. Cont.

R	s-bu	s-bu	s-bu	s-bu	s-bu	s-bu	s-bu	s-bu	s-bu
T (°C)	300	500	500	600	600	700	700	800	800
Θ	Θ_2	Θ_1	Θ_2	Θ_1	Θ_2	Θ_1	Θ_2	Θ_1	Θ_2
-180	355	230	328	128	367	170	391	202	347
-170	360	238	257	124	272	320	322	245	230
-160	246	357	174	78	222	329	165	287	202
-150	89	237	75	57	85	208	49	208	75
-140	14	99	33	18	31	79	18	96	38
-130	2	38	6	6	12	40	3	39	15
-120		22	6	2		17	1	8	4
-110		11	3	1		3		4	
-100		2	4	5				2	
-90				2				1	
-80				9				8	
-70				36				8	
-60				52				15	
-50				92				25	
-40				149				36	
-30				172				33	
-20				162				35	
-10				98				30	
0				74				35	
10				93				27	
20				91				35	
30				61				28	
40				45				24	
50				11				14	
60				4				9	
70				3				4	
80					2			2	
90					3			2	
100		1			7	2		6	
110		2	4	3	18	18	1	18	2
120	19	26	7	32	32	51	1	24	11
130	18	57	34	45	54	54	25	48	27
140	75	122	112	56	129	161	73	86	90
150	142	167	206	80	200	195	215	101	255
160	269	188	352	90	248	201	356	123	311
170	411	203	399	124	318	152	380	132	393

C. Cis/Trans Preference for the Trisubstituted Double Bond

Despite the fact that the double bonds in polyacetylene have a preference

for being trans (Chapter 3), it does not necessarily follow that the trisubstituted double bond in these polymers need have such a strong preference. The relative energies of cis-cis, cis-trans and trans-trans diads were determined using AM1 and the model tetraenes, **3** (Figure 8). All structures were geometry-optimized, so all (except R = H) are nonplanar.

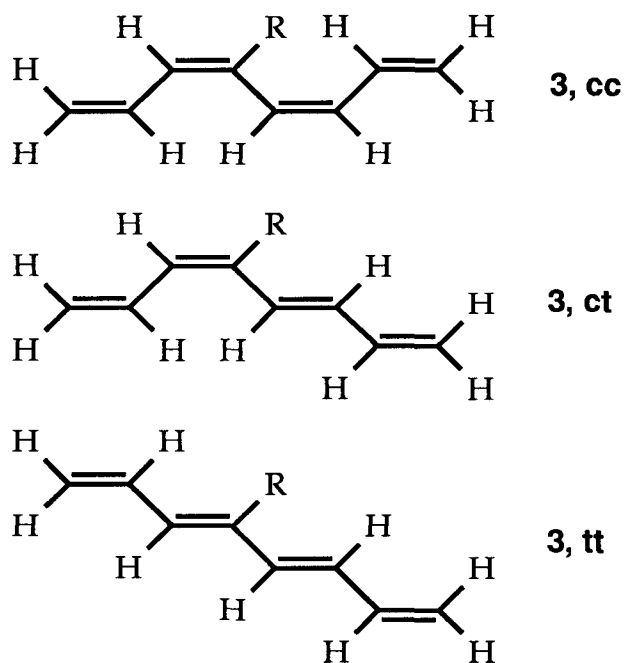


Figure 8. Model tetraenes used to determine heats of formation as a function of side group and isomeric composition.

Heats of formation for each of the three isomers are displayed graphically in Figure 9, and the difference in heat of formation between isomers (and thus a measure of ΔG_0 for the interconversion process) is tabulated in Table 4 (negative ΔE corresponds to an exothermic process).

Table 4. Energy differences between isomers of 3.

R	ΔE^a (cc→ct)	ΔE^a (ct → tt)	ΔE^a (cc → tt)
H	-1.20	-1.13	-2.33
<i>n</i> -butyl	-2.37	+2.00	-0.37
<i>s</i> -butyl	-1.39	+2.21	+0.83
<i>t</i> -butyl	-1.64	+2.22	+0.58
MeO	-0.06	-0.30	-0.36
<i>t</i> -BuO	-2.65	+0.57	-2.08
TMS	-0.95	+0.96	+0.01
Np	-1.19	-0.56	-1.76

^ain Kcal/mol

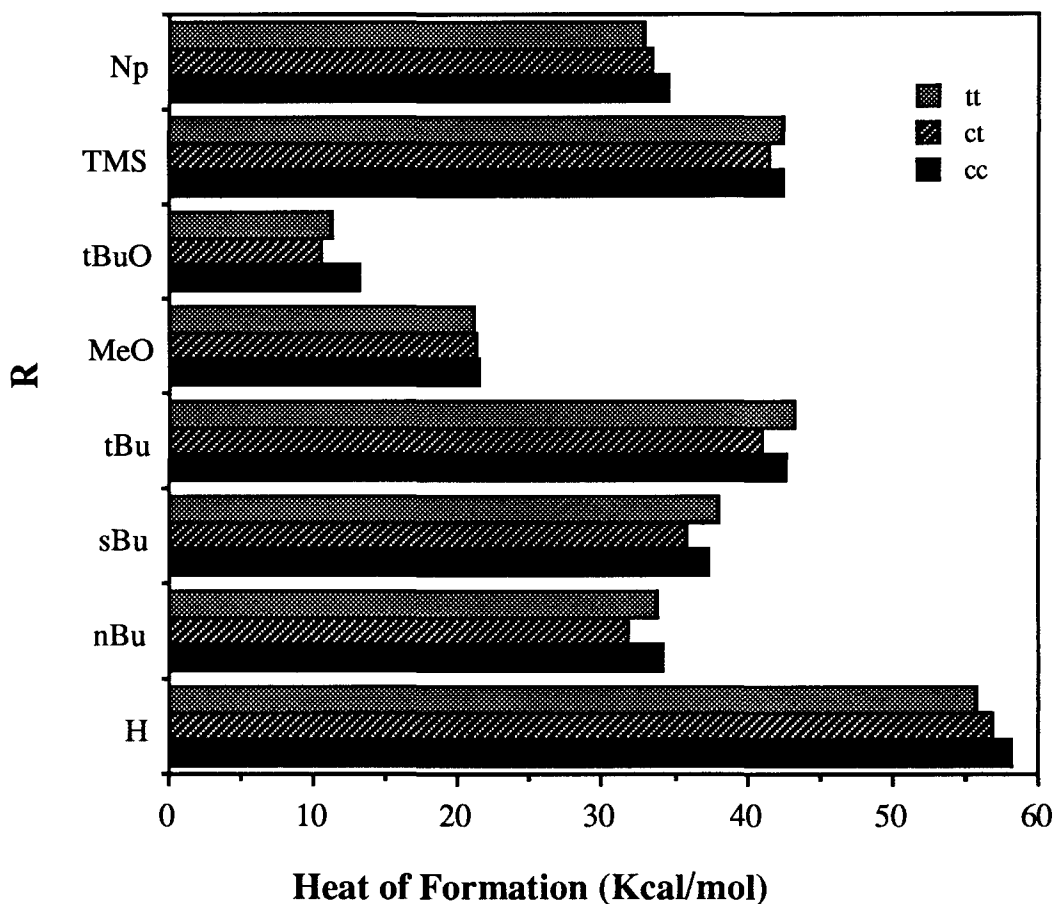


Figure 9. Relative heats of formation of various isomers of 3 as a function of side group.

Thus, AM1 predicts that not every double bond has such a strong preference to be trans with respect to the main chain. Note that the first isomerization (e.g., cc \rightarrow ct, the disubstituted double bond) is always exothermic as expected. Only in a few cases (R = H, MeO, Np) is the second isomerization (e.g., ct \rightarrow tt) exothermic. It is of more interest to examine the relative trends than the quantitative results, since this calculation is a zero K energy calculation. It is, for example, not valid to compare calculated differences in heat of formation for 3_{ct} R = *s*-butyl and 3_{tt} R = *s*-butyl with the ΔG_0 obtained by NMR in the last chapter.

Summary

The picture of twisting and an increased preference for cis linkages in the polyacetylene chain explains both the data presented in Chapter 3 and agrees with the computations presented here. These models are intended to provide a means of visualizing the conformation of the polymer, at least on its smallest-size regime. They have also been useful in the rational design of new polyacetylene derivatives with the goal of solubilizing the highest effective conjugation length possible. This goal appears to have been achieved with polymers containing secondary substituents such as *trans*-poly-*s*-butylCOT and *trans*-polycyclopentyl-COT. By modeling and synthesizing *trans*-polycyclopropylCOT, the limits of solubility appear to have been reached.

Experimental

MM2. MM2 calculations were performed using Batchmin¹⁴ Version 3.1b (on a DEC MicroVax 3500) or Version 2.6 (on a Silicon Graphics Iris 4D/220GTX

workstation). In all MM2 calculations, the default force field was used. The derivatives-convergence criterion was employed, with convergence defined to be the point when the root mean square of the first derivative reached 0.1. A typical command file, run on the Iris, is shown below.

```

/user/cbg/cistuff/sbuccc.mcm
/user/cbg/cistuff/sbuccc.mco
DEBG      28      102
#1=mm2 2=charmm 3=amber 5=opls/a
FFLD      1
READ
CONV      2      1
MINI      3      0      500

```

π -Calculations. Programs are available that perform Hückel π calculations in an iterative manner with molecular mechanics geometry optimization.¹⁹ In this technique, bond orders calculated with the π calculation for a given geometry are used to adjust molecular mechanics torsional potentials; the geometry calculated by the molecular mechanics routine is in turn used to calculate new bond orders. The calculation shuttles back and forth in this fashion until specified convergence criteria are met. (These routines exist primarily because older molecular mechanics programs were unable to differentiate between the single and double bonds of a conjugated system, so the bond orders had to be calculated first. Newer programs, such as Macromodel, are equipped to read input that explicitly gives bond orders, so the calculation is not necessary.) Some preliminary calculations on substituted polyenes were done with this procedure, using PCModel (Serena Software) on an Apple Macintosh II personal computer.

AM1. Semiempirical calculations were done using AM1 version 1.00²⁰ on a DEC MicroVax 3500. The AM1 Hamiltonian was employed. The minimization output

usually included the message: "Gradient test not passed, but further work not justified. SCF field was achieved." A typical command file, excluding all but 5 lines of the starting geometry of the molecule, is shown below.

```
AM1 XYZ T=1000000  
  
C      14.4487  1      2.0977  1      -5.8480  1  
H      14.5021  1      1.3587  1      -5.1470  1  
C      13.1165  1      2.5541  1      -6.2697  1  
H      13.0625  1      3.2931  1      -6.9707  1  
C      11.9912  1      2.0282  1      -5.7608  1
```

Molecular Dynamics.¹ Molecular mechanics force fields are used, but instead of searching for the lowest energy (0 K) structure, the geometry of the molecule is adjusted to keep the temperature at a specified (nonzero) value. At a finite temperature, the atoms have finite velocities, which are monitored. The kinetic energy that is due to atomic motion and the potential energy that is due to the constraints of the force field are calculated at specified intervals. Algorithms have been developed to keep the system at a specified temperature within a certain level of random fluctuation, given constraints such as bond lengths and bond angles.¹⁸

Molecular dynamics calculations were run at 300 K for 20 ps, using Batchmin.¹⁴ A typical command file for molecular dynamics on the MicroVax computer (Batchmin Version 3.1b) is shown below.

It is unclear whether or not a phenyl ring is a good candidate for the transmission of electronic effects. Certainly there are problems with the polymerization and the solubility of the resulting polymer. However, it was not certain whether the phenyl ring would be coplanar with the main chain. At the simplest level of reasoning, if the phenyl ring was twisted 90° with respect to the main chain, there would be no overlap between the two and no electronic effects (aside from inductive effects through the σ bonds) would be transmitted.

Molecular mechanics calculations were performed on trimer 4. However, in these calculations, the dihedral angle between the central phenyl ring and the main chain was fixed in several increments, and the relative energy of the resulting structure was plotted versus this angle after the remainder of the structure had been minimized (using Batchmin's FXTA option). The results in Figure 11 indicate that most of the steric strain can be relieved before the overlap between the phenyl ring and the main chain is lost ($\text{overlap} \propto \cos(\Theta)$ is graphed on the same scale). This computation indicates that the phenyl group tends to align perpendicularly to the main chain but can still reside in conformations in which it overlaps with the main chain.

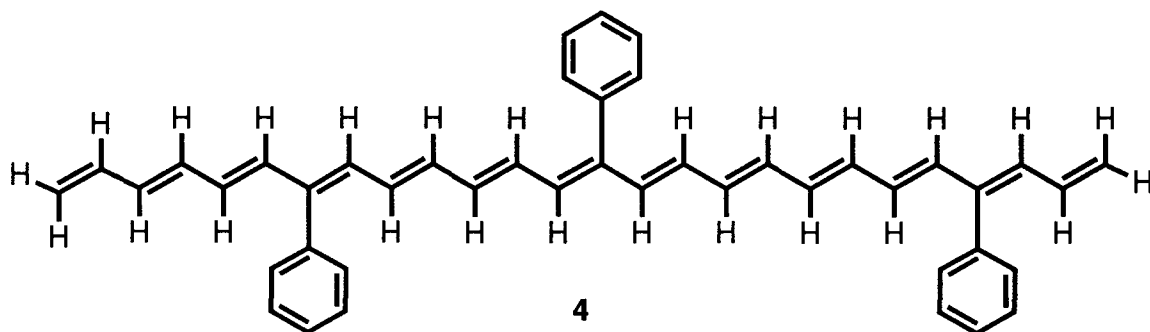


Figure 10. Trimer 4 used in molecular mechanics determination of relative energy as a function of phenyl ring twist (see Figure 11).

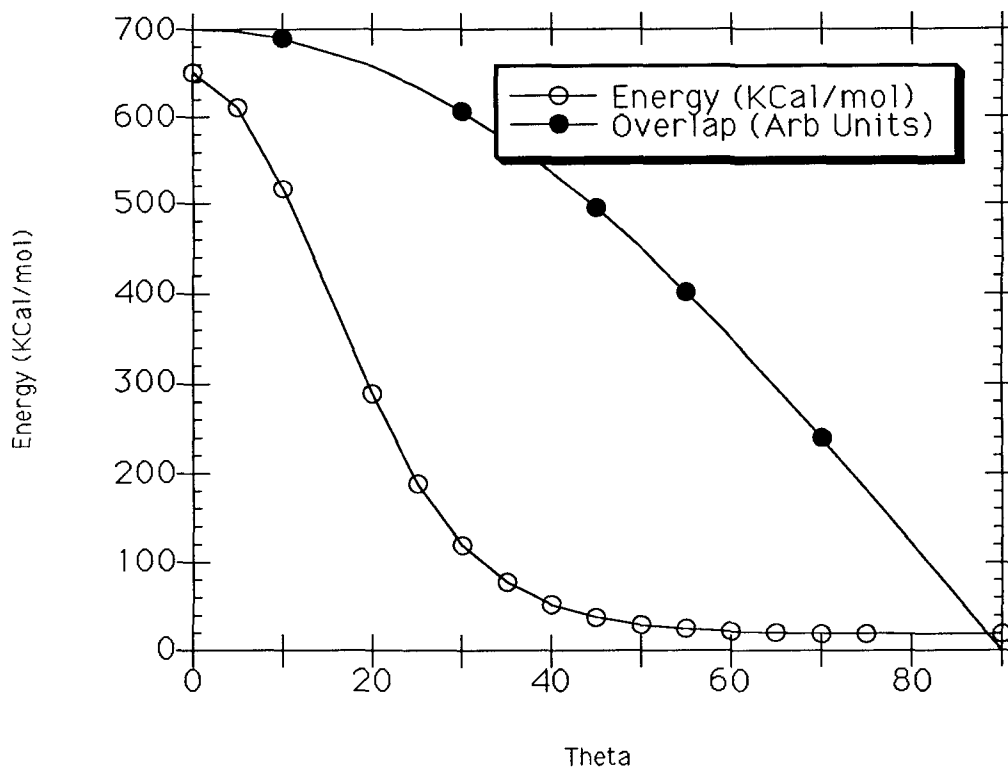


Figure 11. Relative energy of trimer **4**, (0° = phenyl ring is coplanar with backbone).

References and Notes

- (1) Gunsteren, W. F. v.; Berendsen, H. J. C. *Angew. Chem. Int. Ed. Engl.* **1990**, *29*, 992-1023.
- (2) Thémans, B.; André, J. M.; Brédas, J. L. *Synth. Met.* **1987**, *21*, 149-156.
- (3) Clark, T. A. *A Handbook of Computational Chemistry*; Wiley: New York, 1985.
- (4) Leclerc, M.; Prud'homme, R. E. *J. Polym. Sci. Polym. Phys. Ed.* **1985**, *23*, 2021-2030.

- (5) Cis/trans content has been probed for some polymers, and it appears that bulkier side groups increase the cis content of the polymer: Leclerc, M.; Prud'homme, R. E.; Soum, A.; Fontanille, M. J. *Polym. Sci. Polym. Phys. Ed.* **1985**, *23*, 2031-2041.
- (6) Ciardelli, F.; Lanzillo, S.; Pieroni, O. *Macromolecules* **1974**, *7*, 174-179.
- (7) Rao, B. K.; Kestner, N. R.; Darsey, J. A. Z. *Phys. D.* **1987**, *6*, 17-20.
- (8) Brédas, J. L.; Street, G. B.; Thémans, B.; André, J. M. *J. Chem. Phys.* **1985**, *83*, 1323.
- (9) Brédas, J. L. in *Electronic Properties of Polymers and Related Compounds*; Kuzmany, H.; Mehring, M.; Roth, S. Eds.; Springer Ser. Solid State Sci. 63; Springer-Verlag: New York, 1985; pp 166-171.
- (10) Cui, C. X.; Kertesz, M. *Phys. Rev. B.* **1989**, *40*(14), 9661-9670.
- (11) Ginder, J. M.; Epstein, A. J. *Phys. Rev. B.* **1990**, *41*(15), 10674-10685.
- (12) Brédas, J. L.; Heeger, A. J. *Macromolecules* **1990**, *23*(4), 1150-1156.
- (13) MM2 employs a Lennard-Jones potential of the form $E = a/r^6 + b/r^{12}$.
- (14) Still, W. C.; Columbia University.
- (15) Liljefors, T.; Tai, J. C.; Li, S.; Allinger, N. L. *J. Comp. Chem.* **1987**, *8*, 1051-1056.
- (16) Cernia, E.; D'ilario, L. *J. Polym. Sci. Polym. Chem. Ed.* **1983**, *21*, 2163-2176.
- (17) Ginsburg, E. J., Ph. D. Thesis, California Institute of Technology, 1990.
- (18) Ryckaert, J. P.; Ciccotti, G.; Berendsen, H. J. C. *J. Comp. Phys.* **1977**, *23*, 327-341.
- (19) Kao, J.; Allinger, N. L. *J. Am. Chem. Soc.* **1977**, *99*, 975-986.
- (20) Dewar, M. J. S.; Zoebisch, E. G.; Healy, E. F.; Stewart, J. J. P. *J. Am. Chem. Soc.* **1985**, *107*(13), 3902-9.
- (21) Jozefiak, T. H.; Lewis, N. S.; Grubbs, R. H. Unpublished results.

CHAPTER 5**SOLUBLE, CHIRAL POLYACETYLENES: SYNTHESSES AND
INVESTIGATION OF THEIR SOLUTION CONFORMATION**

This work has appeared in the literature (Moore, J. S.; Gorman, C. B.; Grubbs, R. H. *J. Am. Chem. Soc.*, **1991**, *113*(5), 1704-1712) and was performed with Dr. Jeffrey Moore.

Introduction

Polyacetylene has been the subject of intensive experimental and theoretical study.¹ Its extended π system is highly polarizable and capable of supporting mobile carriers created by oxidizing or reducing the polymer, and these phenomena lead to a variety of interesting optical and electrical properties. One of the most important features of a highly conjugated system is the low energy $\pi \rightarrow \pi^*$ electronic absorption (1.8 eV for *trans*-polyacetylene²). The electronic-absorption spectrum provides a probe of backbone conformation, since any deviation from planarity in the backbone will disrupt the conjugation of the olefins and will increase the energy of the electronic absorption. Polymerization of substituted acetylenes, for example, results in materials with low effective conjugation lengths as shown by their high-energy, visible-absorption spectra and comparatively low iodine-doped conductivities.³ This low conjugation length is presumably due to twisting around the single bonds in polyacetylene as a result of steric repulsions between the side groups (Figure 1a).⁴

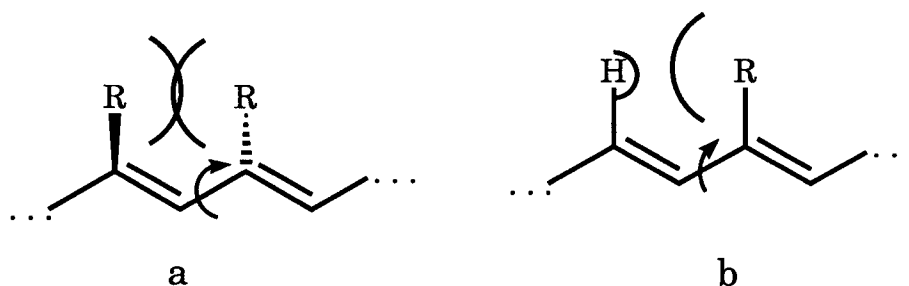


Figure 1. Chain Twisting in Polyacetylene.

Recently, the synthesis of polyacetylene by the ring-opening metathesis polymerization (ROMP) of cyclooctatetraene (COT) was reported.^{5,6} This chemistry has been extended to the ROMP of substituted cyclooctatetraenes,

providing a convenient route to a variety of partially substituted acetylenes (Figure 2).⁷ With the side group spaced, on the average, every eight carbons apart rather than two, the dominant steric interaction is between the side group and a β -hydrogen, reducing the amount of twisting and allowing for a soluble polymer with a much higher conjugation length (Figure 1b). Empirically, secondary or tertiary substituents immediately adjacent to the main chain render the polymer soluble in both the predominantly cis and trans forms. The polymer backbone is thought to twist around single bonds in the main chain adjacent to the substituent. This twist increases disorder in the polymer, imparting solubility. Yet, compared to the parent, unsubstituted polyacetylene, the π system is only minimally perturbed in most cases.⁸

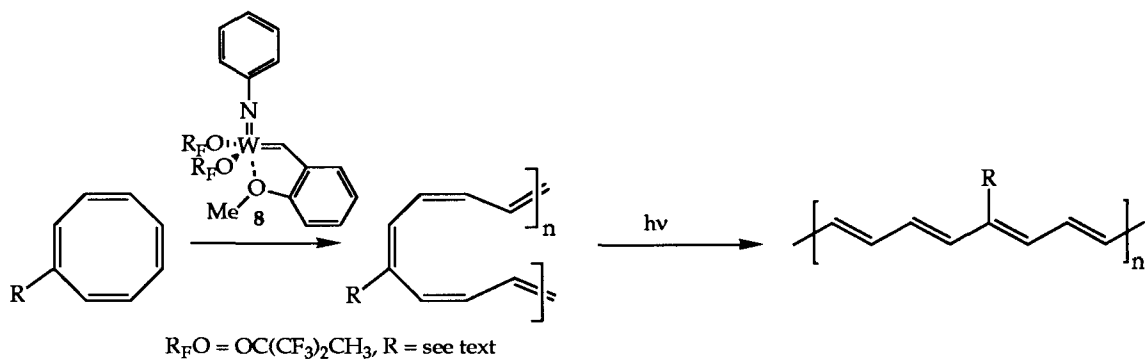


Figure 2. ROMP of COT Derivatives.

Ciardelli et al. have concluded that the polymerization of acetylenes with chiral substituents produces chiral, nonplanar polyacetylenes in which the rotation angle between successive double bonds has a predominantly single sense of twist.⁹ These workers further concluded that the nonplanar conformation of the polyene must be a helix with a predominant screw sense. However, the high-energy $\pi \rightarrow \pi^*$ absorptions reported for these polymers (290-325 nm in *n*-heptane) indicate that their effective conjugation lengths are very

short. Moreover, the polyacetylenes synthesized in this study had a *cis* configuration with respect to the main chain, and there is no discussion of the properties of these polymers in the *trans* form. Nevertheless, these polymers are very susceptible to twisting, which can be influenced by the chiral side groups.

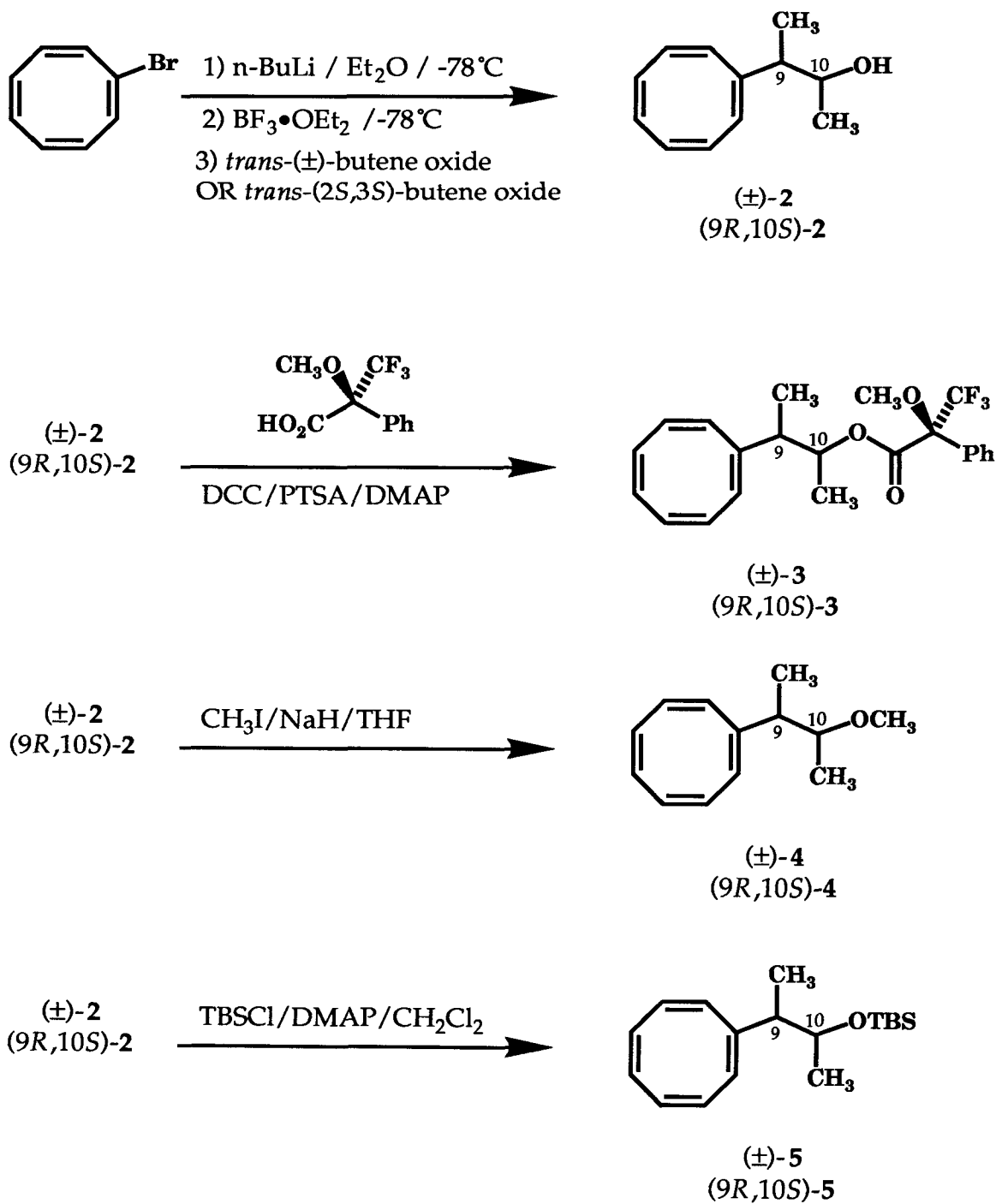
The magnitude of the circular dichroism (CD) of a molecule can be used to differentiate between a sterically perturbed, dissymmetric chromophore in which the chromophore itself is chiral and an asymmetric chromophore, which is merely a symmetric chromophore electronically perturbed by an asymmetric center in the same molecule.¹⁰ An example is the difference in magnitude of circular dichroism of nonplanar, conjugated dienes¹¹ and benzenes with asymmetric substituents.¹²

In the present work, a new class of chiral polyacetylenes are synthesized by ROMP of monosubstituted COT derivatives with chiral side groups. These polymers differ from those discussed above in that they have fewer side groups and are more conjugated as indicated by their higher-wavelength electronic-absorption maxima. Both of these properties impede geometric distortion of the main chain. However, to the extent that each side group twists the main chain, each should contribute to the formation of a dissymmetric chromophore, rather than merely act as a chiral perturbation on an inherently symmetric (flat) chromophore. The magnitude of the CD should indicate the degree of dissymmetry of the main chain. Other chiral conductive polymers have been synthesized¹³ with the goal of producing, for example, asymmetric electrodes for chiral electrosynthesis and ferroelectric liquid crystals. These ideas all fall into the realm of potential applications for the polymers discussed here.

Results and Discussion

If side groups twist the main chain of the polymer, it is of interest to determine if a chiral side group twists the main chain in predominantly one direction. Computer modeling and experimental evidence suggest that the twisting arises from the steric bulk at only the α carbon of the side chain. For example, the soluble polymer *trans*-poly-*t*-butylcyclooctatetraene is substantially twisted as indicated by its orange-red color ($\lambda_{\text{max}} = 432$ nm in THF). *trans*-Polyneopentylcyclooctatetraene in which the *t*-butyl group is displaced from the main chain by a methylene linkage is almost completely insoluble. The small amount of this polymer that is soluble in THF is intensely blue in color, indicative of a highly conjugated main chain with very little twisting ($\lambda_{\text{max}} = 634$ nm in THF).^{7b} In light of this observation, we designed a chiral polymer with the stereogenic center α to the main chain. A polymer with the stereogenic center spaced farther away from the main chain was synthesized as a control. Ciardelli et al.⁹ note that in polymers of chiral acetylenes, the magnitude of circular dichroism is substantially higher in a polymer with the stereogenic center α to the main chain than in polymers with the stereogenic center spaced further away from the main chain. This observation suggests that the steric effects in substituted acetylene polymers are similar to those postulated for polyRCOTs. It also suggests that the magnitude of the CD spectra of the polyR*COTs should be very different for the different spacings noted above.

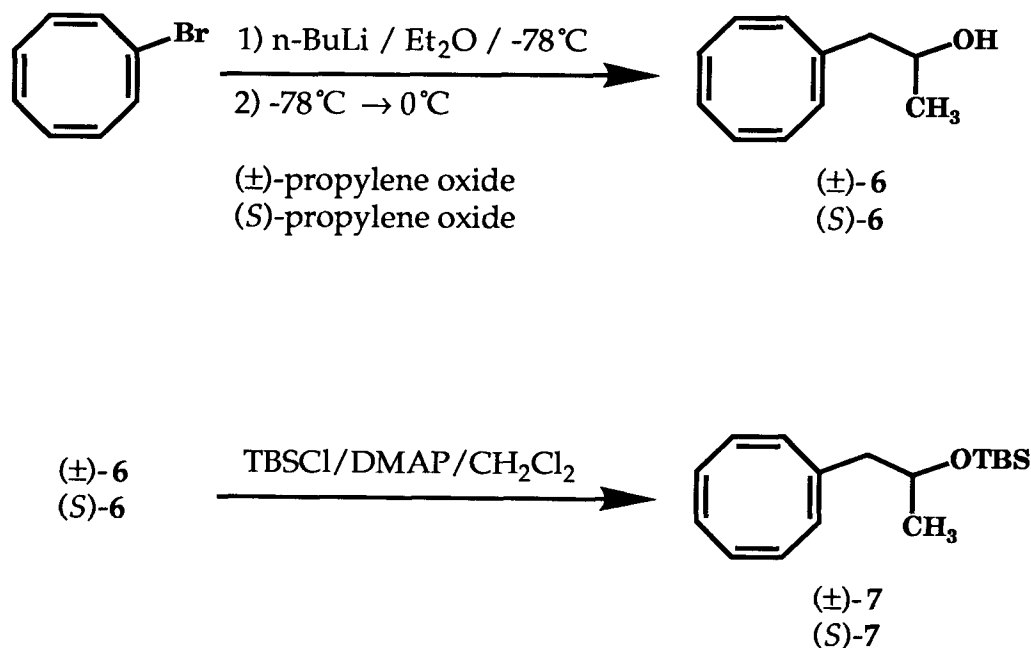
A. Monomers



Scheme 1. Syntheses of 2, 3, 4, 5.

Monomers were synthesized as outlined in Schemes 1 and 2. The opening of ethylene oxide with LiCOT has been reported in the literature,¹⁴ but $\text{BF}_3 \cdot \text{Et}_2\text{O}$ is necessary for the opening of the sterically more encumbered *trans*-2-butene oxide.¹⁵ Propylene oxide can be opened with or without $\text{BF}_3 \cdot \text{Et}_2\text{O}$, giving the same product in each case as determined by NMR and GC/MS.

Proof that the configuration about the two stereogenic centers is retained during the ring-opening of the epoxide is furnished by synthesizing the MTPA esters¹⁶ ((\pm)-**3** and (9*R*,10*S*)-**3**) of the resulting alcohols. Two well-resolved peaks, corresponding to the methoxy groups of two diastereomers are observed in the ^1H NMR spectra of the reaction mixture using (\pm)-**2**, and only one peak is observed in the reaction mixture using (9*R*,10*S*)-**2**. Thus, the chiral alcohol is enantiomerically pure within the limits of ^1H NMR detection (> 95% ee).



Scheme 2. Syntheses of **6**, **7**.

NMR signals were doubled in the spectra of some monomers. In particular, the 125 MHz ^{13}C NMR spectrum of **2** showed two resonances for each of the methine carbons on the side chain, and the 125 MHz ^{13}C NMR spectrum of **4** showed a doubling of one of the upfield methine resonances. The NMR spectra of **5** showed no unusual behavior. Compounds **2** and **4** are undergoing a dynamic process to produce two conformers that are distinguishable in the ^{13}C NMR spectra. ^{13}C NMR spectra of **2** and **4** at 22.5 MHz do not show this behavior, although a decoupled ^{13}C NMR spectrum of **2** at 22.5 MHz shows resonances 4-7 ppm wide for the carbons in the side chain. On the basis of extensive work by Paquette and co-workers,¹⁷ we assume that a dynamic ring inversion between the two forms of this molecule is occurring (Figure 3). Variable temperature ^1H NMR spectra of the monomers are consistent with these conclusions. For example, the *b*-methyl group in alcohol **2** is a broad singlet at 90 MHz and 20 °C but resolves into a sharp doublet at 90 °C. Apparently, the size of the TBS group of **5** sterically inhibits formation of one of the conformers. Thus, except for **5** and **7**, ^{13}C NMR spectra were recorded at 22.5 MHz.

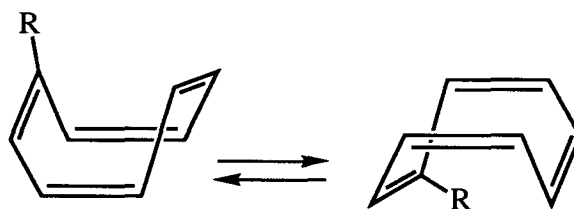


Figure 3. Ring Inversion in Mono-Substituted COT's.

Both **4** and **5** display circular dichroism, the magnitude of which increases monotonically with decreasing temperature (Figures 4 and 5). This behavior is consistent with the "freezing out" of one COT tub conformation. In both

monomers, the maximum CD effect is observed at 306 nm (THF) although the absorbance maximum of the molecule in the near UV is at approximately 280 nm (4: λ_{max} 282 nm, ϵ 348 M⁻¹ cm⁻¹; 5: λ_{max} 284 nm, ϵ 360 M⁻¹ cm⁻¹).

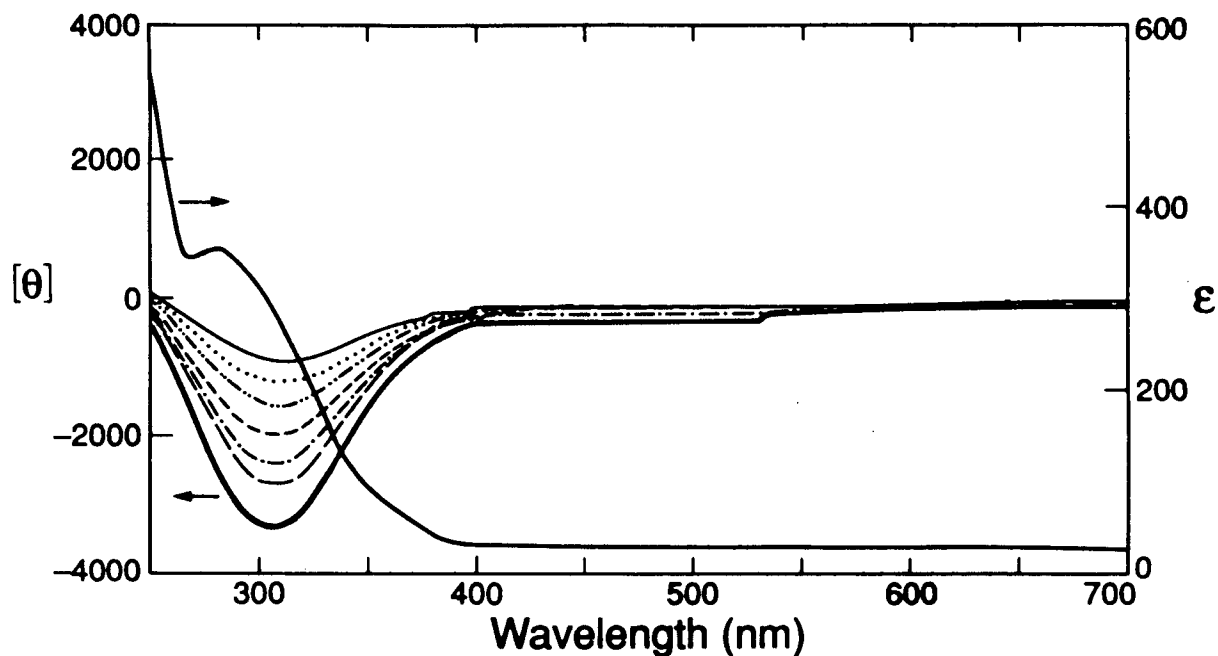


Figure 4. Variable Temperature Circular Dichroism of (9R,10S)-4: (—) 20 °C, (····) 0 °C, (-·-·-) -20 °C, (- - - -) -35 °C, (- · - · -) -50 °C, (- - -) -65 °C, (—) -75 °C.

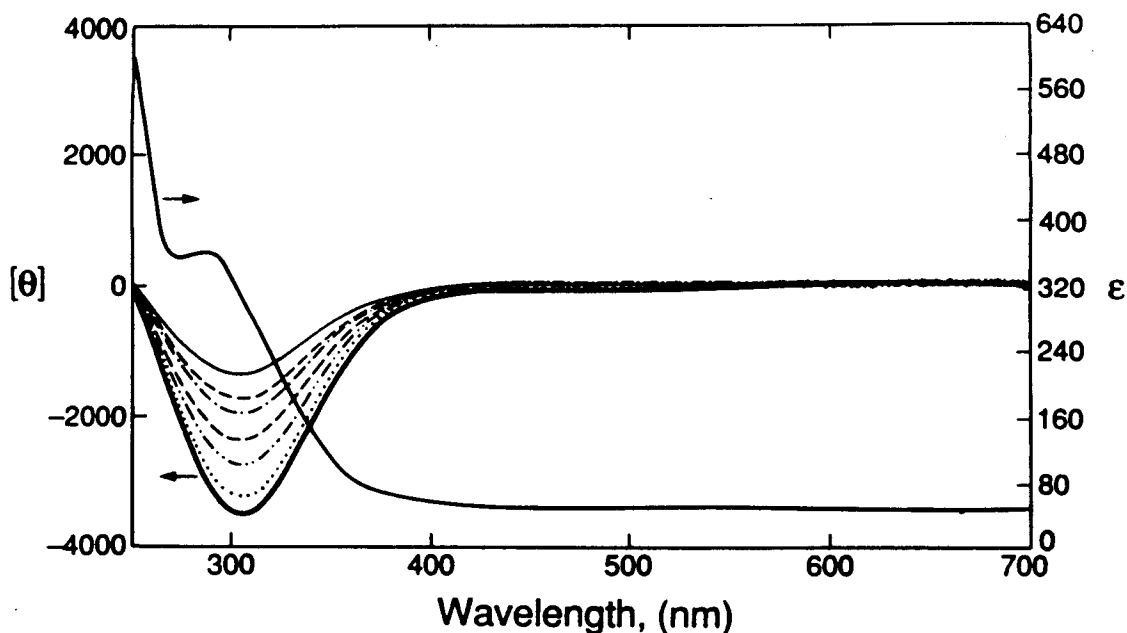


Figure 5. Variable Temperature Circular Dichroism of (9R,10S)-5: (—) 20 °C, (- - -) 0 °C, (- · - ·) -20 °C, (— —) -35 °C, (- · · -) -50 °C, (· · · ·) -65 °C, (—) -73 °C.

B. Polymers.

In the syntheses of these polymers, a monomer/catalyst ratio of 150:1 was found to be ideal. Both 4 and 5 were polymerized at lower (50:1) and higher (300:1) ratios. At 50:1 ratio, the molecular weight versus polystyrene as determined by GPC was $M_n = 28,000$ for *cis*-poly-5. Since the correction factor versus polystyrene could conceivably be large, and we wanted to use high polymer, a higher monomer/catalyst ratio was employed. At a 300:1 ratio, molecular weights were no higher than using a 150:1 monomer/catalyst ratio ($M_n = 110,000$ for *cis*-poly-5), and molecular weight distributions were bimodal in some cases. The tungsten alkylidene catalyst used in this study ($W(CH_2-O(OCH_3)C_6H_4)(NPh)-(OCMe(CF_3)_2)_2(THF)$) (8, Figure 2) was prepared by a

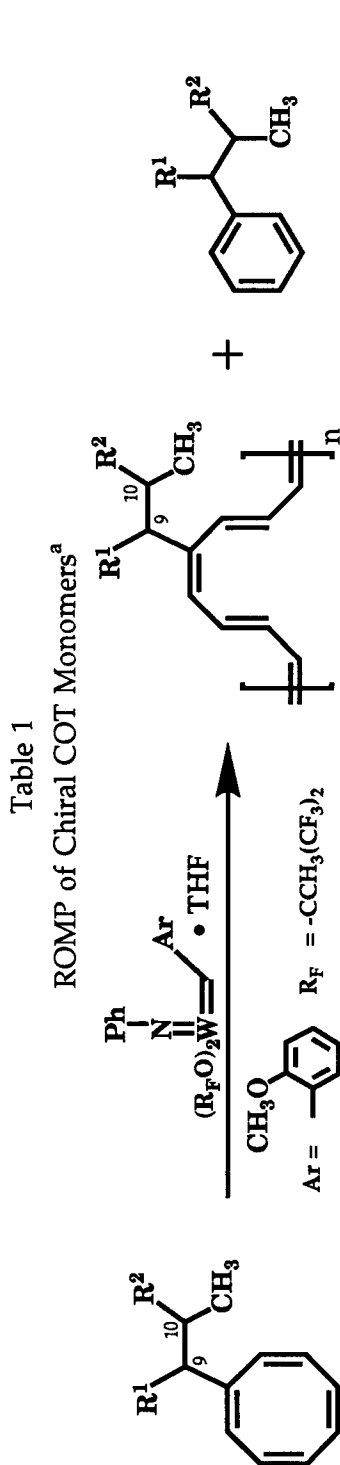
recently described procedure¹⁸ and is similar in many ways to the catalysts first described by Schrock and co-workers,¹⁹ which were used in previous polyRCOT work.⁷ Among other features, the catalyst used here is easily synthesized and has a molecule of THF precoordinated to the metal center. The THF coordinates reversibly and slows down the polymerization so that the reaction mixture can be handled easily. This catalyst allows us to avoid adding THF to the reaction mixture as was done previously, resulting in a controlled, reproducible polymerization rate and the formation of high-quality poly-RCOT films. All COT polymerizations involve some metathesis of olefins in the polymer chain, mostly to produce benzene, and the extent of this process can be determined as shown in the experimental section of Chapter 2 and is accounted for in Table 1.

Although the electronic-absorption spectra, Raman and infrared spectra, and molecular weights (GPC) of these polymer films and solutions did not measurably change over the course of 2-3 hours in air, samples decomposed visibly overnight in air, so air exposure was avoided. The films produced were flexible but tough, indicative of high polymer. Dissolution of polymer films in an organic solvent initially produced green/brown solutions that converted to purple solutions during photolysis or over the course of several hours to days in the light under inert atmosphere. In the dark, this conversion is much slower, although the only way to prevent it is to store solutions below -20 °C in the dark. This change in color is thought to be due to a cis/trans isomerization of the double bonds in the main chain.⁷ NMR evidence suggests that this isomerization is more complicated than initially thought (*vide infra*), but in the body of this paper, references to cis polymer or a cis structure denote the initially synthesized, predominantly cis polymer, and trans refers to the predominantly trans polymer. Both isomers of poly-4 and poly-5 are completely soluble as is observed in all

poly-RCOT's with a secondary or tertiary substituent in the position α to the main chain. Poly-7 is soluble in the initially synthesized (*cis*) form, but precipitates or aggregates (*vide infra*) as it isomerizes to the predominantly *trans* form, characteristic of all poly-RCOT polymers with a methylene (primary) substituent in the position α to the main chain.

There is a dramatic difference in reactivity between 4 and 5. Qualitatively, the rate of polymerization of 5 is roughly the same as that of all other COT monomers. The polymerization of 4, however, occurs very slowly at room temperature and requires a temperature of 50-60 °C to proceed at a rate comparable to the other monomers (Table 1). This elevated polymerization temperature isomerizes the polymer to some extent, making characterization of predominantly *cis*-poly-4 impossible. One rationale for this rate difference is that the OMe group in 4 can reversibly bind to the catalyst, slowing down polymerization, but the OTBS group in 5 is too bulky to bind.

Gel permeation chromatography indicates that these polymers have high molecular weights. Molecular weights were reproducible within approximately 20% from polymerization to polymerization and are comparable for homochiral versus racemic polymers (Table 1). Retention times decreased upon isomerization to the *trans* polymer. This decrease occurs presumably because the polymer becomes stiffer and more rodlike upon isomerization to the *trans* form with a concomitant increase in hydrodynamic radius (R_H). This increase in R_H will increase the apparent molecular weight versus polystyrene. Polydispersity also decreases upon photoisomerization, possibly because the microstructure is becoming more homogeneous.



polymer	R1	R2	stereochem	polymerization time (min)	polymerization temp (°C)	% conv ^b	% back-biting ^b	GPC mol wt ^c	
								cis (Mw/Mn)	trans (Mw/Mn)
5	CH ₃	OTBSd	9R, 10S	90	20	82	4.9	499/233	817/626
5	CH ₃	OTBSd	racemic	60	20	66	3.1	820/497	889/630
4	CH ₃	OCH ₃	9R, 10S	65	20	12	6.6	-	-
4	CH ₃	OCH ₃	9R, 10S	45	55	75	2.8	e	485/330
4	CH ₃	OCH ₃	racemic	25	55	93	4.1	323/154	404/272
7	H	OTBS	10S	60	20	93	7.9	1240/746	3.9/2.2 ^f
7	H	OTBS	racemic	60	20	83	<5	995/727	-

^aAll polymerizations were performed with a monomer : catalyst ratio of 150:1. ^b See Chapter 2. ^c Mol wt relative to polystyrene. All values listed are x 10⁻³. Cis and trans refer to backbone olefin geometry (see text). ^d OTBS = tert-butyltrimethylsilyloxy. ^e The "as polymerized" material was highly trans and thus no cis mol wt data could be obtained. ^f Material obtained after filtration (see text).

Table 2
¹H NMR Chemical Shift Data of Substituted Poly(COT)'s^a

resonance				
olefin ^b	5.6-7.0 {5.91, 6.31, 6.68}	6.1-7.1 {6.39, 6.61, 6.76, 6.95}	5.6-7.0 {5.93, 6.29, 6.65}	6.1-7.1 {6.41, 6.77, 6.95}
H ^β	c	3.28, 3.51	3.74	3.94, 4.16
H ^α	2.36	2.82, 3.02	2.33	2.79, 3.11
CH ₃ ^β	1.28	1.41, 1.51	1.24	1.35, 1.46
CH ₃ ^α	1.07	1.12	1.16	1.23
OR	3.13 (OCH ₃)	3.20 (OCH ₃)	1.03 (SiC(CH ₃) ₃) 0.06 (SiCH ₃)	1.04 (SiC(CH ₃) ₃) 0.18, 0.11 (SiCH ₃)
				5.7-7.0 {6.01, 6.36, 6.64}

^a Chemical shift values in ppm. Spectra were recorded at 400MHz in d₆-benzene.

^b Olefin region was broad and peaks were poorly resolved. The range of olefin chemical-shift values is reported. Peak maxima are listed in brackets.

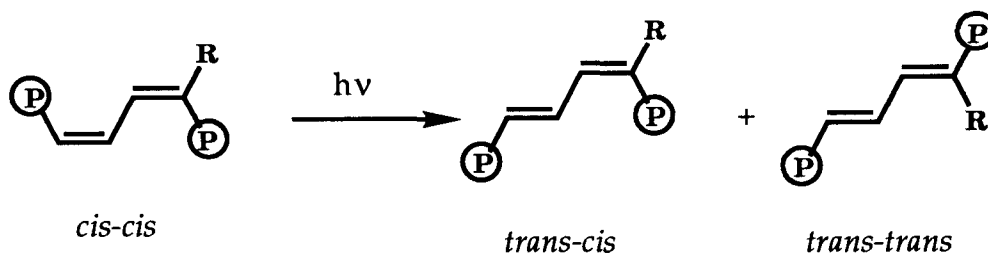
^c H_β for this polymer was coalesced with the methoxy resonance.

This decrease in polydispersity also indicates that photoisomerization is not accompanied by cross-linking or chain-scission reactions. In comparing the molecular weights of two polymers, it is most useful to compare the numbers for the trans forms since any given cis sample has a polymer size that is changing because of isomerization at room temperature.

A blue solution of *trans*-poly-7 in toluene was produced by allowing a red toluene solution of *cis*-poly-7 to isomerize for 2 days in ambient light under inert atmosphere. Some of the material had precipitated out of solution onto the sides of the vial during isomerization. Upon filtration (0.5 mm Millex-SR filter), blue material remained behind in the filter and a purple solution was produced. This solution was too dilute for GPC analysis using refractive index detection. However, GPC with UV detection at the λ_{max} of the solution (575 nm) showed the solution to contain substantially lower molecular weight material (M_n 700; M_w 733). Thus, the bulk of *trans*-poly-7 is insoluble.

^1H NMR data of the polymers are summarized in Table 2. The NMR spectra for the racemic and homochiral forms of each polymer are identical. A series of broad resonances are observed downfield, bordering on the aromatic region, indicative of a polymeric, olefinic chain. Backbone isomerization can be followed by NMR spectroscopy. The peaks that are due to protons in the side chain of the *cis* polymer gradually disappear, and new peaks that are due to *trans* polymer grow in as the sample isomerizes. It is noticed, however, that two peaks grow in for some protons, most notably, H^α and H^β . This behavior has been noticed first in these polymers, possibly because of the ample separation of the chemical shifts of the protons in the side chain. These two chemical species formed upon isomerization are tentatively assigned as detailed below (Figure 6).

It is possible that tri-substituted olefins do not display an overwhelming preference to be trans with respect to the main chain, and that the two resonances are indicative of two diads. Further investigation of this behavior is warranted before definitive conclusions can be drawn.



Designation of olefin geometry is with respect to the main chain

Figure 6. Possible species formed during isomerization of *cis*-polyRCOT's.

In unsubstituted polyacetylene, the infrared C-H stretching vibrations at 740 cm^{-1} and 1015 cm^{-1} are diagnostic for *cis* and *trans* material, respectively.^{1b} The infrared spectra of the substituted polyacetylenes are not as useful, as the vibrations of the side chains obscure those of the main chain. Raman spectroscopy, however, provides structure proof for a polyconjugated chain. Two peaks, assigned as the A_g C-C stretch (ν_1) and A_g C=C stretch (ν_2) in *trans*-polyacetylene, are observed in spectra of all the polymers (Table 3). No peaks are observed that correspond to the *cis* form of polyacetylene, probably since no precautions were taken to prevent isomerization by the 488 nm laser light employed. The position of ν_2 is indicative of the conjugation length of the chain and indicates that the conjugation is reduced compared to polyacetylene.^{20,21} The value of A_g (C=C) in polyacetylene is dependent on excitation frequency. It has been suggested that different excitation wavelengths selectively resonance-enhance different conjugation lengths in the polymer.²² The exact nature of the conformational and/or chemical defects that give rise to this conjugation length

dispersion is still an unresolved issue. The Raman spectra of these polymers are thus compared with a spectrum of polyacetylene recorded with a 488 nm excitation source. In this spectrum, the $A_g(\text{C}=\text{C})$ peak is observed at approximately 1500 cm^{-1} .^{22b}

Table 3. Raman Data, 488 nm excitation.

Polymer	ν_1 (A_g C-C stretch) ^a	ν_2 (A_g C=C stretch) ^a
Polyacetylene	1090-1120	1500
Poly-(±)-4	1132	1522
Poly-(9R,10S)-4	1133	1522
Poly-(±)-5	1131	1518
Poly-(9R,10S)-5	1132	1519
Poly-(±)-7	1120	1491
Poly-(9R,10S)-7	1124	1495

^a in cm^{-1}

C. Electronic transitions and circular dichroism

UV/Vis spectra were acquired for both the cis and trans forms of both the racemic (±) and optically active (9R,10S) forms of 4, 5, and 7. Absorption maxima and extinction coefficients for the optically active polymers are reported in Table 4 and are similar within experimental error to the racemic polymers. Extinction coefficients for the cis polymers are of value only as empirical numbers since there is little control over their cis/trans content. One can notice, however, the shift to higher wavelength (lower energy) upon isomerization and the increase in extinction coefficient. Both of these effects have been observed in cis/trans isomerizations of polyenes.²³ *trans*-Poly-7 has both a lower energy absorption

and higher extinction coefficient than poly-4 or poly-5, indicative of the higher conjugation that is expected for a polymer with $-\text{CH}_2\text{R}$ versus $-\text{CHRR}'$ in the position α to the main chain.

Table 4. Electronic-Transition Data of Poly(COT)'s.

polymer	cis				trans			
	UV-vis data ^a		CD data ^a		UV-vis data ^a		CD data ^a	
	λ_{max}	ϵ_{max}	λ_{CD}	$[\theta]_{\text{max}}$	λ_{max}	ϵ_{max}	λ_{CD}	$[\theta]_{\text{max}}$
(9R,10S)-5	302	11400	297	-2100	560	22400	563	-7100
	376	10100	341	+8000				
			417	-2400				
			495	+2100				
(9R,10S)-4	b	b	b	b	560	23100	587	-5100
							425	+1500
(10S)-7	306	12000			594	35600		
	416	14800						

^a Spectra were recorded in THF at 20°C.

^b The 'as polymerized' material was highly *trans* and thus no data on the *cis* polymer could be obtained.

Both the UV/Vis and CD transitions reported in Table 4 are assigned to $\pi \rightarrow \pi^*$ transitions and represent the absorption with the highest extinction coefficient in the UV/Vis spectrum. Transitions of higher energy than the ones reported remained unassigned, but could be attributed to excitations into orbitals of higher energy than the LUMO, absorptions of parts of the polymer with lower effective conjugation because of more severe twisting, photolytic or chemical degradation, or any other defect that reduces conjugation.

CD data for the polymers prepared from **4** and **5** are reported in Table 4. CD spectra for all racemic polymers were obtained, and no CD activity was found. The magnitude of the CD effect (molar ellipticity, $[\Theta]$) at the UV/Vis λ_{\max} in both *cis*- and *trans*-poly-(9*R*,10*S*)-**5** is of the order of magnitude for dissymmetric chromophores.¹¹ *Thus, the side group acts as a dissymmetric perturbation on the main chain by twisting it with a preference for one screw sense.* Moreover, the magnitude of the CD effect observed for these polymers is on the same order as that observed for polymers of chiral acetylenes.⁹ Thus, the chirality imparted to the backbone by the substituent is not greatly influenced by the proximity of neighboring substituents. CD examination of *cis*-(9*R*,10*S*)-**4** was not possible since the higher temperature of polymerization resulted in a material that, as mentioned before, had a low *cis* content. However, *trans*-(9*R*,10*S*)-**4** and *trans*-(9*R*,10*S*)-**5** both display substantial circular dichroism at their UV/Vis λ_{\max} (Figure 7).

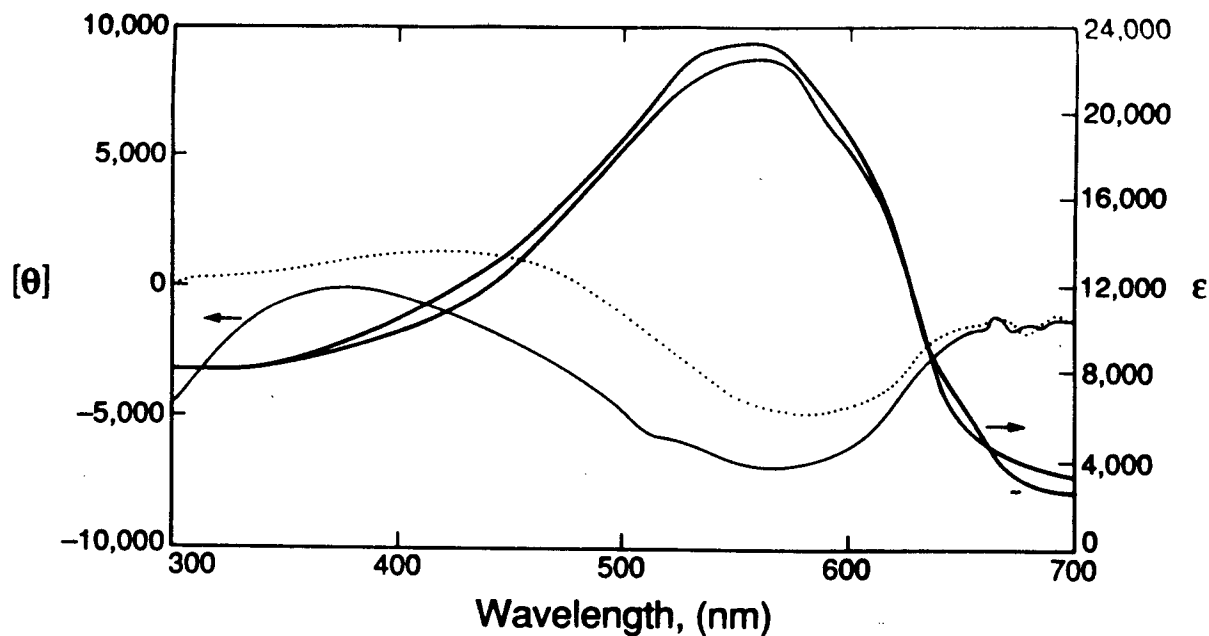


Figure 7. Circular Dichroism of Poly-*trans*-(9R,10S)-4 and Poly-*trans*-(9R,10S)-5: (a) Absorption spectrum of 4, (b) Absorption spectrum of 5, (· · · ·) CD spectrum of 4, (—) CD spectrum of 5.

CD spectra were recorded of both *cis*- and *trans*- poly-(9R,10S)-5 in hexane, and toluene as well as THF. Solvatochromic shifts in the UV/Vis and CD spectra were minimal between these solvents. Additionally, poly-(9S,10R)-5 was synthesized, and its CD spectra were recorded and compared to that of its enantiomer. Although the enantiomeric excess of the former was lower (see experimental section) and the monomer/catalyst ratio was different (50:1 and 300:1), the spectra were mirror images over the 300-700 nm wavelength range studied.

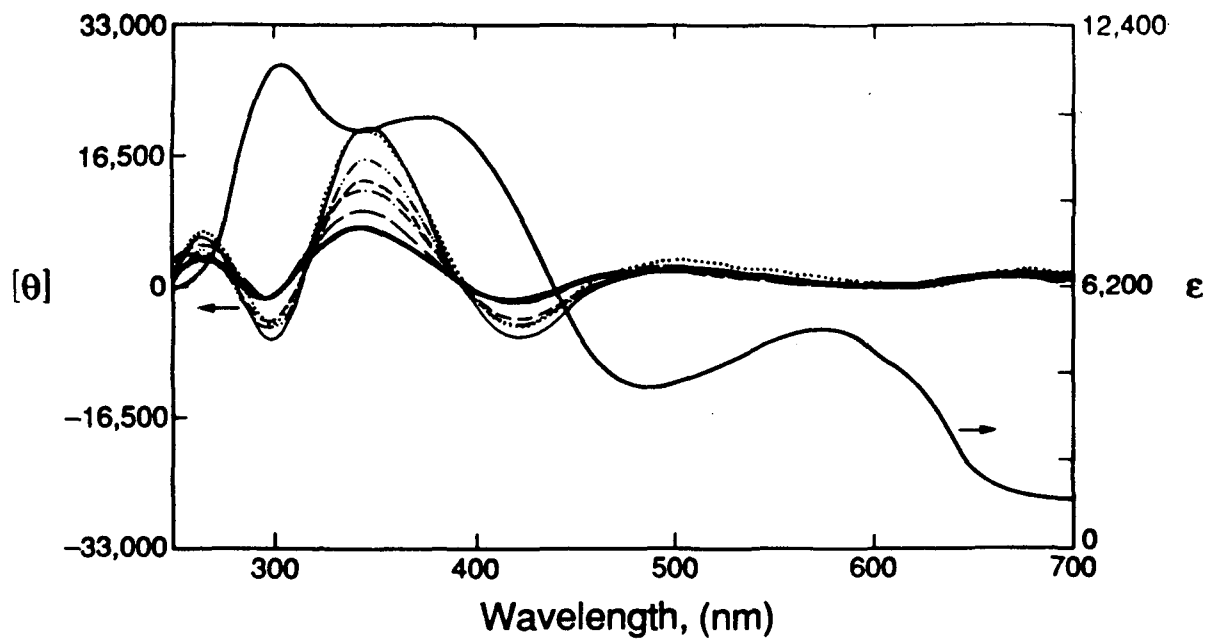


Figure 8. Variable Temperature Circular Dichroism of Poly-*cis*-(9R,10S)-5:
 (—) 20 °C, (— —) 0 °C, (- - -) -20 °C, (- - -) -35 °C, (- · · ·) -50 °C, (· · ·) -65 °C,
 (— · —) -73 °C.

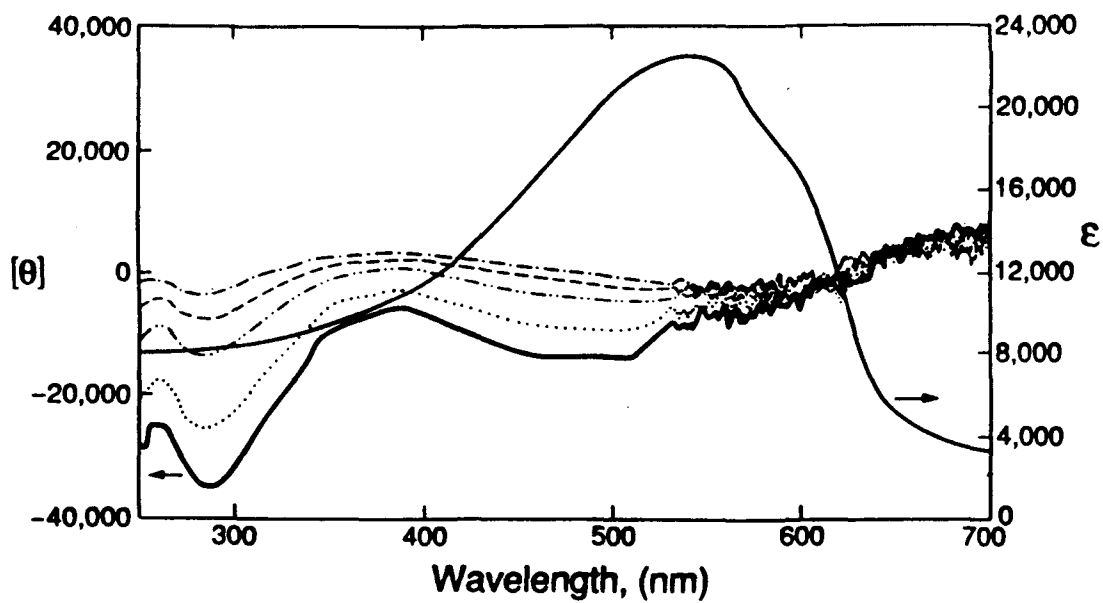


Figure 9. Variable Temperature Circular Dichroism of Poly-*trans*-(9R,10S)-5:
(- · -) 20 °C, (- - -) 0 °C, (- · · -) -20 °C, (· · ·) -35 °C, (—) -50 °C

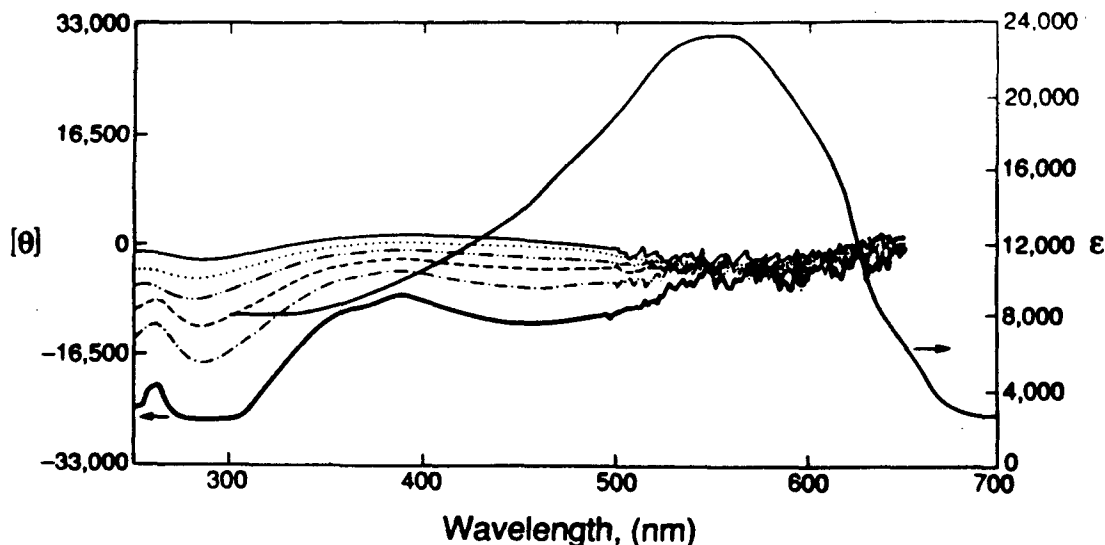


Figure 10. Variable Temperature Circular Dichroism of Poly-*trans*-(9R,10S)-4: (—) 15 °C, (···) -5 °C, (- · · ·) -20 °C, (- - -) -35 °C, (- · - ·) -50 °C, (— · —) -65 °C.

Thermochromic behavior was observed in the UV/Vis spectra of these polymers. For example, upon cooling to -196 °C (2-MethylTHF glass), poly-*cis*-5 shows a red shift of approximately 25 nm and an approximately 20% increase in extinction coefficient. Poly-*trans*-5 also shows a 20-25 nm red shift upon cooling to -196 °C, but more dramatically, shows a 300% increase in extinction coefficient. An approximately 200% increase in extinction coefficient is observed upon cooling from room temperature to -78 °C.

Figures 8-10 show the variable temperature CD spectra over the temperature range of 20 °C to -75 °C of poly-*cis*-(9R,10S)-5, poly-*trans*-(9R,10S)-5, and poly-*trans*-(9R,10S)-4, respectively. Attempts to observe the electronic spectra of similar polymers at elevated temperatures failed because of

decomposition of the polymer, so examination of circular dichroism above room temperature was not attempted. In each case, the magnitude of $[\Theta]$ increases smoothly with decreasing temperature. Moreover, over this temperature range, the magnitude of $[\Theta]$ for poly-*cis*-(9*R*,10*S*)-5 increases with decreasing temperature far more dramatically than does the extinction coefficient, ϵ . In contrast, although the CD spectrum of the poly-*trans*-(9*R*,10*S*)-5 shows a great deal of temperature dependence below 300 nm, $[\Theta]$ is much less temperature-dependent at its λ_{CD} ; certainly less temperature-dependent than the magnitude of ϵ in the UV/Vis spectrum. This behavior, coupled with the knowledge that *cis*-*n*-alkyl poly-COTs are soluble, although the *trans* forms of these polymers are not, suggests that *cis* polyacetylene units are more conformationally flexible than *trans* units. This idea is further supported by the general observation that *cis* polyenes have higher energy UV/Vis absorptions (and thus lower effective conjugation lengths) than all-*trans* polyenes. Although there is experimental evidence that *cis*-polyacetylene is planar in the solid state,²⁴ both experiments²⁵ and calculations²⁶ suggest that it can be helical in an amorphous form or in solution, although calculations disagree on the energy required to untwist and flatten the helix. Uncertainty as to the exact nature of the electronic transitions in this polymer discourages us from speculating on the helical nature of the *cis* form of 5.

Since the nature of the electronic transitions below 550 nm in the *trans* polymers is not known with certainty, one can say only that the chromophores responsible for these transitions are much more conformationally mobile and are considerably influenced by the chiral perturbation. This behavior suggests that rather than seeing transitions to higher energy states, we are observing less conjugated segments of the polymer. The idea that polyacetylene consists of a

dispersion of conjugation lengths has been promoted in the literature (vide supra).^{22b}

Within the signal-to-noise ratio of the spectrophotometer employed, no CD was observed for poly-(10S)-7. One problem encountered was the poor solubility of this polymer. Its CD spectra often had background signal that could not be subtracted simply with a solvent blank. The background artifact may have been caused by an insoluble particulate. Filtering of these solutions did not correct the problem. The second problem encountered with the CD of poly-(10S)-7 is the poor signal-to-noise ratio, which could have arisen from two sources. First, the magnitude of the extinction coefficient for poly-*trans*-7 is much larger than for poly-*trans*-4 or -5 (Table 4). Second, on the basis of the work of Ciardelli et al.,⁹ we suspect that the magnitude of CD decreases as the stereocenter is moved away from the chain. The combination of increasing ϵ and decreasing magnitude of CD dramatically reduces the ratio of $[\Theta]/\epsilon$ and hence the signal-to-noise ratio.²⁷

Conclusions

Soluble and highly conjugated polyacetylene derivatives bearing chiral appendages have been synthesized and characterized. The backbone $\pi \rightarrow \pi^*$ transition of these polymers showed substantial circular dichroism. The magnitude of the CD for the polymers is characteristic of a dissymmetric chromophore. Thus, the chiral side groups twist the main chain in predominantly one sense rather than just electronically perturb that chromophore. The data are consistent with a model described for similar, achiral polymers in which the polymer main chain is comprised of flat, conjugated

segments disturbed by kinks produced by twists about the single bonds adjacent to the side chain substituent.⁸ However, given the optical absorption maximum for the polymer (560 nm for both *trans*-poly-4 and -5) and extrapolations of the absorption maxima of discreet polyenes as the number of conjugated double bonds in the molecule increases,²⁸ the chromophores of these polymers have effective conjugation lengths of at least 20 double bonds.

No significant solvatochromism was observed in the UV/Vis or CD of the polymers. Small differences in CD were observed between polymers having β -methoxy and the more bulky β -silyloxy substituents. The ellipticity observed for the polyacetylenes studied here, having an α -branched substituent on only one of every eight backbone atoms, is of the order of magnitude observed for previously studied chiral polyacetylenes, which had α -branched substituents on every other backbone atom. This observation suggests that the chirality imparted to the backbone by the substituent is not greatly influenced by the proximity of neighboring substituents. These polymers also offered the opportunity to examine both the *cis* and *trans* isomers of the backbone, a comparison not addressed in the past. Decreasing temperature had much more influence on the CD of the *cis* polymers than on the CD of the *trans* polymers in their respective $\pi \rightarrow \pi^*$ regions. *cis*-PolyRCOT's are much more conformationally flexible and may contain helical regions, although the CD data do not provide conclusive evidence of this conformation. ¹H NMR of the polymers suggests that the olefinic units are probably not entirely *cis* or *trans* with respect to the main chain of the polymers studied, and this irregularity might prevent long-range (helical) order. These conclusions are consistent with previous results from our laboratory on solubility behavior of substituted polyCOT's.

Experimental

Instrumentation. All syntheses are air- and moisture-sensitive and were performed using standard Schlenk techniques under argon purified by passage through columns of BASF RS-11 (Chemalog) and Linde 4Å molecular sieves. Polymerizations and subsequent handling of polymer films and preparation of polymer solutions were done in a nitrogen-filled Vacuum Atmospheres drybox. NMR spectra were recorded with either a JEOL FX-90Q (89.60 MHz ^1H ; 22.51 MHz ^{13}C), a Bruker AM-500 (500.14 MHz ^1H , 125.13 MHz ^{13}C) or a JEOL GX-400 (399.65 MHz ^1H , 100.40 MHz ^{13}C) spectrometer. Optical rotations were determined using a Jasco DIP-181 digital polarimeter. Low-resolution mass spectra were obtained with a Hewlett-Packard 5890/5970 GC/MS. Gas chromatographic analysis was performed on a Hewlett-Packard 5890 using an Alltech Chirasil-Val III column. Ultraviolet-visible absorption spectroscopy was performed on an HP 8451A diode-array spectrophotometer. Circular dichroism was performed on a JASCO J-600 circular dichroism spectrophotometer. Gel permeation chromatography was performed on a Waters 150C ALC/GPC with differential refractometer detector and 5 styragel columns, using toluene at a flow rate of 1.5 mL/min except for the GPC of *trans*-poly-7 (vide infra), which was performed on an instrument employing an Altex 110A pump, three Shodex KF columns (KF-803, KF-804, KF-805) and a Kratos spectroflow 757 UV detector (detection @ 575 nm). The toluene solution was diluted by a factor of 4 into the GPC solvent (CH_2Cl_2), and simultaneous refractive index detection showed that the oligomeric material (detected by UV) was separated from the toluene in which it was originally dissolved (detected by RI). Molecular weights are reported relative to narrow molecular weight polystyrene standards (refractive

index or UV @ 254 nm). Raman spectra were obtained from a 488 nm excitation wavelength provided by an argon ion laser source. Spectra were obtained of the light scattered off the surface of polymer films.

Materials: Pentane, tetrahydrofuran, toluene and diethyl ether were distilled from sodium benzophenone ketyl. Methylene chloride and chloroform were vacuum-transferred from calcium hydride. COT was purchased from Strem and was distilled from calcium hydride before use. Bromocyclooctatetraene was synthesized by the method of Gasteiger et al.²⁹ All reagents, including racemic *trans*-2,3 butene oxide, racemic propene oxide, (S)-(-)-propylene oxide ($[\alpha]_{25}^D$ -13.34°, 99% ee), and (2S,3S)-(+)-butanediol ($[\alpha]_{25}^D$ +13.28°, 99% ee) and (2R,3R)-(-)-butanediol ($[\alpha]_{25}^D$ -12.08, 90 % ee) were purchased from Aldrich unless otherwise noted. Tungsten catalyst **8** was synthesized as described in the literature.¹⁹

Syntheses: All procedures are identical for both the homochiral and the racemic forms of the monomer unless otherwise indicated.

***trans*-(2S,3S)-2,3-Epoxybutane and *trans*-(2R,3R)-2,3-Epoxybutane (1).**

Synthesis was done by the method of Schurig et al.³⁰ except that when complete, methyl ethyl ketone was discovered as an impurity (IR 1719 cm⁻¹, NMR 1.05 (t), 2.12 (s), 2.43 (q)). A representative procedure for removal of the ketone follows. A mixture of the epoxide/ketone (8.08 g, approx. 3% ketone impurity by GC) was vacuum-transferred onto an excess of solid methyl lithium (375 mg) at liquid nitrogen temperature, and the solution was allowed to warm to -10 °C with stirring over the course of an hour. Keeping the solution below 0 °C, the volatile material was returned to the original flask by vacuum transfer. (2S,3S): α_{25}^D -

47.17°, %ee ≈ 100%; (2R, 3R): α^{25}_{D} +44.28°, %ee ≈ 94%.

(3-Hydroxy)-s-Butylcyclooctatetraene (2). *n*-Butyl lithium (11.5 mL, 37.4 mmol, 3.25 M solution in ether, titrated before use) was added dropwise via cannula to 6.49 g (35.5 mmol) of bromocyclooctatetraene and 100 mL of diethyl ether in a 500 mL Schlenk flask at -78 °C with efficient stirring. An orange solution resulted, which was stirred at -78 °C for an additional 2 hours. $\text{BF}_3 \cdot \text{Et}_2\text{O}$ (4.4 mL, 5.03 g, 35.5 mmol, Aldrich gold label, distilled from calcium hydride at atmospheric pressure and vacuum-transferred before use) was added slowly via syringe. Immediately afterwards, 2.38 mL (1.91 g, 26.5 mmol, 0.75 equiv) of *trans*-2,3-epoxybutane that had been vacuum-transferred into a graduated tube with a teflon screw top was added via cannula with efficient stirring. A color change from dark-orange to yellow was observed with this addition. The reaction mixture was stirred for an additional 30 minutes at -78 °C, and 30 mL of a saturated NaHCO_3 solution were added and the mixture was allowed to warm to room temperature. Water was added and the mixture was transferred to a separatory funnel and extracted with diethyl ether (3x100mL). The organics were dried (MgSO_4) and concentrated. Residue was flash chromatographed over silica (CH_2Cl_2 and then 5% $\text{Et}_2\text{O}/\text{CH}_2\text{Cl}_2$ eluents). The yellow band was collected and concentrated. The resulting oil was distilled (short path distillation, 0.01 mm, 55-60 °C, first fraction discarded) to produce 2.35 g (50.2% based on epoxide) of the alcohol. ^1H NMR (90 Mhz, CDCl_3) d 5.70, 5.49 (m, 7H, COT), 3.54 (br, 1H, COT-CH-), 2.21 (bs, 1H, -OH, (m 2.09 in *d*₈-toluene)) 2.02 (m, 1H, -CH-OH), 1.10 (d, *J* = 6.3 Hz, 3H, COT-CH-CH₃), 0.96 (d, *J* = 7.2 Hz, 3H, HO-CH-CH₃); ^{13}C NMR (22.5 MHz CDCl_3 , dec.) d 146.21, 132.5-131.2 (br, m), 69.5, 47.8, 21.3, 14.6; MS *m/z* 176 [parent], 143, 131, 117 [base], 103, 91; (9R,10S): $[\alpha]^{20}_{\text{D}}$ (CDCl_3) +75.5°. *m/e* calcd 176.1201 found 176.1193.

Ester of (R)-(+)- α -Methoxy- α -(Trifluoromethyl)Phenylacetic acid and (3-Hydroxy)-*s*-Butylcyclooctatetraene (3). 59 mg (0.33 mmol) of **2**, 34 mg (0.28 mmol) of dimethylaminopyridine, 130 mg (0.56 mmol) of (R)-(+)- α -methoxy- α -(trifluoromethyl)phenylacetic acid, and 20 mg (0.11 mmol) of *p*-toluenesulfonic acid were combined in a round bottomed flask and the flask was purged with argon. 275 mg (1.33 mmol) of dicyclohexylcarbodiimide in 2 mL of methylene chloride were added and the reaction was monitored by TLC (5% Et₂O/CH₂Cl₂). After 20 hours, no alcohol remained. The reaction mixture was passed through a 10 cm x 10 mm plug of silica and concentrated. ¹H NMR (CDCl₃) of the racemic ester showed two peaks of equal intensity at δ 3.55 and 3.51 ppm. Only the peak at 3.55 ppm was observed in the ¹H NMR spectrum of the ester synthesized with the chiral alcohol.

(3-Methoxy)-*s*-Butylcyclooctatetraene (4). A 3-necked 50 mL round bottomed flask was charged in the drybox with 520 mg (1.75 equiv) of NaH, fitted with a septum, stopper, and reflux condenser topped with a teflon valve. The flask was removed from the drybox, and 20 mL of tetrahydrofuran were added via cannula. The suspension was cooled to -78 °C with stirring, and a solution of 2.18 g (12.37 mmol) of **2** and 7.5 mL of methyl iodide was added. The flask was warmed to 35 °C and stirred for 5 hours under argon. A white suspension developed over this time. After cooling to room temperature, the reaction mixture was cautiously added to a separatory funnel containing 100 mL diethyl ether, 100 mL of a saturated sodium hydrogen carbonate solution, and 50 g of ice. The mixture was cautiously shaken, separated, and the aqueous layer was extracted with diethyl ether (2x100mL). The organic layers were combined, dried (MgSO₄), concentrated, and purified by flash chromatography on silica (5%

Et₂O/Pet. ether eluent). The yellow band was collected, concentrated, and fractionally distilled from calcium hydride into a flask with a teflon screw top (52 °C, 0.03 mm) to produce 1.70 g (72%). ¹H NMR (90 Mhz, CDCl₃) d 5.73, 5.54 (m, 7H, COT), 3.25 (s, 3H, OCH₃), 3.00 (br, 1H, COT-CH), 2.14 (m, 1H, CH₃O-CH), 1.13 (d, J = 6.3 Hz, 3H, COT-CH-CH₃), 1.04 (d, J = 6.3 Hz, 3H, CH₃O-CH-CH₃); ¹³C NMR (22.5 Mhz, CDCl₃) d 146.5, 135.1 (br), 130.0, 128.2 (br), 123.3, 79.5 (d, CH₃O-CH-, J_{CH} = 137.5 Hz), 56.1 (qd, -OCH₃, J_{CH} = 140.0 Hz, ³J_{CCH} = 4.4 Hz), 48.0 (d, C₈H₇-CH-, J_{CH} = 122.9 Hz), 17.0 (qd, -C^bH-C^bH₃, J_{CH} = 125.7 Hz, ³J_{CCH} = 2.9 Hz), 15.8 (q, -C^aH-C^aH₃, J_{CH} = 125.7 Hz); MS m/z 190 [parent], 158, 131, 115, 91, 77, 59 [base]; d₂₀ 0.962; (9R,10S): [α]_D²⁰ (CH₂Cl₂) + 28.6°.

Anal. Calcd. for C₁₃H₁₈O: C, 82.06; H, 9.53. Found: C, 82.01; H, 9.58.

(3-*t*-Butyldimethylsiloxy)-*s*-Butylcyclooctatetraene (5). A 3-necked 50 mL round bottomed flask was charged with 1.64 g (9.28 mmol) of **2**, 20 mL of methylene chloride, and 1.70 g (13.9 mmol) of dimethylamino pyridine. A solution of 2.25 g (14.9 mmol) of TBSCl (Petrarch) in 5 mL of methylene chloride was added and the contents were stirred overnight at room temperature. After 14 hours, TLC (4% Et₂O in pet. ether followed by elution with 5% Et₂O in CH₂Cl₂) showed that nearly all starting material had reacted. Contents were poured into 2M HCl/water (50:50, 100 mL total volume) and extracted with methylene chloride (3x50mL). Organic layers were dried (MgSO₄), concentrated, and the residue flash chromatographed over silica gel (3% Et₂O in pet. ether). Yellow band was collected, concentrated, and distilled (72-75 °C, 0.01 mm) to give 2.29 g (85%). ¹H NMR (400 Mhz, CDCl₃) d 5.77, 5.56 (m, 7H, m COT), 3.47 (br, 1H, COT-CH), 2.13 (m, 1H, OTBS-CH), 1.18 (br, 3H, COT-CH-CH₃), 1.03 (d, 3H, OTBS-CH-CH₃) 0.87 (s, 9H, SiC(CH₃)₃), 0.01 (s, 6H, Si(CH₃)₂); ¹³C NMR (125

Mhz, CDCl₃) d 146.9, 132.7, 132.5, 132.3, 132.0, 131.6, 131.5, 131.3, 131.1, 130.1, 130.0, 127.6 (br), 126.2 (br), 71.4 (dq, -CH-OTBS, J_{CH} = 139.0 Hz, ³J_{CCH} = 4.9 Hz), 50.7 (d, C₈H₇-CH-, J_{CH} = 125.8 Hz), 25.8 (qsep., -SiC(CH₃)₃, J_{CH} = 124.9 Hz, ⁴J_{CSiCH} = 5.6 Hz), 22.6 (q, -C^bH-C^bH₃, J_{CH} = 125.8 Hz), 17.9 (s, -SiC(CH₃)₃), 16.9 (q, -C^aH-C^aH₃, J_{CH} = 126.5), -4.19 (q, Si-CH₃, J_{CH} = 118.1 Hz), -4.79 (q, Si-CH₃', J_{CH} = 118.8 Hz); MS m/z 290 [parent], 233, 189, 159, 115, 103, 73 [base]; *d*₂₀ 0.932; (9R,10S): [α]²⁰_D (CDCl₃) +13.44°

Anal. Calcd. for C₁₈H₃₀OSi: C, 74.41; H, 10.41. Found C, 74.06; H, 10.39.

(2-Hydroxy)*n*-Propylcyclooctatetraene (6): *n*-Butyl lithium (12.8 mL, 33.9 mmol, 2.65 M solution in ether, titrated before use) was added dropwise via cannula to 5.91 g (32.3 mmol) of bromocyclooctatetraene and 100 mL diethyl ether in a 500 mL Schlenk flask at -78 °C with efficient stirring. An orange solution resulted, which was stirred at -78 °C for an additional 2 hours. Propylene oxide (3.4 mL, 2.8 g, 48.2 mmol) was added via syringe at -78 °C, and the solution was allowed to warm to room temperature over the course of 2 hours. The solution was cooled to -78 °C, and 50 mL of a saturated NaHCO₃ solution were added and the solution was again allowed to warm up. The solution was transferred to a separatory funnel and the organic layer was separated. The aqueous layer was washed with diethyl ether (3 x 50 mL). The organics were combined, dried (MgSO₄) and concentrated. Flash chromatography over silica (3% Et₂O/CH₂Cl₂) yielded 1.7 g (32.5%). ¹H NMR (400 Mhz, CDCl₃) d 5.77, 5.55 (m, 7H, COT), 3.71 (br, 1H, -CH-), 2.19 (br, 1H, -OH), 2.10 (br, 2H, -CH₂-), 1.14 (d, J = 6.4 Hz, 3H, -CH₃); ¹³C NMR (22.5 MHz, CDCl₃) d 140.6, 137.3, 135.0, 132.8, 130.4, 128.0, 125.9 (br), 65.6 (d, -CH₂-CH-OH, J_{CH} = 139.1 Hz), 47.3 (t, -CH₂-, J_{CH} = 128.7 Hz), 21.2 (q, -CH₃, J_{CH} = 125.8 Hz); MS m/z 162 [parent], 144, 117 [base], 91, 78, 65; 10S:

$[\alpha]^{20}_{\text{D}}$ (CDCl_3) +8.03°. m/e calcd 164.1045 found 162.1034.

(2-*t*-Butyldimethylsiloxy)*n*-Propylcyclooctatetraene (7): 1.96 g (12.1 mmol) of **6** and 35 mL of methylene chloride were placed in a round bottomed flask and purged with argon. 2.44 g (20 mmol) of dimethylaminopyridine and 3.02 g (20 mmol) of *t*butyldimethylsilylchloride (Petrarch) (solution in 10 mL of methylene chloride) were added. The reaction was stirred overnight at room temperature under argon, washed with 5% HCl (3 x 50 mL) and water (1 x 50 mL). Aqueous layers were washed with methylene chloride and all organic layers were combined, dried (MgSO_4) and concentrated. The residue was flash chromatographed over silica (3% Et_2O /Pet. Ether), discarding the first yellow fraction. The remainder of the yellow solution was collected, concentrated, and distilled (74-79 °C, 0.01 mm, forerun discarded), to produce 1.96 g (58%). ^1H NMR (400 Mhz, CDCl_3) d 5.75, 5.54 (m, 7H, COT), 3.83 (m, 1H, -CH-), 2.23 (m, 1H, -CH₂- [dias.]), 2.06 (dd, $J_2 = 13.1$ Hz, $J_3 = 7.6$ Hz, 1H, -CH₂- [dias.]), 1.16 (d, $J = 5.9$ hz, 3H, -CH₃), 0.86 (s, 9H, $\text{SiC}(\text{CH}_3)_3$), 0.28 (s, 6H, $\text{Si}(\text{CH}_3)_2$); ^{13}C NMR (125 Mhz, CDCl_3) d 141.3 (s), 135.4 (br), 133.8 (br), 132.5 (m), 131.4 (m), 130.3 (s), 129.3 (s), 128.1 (s), 67.6 (d, -CH-OTBS, $J_{\text{CH}} = 144.7$ Hz), 48.2 (t, C_8H_7 -CH-, $J_{\text{CH}} = 127.5$ Hz), 25.8 (qsep, - $\text{SiC}(\text{CH}_3)_3$, $J_{\text{CH}} = 124.8$ Hz, $^4J_{\text{CSiCH}} = 5.7$ Hz), 23.3 (q, -CH-CH₃, $J_{\text{CH}} = 126.8$ Hz), 18.0 (s, - $\text{SiC}(\text{CH}_3)_3$), -4.56 (q, -SiCH₃, $J_{\text{CH}} = 118.4$ Hz), -4.71 (q, -SiCH₃', $J_{\text{CH}} = 118.5$ Hz); MS m/z 276 [parent], 261, 219, 175, 159, 103, 73 [base]; d_{20} 0.923; 10S: α^{20}_{D} -24.70.

Anal. Calcd. for $\text{C}_{17}\text{H}_{28}\text{OSi}$: C, 73.85; H, 10.21. Found C, 73.52; H, 10.01.

Polymerization of 4, 5, 7: All polymerizations were done in the drybox. **5** and **7** were polymerized at drybox temperature (20 °C), but **4** was polymerized at 60 °C

as described below. The procedure was identical for the chiral and racemic monomers. In a typical polymerization, 4.3 mg of **8** were placed in a vial and dissolved in a minimum of pentane (2-3 drops). 151.4 mg (154 equiv) of (\pm)-**4** were then added. The contents of the vial were stirred with a pipette tip and after ca. 15 seconds, the solution was transferred by pipette to a glass slide sitting on a hotplate that had been thermally equilibrated to 60 °C. Over the course of 1-2 minutes, the mixture turned from yellow/brown to orange, red, and finally black in color. The film that was produced was peeled off the slide after 25-90 minutes (See Table 1). Polymerization at 20 °C was accomplished in the same manner, but the slide was on the drybox floor during the polymerization instead.

Cis-trans isomerization of poly-4, 5, 7: Isomerization could be accomplished over time by allowing solutions to sit in the light at room temperature under inert atmosphere. However, this procedure describes the photolysis used to convert predominantly cis polymer into predominantly trans material to be used for UV/VIS and CD measurements. The procedure was identical for all polymers. In a typical photolysis, 3.8 mg of poly-(9R,10S)-**5** were dissolved in 5 mL of THF. 190 mL of this solution were diluted to a total volume of 10 mL of THF to produce a 5×10^{-5} M (per monomer repeat unit) solution. The sample was exposed to light from a Pyrex-filtered, 350 watt, medium-pressure mercury Hanovia lamp for a total of 4 - 2 minute intervals until the visible absorption spectrum showed no change. The number of exposures can vary depending on the concentration of the solution, efficiency of the lamp, etc. Overexposure resulted in a decrease in color, indicating decomposition of the material in solution. THF, toluene and benzene were suitable solvents for this experiment, but chlorinated solvents were not acceptable.

References and Notes

- (1) (a) *Handbook of Conducting Polymers*; Skotheim, T. A., Ed. Marcel Dekker: New York, 1986; Vol. 1 and 2. (b) Chien, J. C. W. *Polyacetylene: Chemistry, Physics, and Material Science*; Academic: Orlando, 1984.
- (2) A. O. Patil, A. J. Heeger, F. Wudl, *Chem. Rev.*, **1988**, *88*, 183.
- (3) (a) Zeigler J. M., U.S. Patent Appl. US 760 433 AO, 21 November, 1986; *Chem. Abstr*, **1986**, *20*, 157042. (b) Zeigler J. M. *Polym. Prepr.* **1984**, *25*, 223. (c) Okano, Y; Masuda, T.; Higashimura, T. *J. Polym. Sci.: Polym. Chem. Ed.* **1984**, *22*, 1603. (d) Masuda, T.; Higashimura, T. *Adv. in Polymer Science* **1987**, *81*, 121.
- (4) Leclerc, M.; Prudhomme, R. E. *J. Polym. Sci: Polym. Phys. Ed.* **1985**, *23*, 2021.
- (5) (a) Tlenkopachev, M. A.; Korshak, Yu. V.; Orlov, A. V.; Korshak, V. V. *Dokl. Akad. Nauk SSSR, (Engl. Transl)* **1986**, *291*, 1036; *Dokl. Akad. Nauk SSSR*, **1986**, *291*, 409. (b) Korshak, Y. V.; Korshak, V.; Kansichka, G.; Höcker, H. *Makromol. Chem. Rapid Commun.* **1985**, *6*, 685.
- (6) Klavetter, F. L.; Grubbs, R. H. *J. Am. Chem. Soc.* **1988**, *110*, 7807.
- (7) (a) Ginsburg, E. J.; Gorman, C. B.; Marder, S. R.; Grubbs, R. H. *J. Am. Chem. Soc.*, **1989**, *111*, 7621. (b) Gorman, C. B.; Ginsburg, E. J.; Marder, S. R.; Grubbs, R. H. *Angew. Chem. Adv. Mater.*, **1989**, *101*, 1603.
- (8) (a) Gorman, C. B.; Ginsburg, E. J.; Marder, S. R.; Grubbs, R. H. *Polym. Prepr.*, **1990**, *31(1)*, 386. (b) Gorman, C. B.; Ginsburg, E. J.; Marder, S. R.; Grubbs, R. H. manuscript in preparation.
- (9) Ciardelli, F.; Lanzillo, S.; Pieroni, O. *Macromolecules*, **1974**, *7*, 174.
- (10) (a) *Optical Rotatory Dispersion and Circular Dichroism in Organic Chemistry*; Sneath, G. Ed. Heyden and Son: London, 1967. (b) Charney, E. *The Molecular Basis of Optical Activity*; John Wiley and Sons: New York, 1979.

- (11) (a) Weiss, U.; Ziffer, H.; Charney, E. *Tetrahedron*, **1965**, *21*, 3105. (b) Charney, E.; Ziffer, H.; Weiss, U. *Tetrahedron*, **1965**, *21*, 3121.
- (12) Crabbé, P.; Klyne, W. *Tetrahedron*, **1967**, *23*, 3449.
- (13) (a) Kotkar, D.; Joshi, V.; Ghosh, P. *J. Chem. Soc. Chem. Commun.*, **1988**, 917. (b) Salmon, M.; Bidan, G. *J. Electrochem. Soc.*, **1985**, *132*, 1897.
- (14) Paquette, L. A.; Henzel, K. A. *J. Am. Chem. Soc.*, **1975**, *97*, 4649.
- (15) Eis, M. J.; Wrobel, J. E.; Ganem, B. *J. Am. Chem. Soc.*, **1984**, *106*, 3693.
- (16) Dale, J. A.; Dull, D. L.; Mosher, H. S. *J. Org. Chem.*, **1969**, *34*, 2543.
- (17) For reviews, see: (a) Paquette, L. A. *Tetrahedron*, **1975**, *31*, 2855. (b) Paquette, L. A. *Pure and Appl. Chem.*, **1982**, *54*, 987. And most recently: (c) Paquette, L. A.; Trova, M. P.; Luo, J.; Clough, A. E.; Anderson, L. A. *J. Am. Chem. Soc.*, **1990**, *112*, 228 (d) Paquette, L. A.; Wang, T. Z.; Luo, J.; Cottrel, C. E.; Clough, A. E.; Anderson, L. B. *J. Am. Chem. Soc.*, **1990**, *112*, 239.
- (18) Johnson, L. K.; Virgil, S. C.; Grubbs, R. H.; Ziller, J. W. *J. Am. Chem. Soc.*, **1990**, *112*, 5384.
- (19) Schrock, R. R.; DePue, R. T.; Feldman, J.; Schaverien, C. J.; Dewan, J. C.; Liu, A. H. *J. Am. Chem. Soc.*, **1988**, *110*, 1423.
- (20) Schuegerl, F. B.; Kuzmany, H. *J. Chem. Phys.*, **1981**, *74*, 953.
- (21) Lichtmann, L. S. Ph. D. Thesis, Cornell University, 1980.
- (22) (a) Lichtmann, L. S.; Fitchen, D. B.; Temkin, H. *Synth Met.*, **1979/1980**, *1*, 139. (b) Kuzmany, H. *Pure & Appl. Chem.*, **1985**, *57*, 235. (c) Kuzmany, H. *Phys. Stat. Sol.*, **1980**, *97*, 521. (d) Baruya, A.; Gerrard, D. L.; Maddams, W. F. *Macromolecules*, **1983**, *16*, 578.
- (23) Rao, C. N. R. *Ultra-Violet and Visible Spectroscopy*; Plenum Press: New York, 1967; p. 95.
- (24) Baughman, R. H.; Hsu, S. L.; Pex, G. P.; Signorelli, A. J. *J. Chem. Phys.*,

1978, 68, 5405.

(25) Bates, F. S.; Baker, G. L. *Macromolecules*, **1983**, 16, 1015.

(26) (a) Cernia, E.; D'Ilario, L. *J. Polym. Sci. Polym. Chem. Ed.*, **1983**, 2163. (b) Rao, B. K.; Darsey, J. A.; Kestner, N. R. *Phys. Rev. B.*, **1985**, 31, 1187. (c) Elert, M. L.; White, C. T. *Phys Rev. B.*, **1983**, 28, 7387.

(27) Verbit, L.; Rao, A. S.; Clark-Lewis, J. W. *Tetrahedron*, **1968**, 24, 5839. These authors refer to the ratio $\Delta\epsilon/\epsilon$. However, $\Delta\epsilon$ is related to $[\Theta]$: $[\Theta] \approx 3300\Delta\epsilon$.

(28) Schaffer, H. E.; Chance, R. R.; Knoll, K.; Schrock, R. R.; Silbey, R. in *Conjugated Polymeric Materials: Opportunities in Electronics, Optoelectronics, and Molecular Electronics*; Bredas, J. L. and Chance, R. R., Eds. Nato ASI Series E 182. Kluwer Academic: Boston, 1990; pp. 365-376.

(29) Gasteiger, J.; Gream, G.; Huisgen, R.; Konz, W.; Schnegg, U. *Chem. Ber.*, **1971**, 104, 2412.

(30) Schurig, V.; Koppenhoefer, B.; Buerkle, W. *J. Org. Chem.*, **1980**, 45, 538.